

VICTORIA UNIVERSITY
MELBOURNE AUSTRALIA

NEUROPROTECTIVE AND ANTI-CANCER
EFFICACY OF APX3330 GIVEN IN
COMBINATION WITH IRINOTECAN AND
OXALIPLATIN

MAYA SHAKYA BISHOP

THESIS SUBMITTED IN FULFILMENT OF THE REQUIREMENTS FOR THE DEGREE
OF MASTER OF RESEARCH

VICTORIA UNIVERSITY, AUSTRALIA
INSTITUTE FOR HEALTH AND SPORT

July 2022

ABSTRACT

Colorectal Cancer (CRC) is considered one of the most aggressive cancers and causes the second most cancer-related deaths in Australia. Chemotherapy is the standard first-line treatment for stage three or metastatic cancer. It is given as a combination of two or more chemotherapeutic drugs with other medications by themselves or with radiation. Oxaliplatin (OXL) and Irinotecan (IRI) are the most common chemotherapy medications used in the clinical setting for CRC treatment. Regardless of the success rate of reducing disease progression and increasing survival, these drugs cause acute and chronic toxicities that lead to immediate and long-term adverse effects. Most medications currently in clinical use to alleviate the gastrointestinal side-effects of anti-cancer chemotherapy cause adverse effects and, in many cases, are of limited efficacy; therefore, searching for novel targets and therapies is crucial.

Apurinic/aprimidinic endonuclease 1/ Reduction-oxidation factor-1 (APE1/Ref-1), is the recent therapeutic target that addresses both oxidative stress damage and DNA repair damage due to pathological condition of cancer. APE1/Ref-1 functions as a dual-functioning molecule containing a redox-active site and a DNA repair active site. The redox-active site of the protein mainly regulates cellular antioxidant response while the DNA repair active site is highly attuned to cell survival and preventing apoptosis. Therefore, we hypothesised that APE1/Ref-1's capacity in regulating DNA repair pathway potentially leads to alleviating the damage to the enteric nervous system (ENS) that causes gastrointestinal (GI) dysfunction. APX3330, a small molecular inhibitor of APE1/Ref-1, was used in this study. A murine model with and without CRC was subjected 1) to investigate the efficacy of APX3330 treatment given in combination with IRI and OXL to alleviate neuronal toxicity associated with these chemotherapeutics, and 2) to assess the anti-tumour efficacy of combination treatment compared to treatment with individual chemotherapeutics. Assessment of body weights, faecal water content, and quantification of faecal lipocalin-2 were performed as a part of the evaluation of

clinical parameters. *Ex vivo* experiments to study morphological, immunological, and molecular mechanistic parameters were also utilised to address those aims. This thesis aimed to identify novel therapeutic targets to alleviate ENS neuropathy due to the side-effects of Irinotecan and Oxaliplatin treatments and examine the neuroprotective and anti-tumour efficacy of APX3330 for CRC, which has not been explored yet.

Based on our research findings, it is fair to conclude that the mechanisms underlying chemotherapy-induced gastrointestinal dysfunction arise because of complex and multifaceted mechanisms. Importantly, our research presented for the first time APX3330 showed enhanced enteric neuronal survival and improved GI function following Oxaliplatin and Irinotecan treatment. APX3330 treatment reduced the severity of constipation following Oxaliplatin treatment and alleviated Irinotecan-induced diarrhoea. Furthermore, results show that the impediment of the APE1/Ref-1 redox signalling pathway alleviated myenteric neuronal damage and it exhibited anti-tumour properties that aid in attenuating tumours and diminishing tumour metastasis.

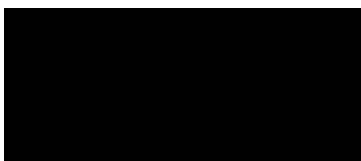
This thesis has demonstrated that individual administration of Oxaliplatin and Irinotecan caused neuronal damage and substantial reduction of myenteric neurons in the distal colon, significantly correlated with gastrointestinal dysfunction. While the effects of combination chemotherapeutic treatments on the enteric nervous system have yet to be further investigated, present work on using APX3330 combined with Oxaliplatin and Irinotecan to treat CRC successfully provides the groundwork for investigating consequent enteric neuronal survival and improved gastrointestinal dysfunction. Future research needs to be conducted to determine the molecular level interactions and possible regulatory pathways to better understand the subcellular interactions of the treatment agents and other proteins. Our research and previous findings show that pharmacologically protecting enteric neurons holds a robust future direction to alleviate chemotherapy-induced enteric neuropathy and gastrointestinal dysfunction.

CANDIDATE DECLARATION

“I, Maya Bishop, declare that the Master by Research thesis entitled ‘Neuroprotective and Anti-Cancer Efficacy of APX3330 Given in Combination with Irinotecan and Oxaliplatin’ is no more than 60,000 words in length including quotes and exclusive of tables, figures, appendices, bibliography, references, and footnotes. This thesis contains no material that has been submitted previously, in whole or in part, for the award of any other academic degree or diploma. Except where otherwise indicated, this thesis is my own work.”

I have conducted my research in alignment with the Australian Code for the Responsible Conduct of Research and Victoria University’s Higher Degree by Research Policy and Procedures.

“All research procedures reported in the thesis were approved by the Victoria University Animal Ethics Committee AEC 19-010.”



Signature

Date: 27/07/2022

DECLARATION OF CONTRIBUTION TO WORK

Chapter 1: Assistance in preparing the manuscripts that contributed to this chapter was provided by Assoc/Prof Kulmira Nurgali

Chapter 2: Dr. Nyanbol Kuol and Majid Hassanzadeganroudsari provided training and assistance with CRC induction surgeries. Dr. Sean Yan and Jia Li provided training for Western Blot experiments. Lauren Sahakian assisted with the assessment of the faecal lipocalin-2 level. Rhiannon Filippone was provided with some training in immunohistochemistry. Valentina Jovanosvska provided training for confocal microscope imaging. Assistance in preparing the manuscripts that contributed to this chapter was provided by Assoc/Prof Kulmira Nurgali

Chapter 3: Dr. Nyanbol Kuol and Majid Hassanzadeganroudsari provided training and assistance with CRC induction surgeries. Dr. Sean Yan and Jia Li provided training for Western Blot experiments. Majid Hassanzadeganroudsari provided training for CT-26 cell culture protocol. Assistance in preparing the manuscripts that contributed to this chapter was provided by Assoc/Prof Kulmira Nurgali

Chapter 4: Assistance in preparing the manuscripts that contributed to this chapter was provided by Assoc/Prof Kulmira Nurgali

MEDIA RELEASES FROM THIS THESIS

1. Colorectal Cancer Role of the Enteric Nervous System in Gastrointestinal side-effects of Chemotherapy (Previously Shakya Dayaratne - Maya Bishop)

<http://jglobal.jst.go.jp/en/public/202002222384893709>

2. Under the Coverslip 2021 Kunstmatrix (Previously Shakya Dayaratne - Maya Bishop)

<https://art.kunstmatrix.com/fr/node/1098852>

PRESENTATIONS

The following presentation has been made at a scientific meeting based on the studies contained within this thesis:

Maya Bishop (2021) Neuroprotective and Anti-Cancer Efficacy of APX3330 Given in Combination with Irinotecan and Oxaliplatin, Institute of Health and Sports, Victoria University, Melbourne, August 2021.

ACKNOWLEDGEMENTS

The completion of this thesis would not have been possible without the support and guidance of many people.

Firstly, I would like to express my sincere gratitude to my principal supervisor **A/Prof Kulmira Nurgali** for her supervision and patience over the last three years. I genuinely thank you for years of guidance, invaluable support, knowledge, direction, and tireless efforts during this journey. I sincerely appreciate every second you have sacrificed away from your family and busy schedules to stay up late proofreading my chapters and manuscript drafts. Your dedication, passion for research, compassion, and selflessness have inspired me to become a better researcher. Thank you for pushing me out of my comfort zone and making me realise my true potential. I sincerely appreciate everything you have done for me over the last couple of years and I appreciate all your efforts in moulding me into the best researcher I could be.

I would also like to express my sincere gratitude to my co-supervisor, **Dr. Sean Yan**, for your support and guidance and, most importantly, for encouraging and trusting me with my capabilities as a young researcher. Thank you for your invaluable knowledge, direction, and experience throughout this degree. Your contribution often presented new experimental procedures, making me a better researcher.

I would like to thank **Professor John Price** and **Professor Alan Hayes** for their constant support, understanding, and guidance. Thank you for making me realise my strengths and use them to achieve my dreams. Thank you for being patient with me and constantly extending a helping hand when needed.

I would like to thank **Mrs. Valentina Jovanovska** for your unwavering support, encouragement, and guidance in training me in a number of techniques. Thank you for your kind words, nurturing nature, and always having the warmest smile on your face that made the lab a happy and comforting environment.

To **Dr. Nyanbol Kuol** for taking time out of your demanding schedule to assist me with CRC induction surgeries; your knowledge and expertise are greatly appreciated.

To my dearest friend and work colleague **Majid Hassanzadeganroudsari**- for all your assistance and time teaching me various lab protocols. I sincerely appreciate your support, laughs, and the friendship you have given me during this time.

To **Jia Li** – I extend my most excellent thanks for sharing your expertise in Western Blotting and putting up with my constant distraction during troubleshooting and analysis. Thank you for being generous with your time even when you were busy with your studies.

To all my lab members at WCHRE past and present, **Lauren, Majid, Jeannie, Jimsheena, Amanda, Rhiannon, and Maryam**, you have all contributed to making this journey an enjoyable one.

To my fellow lab members at Footscray Park campus; **Shavin, Alex, and Victoria**. I feel fortunate to have shared the lab with you. Your willingness to help and support each other had an immense impact on making this experience a pleasant one. Thank you to the lab manager **Sudinna Hewakapuge**.

I want to extend my gratitude to my mother, **Indrani Abeysinghe**, and my brother

Chamil Eranda for sending me love and blessings even though you live far away.

Finally, I would like to offer my heartfelt gratitude to my beautiful daughter **Senudi Nelara**. I dedicate this achievement to you, my darling Senu. I do not know anyone who possesses such resilience, courage, strength, and kindness in life as you. I could not have overcome the countless challenges and obstacles we have faced together in our lives if you were not there with me. You give me such a remarkable yet invisible strength that always served as the hidden driving force to conquer several exceptional achievements in my life. I indeed gave you life, but the truth is you gave me mine. You showed me why I should never give up, never surrender, and walk-through life gracefully with a smile. When life got hard, and I felt alone, you reminded me with those beautiful eyes that this little girl was watching me who wanted to be just like me in the future. So, I got myself back up again because I wanted to show you that dreams can come true. Thank you for sharing all the difficulties and hardships and understanding the obligation and commitment of a Masters degree. I will never forget the nights you slept by the side of my workstation until I got the work done. Thank you for sacrificing your holidays, playtime, and freedom for all these years and for giving me unconditional love in return. Thank you for waking up early morning and staying late with me to remind me of the purpose of my life. Your beautiful, innocent smile gave me the energy and strength to build a happier and safer future for you and me. Having you in my life has always been my inspiration and strength to push myself forward and will always be the greatest joy in my life. My darling daughter, I have no words to express my love or gratitude but to tell you I love and protect you with everything I have.

TABLE OF CONTENTS

ABSTRACT.....	i
CANDIDATE DECLARATION	iii
DECLARATION OF CONTRIBUTION TO WORK.....	iv
MEDIA RELEASES FROM THIS THESIS.....	v
PRESENTATIONS.....	vi
ACKNOWLEDGEMENS	vii
TABLE OF CONTENTS.....	x
LIST OF FIGURES	xvi
LIST OF TABLES	xx
LIST OF ABBREVIATIONS.....	xxi
 CHAPTER 1: LITERATURE REVIEW	
1.1 Colorectal Cancer.....	2
1.2 Multimodality Treatment Approaches for Colorectal Cancer	2

1.2.1	Chemotherapeutics for the Treatment of CRC That Will be Used in This Study.....	4
1.2.1.1	Oxaliplatin.....	4
1.2.1.2	Irinotecan.....	6
1.3	Common Gastrointestinal Side-Effects of Chemotherapy	7
1.3.1	Oxaliplatin-Induced Side-Effects	8
1.3.1.1	Oxaliplatin-Induced Constipation.....	9
1.3.1.2	Current Treatments for Oxaliplatin-Induced Constipation.....	11
1.3.2	Irinotecan-Induced Gastrointestinal Side-Effects.....	12
1.3.2.1	Irinotecan-Induced Diarrhoea.....	12
1.3.2.2	Current Treatments for Irinotecan-Induced Diarrhoea.....	14
1.4	Effects of Oxaliplatin and Irinotecan on The Enteric Nervous System....	15
1.4.1	The Myenteric Plexus.....	17
1.4.2	The Submucosal Plexus.....	18
1.4.3	The Role of the Enteric Nervous System in Chemotherapy-Induced Gastrointestinal Dysfunction.....	19
1.4.4	Chemotherapy-Induced Enteric Neuropathy and Gastrointestinal Dysfunction.....	20
1.4.5	Oxidative Stress Associated with Enteric Neuropathy.....	21
1.4.5.1	Oxaliplatin-Induced Oxidative Stress and the Expression of Neuronal Nitric Oxide Synthase	23
1.4.6	Chemotherapy-Associated Mitochondrial Damage.....	24
1.4.7	Irinotecan-Induced Intestinal Mucositis and Oxidative Stress.....	27
1.5	Inhibition of APE1/Ref-1 Redox Signalling as a Novel Anti-cancer Treatment.....	29

1.5.1	APE1/Ref-1 Function in DNA Repair.....	30
1.5.2	APE1/Ref-1 in Redox Regulation.....	31
1.5.3	Other APE1/Ref-1 Protein-Protein Interactions.....	32
1.5.4	APE1/Ref-1 Angiogenesis.....	34
1.5.5	APE1/Ref-1 and Its Involvement in Inflammation.....	36
1.5.6	APE1/Ref-1 Function in Tumour Cell Metabolism.....	37
1.5.7	Modulating APE1/Ref-1 Function in the Cancer Treatment Milieu.....	38
1.5.8	APE1/Ref-1 Function in Chemotherapy-Induced Peripheral Neuropathy.....	38
1.5.9	Therapeutic Potential of APX3330 as a Cancer Treatment	40
1.5.10	APX3330 Clinical Progress as a Cancer Treatment	42
1.6	Summary	43

CHAPTER 2: INVESTIGATING THE NEUROPROTECTIVE AND ANTI-CANCER EFFICACY OF APX3330 IN COMBINATION WITH IRINOTECAN IN THE MURINE MODEL OF CRC

2.1	Summary	47
2.2	Introduction	49
2.3	Methods	52
2.3.1	Animals.....	52
2.3.2	Cell culture.....	52
2.3.3	Orthotopic Implantation of CT-26 tumour cells.....	53

2.3.4	Treatments.....	54
2.3.5	Clinical parameters.....	56
2.3.5.1	Body weights.....	56
2.3.5.2	Faecal water content.....	56
2.3.5.3	Faecal Lipocalin-2.....	58
2.3.6	Tissue Collection.....	59
2.3.6.1	Immunohistochemistry in wholemount preparations.....	59
2.3.6.2	Immunohistochemistry in cross-sections.....	60
2.3.6.3	Imaging.....	62
2.3.7	Morphometric analysis of tumours and tumour metastasis	62
2.3.8	Western blot analysis.....	65
2.3.9	Data and statistical analysis.....	66
2.4	Results	68
2.4.1	Effects of treatments on clinical symptoms.....	68
2.4.2	Anti-Inflammatory and Neuroprotective properties of APX3330.....	80
2.4.3	Neuroprotective effects of APX3330 in combination with Irinotecan.....	97
2.4.4	Effects of the treatments on APE1/Ref-1 expression	108
2.4.5	Effects of the treatments on transcription factors	124
2.4.6	Effects of treatments on tumour growth and metastasis in the colon	139
2.5	Discussion	147
2.6	Conclusion	155

CHAPTER 3: INVESTIGATING THE NEUROPROTECTIVE AND ANTI-CANCER EFFICACY OF APX3330 IN COMBINATION WITH OXALIPLATIN IN THE MURINE MODEL OF CRC

3.1	Summary.....	157
3.2	Introduction.....	160
3.3	Methods.....	165
3.3.1	Animals.....	165
3.3.2	Cell culture.....	165
3.3.3	Orthotopic implantation of CT-26 tumour cells.....	166
3.3.4	Treatments.....	167
3.3.5	Clinical parameters.....	168
3.3.5.1	Body weights.....	168
3.3.5.2	Faecal water content.....	170
3.3.6	Tissue Collection.....	170
3.3.6.1	Immunohistochemistry in wholemound preparations.....	170
3.3.6.2	Imaging.....	173
3.3.7	Morphometric analysis of tumours and tumour metastasis	173
3.3.8	Western Blotting.....	173
3.3.9	Data and Statistical Analysis.....	175
3.4	Results	177
3.4.1	Effects of treatments on clinical symptoms.....	177
3.4.2	Neuroprotective effects of APX3330 in combination with Oxaliplatin.....	189
3.4.3	Effects of the treatments on APE1/Ref-1 expression.....	195

3.4.4	Effects of the treatments on cytochrome c and STAT3 expression	210
3.4.5	Effects of the treatments on tumour growth and metastasis.....	225
3.5	Discussion	233
3.6	Conclusion	239

CHAPTER 4: GENERAL DISCUSSION AND CONCLUSION

4.1	General Discussion.....	242
4.2	Chemotherapy-Induced Enteric Neuropathy and Gastrointestinal Dysfunction.....	243
4.3	Conclusion and Future Directions	258

CHAPTER 5: REFERENCES.....	265
-----------------------------------	------------

CHAPTER 6: APPENDIX	315
----------------------------------	------------

LIST OF FIGURES

CHAPTER ONE

Figure 1.1	Institution of the enteric nervous system and affiliated muscle layers.	16
Figure 1.2	Role of APE1/Ref-1 in cancer cells vs neurons.....	41

CHAPTER TWO

Figure 2.1	Induction of CRC with CT26 murine cells in a Balb/c mouse	54
Figure 2.2	Effect of IRI and APX3330 treatment on body weight of mice without CRC.....	72
Figure 2.3	Average body weight following 14 days of treatments in CRC-induced mice.....	74
Figure 2.4	Effects of Irinotecan and APX3330 treatment on the faecal water content compared to untreated mice.....	76
Figure 2.5	Effects of the treatments on the faecal water content in CRC-induced mice.....	78
Figure 2.6	Neutrophil gelatinase-associated protein lipocalin-2 levels measured in the faeces from untreated, IRI-treated, and APX3330-treated mice without CRC.....	85
Figure 2.7	Neutrophil gelatinase-associated protein lipocalin-2 levels measured in CRC-induced mice.....	87
Figure 2.8	Effects of treatments on the number of CD45+ immune cells and β -Tubulin III-immunoreactive (IR) neuronal fibre density in the distal colon of mice without cancer.....	89
Figure 2.9	The number of CD45+ immune cells and neuronal fibre density in the distal colon of CRC-induced mice.....	91

Figure 2.10	The level of myeloperoxidase (MPO) and neuronal fibre density in the distal colon of mice without cancer.....	93
Figure 2.11	The level of myeloperoxidase (MPO) and neuronal fibre density in the distal colon of CRC-induced mice.....	95
Figure 2.12	Effect of <i>in vivo</i> treatments on ChAT-IR neurons in mice without cancer.....	100
Figure 2.13	Effect of <i>in vivo</i> treatments on ChAT-IR neurons in mice with CRC.....	102
Figure 2.14	Effect of the treatments on the density of cholinergic fibres in mice without cancer.....	104
Figure 2.15	Changes in the density of cholinergic fibres in mice with CRC.....	106
Figure 2.16	APE1/Ref-1 expression in the distal colon following 14-day treatment with Irinotecan and APX3330.....	112
Figure 2.17	Quantitative analysis of the APE1/Ref-1 expression in the distal colon myenteric ganglia of mice without cancer.....	114
Figure 2.18	APE1/Ref-1 protein expression in the distal colon.....	116
Figure 2.19	APE1/Ref-1 expression in the distal colon following 14-day treatments in CRC-induced mice.....	118
Figure 2.20	Quantitative analysis of the APE1/Ref-1 expression in the distal colon myenteric ganglia of CRC-induced mice.....	120
Figure 2.21	APE1/Ref-1 protein expression in the distal colon of mice with CRC.....	122
Figure 2.22	NF- κ B protein expression in the distal colon from mice without cancer.....	127
Figure 2.23	NF- κ B protein expression in the distal colon from CRC-induced mice.....	129
Figure 2.24	Signal transducer and activator of transcription 3 (STAT3) protein expression in the distal colon of mice without cancer.....	131

Figure 2.25	Phosphorylated signal transducer and activator of transcription 3 (pSTAT3) protein expression in the distal colon of mice without cancer.....	133
Figure 2.26	Signal transducer and activator of transcription 3 (STAT3) protein expression in the distal colon of mice with CRC.....	135
Figure 2.27	Phosphorylated signal transducer and activator of transcription 3 (pSTAT3) protein expression in the distal colon of mice with CRC.....	137
Figure 2.28	Effects of the treatments on tumour growth.....	141
Figure 2.29	Tumour metastasis in the distal colon.....	143
Figure 2.30	Vascular endothelial growth factor (VEGF) protein expression following treatments in mice with CRC.....	145

CHAPTER THREE

Figure 3.1	Effect of OXL and APX3330 treatment on body weight of mice without cancer.....	181
Figure 3.2	Average body weight following 14 days of treatments in CRC-Induced mice.....	183
Figure 3.3	Effects of Oxaliplatin and APX3330 treatment on the faecal water content of mice without cancer.....	185
Figure 3.4	Effects of the treatments on the faecal water content in CRC-induced mice.....	187
Figure 3.5	Effect of <i>in vivo</i> treatments on neuronal nitric oxide synthase (nNOS)-immunoreactive neurons in mice without cancer.....	191
Figure 3.6	Effect of <i>in vivo</i> treatments on nNOS-IR neurons in CRC-induced mice.....	193
Figure 3.7	APE1/Ref-1 expression in the distal colon following 14-day treatment with Oxaliplatin and APX3330.....	198

Figure 3.8	Quantitative analysis of the APE1/Ref-1 expression in the distal colon myenteric ganglia of mice without cancer.....	200
Figure 3.9	APE1/Ref-1 protein expression in the distal colon of mice without cancer.....	202
Figure 3.10	APE1/Ref-1 expression in the distal colon following 14-day treatments in CRC-induced mice.....	204
Figure 3.11	Quantitative analysis of the APE1/Ref-1 expression in the distal colon myenteric ganglia of CRC-induced mice.....	206
Figure 3.12	APE1/Ref-1 protein expression in the distal colon of mice with CRC.....	208
Figure 3.13	Cytochrome c protein expression in the distal colon from mice without cancer.....	213
Figure 3.14	Cytochrome c protein expression in the distal colon from mice with CRC.....	215
Figure 3.15	Signal transducer and activator of transcription 3 (STAT3) protein expression in the distal colon of mice without cancer.....	217
Figure 3.16	Phosphorylated signal transducer and activator of transcription 3 (pSTAT3) protein expression in the distal colon of mice without cancer.....	219
Figure 3.17	Signal transducer and activator of transcription 3 (STAT3) protein expression in the distal colon of CRC-induced mice.....	221
Figure 3.18	Phosphorylated signal transducer and activator of transcription 3 (pSTAT3) protein expression in the distal colon of CRC-induced mice.....	223
Figure 3.19	Effects of the treatments on the tumour growth.....	227
Figure 3.20	Tumour metastasis in the distal colon.....	229
Figure 3.21	Vascular endothelial growth factor (VEGF) protein expression following treatments in mice with CRC.....	231

LIST OF TABLES

CHAPTER TWO

Table 2.1	Treatment Regimens	57
Table 2.2	Primary and Secondary Antibodies Used in Wholemout Preparations	63
Table 2.3	Primary and Secondary Antibodies Used in Cross-sections	64
Table 2.4	Primary and Secondary Antibodies Used for Western Blotting	67

CHAPTER THREE

Table 3.1	Treatment Regimens	169
Table 3.2	Primary and Secondary Antibodies Used in Wholemout Preparations	172
Table 3.3	Primary and Secondary Antibodies Used for Western Blotting	176

LIST OF ABBREVIATIONS

AKT	Serine /Threonine-specific Protein Kinases
AMD	Neovascular Age-Related Macular Degeneration
ANOVA	Analysis of Variance
AP-1	Activator Protein 1
APE1/REF-1	Apurinic/ apyrimidinic Endonuclease
APE1/Ref-1	Apurinic/ Apyrimidinic Endonuclease/ Redox Effector Factor 1
APX	APX3330
BCL-xl	B-Cell Lymphoma -xl
BER	Base Excision Repair
bFGF	Basic Fibroblast Growth Factor
BSA	Bovine Serum Albumin
CCL5	Chemokine Ligand 5
CD 80/86	A cluster of Differentiation 80/86
CD45	Cluster of Differentiation
CD45+	Lymphocyte Common Antigen- Receptor-linked Protein Tyrosine Phosphatase
CGRP-IR	Calcitonin Gene-related Peptide
ChAT	Choline Acetyltransferase
CHT1	Choline Transporter 1
CIPN	Chemotherapy-Induced Peripheral Neuropathy
CO ₂	Carbon Dioxide
CRC	Colorectal Cancer
CREB	Cyclic-AMP Response Element-Binding Protein

CTL1	Choline Transporter-like1
CXCL 10	C-X-C Motif Chemokine 10
DAPI	4'6-diamidine-2'-phenylindoloe dihydrochloride
DME	Diabetic Macular Edema
DMSO	Dimethyl Sulfoxide
DR	Damage Response
DR	Diabetic Retinopathy
ECL	Enhanced Chemiluminescence
Egr-1	Early Growth Response-1
EMT	Epithelial to Mesenchymal Transition
ENS	Enteric Nervous System
FBS	Foetal Bovine Serum
FOLFOX	5-Fluorouracil, Leucovorin, Oxaliplatin
5-FU	5 Fluorouracil
GGR	Global Genomic Repair
GI	Gastrointestinal
HIF1- α	Hypoxia-Inducible Factor-1 Alpha
HOCL	Hypochlorous acid
HR	Homologous Recombination
HRP	Horseradish Peroxidase
IFN- β/γ	Interferon Beta and Gamma
IFN- γ	Interferon- γ
IL-1	Interleukin 1
IL-6	Interleukin 6
IL-8	Interleukin 8

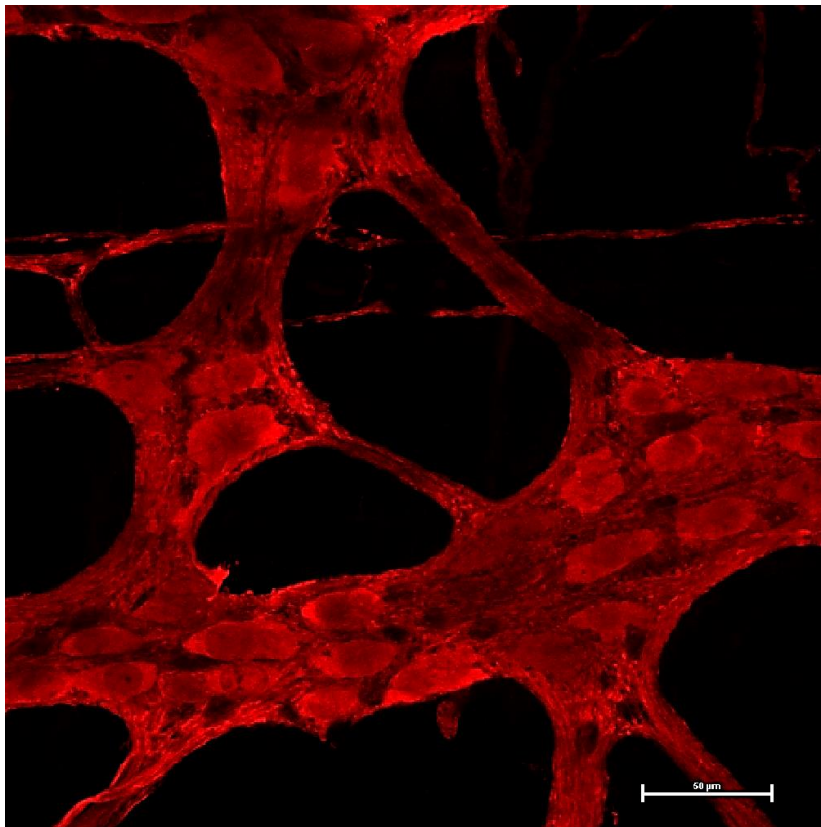
IL-10	Interleukin 10
IL-12	Interleukin 12
IL-18	Interleukin 18
IL-1 β	Interleukin 1 β
IR	Immunoreactive
IRI	Irinotecan
JAK	Janus Kinase
LCN-2	Neutrophil Gelatinase Associated Protein- Lipocalin II
LMMP	Longitudinal Muscle Myenteric Plexus
LPS	Lipopolysaccharide
MAPK	Mitogen-activated Protein Kinase
MHC class II	Major Histocompatibility Complex II
MMPs	Matrix Metalloproteins
MMR	DNA Mismatch Repair
MPO	Myeloperoxidase
mRNA	Messenger Ribonucleic Acid
MYC	MYC Proto-Oncogene
NA	Deoxyribonucleic Acid
NADP+	Nicotinamide Adenine Dinucleotide Phosphate
NF κ B	Nuclear Factor Kappa-light-chain- enhancer of Activated B Cells
NHMRC	National Health and Medical Research Council
NLRP3	Inflammatory Cascade
nNOS	Neuronal Nitric Oxide Synthase
NO	Nitric Oxide
NOS	Nitric Oxide Synthase
OCT	Optimum Cutting Temperature

OCTs	Organic Cation Transporter
OXL	Oxaliplatin
OXL APX	Oxaliplatin, APX3330
OXL VEH	Oxaliplatin Vehicle
P53	Tumour Protein
PAX-5	Paired Box Genes-5
PAX-8	Paired Box Genes-8
PBS	Phosphate Buffered Saline
PBST	Phosphate Buffered Saline with Triton
PCR	Polymerase Chain Reaction
PDGF	Platelet-derived Growth Factor
PD-L1	Programmed Death Ligand 1
PD-L2	Programmed Death Ligand 2
PEBP-2	Phosphatidylethanolamine – Binding Protein
PGP 9.5	Protein Gene Product 9.5
pSTAT3	Phosphorylated Signal Transducer and Activator of Transcription 3
PVDF	Polyvinylidene Fluoride
RIPA	Radioimmunoprecipitation Assay Buffer
RNA	Ribonucleic Acid
ROS	Reactive Oxygen Species
RPMI	Roswell Park Memorial Institute
SD	Standard Deviation
SDS-PAGE	Sodium Dodecyl-sulfate Polyacrylamide Gel Electrophoresis
SEM	Standard Error of the Mean
STAT3	Signal Transducer and Activator of Transcription 3
TCA	Tricarboxylic Acid Cycle

TBST	Tris Buffered Saline with Tween
TGF- α	Transforming Growth Factor-Alpha
TGF β	Transforming Growth Factor Beta
TME	Tumour Microenvironment
TNF- α	Tumour Necrosis Factor Alpha
TTF-1	Thyroid Transcription Factor
VACht	Vascular Acetylcholine Transporter
VEGF	Vascular Endothelial Growth Factor
VEH	Vehicle
WCHRE	Western Centre for Health Research and Education
β -Tubulin III	Class III β -tubulin

1

LITERATURE REVIEW



Wholemout preparation of the myenteric ganglia from the distal colon of OXL+APX3330-treated mouse with CRC labelled with a pan-neuronal marker anti-PGP9.5 antibody (red) (Scale bar = 50μm)

1.1 Colorectal Cancer

Colorectal Cancer (CRC) is one of the most common cancers and is the third most common cause of cancer-related deaths in Australia. According to recent statistics, 15,540 Australians are diagnosed with bowel cancer annually, including 1542 individuals under the age of 50 (Bowel Cancer Australia, 2021). Bowel cancer-related fatality tolls 5,295 Australian lives every year, including 292 individuals under the age of 50 (Bowel Cancer Australia, 2021). Age, gender, and race/ethnicity are the most common epidemiological factors associated with colorectal cancer (Haggard and Boushey, 2009, Amersi et al., 2005). CRC tends to have a higher incidence rate in westernised countries, indicating geographic variations (Haggard and Boushey, 2009, Boyle and Langman, 2000). Obesity, smoking, nutritional practices, physical activity, inherited genetics, heavy alcohol consumption, inflammatory bowel disease, and familial history of adenomatous polyps are primary risk factors for CRC (Haggard and Boushey, 2009, Centre et al., 2009). Since the early stages of CRC are often asymptomatic, in most cases, it is diagnosed at the advanced stages. Hence the five-year survival expectancy is less than 10 percent (Bowel Cancer Australia, 2020). Weight loss, altered bowel habits, rectal bleeding, unexplained extreme tiredness, lump or swelling in the abdomen, and abdominal pain commonly occur in the later stages of the disease progression (Adelstein et al., 2011, Cappell, 2005). Surgical resection is the most common treatment approach for the early stages of CRC, including stage I and stage II. Chemotherapy is the standard first-line treatment for stage III or metastatic cancer. It is given as a combination of two or more chemotherapeutic drugs or with radiation for rectal cancer (Johnston et al., 2012, Chibaudel et al., 2012). Oxaliplatin (OLX), Irinotecan (IRI), and 5-fluorouracil (5-FU) are the most common chemotherapy medications that are used in the clinical setting for CRC treatment (Wang and Li, 2012, Sharif et al., 2008, Marschner et al., 2015).

1.2 Multimodality Treatment Approaches for Colorectal Cancer

Therapeutic options for CRC depend on the location and the characteristics of the tumour. Around 65% of colon tumours are located further away from the splenic flexure that can be detectable via sigmoidoscopy, whereas 35% of primary tumours are found proximal to the sigmoid colon, which makes it indistinguishable from detection at the early stages (Martini et al., 2017, Church, 2005, McCallion et al., 2001). Due to the ambiguity of the symptoms that distinguish CRC from other pathologies, only rectal bleeding, and weight loss can be considered the definitive symptoms of CRC (McCulloch et al., 2020, Adelstein et al., 2011, Oldie et al., 2010). As a result of poor prognosis, the 5-year survival rate for stage I and stage II CRC patients sit at 63%, whilst stage III and metastatic (stage IV) cancer patients' 5-year survival rate drops down to less than 10% (Jiang et al., 2022, Jemal et al., 2008, Hagger and Boushey, 2009, Goldberg, 2005, Ries et al., 2008). Based on current treatment approaches, patients with chemotherapy-refractory colorectal liver metastasis have 4-6 months of survival, including optimum palliative care (Hong et al., 2020, Amado et al., 2008). Most CRC patients diagnosed after stage III mainly depend on the application of chemotherapeutics as the mainstay treatment (Dienstmann et al., 2017, Bockelman et al., 2015, Siegel et al., 2014).

Surgical resectioning is a common therapeutic approach for CRC, and approximately two-thirds of patients undergo surgical resectioning followed by chemotherapy (McQuade et al., 2017, Scheer and Auer, 2009). Regrettably, cancer recurrence is as high as 90% in the first five years in 30-50% of the patients who undergo surgical resection (Van der Stok et al., 2017, Granados-Romero et al., 2017, Bohm et al., 1993). Preoperative chemotherapeutics have shown improved outcomes that led to the development of several treatment regimens improving five-year survival expectancy for locally resected stage III CRC (Favoriti et al., 2016, Souglakos et al., 2006, Haller, 2000). The structure of the treatment has changed in recent years along with multi-agent regimens instated of administering singular cytotoxic agents (Spiegel et al., 2020, Jalaeikhoo et al., 2019, Markovina et al., 2017, Casadaban et al., 2016). Current chemotherapeutic approaches focussing on administering a combination of plant alkaloids, platinum agents, and antibiotics to adjuvant and neoadjuvant before chemotherapy treatment have shown

successful results in improving colorectal cancer patients' 5–10-year survival expectancy (Manjelievskaia et al., 2017, Al-Hajeili et al., 2016). This demonstrates the importance of ongoing research in developing new treatment approaches for CRC (Shiao et al., 2020, Cassidy et al., 2017, Bradley et al., 2016, Cassidy et al., 2004, Haller et al., 2011, De Gramont et al., 2000, Grothey et al., 2004, Douillard et al., 2000, Saltz et al., 2000).

1.2.1 Chemotherapeutics for the Treatment of CRC That Will be Used in This Study

1.2.1.1 Oxaliplatin

The incidental discovery of biologically active platinum complexes in the early 1960s (Rosenberg et al., 1965) triggered a rejuvenation of thousands of platinum analogues as a chemotherapeutic medication (Kelland, 2007). Consequently, platinum-based chemotherapeutics such as Cisplatin and Oxaliplatin are now being used in the clinical setting to treat a broad range of cancers, including CRC. Cisplatin and carboplatin are the first- and second-generation platinum-based chemotherapeutics used to treat a wide range of malignant diseases (McQuade et al., 2017, Cortejoso et al., 2013, Ali et al., 2013, Kelland, 2007). Oxaliplatin ($C_8H_{14}N_2O_4Pt$) is a third-generation platinum-based chemotherapeutic medication used in clinical settings for stage III and metastatic CRC as a single agent or as a combination therapy with 5-FU (Carlsen et al., 2021, Gu et al., 2019, Stintzing, 2014). The primary mechanism of action of platinum-based agents is the formation of platinum-based adducts resulting in intra and inter-strand crosslinks at the DNA level, leading to disruption of the DNA transcription as well as DNA replication processes (Chen et al., 2019, Cortejoso et al., 2013, Fuertes et al., 2003, Jamieson and Lippard, 1999, Noll et al., 2006). This triggers the halting of the mitotic cell cycle and stimulates the cell death of newly dividing cells via apoptosis (Goodisman et al., 2006, Graham et al., 2000). These platinum adducts cause deformities in DNA strands that are recognised by several cellular proteins, including the proteins

involved in the DNA repair pathways of the cell (Chaney et al., 2004) and they usually lead to the activation of cytotoxic pathways, resulting in apoptosis (Guo et al., 2015, Gaur et al., 2014, Eastman, 1989). Moreover, the exact path of apoptosis triggered by platinum-based chemotherapeutics remains unclear (Kelland, 2007). Recent studies suggest several pathways that lead the cancer cells to apoptotic death via ribosomal biogenesis stress (Sutton and DeRose, 2021), induction of immunogenic cell death (ICD), via modulation of the tumour immune microenvironment (Zhu et al., 2020), or as a result of anti-tumour immunity (Park et al., 2019).

Oxaliplatin is currently used in the clinical setting as the first line of treatment for metastatic CRC (Abraham et al., 2021, Innominato et al., 2021, Landre et al., 2018, Petrioli et al., 2008, De Gramont et al., 2000). When used at clinically recommended doses, Oxaliplatin causes less damage to renal, haematologic, and auditory systems compared to other platinum-based chemotherapeutics such as cisplatin and carboplatin (Um et al., 2019, Oun et al., 2018, Raymond et al., 1998). Oxaliplatin seems to cause a significantly different pattern of side-effects compared to carboplatin and cisplatin, distinguishing it from the rest of the platinum-based chemotherapeutics (Um et al., 2019, Oun et al., 2018). Patients have reported Oxaliplatin-related side-effects including gastrointestinal toxicity, peripheral sensory neuropathy, and hematologic toxicity (Branca et al., 2021, Drott et al., 2019, McQuade et al., 2016, Cassidy and Misset, 2002). Oxaliplatin has been reported significantly improve the efficacy of treatment against many tumours resistant to other chemotherapeutic medications (Louvet et al., 2002, Machover et al., 1996). Since then, several studies have been conducted to evaluate the efficacy of Oxaliplatin as a first-line and second-line treatment in combination with 5-Fluorouracil and Leucovorin for CRC, thus, discovering the more significant therapeutic potential of Oxaliplatin in combination with other medications as an anti-cancer medication (Abraham et al., 2021, Innominato et al., 2021, Landre et al., 2018, Andre et al., 2004, Machover et al., 1996, Levi et al., 1993, Giacchetti et al., 2000). The therapeutic potential of Oxaliplatin in combination treatments sheds light on novel therapeutic pathways that allow patients to undergo secondary surgeries

following chemotherapy regimens as curative surgeries (Wang et al., 2019, Cercek, et al., 2014, Oechsle et al., 2011).

1.2.1.2 Irinotecan

Twenty-eight years ago, Irinotecan was approved as a cytotoxic medication for the treatment of cancer in Japan (Bailly, 2019). Since then, Irinotecan has been used for the treatment of solid tumours worldwide for more than two decades. Irinotecan is the semi-synthetic version of naturally occurring quinoline alkaloid camptothecin (Martino et al., 2017, Xu and Villalona-Calero, 2002). Irinotecan ($C_{33}H_{38}N_4O_6$) exerts its anti-tumour efficacy by inhibiting DNA topoisomerase (Mastrangelo et al., 2022, Dickens and Ahmed, 2018). Its active metabolite, SN-38, induces irreversible DNA damage to tumour cells and causes cell death (Lee et al., 2019, Shin et al., 2016). Topoisomerase I is an essential component in DNA transcription that modulates its action via cutting, relaxing, and reannealing DNA strands (Mastrangelo et al., 2022). Irinotecan's active metabolite SN-38 binds to topoisomerase I and forms a stable ternary structure that prevents DNA binding activity, thus promoting DNA damage, ultimately leading to apoptosis (Dickens and Ahmed, 2018). Irinotecan induces a conversion from single-strand breaks into double-strand breaks during the S-phase of the cell cycle due to the collapse of the replication fork halted by Irinotecan's active metabolite SN-38 and DNA (Dickens and Ahmed, 2018, Pommier et al., 2003, Grivicich et al., 2001). The recent discovery of Irinotecan's mechanism of action that targets FUBP1 protein involved in binding single-strand DNA aids in understanding and better managing the main limiting toxicities of the treatment (Bailly, 2019). During phase II clinical trials conducted in the late 1990s to investigate the overall benefit of Irinotecan as a second-line treatment for patients who have been treated with 5-FU therapy, Irinotecan showed positive results by prolonging survival compared to patients who receive palliative care (Jia et al., 2019, Cascinu et al., 2017, Passardi et al., 2015, Cunningham et al., 1998). Patients with stage IV CRC have a poor survival rate with a less than 6% chance of a five-year survival rate (Cassidy et al., 2008, Colucci et al., 2005,

Tournigand et al., 2004). The treatment for unresectable tumours for advanced-stage CRC is using a combination of 5-FU with leucovorin that increases the survival from approximately 6-12 months. Researchers have found that the addition of Irinotecan (FOLFIRI) and Oxaliplatin (FOLFOX) prolongs survival by approximately 20 months (Tournigand et al., 2004). Numerous research has shown successful outcomes for the treatment of advanced-stage cancers when using combination treatments that target different aspects of cancer that inhibit the molecular level progression of cancer rather than using single-agent cancer treatments. Alternative treatment regimens with Irinotecan and Oxaliplatin with other chemotherapeutics have shown less toxicity for the patients when used in an alternative schedule even when the patients are exposed to 100% doses (Koopman et al., 2007).

1.3 Common Gastrointestinal Side-Effects of Chemotherapy

Regardless of the successful reduction of the disease progression and increasing the survival rate, these medications cause acute and chronic toxicities that lead to immediate and long-term adverse effects (Axelrad et al., 2017, McQuade et al., 2016, Keefe et al., 2014). Eighty to ninety percent of the patients have experienced diarrhoea, constipation, nausea, vomiting, and oral mucositis as side-effects of standard first-line chemotherapeutic drugs that are in the clinical setting (McQuade et al., 2016b, McQuade et al., 2016a, Keefe et al., 2014, Andreyev et al., 2014). These side-effects cause severe dehydration and malnutrition, resulting in significant weight loss and a weakened immune system (Bossi et al., 2021, Nishikawa et al., 2021, Andreyev et al., 2014, Aprile et al., 2015). Intestinal inflammation, bowel wall thickening, ulceration in the bowel wall, and bowel perforation are the complications of chemotherapy side-effects (Reginelli et al., 2021, Gray et al., 2016, Lecarpentier et al., 2010). These side-effects lead to the reduction of the dose of the chemotherapeutics to limit the adverse side-effects, potentially lowering the efficacy of the treatment (McQuade et al., 2016, Arbuckle et al., 2000). Diarrhoea and constipation are the most common gastrointestinal side-

effects of chemotherapeutic drugs (Moschen et al., 2022, Anthony and Chauhan, 2018). Up to 14-49% of cancer survivors have experienced post-treatment diarrhoea and, in some cases, the side effects lasted more than ten years (Han et al., 2020, Miller et al., 2019, Delinger et al., 2009). These side-effects cause a considerable negative impact on the quality of life of the patients and the carers. The drugs that are targeted the gastrointestinal (GI) side-effects of chemotherapeutic drugs have their own adverse effects, and, therefore, the efficacy of the treatment is being compromised (Kroschinsky et al., 2017, Banerjee et al., 2017, Kwon, 2016, Feyer et al., 2011). Hence, novel treatments and therapeutic targets are crucial for later-stage aggressive cancers such as CRC.

1.3.1 Oxaliplatin-Induced Side-Effects

Recent literature supports that platinum-based agents are more susceptible to gastrointestinal side-effects, with up to 90% of patients experiencing vomiting, diarrhoea, and/or nausea throughout the treatment (Abu-Sbeih et al., 2020, Breen et al., 2020, Oun et al., 2018, Sharma et al., 2005). Even though combination regimes such as FOLFOX with 5-fluorouracil, leucovorin, and oxaliplatin reported successful outcomes for dose tolerance for a longer duration, they have a high incident rate of chronic constipation and treatment-related death making it harder to use the platinum-based chemotherapeutics even for combination therapy (Souglakos et al., 2006). Chemotherapy-related gastrointestinal side effects can last up to 10 years after the cessation of the treatment (Denlinger and Barsevick, 2009, Di Fiore and Van, 2009, Grabenbauer et al., 2016). The main side effect related to platinum-based chemotherapeutics is peripheral neuropathy developed during acute and chronic administration (Mauri et al., 2020, Ranieri et al., 2019, Zajackowska et al., 2019, Staff et al., 2017, Zedan et al., 2014, Evans et al., 2000, Bennett et al., 1996). Cisplatin treatments cause peripheral neuropathy in the long term, even after the cessation of the treatment, and some of these cases are irreversible considering the damage that has occurred (Starobova et al., 2017, Brewer et al., 2016, Dar et al., 1995, Bennett et al., 1996, Sidorenko et al., 2007).

Oxaliplatin also causes peripheral neuropathy, but in contrast to other chemotherapeutics, Oxaliplatin causes acute and irreversible neurotoxicity (Mauri et al., 2020, Ranieri et al., 2019, Tanioka et al., 2019, Reddy et al., 2016) manifested as pain, and increased sensitivity to cold (Wasilewski and Mohile, 2021, Cavaletti and Marmiroli, 2020, Campalans et al., 2005, Dianova et al., 2001, Ranalli et al., 2002, Dar et al., 1995).

1.3.1.1 Oxaliplatin-Induced Constipation

Constipation is considered a frequent chemotherapy-related complication in advanced CRC patients, yet overseen in many instances (Podolski and Gucalp, 2021, Bertaut et al., 2021, Avci et al., 2020, Fox et al., 2017, Mancini and Bruera, 1998). Based on the nature of the individual experience of constipation, it is challenging to set definitive guidelines to explain constipation. The broadly accepted method is a mixture of increased stool consistency accompanied by reduced frequency of bowel action (Conolly and Larkin, 2012). It was found that 50-78% of advanced cancer patients experience constipation as a common side-effect of chemotherapy (Abernethy et al., 2009). Other studies report that approximately 16% of patients who receive cytotoxic chemotherapy experience constipation as a common side-effect, with 5 having severe symptoms and 11% experiencing moderate symptoms following treatments (Yamagishi et al., 2009, Anthony, 2010).

Even though chemotherapy-induced constipation is a relatively common occurrence in patients who receive chemotherapeutics such as Oxaliplatin (Donald et al., 2017, Zimmerman et al., 2016) minimal studies have been done regarding the mechanisms underlying chemotherapy-induced constipation (CIC) (Belsky et al., 2021, Zajackowska et al., 2019). Medications such as anti-emetics prescribed for nausea and vomiting, and opioids given for pain, also induce constipation, and it is misunderstood as chemotherapy-induced constipation since those medications are also given relatively at the same time as chemotherapy (Gibson and Keefe,

2006). It is difficult to draw a conclusion inclusive of all chemotherapy-induced constipation due to the lack of data regarding the prevalence and severity of chemotherapy-related constipation but to discuss individual chemotherapeutics and their susceptibility to inducing the symptoms. Recent research has focused on specific chemotherapeutics such as cisplatin, thalidomide, vinorelbine, and vinblastine that definitively induce CIC in up to 80-90% of patients and are used as guidance to assess the symptoms induced by other chemotherapeutics (Podolski and Gucalp, 2021, Belsky et al., 2020, Ghobrial and Rajkumar, 2003).

Since constipation is relatively manageable compared to uncontrollable diarrhoea, another side effect of chemotherapy, it is not given critical clinical importance until it causes physical risks to the patient or affects the patient's quality of life. Constipation causes several symptoms such as having lumpy or hard stools, reduced bowel emptying dropping below three times a week, straining to empty the bowels, feeling of blockage in the rectum that prevents from emptying the bowels, sensation of the inability to completely empty the stools from the rectum (Forootan et al., 2018). Patients usually experience abdominal distention and a severe, abrupt episode of abdominal pain because of prolonged constipation (Falcon et al., 2016). Rectal tearing, rectal fissures, and haemorrhoids are also caused by passing hard, dry stool (Walke and Sakharkar, 2021, Leung et al., 2011). Untreated longstanding constipation can lead to a severe form of constipation called obstipation, and the patient could face serious consequences such as faecal impaction and bowel obstruction (Walke and Sakharkar, 2021, Leung et al., 2011). Faecal impaction accumulates a mass of stool that obstructs the colon and gradually starts to increase intraluminal pressure that leads to ischemic necrosis of the mucosa and inflicting pain in the lower abdomen, bleeding, and bowel perforation (Walke and Sakharkar, 2021). It is common in elderly patients that faecal impaction causes urinary incontinence that usually requires medical intervention (Guinane and Crone, 2018, MacDonald et al., 2002). Constipation can also cause rapid onset of nausea that occurs with or without vomiting, confusion, liver pain, pain in the intraperitoneal region of the abdominal cavity, intestinal blockage leading to the malfunctioning GI tract, and inadequate to absorb oral drugs (Leslie, 2019, Mancini and Bruera, 1998)

including chemotherapy medications, having a massive impact on the tolerability and the efficacy of the treatments (Gupta et al., 2021). Several studies report that self-reported constipation and functional constipation have a significant effect on the patient's quality of life (Dennison et al., 2005, Talley, 2003). Recent research conducted to evaluate the therapeutic potential of resveratrol in combination of Oxaliplatin has found that Oxaliplatin caused significant changes to the myenteric neurons, decreased GI muscle wall thickness, and increased damage to the mucosal lining that led to GI motor dysfunction due to decreased amplitude of colonic muscle contractions resulted in severe constipation (Donald et al., 2017). The research conducted by McQuade et al., 2016, suggests that chemotherapy-induced CID and CIC arise as a result of a multifactorial involvement of GI dysmotility, alterations in GI innervation, inflammation, and secretory dysfunction. Current treatment approaches target reducing the severity of the symptoms rather than addressing the pathophysiological dysfunctions that cause the symptoms. Despite the debilitating impacts experienced by cancer-suffers who are receiving chemotherapy due to acute and chronic severe constipation, minimal efforts have been undertaken to rationalise prevalence and underlying mechanisms.

1.3.1.2 Current Treatments for Oxaliplatin-Induced Constipation

The management of constipation can be subdivided into general interventions and therapeutic measures. The general intervention approach incorporates increasing fluid intake and more dietary fibre intake, encouraging more physical exercise, and providing privacy, convenience, and comfort during defecation followed by the extermination of any medical factors that may contribute to constipation (Mancini and Bruera, 1998). Therapeutic approaches for CIC include the administration of both oral and/or rectal stimulants, emollients, bulk-forming, osmotic/saline, and lubricant laxatives (Connolly and Larkin, 2012). There are several categories of laxatives depending on the mechanism of action. Research conducted by McQuade et al., 2016, found that BGP-15 co-treatment alleviates the Oxaliplatin-induced

neuronal loss as well as mitigates the gastrointestinal dysfunction induced by Oxaliplatin treatment (McQuade et al., 2016, McQuade et al., 2018).

1.3.1 Irinotecan-Induced Gastrointestinal Side-Effects

Nausea, vomiting, dyspnoea, cholinergic syndrome, constipation, and neutropenia are common Irinotecan-associated side-effects that cause severe impacts on the quality of patients' day-to-day lives (Badgett et al., 2017, Rougier et al., 1998, Cunningham et al., 1998). The major dose-limiting factor for Irinotecan treatment is diarrhoea. Approximately 60-80% of patients experienced acute diarrhoea within 24 hours following Irinotecan administration (Okunaka et al., 2021, Gibson and Keefe, 2006). Acute diarrhoea is believed to be caused primarily by increased secretion and is treated with atropine indicating the involvement of cholinergic nature (Ribeiro et al., 2016, Gibson and Stringer, 2009, Gibson et al., 2003). Approximately 80% of patients have experienced delayed onset of diarrhoea and it usually occurs within 24-48 hours of Irinotecan administration (Baily, 2019, Ribeiro et al., 2016, Saliba et al., 1998). The delayed onset of diarrhoea is believed to be associated with the enzymic activity of β -glucuronidase found in intestinal microflora (Cheng et al., 2019). In the lumen of the gastrointestinal tract, SN-38 glucuronide is catalysed by β -glucuronidase to form its active metabolite SN-38 believed to be contributed to delayed onset diarrhoea (Takasuna et al., 1998).

1.3.2.1 Irinotecan-Induced Diarrhoea

Generally, chemotherapy-induced diarrhoea (CID) has a significant impact on the morbidity and mortality of cancer patients, thus frequently underrecognized by its impact (Nurgali et al., 2018, Maroun et al., 2007). The dosage and the frequency of chemotherapy regimen administration play a vital part in the prevalence and severity of CID (Smith et al., 2020). A direct correlation between cumulative dose and the severity of CID was found, as well as a correlation between that high dose

chemotherapy regimens and increased susceptibility to CID (Smith et al., 2020, Verstappen et al., 2003). The occurrence of CID has been associated with several patient and treatment-related risk factors (Athauda et al., 2020). Age (>65), gender (female), genetic predisposition (Gilbert's syndrome, Crigler-Najjar syndrome), biliary obstruction, and associated bowel pathology such as chronic inflammation or malabsorption are among the main patient-associated risk factors (Richardson and Dobish, 2007). Weekly chemotherapy schedule, prior history of CID, bolus 5-FU and prior or concomitant radiotherapy are considered treatment-associated risk factors (Walder et al., 1998, Saltz et al., 2003, Dranitsaris et al., 2005). The treatment regimens containing Irinotecan and 5-FU are especially prone to induce diarrhoea and recent research has found that up to 80% of patients experienced CID following Irinotecan or 5-FU administration (Richardson and Dobish, 2007, Benson et al., 2004) with one-third of the patients experienced severe diarrhoea that had debilitating effects on their quality of life (Maroun et al., 2007).

CID often results in dose reductions of chemotherapy (~22%), treatment alterations (~60%), treatment delays (~28%), and complete termination of the treatment in approximately 15% of patients resulting in debilitating effects on patient health and wellbeing as well as patient mortality (Seo et al., 2016, Dranitsaris et al., 2005, Arbuckle et al., 2000). Chemotherapy-related severe and persistent diarrhoea is often associated with malnutrition and dehydration commonly leading to significant weight loss (cachexia), renal failure, fatigue, perianal skin breakdown, and haemorrhoids (Fox et al., 2017, Seo et al., 2016, Shafi and Bresalier, 2010, Mitchel, 2006). Approximately 5% of patients who receive chemotherapy medications experience severe dehydration that can lead to early death (Rothenberg et al., 2001). Furthermore, chemotherapy-related gastrointestinal side-effects also extend to intestinal inflammation, bowel wall thickening, and ulceration (Marin-Diez and Pozo, 2021, Kuebler et al., 2007a) causing life-threatening ramifications in patients (Srisajjakul et al., 2022, Stein et al., 2010, Benson et al., 2004, Rothenberg et al., 2001). Researchers have found that for over 30% of CID sufferers, CID affects their quality of life including a significant impact on their mental and social lives (Stein et al., 2010). Persistent and uncontrollable CID has

led patients into social isolation, low self-esteem, anxiety, and depression (Viele, 2003) emphasizing the importance of discovering novel therapeutic approaches that had minimal or no side effects (Carelle et al., 2002).

1.3.2.2 Current Treatments for Irinotecan-Induced Diarrhoea

According to the National Cancer Institute's common terminology criteria for adverse effects grading system, CID can be classified as complicated grade 3-4 with one or more complicating signs or symptoms, uncomplicated grade 1-2 with no complications, early-onset occurs less than 24 hours after administration, late-onset occurs after 24 hours of administration, persistent if present for more than 4 weeks and non-persistent if present less than 4 weeks (Stein et al., 2010). Studies have shown that uncomplicated chemotherapy-induced diarrhoea can be managed by diet modification and anti-diarrhoeal medications such as octreotide, loperamide, and tincture of opium while complicated diarrhoea usually requires high-dose anti-diarrhoeal medications and extensive care at a hospital (McQuade et al., 2014). In 1998 the recommendations on the management of CID were published to provide guidelines for the evaluation and management of CID, and it has been updated in 2004 after further evaluation (Ferrell and Coyle, 2006, Walder et al., 1998). Okunaka et al., 2021 conducted a study to evaluate the expression profile of Irinotecan-induced diarrhoea in patients with CRC. Irinotecan-induced delayed-onset diarrhoea is treated with broad-spectrum antibiotics, neomycin which was found to reduce the β -glucuronidase levels to undetectable levels and decreasing the faecal SN-38 levels thus exhibiting no significant effect on haematological toxicity. Irinotecan-induced inflammation and dysbiosis instigate major contributing factors to intestinal toxicity, and β -glucuronidase inhibitors, plant extracts, and probiotics have been used in the clinical setting to limit the side-effects (Baily, 2019). The most recent discovery of Irinotecan's active metabolite SN-38 analogue FL118, SN-38 based immune-conjugates such as Sacituzumab govitecan, and recently approved liposomal form Nal-IRI is believed to dampen severe side-effects caused by original forms of the treatment (Bailly et al., 2019). Neomycin was found to

ameliorate Irinotecan-induced diarrhoea in 86% of patients indicating β -glucuronidase enzyme activity and bacterial involvement in Irinotecan-induced delayed-onset diarrhoea (Kehrer et al., 2001). A study conducted by Mayo et al., 2017 has found that Irinotecan treatment causes alterations in cell proliferation and cell survival pathways, initiates intestinal mucositis, induction of a number of inflammatory pathways as well as early apoptosis that ultimately leads to severe damage to the structure and function of the GI tract resulting in treatment alterations, hospitalisations and complete cessation of the treatment. In that study, they subjected the therapeutic efficacy of glucagon-like peptide-2 analogues (GLP-2 analogue) for the treatment of Irinotecan-induced diarrhoea. They have found that GLP-2 analogues exhibit successful outcomes for Irinotecan induced-toxicity by demonstrating anti-inflammatory, anti-apoptotic as well as intestinotrophic properties. Recent research conducted by McQuade et al., 2017 highlights the involvement and importance of the enteric nervous system (ENS) in Irinotecan-induced gastrointestinal dysfunction. They suggest the damage and death of enteric neurons. The recent advancements in research that benefited the researchers to better understand the detailed knowledge of the metabolism of Irinotecan and its active metabolite SN-38, has enabled the recognising of potential biomarkers, and therefore, to reduce drug-induced toxicities. Regardless of the recent progress, Irinotecan-specific definitive therapeutic biomarker has not been discovered yet (Bailly, 2019). Irinotecan is being used for the treatment of a large range of cancers and advanced solid tumours due to its' versatile nature of combining well with a variety of anti-cancer medications such as immuno-active biotherapeutics, cytotoxic agents, and targeted products. Regardless of its side-effects, Irinotecan remains a largely prescribed, an essential anti-cancer drug even after a quarter of a century after its first launch.

1.4 Effects of Oxaliplatin and Irinotecan on The Enteric Nervous System

According to recent literature, only a few studies have been conducted to examine the effects of chemotherapeutics on the enteric nervous system (Wafai et al., 2013,

Vera et al., 2011). Oxaliplatin and Irinotecan cause significant damage and death of enteric neurons and cause changes in certain sub-populations of myenteric neurons following treatments (McQuade et al., 2017, McQuade et al., 2016). Oxaliplatin treatment causes oxidative stress that contributes to enteric neuropathy, changes in the expression of neuronal nitric oxide synthase (nNOS), changes in microbiota, toll-like receptor 4 (TLR4+) positive cells, enhanced high mobility group box 1 protein (HMGB1) expression (McQuade et al., 2018), increase in s100 β -IR enteric glial cells (Robinson et al., 2016) which may underlie the mechanism of colonic dysmotility in mice (McQuade et al., 2016). Carbone et al., 2016 found that several chemotherapeutic agents, including a combination of Folinic acid, 5-FU, and Oxaliplatin, cause electrophysiological and morphological changes in colonic myenteric neurons. Irinotecan-induced gastrointestinal dysfunction is associated with enteric neuropathy and caused an increase in the sub-population of myenteric neurons (McQuade et al., 2017).

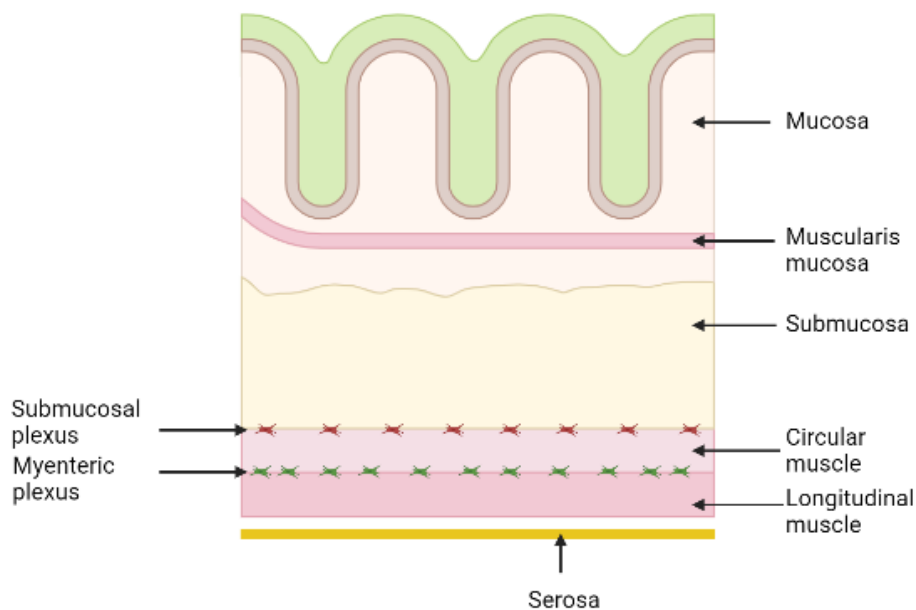


Figure 1.1 Institution of the enteric nervous system and affiliated muscle layers. The enteric nervous system is comprised of two major nerve plexuses, myenteric plexus and submucosal plexus located between the longitudinal and circular muscle layers.

The enteric nervous system (ENS) comprises two main layers namely the myenteric plexus and submucosal plexus. The myenteric (Auerbach's plexus) is found between the circular and longitudinal muscle of the muscular externa and it is responsible for providing motor innervation of the gut (Shahrestani and Das, 2021, Furnes, 2012). Submucosal plexus is located between the circular muscle and muscularis mucosa and it regulates the water and electrolyte balance, vascular tone, and secretion (Shahrestani and Das, 2021, Bornstein et al., 2012, Mourad et al., 2003, Furness et al., 2012). Moreover, these enteric neurons can be further categorised based on their biophysical properties, morphology, projections connectivity, and neurochemistry (Costa and Brooks, 2008). The enteric nervous system can generate its nerve impulses and encompasses the capacity to function on its own without interference with the central nervous system. Therefore, it refers to as the second brain of the body. ENS supplies the intrinsic nerve innervation of the gut via myenteric and submucosal plexus ganglia, primary inter-ganglionic fibre tracts, as well as secondary and tertiary fibres that extend from the gut to the various effector systems including glands, muscles, and blood vessels (Furness, 2012, Hansen, 2003). Predominately gastrointestinal functions are regulated and controlled by the enteric nervous system and damage to the enteric neurons causes gastrointestinal dysfunction (Furness, 2012).

1.4.1 The Myenteric Plexus

Myenteric ganglia can contain up to 5-200 neuronal cell bodies and their size and function can be different from one another depending on the types of neurons (Furness, 2014). The complex motor reflex pathways are primarily governed by three main classes of myenteric neurons. Primary afferent (intrinsic sensory) neurons represent about 30% of myenteric neurons and they respond to muscle tension and length, deformation in the mucosal layer, and responds to chemical stimuli in the intestinal lumen such as amino acids and fatty acids (Costa et al., 2008). The circular muscle layer of the GI tract is also supplied by ascending and descending interneurons as well as excitatory motor neurons and inhibitory motor

neurons, whereas the longitudinal muscle layer is supplied by a separate population of excitatory neurons and inhibitory motor neurons (Costa et al., 2008, Furness et al., 2004, Bornstein et al., 2002, Gwynne and Bornstein, 2007, Bornstein et al., 2006). Extrinsic nerve supply to the gut is mainly provided in an indirect way via providing nerve terminals mainly to the intrinsic ganglionated plexus rather than merging into the muscle layers of the gut except for the striated muscle of the oesophagus and in the sphincters (Furness, 2012). Hence, extrinsic innervation of the gut largely controls the activity of certain parts of the GI tract via modifying enteric neurons and maintaining homeostatic regulation as a common control between extrinsic control and intrinsic control (Bornstein et al., 2002).

1.4.2 The Submucosal Plexus

Submucosal plexus receives nerve supply from the myenteric plexus, sympathetic nervous system, and parasympathetic nervous system to stimulate the mucosal epithelium and the arterioles in the submucosal layers thus, regulating water and electrolyte balance, maintaining vascular tone, and control secretion (Furness et al., 2012, Mourad et al., 2003, Bornstein et al., 2012). The process of movement of fluid and substances between the blood and the intestinal lumen is a complex activity that requires the involvement of neural, endocrine, paracrine as well as autocrine systems (Bornstein et al., 2012). Nutrients in the food are absorbed with fluid from the lumen of the GI tract into the circulation via ion-coupled transporters and returned through secretomotor reflexes. These absorbed water and electrolytes from the lumen and the circulatory system (blood) are moved from the interstitial spaces of the lamina propria to the lumen. This important and complex action is controlled via the sympathetic secretomotor and vasodilator pathways (Furness, 2012) including multiple interacting levels of neural control in the secretion and absorption of water and electrolytes in the gut.

1.4.3 The Role of the Enteric Nervous System in Chemotherapy-Induced Gastrointestinal Dysfunction

The traditional view suggests that the chemotherapy-related GI side-effects are due to mucosal damage (Feyer et al., 2011). It is true to a point that the acute symptoms of anti-cancer drugs are due to mucosal damage whereas the chronic symptoms may be caused by damage to GI tract innervation (McQuade et al., 2016, McQuade et al., 2017). The damage to the specialised neuronal innervation to the GI tract, namely the enteric nervous system (ENS) seems to be the underlying cause of chronic, persistent gastrointestinal side-effects of chemotherapeutic drugs. ENS is responsible for nutrient absorption, secretion, GI sensation as well gastric motility (Spencer and Hu, 2020, Escalante et al., 2017, De Giorgio et al., 2004). Damage and death of ENS neurons due to chemotherapeutic drugs can lead to disorders of motility such as diarrhoea, constipation, and slow transit disorders (Escalante et al., 2017). Anti-tumour medications cause structural and functional changes to the ENS neurons (Carbone et al., 2016) that lead to persistent changes in the GI tract even after a considerable post-treatment time (McQuade et al., 2020, Escalante et al., 2017, McQuade et al., 2016). First-line anti-colorectal drugs caused the death of enteric neurons, axonal damage (McQuade et al., 2020, McQuade et al., 2017, McQuade et al., 2016, Wafai et al., 2013,) and changes in the electrophysiological properties in ENS neurons (Carbone et al., 2016). Evidence suggests that most of these changes occur due to oxidative stress of the neurons (Donald et al., 2017, McQuade et al., 2016). Neurons are structurally and functionally prone to produce larger amounts of free radicals due to their larger size, high level of metabolic activity, and lower capacity for antioxidant defense (Pachman, 2014). It was found that oxaliplatin-treated cells exhibited increased expression of both inducible Nitric Oxide Synthetase (iNOS) and neuronal Nitric Oxide Synthetase (nNOS) and elevated levels of O_2^- (Donald et al., 2017). Elevated level of O_2^- is related to mitochondrial membrane depolarization which results in the release of cytochrome c, and which leads to neuronal death (McQuade et al., 2016). Therefore, it is evident that oxidative stress plays a major role in enteric neuropathy and colonic dysmotility that are associated with anti-cancer chemotherapy drugs.

1.4.4 Chemotherapy-Induced Enteric Neuropathy and Gastrointestinal Dysfunction

Changes in the enteric neurons are found to give rise to several debilitating disorders such as Hirschsprung's disease, Chagas disease, achalasia, intestinal neural dysplasia, severe idiopathic slow transit constipation, and irritable bowel syndrome (Furness et al., 2012, De Giorgio et al., 2004a, De Giorgio and Camilleri, 2004, De Giorgio et al., 2000, Tornblom et al., 2002, Bassotti and Villanacci, 2006, Wingate et al., 2002, Chandrasekaran et al., 2011). The study conducted by Bassotti and Villanacci, 2011 has revealed that even the minor changes to the enteric neurons that are not evident in conventional histological examination contributed to the changes in colonic motor activity that led to constipation (Bassotti and Villanacci, 2011). Another study conducted on patients with slow transit disorders has found abnormalities in the inhibitory neurotransmitters, nitric oxide and vasoactive intestinal peptide, changes in the number of myenteric neurons as well as a reduction in the density of Interstitial Cells of Cajal indicating the importance of enteric neurons and neurotransmitters for the optimal function of the GI tract (He et al., 2000, Tzavella et al., 1996, Cortesini et al., 1995). Regardless the importance of the effects of chemotherapeutics on the ENS and GI function has long been overlooked.

Different chemotherapeutics cause different levels of neurotoxicity varying from moderate to highly toxic and yet, neuronal degeneration and enteric neuropathy are considered benchmark measurements in chemotherapy-induced gastrointestinal dysfunction (McQuade et al., 2016, Pini et al., 2016, Wafai et al., 2013, Vera et al., 2011). Several studies have revealed that repeated administration of chemotherapeutics causes enteric neuronal loss and that has a significant impact on the colonic motor activity and gastric transit (McQuade et al., 2020, McQuade et al., 2018, McQuade et al., 2016, Pini et al., 2016, Wafai et al., 2013, Vera et al., 2011). Several key studies conducted on cisplatin-induced GI side-effects have shown that *in vivo* administration of cisplatin significantly reduced the number of

myenteric neurons in the distal colon and gastric fundus followed by reduced upper gastrointestinal transit and abrogation of colonic contractile activity (Pini et al., 2016, Vera et al., 2011). In another study, the researchers have found that Oxaliplatin administration causes myenteric neuronal death in the distal colon that is related to decrease colonic contractile function (Wafai et al., 2013). In those studies, the researchers have also found that myenteric neuronal loss after Oxaliplatin and cisplatin administration is also correlated with changes in the number and the proportion of NOS-immunoreactive neurons (Pini et al., 2016, Wafai et al., 2013, Vera et al., 2011). The changes in the NOS-immunoreactive neurons have been identified in several other enteric neuropathies such as Hirschsprung's disease, Chagas disease, achalasia, ischemia/reperfusion injury, and diabetic gastroparesis (Rivera et al., 2011a). It is suggested that free radicals and nitric oxide (NO) cause damage to the enteric neurons and cause changes in the expression of NOS-immunoreactive neurons (Donald et al., 2017, Rivera et al., 2011a, Martinez-Ruiz et al., 2011). Chemotherapy-induced oxidative stress is closely linked to the generation of excessive production of NO (Donald et al., 2017). Recent studies have found that platinum accumulation in enteric neurons due to Oxaliplatin treatment causes direct toxicity to the neurons and this may have caused the 30% reduction in total neuronal number in both myenteric and submucosal neurons (Stojanovska et al., 2014, Stojanovska et al., 2016).

1.4.5 Oxidative Stress Associated with Enteric Neuropathy

Oxidative stress arises because of an imbalance between the production of Reactive Oxygen Species (ROS) and the capacity of antioxidant systems to remove them and restore the homeostatic balance without producing elevated amounts of free radicals (Valko et al., 2007). This results in redox imbalance in the cell that affects several other cellular functions including the mitochondrial function. Under closely regulated circumstances, Oxidative stress can modulate several cellular responses including mitochondrial fission which enables the cells to quality control by removing damaged mitochondria and cells by facilitating apoptosis to stop

spreading the damage to nearby cells and other mitochondria, and provide cellular protection (Zhou and Toan, 2020, Denzer et al., 2016, Zorov et al., 2005). Nevertheless, uncontrolled oxidative stress can result in severe consequences such as serious cellular damage, unrequired cell death that ultimately leads to complete organ failure, and death of an organism (Kim and Kim, 2018, Zorov et al., 2014, Zorov et al., 2012). Therefore, it is important to differentiate the adaptive redox response that occurs in physiological processes such as the removal of damaged mitochondria and cellular components from pathological oxidative stress that causes debilitating effects on the cell (Zorov et al., 2014). In a healthy cell, the net ROS production accounts for approximately 2% out of the total oxygen consumed by the mitochondria whereas in pathological cells that rate varies from 0.25 to 11% depending on the species of the animal as well as the different respiratory capacities (Zorov et al., 2014). Hydroxyl (OH^\cdot), nitric oxide (NO), and superoxide (O_2^\cdot) are the most common reactive oxygen species that contribute to oxidative stress. Hydrogen peroxide (H_2O_2) and peroxy nitrite (ONOO^-) are the other molecules that indirectly partake in producing free radicals via several chemical reactions and therefore they are considered an important component in oxidative stress pathways (Uttara et al., 2009).

Oxidative stress-associated neuronal damage is considered one of the main side-effects of several neuropathies including Charcot-Marie neuropathy, acrylamide-induced neuropathy, and diabetic neuropathy (Areti et al., 2014, Vincent et al., 2004, Chandrasekaran et al., 2011, Saifi et al., 2003). Furthermore, chemotherapy-induced peripheral nerve damage is also the main side effect of oxidative stress as well as subsequent mitochondrial damage that cause acute and chronic symptoms in patients (Shim et al., 2019, Ma et al., 2018, Zheng et al., 2011). Several research has identified that oxidative stress-induced neurodegeneration may be caused by biomolecular damage, neuroinflammation, ion channel activation, bioenergetic failure, microtubule disruption, depletion of antioxidant defenses, and or neuronal death via activation of apoptotic cascades (Donald et al., 2017, Areti et al., 2014, McDonald and Winderbank., 2002, Ta et al., 2013, Salvemini et al., 2011). Furthermore, recent research findings have identified a correlation between

oxidative stress-induced apoptosis and mitochondrial dysfunction, and mitochondrial DNA base excision repair imbalance indicating the importance of regulating ROS levels at homeostatic balance for the proper function of mitochondria as well as neuronal survival (Shou et al., 2017, Qi et al., 2017, Harrison et al., 2005).

1.4.5.1 Oxaliplatin-Induced Oxidative Stress and the Expression of Neuronal Nitric Oxide Synthase

Nitric Oxide (NO) is a widely spread neurotransmitter in both the central and peripheral nervous system and it is activated by the enzyme, nitric oxide synthase (NOS) (Subedi et al, 2021, Sheng and Zhu, 2018). Neuronal nitric oxide synthase (nNOS) is the common variety that is typically found in the nervous system (Subedi et al, 2021). NO produced by nNOS neurons in the ENS is predominantly responsible for vasodilation and gastrointestinal relaxation (Idrisaj et al., 2021, Fung et al., 2020, McQuade et al., 2016, Bornstein et al., 2004, Takahashi, 2003). In the enteric nervous system, nNOS is expressed by the descending interneurons and inhibitory motor neurons that supply to the intestinal smooth muscle (Bombardi et al., 2021, Lecci et al., 2002), and the main source of NO in the ENS is supplied by the nNOS neurons (Wafai et al., 2013., Qu et al., 2008). NO released by intestinal smooth muscle cells as well as nNOS neurons in the ENS is essential for a smooth gastrointestinal motor pattern control as it aids to relax the GI tract sphincters as well as generating GI tract motor innervations (Bombardi et al., 2021, Roberts et al., 2008, Roberts et al., 2007, Sarna et al., 1993). Therefore, altered levels of nNOS are indicative of GI tract dysfunction, and elevated nNOS can be indicative of oxidative stress that is related to several pathological conditions (Sampath et al., 2019, Rivera et al., 2011a). It was suggested that oxidative stress can hurt post-mitotic cells including enteric neurons and long-term exposure to oxidative stress and NO leads to neuronal damage and death of neurons (Chandrasekaran et al., 2011). Oxaliplatin exerts its anti-tumour efficacy by forming platinum-DNA adducts that cease the cell cycle and trigger apoptosis of dividing cells (Makovec, 2019,

Graham et al., 2000, Goodisman et al., 2006). Increased levels of nNOS expression had been linked to oxidative stress (Rivera et al., 2011a) which is the main side effect induced by Oxaliplatin. Persistent occurrence of oxidative stress in post-mitotic cells including enteric neurons can lead to neuronal loss and the disintegration of neuronal function mutilating gastrointestinal function (Knauf et al., 2020, Donald et al., 2017, Chandrasekharan et al., 2011). The mechanism of action that oxaliplatin is employing to immobilise cell division results in producing high levels of reactive oxygen species (ROS) and in cancer cells the buffering system that balances ROS in the cellular environment is being impaired leading to the accumulation of high levels of ROS thus diminishes the treatment effectiveness (Bukovski et al., 2020).

1.4.6 Chemotherapy-Associated Mitochondrial and Nuclear Damage

Chemotherapeutics such as Oxaliplatin and Irinotecan are well known for inducing oxidative stress directly and indirectly via a number of cellular pathways. Oxaliplatin induces oxidative stress directly due to the excessive production of ROS while Irinotecan causes Oxidative stress indirectly due to an inflammation-induced cascade. As a result of elevated oxidative stress, a significant amount of ROS is produced in the cell that greatly interferes with mitochondrial function (Angelova and Abramov, 2018, Yang et al., 2016). ROS-induced DNA damage can be varied from single and double-strand breaks to DNA base modifications (Yang et al., 2016). Therefore, it is important to repair the damages as quickly as possible to prevent mutations and maintain the genomic stability of cellular and organelle DNA including mitochondrial DNA (Hakem, 2008).

Damage to nuclear DNA can cause much more complex consequences since it is important for gene expression, survival, and mutations in the cell. The inability to repair or wrongly repaired DNA leads to genomic instability and mutations that are among the hallmarks of cancer (Hanahan and Weinberg, 2011).

The target of primary anticancer therapies, such as chemotherapy and ionising radiation, is to damage both nuclear and mitochondrial DNA driving the damaged cancer cell directly or indirectly, towards cell death (Huang et al., 2021). DNA damage response (DDR) is the mechanism that activates different repair mechanisms with the primary goal to restore DNA integrity (Jurcovicova et al., 2022). DDR plays a profound role not only in cancer development but also in cancer treatment. Defects in DDR genes are known to contribute to the cancer development and the cells with defective or deficient DDR exhibit a significant increase in the sensitivity to DNA-damaging agents (Barnieh et al., 2021) such as chemotherapy and radiotherapy. DNA methylation is a regular and stable epigenetic mechanism to regulate gene expression in cancer cells, DDR components also exhibit alterations in their gene promoter methylation status (Lahtz et al., 2011). MLH1 gene methylation has been used as diagnostic, prognostic, and therapy response biomarkers in various cancer types including colorectal, ovarian, and breast cancers as well as a therapy response biomarker associated with platinum compounds and temozolomide (Gao et al., 2016). Vogelstein and collaborators have identified more than 130 000 different genetic mutations contributing to tumorigenesis including both oncogenes and tumour suppressors that are involved in the regulation of cell survival, genome maintenance, and overall DDR (Vogelstein et al., 2013) and these genes serve as valuable targets for new approaches to cancer treatment.

Compared to nuclear DNA, mitochondrial DNA (mtDNA) is susceptible to oxidative damage partially due to its proximity to the source of endogenous ROS generation (Kowalska et al., 2020, Erol et al., 2017, Yakes and Van Houten, 1997). Another reason for this is mitochondrial DNA is lacking introns that lead to a high rate of transcription activity elevating the risk of oxidative modification of DNA bases in the coding region and culminating in faulty mutated DNA (Glowacki et al., 2013). ROS-induced lesions carry a high susceptibility to mutations in DNA and due to the extra sensitive nature of mitochondrial DNA for ROS-induced mutations, it is critical to repair those DNA damages for the integrity and the survival of mitochondria (Van Houten et al., 2018). Nucleotide excision repair pathway (NER) has been observed

as an essential component for the stability of the nuclear genome and mismatch repair (MMR) and base excision repair (BSR) pathways have been involved in regulating mitochondrial DNA activity (Van Hauten et al., 2018, Glowacki et al., 2013). Significantly high levels of accumulated oxidative stress cause more damage to mtDNA compared to nuclear DNA (nDNA) due to its proximity to the respiratory chain reaction, therefore, effective repair of ROS induced damage in mtDNA is crucial for the survival of the organelle as well as the sustainability of the cell (Kowalska et al., 2020, Yang et al., 2016, Todorov and Todorov, 2009). Furthermore, since mitochondria carry several genes associated with respiratory chain reaction components, defective mitochondrial DNA leads to the production of defective or malfunctioning proteins associated with the respiratory chain reaction that can further aggravate mitochondrial dysfunction by producing larger amounts of ROS, depleted production of ATP, and increased amounts of ROS-induced self-mutated faulty DNA. Mitochondrial DNA damage further exacerbates oxidative stress by decreasing the oxidative phosphorylation that results in depleted cellular ATP generation capacity as well as further increasing the intracellular ROS (Chiang et al., 2017, Glowacki et al., 2013). Increased ROS stimulates further oxidative DNA damage and synthesis of faulty or malfunctioning proteins that lead the cell into a vicious cycle of damaging consequences.

Due to mitochondrial stress and calcium overload, mitochondrial permeability transition pores (mPTP) open in the inner mitochondrial membrane leading to mitochondrial uncoupling and release of proapoptotic factors into the cytosol eventually leading to cell death (Halestrap., 2009). Brief opening of mPTO inevitably aids in maintaining healthy mitochondrial homeostasis, prolonged and sustained opening of mitochondrial permeability transition pores brings disastrous consequences to the cell (Zorov et al., 2014). Activation of mPTO's causes the changes in intra- and inter-mitochondrial oxidative status resulting in the lease of ROS from mitochondria. This physiological phenomenon of ROS production and ROS release is referred to as ROS-induced and ROS release (RIRR) cycle (Zorov et al., 2000). The opening mPTO's is also dependent on the reduction of nicotinamide adenine dinucleotide (NAD⁺) concentration in the cell (Di Lisa et al.,

2001). Even though RIRR plays a crucial physiological role in removing damaged mitochondria and cells, it may cause considerably harmful effects to the organism under pathological conditions by eliminating vital mitochondria and cells.

Several research conducted on animal models reported that chemotherapy-induced neuropathic symptoms were partially dependent on the mitochondrial dysfunction (Trecarichi and Flatters et al., 2019) and peripheral neuronal projections were prone to mitochondrial damage by exhibiting swollen, vacuolated mitochondria (Areti et al., 2014). Studies conducted in Oxaliplatin-treated rats have reported that Oxaliplatin treatment induced elevated oxidative stress, associated with a reduction in mitochondrial capacity in oxidative phosphorylation, resulting in decreased ATP production in nerves (Waseem et al., 2018, Yang et al., 2018, Zheng et al., 2011). Elevated ROS production is correlated with increased susceptibility of DNA strands lesions that stimulate the activation of nuclear poly (ADP-ribose) polymerase (PARP) enzyme (Bardos et al., 2003). When oxidative stress is accompanied by energy depletion, the activation of PARP can quickly convert into the process of activation cell death (Akbar et al., 2016, Du et al., 2003). An increase in NAD⁺ availability via PARP inhibition or NAD⁺ precursors has been associated with ameliorating mitochondrial function and improving mitochondrial oxidative metabolism (Lehmann et al., 2016, Felici et al., 2015, Pirinen et al., 2014, Bai et al., 2011).

1.4.7 Irinotecan-Induced Intestinal Mucositis and Oxidative Stress

Inflammation is considered one of the major causes of indirect toxicity and this is related to a significant amount of neuronal death due to chemotherapy treatment. Studies have demonstrated that 5-FU and IRI can cause long-term intestinal inflammation (McQaude et al., 2016, McQaude et al., 2017). Intestinal mucositis is another chemotherapy-related gastrointestinal side effect that causes adverse effects on patients' quality of life. Irinotecan is one of the chemotherapeutic agents

associated with this condition. Intestinal mucositis can be characterised by extensive damage to the gut mucosa leading to severe gastrointestinal side-effects such as nausea, vomiting, abdominal pain, diarrhoea, bleeding, infections, malnutrition, and bacterial sepsis (Sougiannis et al., 2021, Ribeiro et al., 2016, Vanhoecke et al., 2015). Chemotherapy-induced intestinal mucositis is a common condition. Approximately 40% of patients receiving standard-dose chemotherapy and 100% of patients receiving high dose chemotherapy reported suffering from mucositis while receiving treatment (Cinausero et al., 2017). Dose reductions and treatment delays are the common strategies for chemotherapy-induced intestinal mucositis, decreasing the chances of cancer remission and increasing the mortality rates due to cancer or due to the complications caused by intestinal damage (Ribeiro et al., 2016). Regardless of the debilitating side-effects caused by the Irinotecan treatment, it is still being used in the clinical setting as a leading cancer treatment medication due to its efficacy as an anti-cancer medication and the lack of novel therapeutic options viable in the clinical setting (Fujita et al., 2015). Irinotecan treatment also causes DNA strand breaks leading to direct cellular injury to the basal epithelial cells and cellular damage within the submucosal layer, eventually leading to the activation of apoptotic cascades (Mishra and Jha, 2019, Bowen et al., 2016). Inflammation of the mucosal membranes, elevated production of reactive oxygen species and reactive nitrogen species are directly or indirectly associated with inducing apoptosis (Mishra and Jha, 2019, Ribeiro et al., 2016, Arifa et al., 2014, Sonis, 2004). In a clinical setting, several measurements are being taken to reduce fluid loss and decrease the motility of hyperactivated intestines by administering pharmacological agents such as opioid agonists, increasing oral rehydration, and electrolyte replacement (Andreyev et al., 2014). However, the damage to the enteric nervous system plays an important role in chemotherapy-induced GI dysfunction. Therefore, it is a clinical necessity to find novel therapeutic approaches to target the enteric nervous system to ameliorate chemotherapy-induced GI dysfunction. Identification of potential targets and the discovery of novel therapies to address chemotherapy-induced toxicity has become a robust therapeutic urgency for the disease prognosis as well as to improve the quality of life of the patients.

1.5 Inhibition of APE1/Ref-1 Redox Signalling as a Novel Anti-cancer Treatment

Cancer is an augmentation of errors caused by numerous heterogeneous factors. So, it follows that the pragmatic method to terminate cancer should be to the hindrance of the initial error in cancer's progression or arrest a pathway by cancer to survive itself. The current research focuses on targeting regulatory pathways to block cancer progression because the first approach to kill the cancer has not been achieved therapeutically as hoped for. Since tumour cells accumulate many defects, it is more efficient to focus on a single target that affects multiple pathways to produce a greater therapeutic effect. One of the most promising proteins being studied in this regard is APE1/Ref-1 (Zabransky et al., 2022, Mijit et al., 2021, Chen et al., 2017). Apurinic/apyrimidinic endonuclease 1/ Reduction-oxidation factor-1 (APE1/Ref-1), is the recent therapeutic target that addresses both oxidative stress damage and DNA repair damage due to pathological condition of cancer (Mijit et al., 2021). APE1/Ref-1 functions as a dual functioning molecule containing a redox-active site and a DNA repair active site (Laev et al., 2017, Shah et al., 2017). The redox-active site of the protein mediates the DNA-binding activity of several transcription factors that regulate cellular antioxidant response, cell growth, cell cycle arrest, and inflammation (Shah et al., 2017). The DNA repair active site of APE1/Ref-1 is highly attuned to cell survival and preventing apoptosis (Shah et al., 2017). APE1/Ref-1 is a protein with endonuclease activity that regulates BER pathway minimising oxidative DNA damage. It plays a vital protective role in neurons from mitochondrial and nuclear DNA damage (Frossi et al., 2019). APE1/Ref-1 also functions as a reducing-oxidising (redox) factor that enhances the downstream regulation of oxidative stress by binding several transcription factors to DNA such as NF κ B that are directly related to the cellular stress response as well as neuronal survival (Kelley et al., 2014). Kelley et al., 2014 & 2016 have identified the therapeutic capacity of APE1/Ref-1 for the survival of nondividing post-mitotic cells after oxidative DNA damage. They have developed a novel small molecule compound, namely APX3330 that directly and specifically inhibits APE1/Ref-1 protein's reducing-oxidising pathway and enhances the activity of the BER pathway

to augment the DNA repair in neurons (Kelley et al., 2014 & 2016). When administered in combination with cisplatin, the above compound has shown high efficacy in preventing or reversing cisplatin-induced sensory neuropathy without interfering with the effectiveness of anti-cancer efficacy in the treatment (Shah et al., 2017). It has also exhibited its' effectiveness in tumour-killing properties (Kelley et al., 2014). Numerous studies have demonstrated APX3330's efficacy in inhibiting APE1/Ref-1's redox activity without affecting its' endonuclease activity in tumours and DNA damage repair in neurons (Miller et al., 2016).

1.5.1 APE1/Ref-1 Function in DNA Repair

APE1/Ref-1's endonuclease activity involves repairing DNA damage caused by oxidative stress, alkylating agents, and ionizing radiation via Base Excision Repair (BER). In this realm the damaged bases are removed by number of glycosylases and APE1/Ref-1 endonuclease function then nicks the DNA backbone forging hydroxyl (3'-OH) and 5' deoxyribose phosphate (5'dRp) group allowing the formation of strand of new nucleotides. APE1/Ref-1 is also involved with DNA damage repair caused by reactive oxygen species (Gampala et al., 2021, Silpa et al., 2021). If the damage is beyond repair, genetic instability drives the cells to programmed cell death by activating the apoptotic cascade (Sahakian et al., 2021, Curtis et al., 2021). APE1/Ref-1 interacts with several other DNA repair associated proteins such as DNA glycosylases (Tell et al., 2005), DNA polymerase β (Tell et al., 2005), DNA glycosylases Ogg 1 (Sardar et al., 2018) and flap endonuclease 1 (Sardar et al., 2018, Tell et al., 2005, Shin et al., 2015, Choi et al., 2016) in transcriptional regulation of gene expression (Gianluca et al., 2009). It also influences the DNA repair activities via redox modulation of several transcription factors. APE1/Ref-1 influence the sequence-specific DNA binding that ultimately controls gene expression (Zhang et al., 2018, Codrich et al., 2019). BER, homologous recombination (HR), direct repair (DR), mismatch repair (MMR), and global genome repair (GGR) cell signalling pathways are affected by the expression of p53, activator protein 1 (AP-1), and hypoxia-inducible factor-1 alpha (HIF1- α)

which are directly influenced by APE1/Ref-1 protein (Zhang et al., 2018, Codrich et al., 2019., Zhang et al, 2020, Barchiesi et al., 2020, Barchiesi et al., 2015, Liu et al., 2020, Chattopadhyay et al., 2006).

1.5.2 APE1/Ref-1 in Redox Regulation

As described above, APE1/Ref-1 functions as a dual functioning molecule that has a DNA repair active site and a redox-active site (Laev et al., 2017). This dual functioning capacity is unique to mammals and the redox-active function of signal transduction regulates eukaryotic gene expression (Laev et al., 2017). APE1/Ref-1 protein comprises two distant portions that molecularly and physically separate sites that can work independently without interfering with each other's functions (Li et al., 2008). The APE1/Ref-1 inhibitor, APX3330 has been in clinical trials for solid tumours. Even though the DNA repair function of the protein is well known for decades, the redox function plays an important role in cancer growth, survival, metastasis, and angiogenesis (Kelly et al., 2014). APE1/Ref-1 proteins' redox modulation varies from modulating the number of transcription factors involved in DNA repair, cellular stress responses, and other important cellular functions (Kleih et al., 2019, Cruz-Bermudez et al., 2019, Hu et al., 2019, Kelley et al., 2017, Stone et al., 2016, Dzagnidze et al., 2007, Ta et al., 2006). APE1/Ref-1 is the main regulator of both ubiquitous and tissue-specific transcription factors such as activator protein1 (AP-1), nuclear factor kappa B (NF-kB), early growth response protein 1 (EGR-1), p53, HIF1- α , cyclic AMP response-element binding protein (CREB), paired box protein 5 PAX-5, paired box protein 8 (PAX-8), thyroid transcription factor 1 (TTF-1), phosphatidylethanolamine-binding protein 2 (PEBP-2) (Hu et al., 2018, Stone et al., 2016, El Hadri et al., 2012, Lando et al., 2000, Tell et al., 2000, Ueno et al., 1999, Hirota et al., 1999, Akamatsu et al., 1997, Huang et al., 1993). Some of these transcription factors are directly involved with cancer growth, survival, metastasis, and angiogenesis. For instance, AP-1, NF-kB, PAX, HIF1- α , HLF, and p53 have a direct influence on cancer progression, and targeting APE1/Ref-1, stands a greater chance of effective therapeutic outcomes for the

disease progression (Bokhari and Sharma, 2019). NF- κ B, AP-1, signal transducer and activator of transcription 3 (STAT3), and HIF1- α are four main transcription factors that are under APE1/Ref-1's direct control (Luo et al., 2010, Fishel et al., 2007, Ray et al., 2009, Evans et al., 2000). They have been identified as main driving forces in pancreatic cancer progression, treatment resistance and metastatic potential (Oliveira et al., 2022, Mijit et al., 2021, Choi et al., 2020, Shin et al., 2009, Yang et al., 2009). Therefore, it is essential to target those transcription factors and inhibit their function via their origin to find a better outcome for tumour therapy. Targeting and inhibiting APE1/Ref-1 presents promising hopes based on several important transcription factors modulated under APE1/Ref-1 control.

1.5.3 Other APE1/Ref-1 Protein-Protein Interactions

The redox function of APE1/Ref-1 activates a number of transcription factors such as AP-1, p53, NF- κ B, STAT3, and HIF1- α (Lee et al., 2009, Jedinak et al., 2011, Nassour et al., 2016, Nath et al., 2017). Hence, it affects the gene expression that regulates several cellular processors including inflammatory responses (Su et al., 2011, Li et al., 2018). APE1/Ref-1 also controls several post-translational modifications, including nitrotyrosination, phosphorylation, and acetylation by modulating redox-independent transcriptional regulatory functions (Lopez et al., 2021, Sengupta et al., 2016, Tell et al., 2009). The functional prerogatives of those modifications are yet to be discovered. For instance, acetylation of APE1/Ref-1 protein may affect its intracellular localisation (Bhakat et al., 2009). Several studies reported additional functions of APE1/Ref-1 including regulation of endothelial NO production and vascular tone (Jeon et al., 2004), NK-cell-mediated cell killing via granzyme A (GzmA) (Martinvalet et al., 2005, Fan et al., 2003), concealing the activation of PARP1 while the repair of oxidative DNA damage (Peddi et al., 2006) and inhibition of oxidative stress through negatively controlling Rac 1/GTPase activity (Ozaki et al., 2002). Several other research findings report APE1/Ref-1 protein's retrogressive relationship with Bcl2 protein expression (Jin et al., 2006) and its inverse regulation of PTEN activator and the parathyroid hormone gene

(Bhakat et al., 2003, Kuninger et al., 2002, Chakravarti et al., 2001, Chung et al., 1996, Okazaki et al., 1994).

APE1/Ref-1's versatile functioning capacity also spreads into influencing tumour microenvironment via modulating vascular tone by regulating NO levels, maintaining cell differentiation, enabling the differentiation of angiogenic progenitor cells, preventing apoptosis by repressing pro-apoptotic molecules such as TNF- α as well as upregulating pro-survival NF-kB signalling (Kelley et al., 2021). Researchers have found that APE1/ Ref-1 has a direct effect on NF-kB expression in human pancreatic tumour cell lines (Li et al., 2018, Gampala et al., 2021, Oliveira et al., 2022). Furthermore, the crosslink between NF-kB and STAT3 enhances the downstream regulatory pathways to be affected, including genes that regulate tissue repair, cell cycle progression, and apoptosis (Gampala et al., 2021, Oliveira et al., 2022). APE1/Ref-1 protein's redox activation is required for NF-kB full activation and, therefore, inhibiting specific functions of APE1/Ref-1 protein may hold the capacity for hindering multiple downstream tumorigenic pathways (Lee et al., 2009, Gampala et al., 2021, Oliveira et al., 2022). Since APE1/Ref-1 protein regulates NF-kB, AP-1, STAT3, it directly influences the immune system by controlling the expression of cytokines and chemokines, including interleukin-6 (IL-6), interleukin-8 (IL-8) and tumour necrosis factor-alpha (TNF- α) (Oliveira et al., 2022).

Targeting APE-1/Ref-1's dual function via small molecular inhibitors for the therapeutic inhibition of NF-kB lacks specificity. Tumours usually express high metabolic demands due to the constant cellular activity and neovascularisation plays a critical role in this aspect to supply blood and other essential components to the newly forming tumour cells. Without a proper blood supply, the tumours cannot sustain, and therefore, migrating of endothelial cells in the tumour microenvironment is critical for neo-angiogenesis. Recent research demonstrates that APX3330 inhibits the growth of pancreatic cell lines (Zou et al., 2008), pancreatic cancer-associated endothelial (PCECs), and endothelial progenitor cells

facilitating angiogenesis (Oliveira et al., 2022, Mijit et al., 2021, Choi et al., 2020, Zou et al., 2009).

1.5.4 APE1/Ref-1 Angiogenesis

Angiogenesis falls under the APE1/Ref-1 redox regulation umbrella that is controlled by several transcription factors such as HIF1- α , NF- κ B, and AP-1 (Maulik et al., 2002). APX3330 and its analogues are known to exert anti-angiogenic properties that reduce tumour growth (Nyland et al., 2010, Kelley et al., 2011). Research conducted on *in vitro* murine retina has discovered that APE1/Ref-1 proteins redox activity is an important factor for retinal vascular endothelial cells (RVECs) for the proliferation and forming of tubules (Luo et al., 2010). Research has also found that APE1/Ref-1 protein is highly expressed in murine retinas, RVECs, retinal progenitor cells (RPCs), and choroid/retinal pigment epithelium (RPE) (Luo et al., 2010). These findings suggest the importance of APE1/Ref-1 protein's redox activity for the development of retinal endothelial cell proliferation, migration, and new tubular formation (Luo et al., 2010). It has been demonstrated that a single intravitreal injection of APX3330 impedes the subretinal neovascularization in *vldlr*^{-/-} knockout mice strongly suggesting the involvement of APE1/Ref-1 in retinal neovascularization (Jiang et al., 2009, Hu et al., 2008). APE1/Ref-1 protein's redox inhibitor APX3330 and some of its recently developed analogues (Kelley et al., 2011, Nyland et al., 2010) have demonstrated therapeutic potential for age-related muscular degeneration (AMD). Regardless of its expensiveness and indefinite treatment time, anti-VEGF treatments are being used in the clinical setting as the standard care for wet AMD, it does not improve the patient's vision with the treatment. Therefore, APX3330 could be used as a part of AMD treatment-refractory to anti-VEGF agents. Recent research has been focussing on the efficacy of combining APX3330 with anti-VEGF agents for the treatment of such diseases (Jiang et al., 2011). Studies conducted in normal endothelial cells have demonstrated that APE1/Ref-1 proteins' involvement in multiple cellular pathways that associated with modulating vascular tone by

regulating NO levels (Zou et al., 2009), maintaining cell differentiation, preventing apoptosis by inhibiting pro-apoptotic TNF α signalling pathway and upregulating pro-survival NF- κ B signalling pathway and enabling the differentiation of angiogenic progenitor cells. Considering the research findings of *in vitro* studies and preclinical data of APE1/Ref-1 inhibition, highly suggestive of the influence of APE1/Ref-1 protein in the tumour microenvironment and the potential clinical utility of APX3330. The survival of tumours is mainly dependent on the ready access to a blood supply. Therefore, the migration of endothelial progenitor cells to the tumour microenvironment is essential for the formation of new blood vessels that supply blood to developing tumours. APX3330 inhibits the growth of pancreatic cancer cell lines (Zou et al., 2008), endothelial progenitor cells as well as pancreatic cancer-associated endothelial cells (Zou et al., 2009). Additional studies conducted on the effects of APX3330 on human bone marrow cells, and human umbilical vein endothelial cells demonstrated that APX3330 can impede tumour endothelial VEGF production, reduce the expression of the cognate receptor Flk-1/KDR on pancreatic cancer-associated endothelial cells, hindering a conceivably important angiogenic ligand-receptor interaction in the tumour microenvironment (Zou et al., 2009).

AP-1, NF- κ B, HIF-1 α , p53, HLF, and PAX are some of the main transcription factors involved in tumour promotion and progression (Luo et al., 2010, Ray et al., 2009, Fishel et al., 2007, Evans et al., 2000). NF- κ B, AP-1, HIF-1 α , and STAT3 are four main proteins that come under APE1/Ref-1 redox regulation and a major role in cancer progression, resistance to therapy, and metastatic potential (Ray et al., 2009, Fishel et al., 2007). These transcription factors not only regulate the cellular signalling activity but also influence the tumour microenvironment (Vinita et al., 2009). These transcription factors upregulate downstream activation of several other transcription factors that are further closely linked to cancer cell growth and metastasis (Xie et al., 2006). HIF-1 is one of the major transcription factors that is regulated by APE1/Ref-1 protein, which responds to low oxygen conditions in the intracellular environment (Bristow et al., 2008, Cannito et al., 2008). HIF-1 is a heterodimeric transcription factor that comprises two protein subunits namely, HIF-1 α and HIF-1 β . HIF-1 α is typically overexpressed in cancer and it usually resides in

the cytosol of the cell (Huang et al., 1996). HIF-1 β on the other hand usually resides in the nucleus and usually remains in a dormant state until the HIF-1 α subunit binds and activates it (Huang et al., 1996). Cellular hypoxic conditions cause HIF-1 α subunits to translocate into the nucleus and bind to HIF1- β to produce heterodimeric HIF-1, which further activates its downstream transcription factors such as vascular endothelial growth factor (VEGF) (Forsythe et al 1996, Jiang et al., 1996). VEGF is a major transcription factor that stimulates and enhances the growth of new blood vessels into newly forming tumours (Emami et al., 2021, Pezzuto and Carico, 2018). Therefore, it is imperative to recognise major transcription factors that aid in cancer progression and survival, and it is also important to block or inhibit their function for better cancer treatment and decreased treatment resistance. Therefore, APE1/Ref-1 proves to have a great potential as a therapeutic target to control tumour growth.

1.5.5 APE1/Ref-1 and Its Involvement in Inflammation

Inflammation is an important biological process that is stimulated by various invading pathogens and or endogenous stimuli that aid the immune system in the tissue healing process (Yamabe et al., 1998). Several diseases such as diabetes, cardiovascular disease, osteoarthritis, bowel diseases, and cancers cause chronic inflammation that disrupts the cellular homeostasis of tissue healing and leads to diseases (Grombacher et al., 1998). Long-standing Inflammation is also another risk factor for tumour genesis especially in conditions like ulcerative colitis due to chromosomal instabilities (Guo et al., 2008). The risk factor of developing colorectal cancer increases by 20 to 30-fold with the re-occurrence of the disease for more than 10 years. Intracellular APE1/Ref-1 was found to be higher with Inflammation caused by ROS and other toxic agents (Luo et al., 2010, Tell et al., 2009, Evans et al., 2000). Prolonged cytosolic stress can lead to increased expression of APE1/Ref-1 and the possibility of creating genomic errors also increases. APE1/Ref-1's endonuclease activity can repair damaged DNA via the BER pathway. Yet, prolonged cellular stress increases the chances of accumulating errors in the cell that lead to microsatellite instability in cells (Bapat et al., 2009).

1.5.6 APE1/Ref-1 Function in Tumour Cell Metabolism

Cancer cells are well known for their capacity of adapting to meet their ever-changing biogenetic needs by adapting and reprogramming cellular metabolic pathways. Since tumour cells own unrestricted proliferative capacity, the tumour cells must rely on accumulating secondary fuel sources such as mitochondrial metabolites, fumarate, succinate, and α -ketoglutarate to meet their high energy demands (Porporato et al., 2018). Recent research has found that certain malignant cancers shift their primary energy source from glycolysis to oxidative phosphorylation to meet their constant energy demands (Alameddine et al., 2018). Mitochondrial metabolic plasticity may play a significant role in this bidirectional shift that, consequently, questions the reliability of the Warburg effect that is responsible for all tumour survival and growth. Recent research has found that APE1/Ref-1 can regulate mitochondrial metabolism in addition to its function in redox regulation and endonuclease activity (Codrich et al., 2019). Inhibiting APE1/Ref-1's endonuclease activity seriously impedes mitochondrial respiration (Codrich et al., 2019), and therefore, it is possible to control the metabolic activity of pathological tumour cells. APE1/Ref-1 has been found to translocate into the mitochondria (Barchiesi et al., 2015) through the mitochondrial space import and assembly protein 40 (Barchiesi et al., 2015) when methylated at Arginine 301 (Zhang et al., 2020). It is responsible for maintaining mitochondrial respiration (Barchiesi et al., 2020) as well as maintaining mitochondrial DNS integrity, especially under increased cellular ROS environment (Barchiesi et al., 2020). Recent findings report that mitochondrial APE1/Ref-1 decreases the ROS generation in certain cancer cells and thereby increases Cisplatin resistance (Liu et al., 2020). Truncated and full-length APE1/Ref-1 in mitochondria can repair damaged mitochondrial DNA due to endogenous ROS which is a constant threat to mitochondrial DNA integrity (Li et al., 2008, Chattopadhyay et al., 2006, Tell et al., 2001). Researchers have found that APE1/Ref-1 knockdown cancer cells expressing high levels of HIF1- α have shown to downregulate the glycolysis, TCA cycle (tricarboxylic acid cycle), and oxidative phosphorylation (Gampala et al., 2021), indicating the importance of APE1/Ref-1's endonuclease function within the mitochondria. Furthermore, recent research has

found that APE1/Ref-1's redox function also plays a significant role in mitochondrial metabolism (Silpa et al., 2021). APE1/Ref-1's capacity in orchestrating to provide energy through mitochondrial metabolism for cancer growth and metastasis has significant importance to investigate for finding successful cancer therapy.

1.5.7 Modulating APE1/Ref-1 Function in the Cancer Treatment Milieu

Altered or elevated expression of APE1/Ref-1 has been observed in numerous cancers such as breast cancer, ovarian cancer, gliomas, sarcomas, and multiple myelomas (Langie et al., 2007, Madhusudan et al., 2005, Koshiji et al., 2005, Hanson et al., 2005, Chen et al., 1994, Hainaut et al., 1993) that shed the lights into APE1/Ref-1's association with aggressive tumour proliferation, evaluated levels of neovascularisation, elevated therapeutic resistance, incomplete therapeutic response, poor prognosis, and poor survival rates (Wang et al., 2004, Koukourakis et al., 2001, Bobola et al., 2001, Evans et al., 2000, Moore et al., 2000, Kakolyris et al., 1998, Xu et al., 1997). Increased expression of APE1/Ref-1 is associated with increased chemoresistance (Yang et al., 2007), and developing novel compounds that can modulate APE1/Ref-1 could hold the missing piece for definitive and effective cancer treatment. Anti-tumour efficacy of APE1/Ref-1 by inhibiting redox activation holds a high value because of the number of transcription factors that are governed by this single protein that can control cancer growth, metastasis, survival, and angiogenesis (Fishel et al., 2008, Fishel et al., 2007, Wang et al., 2004., Lau et al., 2004., Ono et al., 1994).

1.5.8 APE1/Ref-1 Function in Chemotherapy-Induced Peripheral Neuropathy

APE1/Ref-1 function in chemotherapy-induced peripheral neuropathy (CIPN) is a chemotherapy-related serious side-effect that can lead to dose reduction and thereby the efficacy of the treatment (Kelley et al., 2016a, Kelley et al., 2016b).

Patients usually experience numbness and tingling sensations increased sensitiveness to touch and cold decreased tendon reflexes and loss of proprioception, especially in the hands and feet due to the damage to peripheral sensory neurons (Gupta and Bhaskar, 2016). A larger portion of patients experience tabbing, burning, and electrical sensations (Seretny et al., 2014) due to chemotherapy, and the treatments are limited by a lack of preventative or therapeutic options (Hu et al., 2019, Stone et al., 2016, Hershman et al., 2014). Several research supports the hypothesis that DNA damage due to platinum-based drugs is a major contributing factor to CIPN. In addition to forming platinum-DNA adducts that cause neural toxicity (Dzagnideze et al., 2007, Ta et al., 2006), platinum-based chemotherapeutics are also correlated with increased formation of ROS that contributes to oxidative DNA damage and neurotoxicity (Xue et al., 2020, Cruz-Bermudez et al., 2019, Shah et al., 2017, Kelley et al., 2017, Kleith et al., 2017, Preston et al., 2009, Siomek et al., 2006). It is critical to maintaining neuronal homeostasis by regulating the damage repair of both endogenous and exogenous DNA damage (Hetman et al., 2010, Fishel et al., 2007, McMurray, 2005, Brooks, 2002). Neurons contain two major DNA damage repair pathways, namely nucleotide excision repair pathway (NER) and Base Excision Repair Pathway (BER) to fix and regulate the homeostatic balance in the cellular environment. NER pathway is mainly regulated to remove relatively large DNA damages such as platinum-DNA adducts that are generated by chemotherapeutics, Oxaliplatin and Cisplatin. BER pathway mainly predominates in removing smaller size DNA mishaps such as oxidation and alkylation within mitochondrial and nuclear DNA (Rolfe and Brown, 1997). BER pathway is more important in the neurons because of the high metabolic nature of the cells (Rolfe and Brown, 1997) results in the steady production of ROS followed by subsequent oxidative DNA damage (Fortini et al., 2010, Barzilai et al., 2008, Fishel et al., 2007). APE1/Ref-1 protein plays an important role in the BER pathway by hydrolysing the phosphodiester backbone of the DNA strand to an apurinic/apyrimidinic site that generates a normal hydroxyl group and an abasic deoxyribose phosphate molecule that can be further processed by a chain of enzymes in the BER pathway. The importance of the endonuclease activity of APE1/Ref-1 in neurons is crucial due to the risk of accumulation of DNA damage that could lead to neuronal death whereas enhancing

APE1/Ref-1 repair activity could mitigate the damage (Fehrenbacher et al., 2017, Kelley et al., 2017, Fishel et al., 2007, Tell et al., 2001). It is important to investigate the efficacy of small molecule compounds such as APX3330 in enhancing APE1/Ref-1's endonuclease capacity to mitigate the neurotoxic effects of chemotherapeutics without arbitrating its anti-tumour properties to prevent or reverse the debilitating side effects of chemotherapy.

1.5.9 Therapeutic Potential of APX3330 as a Cancer Treatment

Recent references have been added to the section. APX3330 ([[(2E)-3-[5-(2,3dimethoxy-6-methyl-1,4-benzoquinoly)]-2-nonyl-2 propanoic acid]]) is a quinone compound that has been originally developed by Eisai (E3330) as an NF- κ B/TNF- α inhibitor for the treatment of inflammatory liver disease and has been studied for its therapeutic potential to inhibit APE1/Ref-1 proteins' redox function (Mijit et al., 2023, Li et al., 2021, Caston et al., 2020, Luo et al., 2008). The direct and selective interaction of APX3330 with APE1/Ref-1's redox function was demonstrated by mass spectrometry, chemical footprinting, and other biochemical data (Li et al., 2021, McIlwain et al., 2018). Inhibition of APE1/Ref-1's redox-signalling and transcription factor activation to regulate oxidative stress response, inflammation, cell cycle and angiogenesis have been demonstrated in patients with neovascular eye disease (Hartman et al., 2021).

Several studies have demonstrated that APX3330 can selectively block APE1/Ref-1's redox activity and, therefore, it blocks APE1/Ref-1's capacity in converting a variety of transcription factors from oxidised to reduced state, preventing specific genes from being "switched on" (Hartman et al., 2021, Caston et al., 2020, Nyland et al., 2010, Luo et al., 2008). Although the possibility of modulating multiple regulatory pathways, redox inhibition of APE1/Ref-1 via APX3330 has not shown any unacceptable toxicity in both animal and human studies (Mijit et al., 2023, Salat, 2020, Kelley et al., 2016). APX3330 has

demonstrated its specificity in inhibiting APE1/Ref-1 proteins' redox regulation, making it a novel therapeutic approach in cancer treatment (Kelley et al., 2016, Curtis et al., 2009, Zou et al., 2009, Zou et al., 2008, Shimizu et al., 2000).

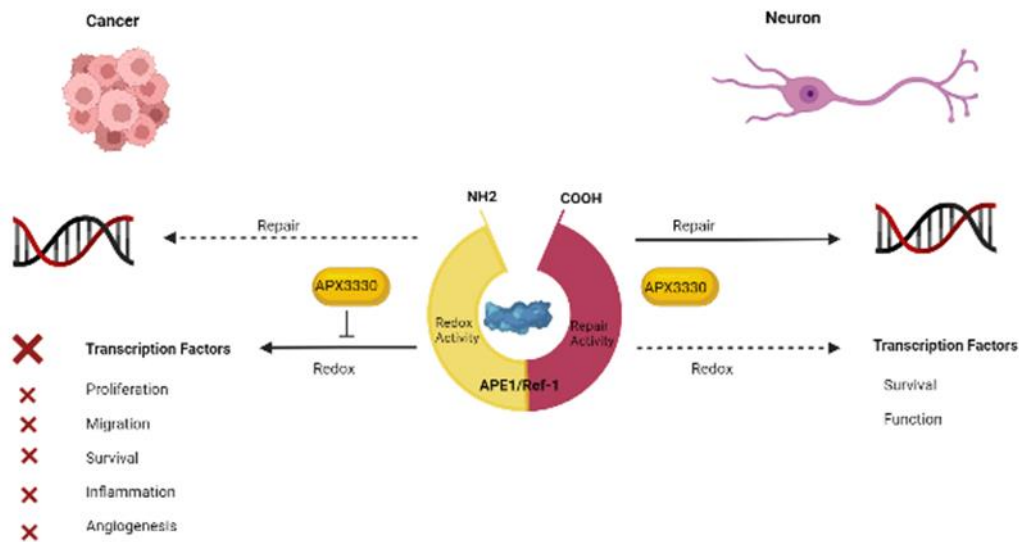


Figure 1.2 Role of APE1/Ref-1 in cancer cells vs neurons. APX3330 selectively inhibiting the redox active site of APE1/Ref-1 protein. In cancer cells, inhibiting redox active site of APE1/Ref-1 by APX3330, prevents the activation of number of transcription factors such as NFkB, AP-1, STAT3, pSTAT3 and HIF1- α that control cell differentiation, proliferation, apoptosis, metastasis, angiogenesis, inflammation and invasion. In neurons, APE1/Ref-1 promotes cell function and survival.

Fehrenbacher and collaborators (2017) found that anti-cancer drugs and ionising radiation causes increased expression of reactive oxygen (ROS) and nitrogen (RNS) species and elevated DNA damage, leading to altered neuronal sensitivity. They have also found that either genetically enhancing the expression of APE1/Ref-1 to increase the DNA repair function or treatment with a small-

molecule modulator such as APX3330 to stimulate APE1/Ref-1's DNA repair activity, results in increased DNA repair and decreased damage in sensory neurons leading to alteration in neuronal function (Fehrenbacher et al., 2017).

1.5.10 APX3330 Clinical Progress as a Cancer Treatment

Emerging evidence suggests that the use of APE1/Ref-1 redox inhibitors has successfully blocked the APE1/Ref-1's redox function and therefore it has impeded the DNA binding of several important transcription factors that aid cancer survival, progression, and metastasis (Luo et al., 2010, Luo et al., 2008, Zou et al., 2009, Zou et al., 2008). Considering its multifunction regulatory capacity, targeting APE1/Ref-1 protein provides an effective approach to modifying and controlling numerous cancer cell survival pathways. Recent developments in this arena include xenograft models and the development of more effective and selective APE1/Ref-1 redox inhibitors to directly and specifically target gene or protein expression. Furthermore, currently APX3330 and its analogues are being used in the clinical setting to establish a standard compound with the highest clinical therapeutic potential. Oral APX3330 has successfully completed Phase I trials as an orally administered chemotherapeutic for the treatment of cancer as well as chemotherapy-induced peripheral neuropathy (Shahda et al., 2019). In patients with solid tumours, APX3330 demonstrated a favourable safety and tolerability profile with up to 600mg over multiple months (Boyer et al., 2022, Hartman et al., 2021). APX3330 has also progressed to Phase IIb clinical trials for the treatment of retinal diseases, diabetic retinopathy (DR) and diabetic macular edema (DME) (Boyer et al., 2022, Hartman et al., 2021). The most common oral APX3330 treatment-related adverse side effects were mild diarrhoea or soft stool reported by 4% of patients treated with APX3330 and 2% with placebo (Boyer et al., 2022). Regardless of the promising results of APX3330 in redox inhibition of APE1/Ref-1 protein, still, several challenges must be overcome to reap the maximum therapeutic potential of the drug. Among the number of newly developing APX3330 analogues, the most effective successor at specifically targeting APE1/Ref-1 redox function as well as

the sub-micromolar concentrations with high selectivity, is yet to be identified. The studies up to date have demonstrated the therapeutic potential of redox-specific APE1/Ref-1 inhibitor APX3330 for the treatment of retinal diseases, AMD and several cancers and there may be other regulatory pathways that involve APE1/Ref-1, which hold the potential for providing novel therapeutic avenues for several other diseases.

1.6 Summary

Colorectal Cancer (CRC) is considered one of the most aggressive cancers and causes the third most common cancer-related death in Australia. According to recent statistics, 15,540 Australians are told they have bowel cancer annually with a fatality toll of 5,295 Australians annually. Age, gender, and race/ethnicity are the most common epidemiological factors associated with colorectal cancer (Haggard and Boushey, 2009, Amersi et al., 2005) and five-year survival expectancy is less than 10 percent (Bowel Cancer Australia, 2020). Weight loss, altered bowel habits, rectal bleeding, unexplained extreme tiredness, lump or swelling in the abdomen, and abdominal pain commonly occur in the later stages of the disease progression (Adelstein et al., 2011, Cappell, 2005). Surgical resection is the most common treatment approach for the early stages of colorectal cancer, including stage I and stage II. Chemotherapy is the standard first-line treatment for stages III and IV or metastatic cancer. It is given as a combination of two or more chemotherapeutic drugs with other medications by itself or with radiation (Johnston et al., 2012, Chibaudel et al., 2012). Oxaliplatin, Irinotecan, and 5-fluorouracil are the most common chemotherapy medications that are used in the clinical setting for CRC treatment (Wang and Li, 2012, Sharif et al., 2008, Marschner et al., 2015).

Oxaliplatin ($C_8H_{14}N_2O_4Pt$) is a third-generation platinum-based chemotherapeutic medication used in clinical settings for stage III and metastatic CRC as a single agent or frequently as a combination therapy with 5-FU (Carlsen

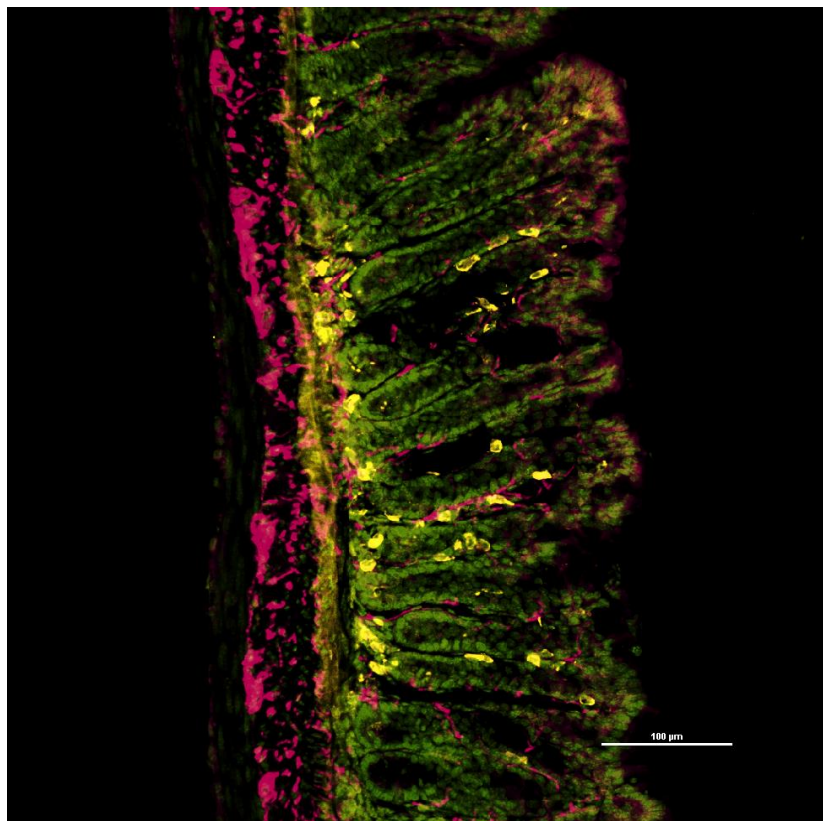
et al., 2021, Gu et al., 2019, Stintzing, 2014). Patients have reported Oxaliplatin-related side-effects including gastrointestinal toxicity, peripheral sensory neuropathy, and hematologic toxicity (Branca et al., 2021, Drott et al., 2019, McQuade et al., 2016, Cassidy and Misset, 2002). Irinotecan ($C_{33}H_{38}N_4O_6$) exerts its anti-tumour efficacy by inhibiting DNA topoisomerase (Mastrangelo et al., 2022, Dickens and Ahmed, 2018). Its active metabolite, SN-38, induces irreversible DNA damage to tumour cells and causes cell death (Lee et al., 2019, Shin et al., 2016). Regardless of the success rate of reducing the disease progression and increasing the survival rate, these medications cause acute and chronic toxicities that lead to immediate and long-term adverse effects (Axelrad et al., 2017, McQuade et al., 2016, Keefe et al., 2014). Eighty to ninety percent of the patients have experienced diarrhoea, constipation, nausea, vomiting, and oral mucositis as side-effects of standard first-line chemotherapeutic drugs that are in the clinical setting (McQuade et al., 2016b, McQuade et al., 2016a, Keefe et al., 2014, Andreyev et al., 2014). These side-effects cause severe dehydration and malnutrition, resulting in significant weight loss and a weakened immune system (Bossi et al., 2021, Nishikawa et al., 2021, Andreyev et al., 2014, Aprile et al., 2015). It is common to experience intestinal inflammation, bowel wall thickening, ulceration in the bowel wall, and bowel perforation because of chemotherapy (Reginelli et al., 2021, Gray et al., 2016, Lecarpentier et al., 2010).

Due to the adverse gastrointestinal side-effects associated with Oxaliplatin and Irinotecan, the dose of the chemotherapeutics is being reduced, limiting the efficacy of the treatment (McQuade et al., 2016, Arbuckle et al., 2000). Diarrhoea and constipation are the most common gastrointestinal side-effects of chemotherapeutic drugs (Moschen et al., 2022, Anthony and Chauhan, 2018). These side-effects cause a considerable negative impact on the quality of life of the patients and the carers. The drugs that are targeted the gastrointestinal side-effects of chemotherapeutic drugs have their side-effects, and therefore, the efficacy of the treatment is being compromised (Kroschinsky et al., 2017, Banerjee et al., 2017, Kwon, 2016, Feyer et al., 2011). Hence, novel treatments and therapeutic targets are crucial for later-stage aggressive cancers such as colorectal cancer. One of the

most promising proteins being studied in this regard is APE1/Ref-1 (Zabransky et al., 2022, Mijit et al., 2021, Chen et al., 2017). APE1/Ref-1 is the recent therapeutic target that addresses both oxidative stress damage and DNA repair damage due to pathological condition of cancer (Mijit et al., 2021). APE1/Ref-1 is a dual-functioning molecule containing a redox-active site and a DNA repair active site (Laev et al., 2017, Shah et al., 2017). The redox-active site of APE1/Ref-1 protein is mainly responsible for DNA repair, inflammatory responses, and angiogenesis and plays a critical role in the tumour microenvironment. Recent data demonstrate APE1/Ref-1s involvement in tumour survival and proliferation as well as altered APE1/Ref-1 protein expression level at the protein or subcellular localisation level in numerous cancers (Puglisi et al., 2002, Koukourakis et al., 2001, Bobola et al., 2001, Puglisi et al., 2001, Robertson et al., 2001, Thomson et al., 2001, Kakolyris et al., 1998). Its significant influence on several important cancer signalling pathways (Luo et al., 2010, Luo et al., 2008, Xie et al., 2006) provides abundant evidence further supporting the therapeutic potential of APX3330 in modulating APE1/Ref-1's redox function as a novel therapeutic approach for cancer treatment. Recent research findings propose the capacity of selectively inhibiting APE1/Ref-1's redox function via chemically knocking down or blocking APE1/Ref-1's redox function may provide great potential for successfully inhibiting tumour growth, modification of tumour microenvironment such as inflammation, that negatively influences tumour survival, growth, and metastasis. Therefore, inhibition of the redox function of APE1/Ref-1 protein via APX3330 underscores its importance as a prime candidate for the treatment of cancer. Recent studies demonstrated that APX3330 exerts anti-inflammatory, neuroprotective, and tumour suppressive effects in DRG neurons (Fehrenbacher et al., 2017, Kelley and Fehrenbacher, 2017). The study presented in chapter 2 aimed to investigate the neuroprotective, anti-inflammatory anti-tumour efficacy of APX3330 against Irinotecan-induced damage to the myenteric neurons and to investigate the molecular mechanisms of APX3330 that modulate its neuroprotective and anti-tumour properties. Chapter 3 is mainly focused on investigation of the neuroprotective and anti-tumour efficacy of APX3330 against Oxaliplatin-induced damage to the myenteric neurons and investigating the molecular mechanisms of APX3330 that modulate its neuroprotective and anti-tumour properties.

2

INVESTIGATING THE NEUROPROTECTIVE AND ANTI-CANCER EFFICACY OF APX3330 IN COMBINATION WITH IRINOTECAN IN THE MURINE MODEL OF CRC



Cross-sectional preparation of the distal colon of APX3330+VEH-treated mouse with CRC labelled with a pan-leukocyte marker anti-CD45 antibody (yellow), neuronal marker anti- β Tubulin III antibody (magenta) and DAPI (green) (Scale bar = 100 μ m)

2.1 Summary

Chemotherapy-induced gastrointestinal (GI) dysfunction is a common side-effect that ultimately leads to treatment delays, dose reductions and, in severe cases, cessation of the treatment (Verstappen et al., 2003, McQuade et al., 2014, Kciuk et al., 2020, Smith et al., 2020, O'Reilly et al., 2020, Okunaka et al., 2021). The GI side effects of chemotherapy could last up to 10 years post-treatment (Di Fiore et al., 2009, Denlinger and Barsevick, 2009, Hino et al., 2022, Lu et al., 2022). Irinotecan is a common chemotherapeutic agent that is used for colorectal cancer (CRC) treatment. In the clinical setting, Irinotecan is commonly used with either 5-fluorouracil or leucovorin as a combination therapy (Cunningham et al., 1998, Khattab et al., 2019, Sun et al., 2020). Irinotecan (IRI) exerts its tumour killing properties by preventing religation of the DNA strand via inhibiting the binding of topoisomerase 1-DNA complex that halts the movement of the replication fork causing lethal double-strand breaks that lead to halting the cell cycle (Ma et al., 2000, Grivicich et al., 2001, Pommier et al., 2003, Wong et al., 2019, Kolb et al., 2020, Elbeddini et al., 2020, Gunasegaran et al., 2020, Carlsen et al., 2021, Parvez et al., 2021, Boeing et al., 2021). The common side-effects associated with Irinotecan treatment are nausea, vomiting, diarrhoea, dyspnoea, constipation, neutropenia, and cholinergic syndrome (Cunningham et al., 1998, Rougier et al., 1998, McQuade et al., 2016, Krishnamurthi and Macaron, 2019, Fumet et al., 2021). However, the main Irinotecan-associated GI side-effect that contributes to dose-limiting factors is acute and delayed onset diarrhoea (Rougier et al., 1998, Cole et al., 2020, Parvez et al., 2021, Vitiello et al., 2021, Wainberg et al., 2021). Acute diarrhoea occurs within the first 24 hours post-Irinotecan administration and usually, 60-80% of patients experience the symptoms that have a considerable impact on their general wellbeing (Gibson and Keefe, 2006, Mego et al., 2014, Campbell et al., 2017, Okunaka et al., 2021, Wong et al., 2021). Approximately 80% of patients experience delayed onset of diarrhoea and it usually occurs 24-48 hours following treatment (Saliba et al., 1998, Hamano et al., 2019, Boeing et al., 2021). It is believed that acute symptoms of chemotherapy-related GI side effects are due to mucosal damage, whereas long-term gastrointestinal side-effects may be caused

by the damage to the enteric nervous system. Previous studies have demonstrated that Irinotecan treatment induces the loss of myenteric neurons, luminal accumulation, and reactivation of SN-38 that leads to continuous aggravation to intestinal microflora, sustained mucosal damage, damage to the intrinsic nervous system of the GI tract and the enteric nervous system where inflammation serves as a main driving force for the instigation of the array of adverse side-effects (McQuade et al., 2017). Recent studies demonstrated that APX3330 exerts anti-inflammatory, neuroprotective, and tumour suppressive effects in DRG neurons (Kelley and Fehrenbacher, 2017). The focus of this study is to investigate the neuroprotective, anti-inflammatory anti-tumour efficacy of APX3330 against Irinotecan-induced damage to the myenteric neurons of the enteric nervous system and to investigate the molecular mechanisms of APX3330 that modulate its neuroprotective and anti-tumour properties. For the study we used 9 weeks old male *Balb/c* mice. Mice were randomly subjected for CRC induction surgeries by injecting 1×10^6 CT-26 cells into the caecum, under sterile conditions. Treatments started on day 6 post-surgery. Mice were divided into the following treatment groups: mice received two vehicles (1), Irinotecan plus vehicle for APX3330 (2), APX3330 plus vehicle for Irinotecan (3) and combination of Irinotecan plus APX3330 (4). A separate cohort of mice that was not subjected to CRC-induction surgeries were randomly divided into three groups: untreated (5), Irinotecan-treated (6) and APX3330-treated (7). Mice were given vehicles (vehicle for Irinotecan, vehicle for APX3330), Irinotecan (30 mg/kg/ x 3 /week), APX3330 (25 mg/kg/ x2/daily) and their combination for two weeks. Morphometric analysis of tumours and tumour metastasis, faecal water content, faecal neutrophil gelatinase-associated protein - lipocalin II (LCN-2), immunohistochemical analysis of myenteric neurons and molecular level Western blot analysis of APE1/Ref-1 redox inhibition pathway proteins were analysed via *ex-vivo microscopically*. Irinotecan caused persistent weight loss throughout the treatment duration for both cohorts with cancer and without cancer. APX3330 treatment in combination with Irinotecan showed steady weight gain during the treatment compared to Irinotecan treatment alone. Irinotecan treated groups in both cohorts experienced diarrhoea throughout the treatment duration and APX3330 treatment seems to alleviate the side-effect by not showing symptoms of diarrhoea in both APX3330 treatment by itself as well

as in combination with Irinotecan. Mucosal damage and inflammation were evident following long-term treatment with Irinotecan. Faecal lipocalin level indicated a positive trend of alleviating GI inflammation induced by Irinotecan treatment following APX3330 treatment with the combination of Irinotecan. Irinotecan induced neuronal loss, mucosal damage, and inflammation following 14-day treatment period. Combination of APX3330 with Irinotecan treatment showed improved neuroprotective and anti-tumour properties compared to individual treatments of either Irinotecan or APX3330.

2.2 Introduction

Irinotecan ($C_{33}H_{38}N_4O_6$) is usually given as a combination with 5-fluorouracil and leucovorin for the treatment of advanced colorectal cancer (Conti et al., 1996, Saltz et al., 2000, Heinemann et al., 2021, Hsieh et al., 2021, Sugiyama et al., 2021, Shinozaki et al., 2021, Zhang et al., 2022, Rong et al., 2022). Irinotecan belongs to the family of quinoline alkaloids, and it is made as a semi-synthetic analogue of camptothecin. Irinotecan exerts its anti-cancer properties via inhibition of topoisomerase I (Xu and Villalona-Calero, 2002, Xu and Villalona-Calero, 2002, Dai et al., 2019, Ozawa et al., 2021). DNA topoisomerase I is an essential component of DNA transcription, and it is responsible for cutting, relaxing, and reannealing DNA strands. SN-38, the active metabolite of Irinotecan binds to DNA topoisomerase I and form a complex stable ternary structure that ceases the replication process of the cell that leads to DNA damage and apoptosis (Dai et al., 2019, Ozawa et al., 2021). Irinotecan has been used for phase II clinical trials in the 1990s as second-line therapy for patients whose first-line treatments were not satisfactory with 5-FU with advanced CRC (Grothey et al., 2004). These studies have revealed that sequential administration of Irinotecan has been showing positive outcomes with patients who receive 5-FU treatment by itself or combination therapy with 5-FU and Leucovorin (Cunningham et al., 1998, Rougier et al., 1998, Heinemann et al., 2021, Sugiyama et al., 2021, Kimura et al., 2021).

Nausea, vomiting, constipation, shortness of breath, and cholinergic syndrome are among the common side effects of Irinotecan treatment (Cunningham et al., 1998, Rougher et al., 1998, Wong et al., 2021, Park et al., 2022, Grierson et al., 2022). The acute and chronic onset of diarrhoea is the most common and dose-limiting side effect of the treatment leads to treatment delays and in severe cases cessation of the treatment. Acute diarrhoea usually starts 24 hours after the administration of treatment, and it is experienced by 60-80% of patients (Gibson and Keefe, 2006, Mego et al., 2015, Sakanaka et al., 2022, Secombe et al., 2022). Approximately 80% of the patients experience delayed onset diarrhoea and it is experienced 24-48 hours following administration of the treatment (Saliba et al., 1998, Leonard et al., 2002, Schulz et al., 2009, Zhao et al., 2021, Secombe et al., 2022). Acute symptoms associated with Irinotecan treatment may be due to mucosal damage and chronic systems such as recurring onset diarrhoea are due to the damage to the enteric nervous system.

Inflammation is a biological process that is enticed by the immune system as a response to several endogenous and exogenous stimuli and it is an essential process for tissue healing (Chen et al., 2018). In certain diseases such as cancer, diabetes, cardiovascular disease, and bowel disease, chronic inflammation disrupts the homeostatic balance in the cellular environment that further enhancing the disease progression (Varade et al., 2021). Number of widely used chemotherapeutics including Irinotecan causes inflammation as a main side-effect of the treatment. Irinotecan causes acute and chronic mucosal damage, inflammation and myenteric neuronal loss as demonstrated in previous studies (McQuade et al., 2017). Immune cells, tumours and cancer-associated fibroblasts are capable of producing cytokines in response to different stimuli (Ray et al., 2016, Peter et al., 2020, Varade et al., 2021). The release of these cytokines functions as a major driving of cytokine receptor activation that activates and enhances downstream activation of several cell signalling pathways including nuclear factor kappa-B (NF- κ B) and activator of transcription (STAT). Some of these cytokines like IL-1, IL-6, and TNF- α stimulate the activation of several transcription factors such as AP-1, STAT3, VEGF, and NF κ B and ultimately modulate the gene

expression (Gadina et al., 2017). APE1/Ref-1 functions as a key modulator of several important transcription factors and their activation of cytokines, chemokines, and other downstream target proteins that promote growth, metastasis, angiogenesis as well as cancer cell survival in the tumour microenvironment (Jiang et al., 2020) Recent research has found that APE1/Ref-1 protein induces lipopolysaccharide (LPS) - induced NLRP3 inflammatory cascade activation along with the production of a larger amount of pro-inflammatory cytokines such as IL-18, TNF- α , IL-1 β in tumour associated macrophages by activating NF-kB pathway. Another research finding has revealed that APX3330 suppressed the secretion of pro-inflammatory cytokines like TNF- α , IL-6, and IL-12 in LPS-stimulated macrophages. They have also found that APX3330 decreases the production of inflammatory mediator nitric oxide (NO) through the hindrance of transcription factors, AP-1, and NF-kB (Jedinak et al., 2011). Collectively, APE1/Ref-1 mediates several inflammatory processors via regulating the expression of important transcription factors that mediate pro-inflammatory cytokines.

Since the use of protein levels of NFkB, STAT3 to infer the activity of transcription factors is not a direct measurement of downstream regulation of APE1/Ref-1 inhibition by APX3330 alone or in combination with chemotherapeutics, further studies to elucidate its mechanism of action are warranted. APE1/Ref-1 is also known for its endonuclease activity that encourages DNA repair and enhances cell survival. In this study, we aimed to investigate the efficacy of APX3330 to protect the enteric neurons from Irinotecan-induced damage and to potentiate the anti-tumour effectiveness of APX3330 in a combination with Irinotecan in an orthotopic model of CRC. We hypothesised that APX3330 will reduce Irinotecan-induced damage to the enteric nervous system (ENS) and gastrointestinal dysfunctions in the murine model of colorectal cancer (CRC). Our study is the first to provide evidence of APX3330 neuroprotective and anti-tumour efficacy in the murine model of CRC. Our study is the first one to exhibit the neuroprotective and anti-tumour efficacy of the combination of APX3330 with Irinotecan. We have also found that APX3330 alleviates the adverse side-effects of Irinotecan treatment

alone and APX3330 treatment combined with Irinotecan has the potential of reducing the Irinotecan dose that inflict number of debilitating side-effects in CRC patients.

2.3 Methods

2.3.1 Animals

Male *Balb/c* mice (n=35) were purchased from the Animal Resources Centre (Perth, Australia) and housed in groups of 5 per cage at the Western Centre for Health Research and Education (WCHRE) for the duration of the project. The animals were kept in a temperature-controlled environment at approximately 22°C with a 12-hour day/night cycle with free access to food and water. The mice were allowed to acclimatise 3-5 days before experiments. All experiments were approved by the Victoria University Animal Experimentation Ethics Committee (Ethics number AEC19-010) and performed according to the guidelines of the National Health and Medical Research Council (NHMRC) Code of Practice for the Care and Use of Animals for Scientific Purposes.

2.3.2 Cell Culture

Murine colorectal cell line CT-26 cells were used to induce cancer in *Balb/c* mice at 9 weeks of age. CT-26 cells were cultured in Roswell Park Memorial Institute (RPMI) 1640 culture medium (Sigma-Aldrich, Castle Hill, Australia). Culture medium was supplemented with 10% Foetal Bovine Serum (FBS), 1% penicillin-streptomycin, and 1% glutamine. The cells were cultured in 5% CO₂ and 95% air atmosphere at 37°C. Cells were grown in 75cm² flasks and once they grow into confluent or semi confluent monolayers, they were further passaged or used for the study. The passaged cells were washed with 1x PBS (Phosphate Buffered Saline)

before passaging and the cells were seeded by using 0.25% trypsin. Once the cells reached 80-90% confluency in the flask they were separated from the bottom of the flask and centrifuged to obtain the condensed cells for the preparation of injections. Cell pellet was suspended in 1mL PBS. One part of cell suspension was mixed with 1 part of 0.4% trypan blue, and the mixture was incubated for 3 minutes in room temperature. A drop of cell/ trypan blue mixture was added to a hemacytometer, and cells were counted within 3-5 minutes. Trypan Blue dye was used to determine the number of cells in each vial. The viability of the cells was determined by observing the blue colour hue on the cell surface and they were counted under a light microscope and used a cell counting formula to calculate the total number of viable cells in 1mL of media. The condensed cell lysate was mixed with 100µL of media and 200 µL of Matrigel to prepare for injections. 1×10^6 cells were mixed with 25µL Matrigel per injection with >95% viability defined by trypan blue exclusion.

2.3.3 Orthotopic Implantation of CT-26 Tumour Cells

The cancer induction was performed by implanting murine CT-26 colorectal cancer cells into the mice caecum. Briefly, mice have received anaesthetics before surgeries using xylazine (10mg/kg) and ketamine (80mg/kg) via intraperitoneal injections. The level of anaesthesia was checked constantly by performing a paw pinch reflex test especially before and during the surgery. The eyes of the mice were covered with Visco Tears to protect them from drying out during the surgery. The surgeries were performed in an aseptic environment and the mice were placed on a heat mat (30-36°C) during surgeries to prevent heat loss. The surgical instruments were autoclaved before the surgeries and only opened on the operating table under an aseptic environment during surgeries. The abdominal area of the mice was shaved and swabbed with 70% ethanol followed by covering with sterile film to prepare the mice for the procedure. A small abdominal incision was made along the midline to exteriorise the caecum and the caecum was placed on sterile gauze during the procedure. One million (1×10^6) CT-26 murine colorectal tumour cells, that were suspended in 25µL of Matrigel with >95% viability, was injected into

the caecum using an insulin needle. The tumour cells were injected into the outer layer of the caecum (Figure 2.1) and a visible bulla formation was observed. The injections were carried out in a way to prevent any extra-caecal fluid leakage to complete the criteria for successful injection. The caecum was returned into the abdominal cavity, the abdominal muscles were sutured using polygalaceous sutures and the skin was sutured using surgical silk or dissolvable skin sutures. The incision area in the abdomen was swabbed with saline, followed by sterilising with iodine to aid the recovery process. After the surgery, the mice were given an analgesic, Temgesic/ buprenorphine (0.05mg/kg) subcutaneously. After returning to the recovery cage, the mice were closely monitored for 1-2 hours until they were conscious and moving around the cage and they returned into the animal house until the end of the treatment period.

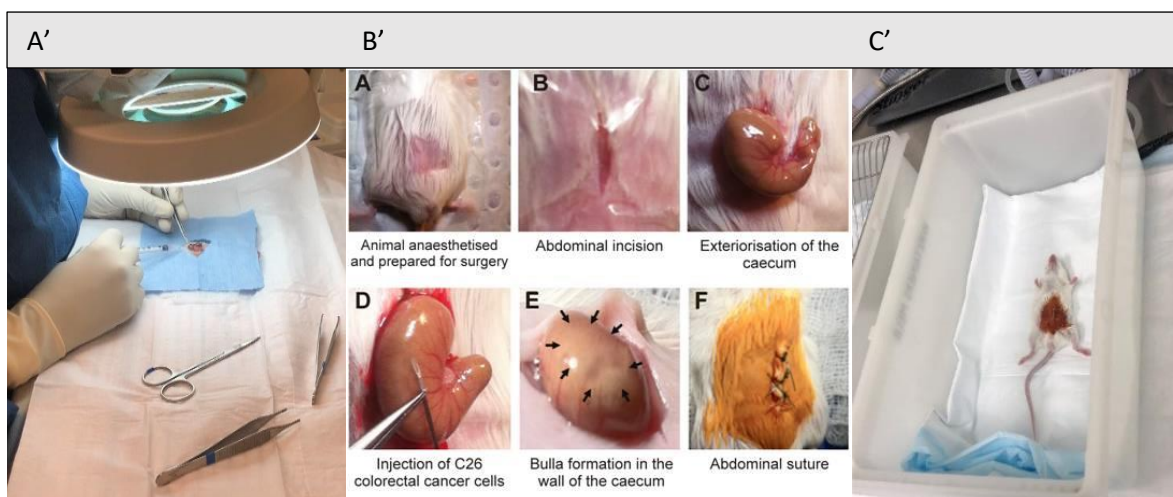


Figure 2.1 Induction of CRC with CT26 murine cells in a Balb/c mouse. Injecting anaesthesia before surgery (A'), CRC induction surgery (B'), mouse placed in the recovery cage following surgery (C').

2.3.4 Treatments

Mice without CRC (n=15/cohort) cohort was randomly divided into three groups including untreated (n=5), Irinotecan-treated (n=5), and APX3330-treated (n=5) received treatments twice as per the treatment plan (Table 2.1). Following CRC-induction surgery mice with cancer (n=19/cohort) were randomly divided into four groups including a two vehicles-treated group (n=5), Irinotecan plus vehicle for APX3330-treated (n=5), APX3330 plus vehicle for Irinotecan (IRI)-treated (n=4) and a combination of Irinotecan plus APX3330 (n=5) group (Table 2.1). All groups received treatments for two weeks starting from day 6 post-surgery. In cancer-free mice cohort, the untreated group (n=5) did not receive any treatments and were subjected to final experiments on day 15. Irinotecan-treated without cancer mice received treatments every second day with a maximum of 3 injections per week for 14 days and APX3330-treated cancer-free mice received treatments twice a day with 12 hours duration for 14 days. CRC-induced, two vehicles-treated (vehicle for Irinotecan plus vehicle for APX3330), Irinotecan plus vehicle for APX3330-treated, APX3330 plus vehicle for Irinotecan-treated, and combination of Irinotecan with APX3330-treated mice received treatments twice daily with 12-hours interval. Details of the treatment groups and treatment regimens are outlined in the Table 2.1. Mice received intraperitoneal injections (IP) of Irinotecan (IRI) (Sigma Aldrich) (30 mg/kg/dose) (3 times a week, 2 weeks) via a 30 ½ gauge needle. IRI was dissolved in sterile water to make stock solutions and they were refrigerated at -20°C until they were further be diluted to make working solutions for the intraperitoneal injections (McQuade et al., 2016). The dose of the Irinotecan was calculated to achieve a cumulative dose correspondent to an average human dose (Reagan-Shaw et al., 2008, Kohne et al., 2012). APX3330 (25 mg/kg) dose was given to mice 2x daily with 12 h interval for 14 days via intraperitoneal injections starting on the same day as IRI. APX3330 was dissolved in 2% Cremophor, 2% Ethanol, and 96% sterile water, due to the poor dissolvability of APX3330. APX3330 dose was based on our previous study that showed neuroprotective and anti-inflammatory effects in mice with chronic intestinal inflammation (Sahakian et al., 2021). The volumes for all injections were calculated to the animal's body weight every day with less than 200µL per injection (Table 2.1).

2.3.5 Clinical Parameters

2.3.5.1 Body Weights

Mice were weighed daily before the treatments starting three days after acclimatisation. They were weighed throughout the treatment period until the day of the final experiments. Body weight data were used as an indicator of the general health and wellbeing of mice.

2.3.5.2 Faecal Water Content

Faecal water content was calculated by analysing the percentage difference between wet and dry faecal weights to wet pellet weights using the following formula:

$$\text{Faecal water content (\%)} = \frac{\text{Wet pellet weight} - \text{Dry pellet weight}}{\text{Wet pellet weight}} \times 100$$

The wet weight of the faecal pellets was measured immediately after the sample collection. Samples were placed in a 60°C oven overnight and then the dry weights of the samples were measured. Faecal water content was analysed before the commencement of the treatment (day 0), the middle (day7), and the end of the treatment (day 14). Acute diarrhoea was confirmed by measuring water content in faecal pellets collected on day 7 of Irinotecan treatment (dose 3). Chronic diarrhoea was confirmed by measuring water content in faecal pellets collected on day 14, two days after receiving the last dose (dose 6) of Irinotecan treatment.

Table 2.1 Treatment Regimens

Treatment Group	Number of Mice	Treatment
Mice without CRC		
Untreated	n=5	No Treatment
Irinotecan-treated	n=5	IRI: 30 mg/kg/dose (dissolved in sterile water) 3 times a week, 2 weeks
APX3330-treated	n=5	APX3330: 25 mg/kg/dose (dissolved in 2% Cremophor: 2% EtOH and 96% sterile water) 2x daily with 8 h interval, 2 weeks
Mice with CRC		
Vehicle 1 + Vehicle 2-treated	n=5	Vehicle 1: sterile water 3 times a week, 2 weeks Vehicle 2: 2% Cremophor: 2% EtOH and 96% sterile water 2x daily with 8 h interval, 2weeks
APX3330 + Vehicle-treated	n=4	APX3330: 25 mg/kg/dose 2x daily with 8 h interval, 2 weeks Vehicle 1: sterile water 3 times a week, 2 weeks
Irinotecan + Vehicle-treated	n=5	IRI: 30 mg/kg/dose 3 times a week, 2 weeks Vehicle 2: 2% Cremophor: 2% EtOH and 96% sterile water 2x daily with 8 h interval, 2weeks
Irinotecan + APX3330-treated	n=5	IRI: 30 mg/kg/dose 3 times a week, 2 weeks APX3330: 25 mg/kg/dose 2x daily with 8 h interval, 2 weeks

2.3.5.3 Quantification of Faecal Lipocalin-2

Fresh faecal samples were collected on days 0, 7, and 14 to detect the changes in faecal lipocalin-2 levels. Faecal samples were immediately snap-frozen in liquid nitrogen after sample collection to preserve samples from further degradation. On the experimental day, the faecal samples were suspended in 0.1% Triton (100mg/ml) before sonicating the samples to agitate the particles in the samples. Then the samples were centrifuged at 12,000rpm at 4°C for 10 minutes. DuoSET ELISA Mouse Lipocalin-2 kit (R&D Systems, Minneapolis, USA) was used to quantify the lipocalin-2 levels in the supernatant of the faecal samples. Mouse lipocalin-2 capture antibody, mouse lipocalin-2 detection antibody, mouse lipocalin-2 standard, and streptavidin-horseradish peroxidase (HRP) were diluted with their diluent reagents according to instructions to prepare the working solutions. Plate preparation was done by coating the 96-well microplates with diluted capture antibody in PBS without carrier protein. Each well was coated with 100µL of diluted capture antibody and the sealed 96-well plates were incubated overnight at room temperature a day before the commencement of the experiment. On day 2, the solution was aspirated from the plate and the plate was washed three times with 400µL of wash buffer followed by complete removal of the liquid each time for increased performance. Once the plate was completely washed and dried with wash buffer, 300µL of blocking solution was added to the plates followed by a minimum of 1-hour incubation at room temperature. The plate was aspirated properly and was washed three times with wash buffer to prepare the plate for sample addition. The assay procedure was executed by adding 100µL of samples or standards to each well, covering the plate with an adhesive strip, and incubating for 2 hours at room temperature. The plate was aspirated carefully and washed three times with wash buffer after 2 hours incubation period. Each well of the plate was then covered by 100µL of detection antibody which was diluted in reagent diluent. Again, the plate was covered with a new adhesive strip and incubated at room temperature for 2 hours followed by aspiration and three washes with wash buffer before adding 100µL of streptavidin-HRP to each well. The plate was covered with aluminium foil to protect it from light and the plate was incubated 20 minutes at room temperature before aspirating the liquid and washing it three times with wash buffer.

Lastly, 100µL of substrate solution was added to each well and covered the plate with an aluminium foil to protect it from direct sunlight and incubated the plate for another 20 minutes at room temperature followed by adding 50µL of stop solution to each well to stop the enzymic reaction. The plate was tapped gently to ensure through mixing since it is important to have a consistent density in each well. The optical density of each well was read by using a microplate reader set to 450 nm. The readings were then subtracted by 570nm from the readings at 450nm to obtain the readings corrected for optical imperfections in the plate.

2.3.6 Tissue Collection

On the day 6 post-surgery the mice started receiving Irinotecan, APX3330, Vehicle or a combination of treatments for 14 days. After the treatments mice were culled by giving a lethal injection of phenobarbital. The caecum was exteriorised and examined for tumour growth. Samples of the caecum, distal colon, and secondary spread of tumour samples in the abdominal cavity were immediately snap-frozen in liquid nitrogen for Western blot analysis. Fresh colon samples were collected and processed for immunohistochemistry experiments as described below.

2.3.6.1 Immunohistochemistry in Wholemout Preparations

Immunohistochemistry was performed as described in Robinson et al. (2014) and Wafai, et al. (2013). The distal colon tissue samples from each animal were collected and placed in oxygenated phosphate-buffered saline (PBS, pH7.2) that contained nifedipine (3µM) for 20 minutes to inhibit smooth muscle contractions. Wholemout preparation sample tissues were maximally stretched and pinned flat with the mucosal side up into the dish. Then the tissue samples were fixed with Zamboni's fixative (2% formaldehyde containing 0.2 % picric acid) overnight at 4°C. The next day, the tissue sections were washed with dimethyl sulfoxide (DMSO,

Sigma-Aldrich, Australia) three times 10 minutes apart to clear off the fixative followed by three times ten-minute washes of phosphate-buffered saline (PBS). Tissue samples of the distal colon that were prepared for Immunohistochemistry wholemounts were then placed in 10mL of PBS+0.01g of Sodium Azide solution and stored at 4°C for long-term storage.

The tissues processed for wholemount preparations were then washed (2x5 mins) with phosphate-buffered saline with 0.01% Triton X 100 (PBST) and then peeled the mucosal layer, submucosal muscle layer, and the circular muscle layer off to visualise the myenteric plexus of the colon. Once the longitudinal muscle-myenteric plexus (LMMP) of the wholemount preparation is neatly dissected, the tissues were incubated in a humidified box with 10% normal donkey serum (Chemicon, USA) for 1 hour at room temperature. The tissues were then washed (3 x 5 mins) with PBST followed by incubating with primary antibodies (Table 2.2) overnight at room temperature. The following day, the tissue preparations were washed in PBST (3x10 min) before incubation with species-specific secondary antibodies (Table 2.2) that were developed to detect and bind to the primary antibody. The tissue sections were incubated in a dark humidified box for two hours at room temperature before washing in (3x10 min) PBST. After the third PBST wash, the sections were incubated with 4'6-diamidine-2'-phenylindole dihydrochloride (DAPI) (D1306, Life Technologies, Australia) for 1 minute which serves as a fluorescent nucleic acid stain. Tissues were then further subjected to PBST washes (2x10 min) and then mounted on glass slides using fluorescent mounting medium (DAKO).

2.3.6.2 Immunohistochemistry in Cross-Sections

The distal colon tissue samples from each animal were collected and placed in oxygenated phosphate-buffered saline (PBS, pH7.2) that contained nifedipine (3µM) for 20 minutes to inhibit smooth muscle contractions. Cross-section

preparation sample tissues were pinned flat with the mucosal side up without stretching into the dish. Then the tissue samples were fixed with Zamboni's fixative (2% formaldehyde containing 0.2 % picric acid) overnight at 4°C. The next day, the tissue sections were washed with dimethyl sulfoxide (DMSO, Sigma-Aldrich, Australia) three times 10 minutes apart to clear off the fixative followed by three times ten-minute washes of phosphate-buffered saline (PBS). After washing three times with PBS, the tissue samples that were prepared for Immunohistochemistry cross-sections were placed in moulding trays and then embedded in optimum cutting temperature (OCT) compound. The moulding cases were then placed in a liquid nitrogen canister after placing the mould in a 2-methyl butane (isopentane) container. The prepared OCT blocks were stored in a -80°C freezer for long-term storage.

The OCT blocks that contained distal colon segments were cryo-sectioned at 10µm section thickness using a Leica CM1950 cryostat (Leica Biosystems, Germany). The sections were adhered to glass slides immediately after cutting and they were left at room temperature for 1hr before commencing the immuno-staining process. Residual OCT was washed off from the slides by washing the slides three times with 0.01% Triton x100 (PBST) for five minutes apart. The samples were outlined by using a liquid Blocker Super Pap Pen to reduce the use of the antibodies. Then 10% normal donkey serum (Chemicon, USA) in x1 PBS was added to the samples to block the endogenous activity of the samples. The glass slides were stored in a humidified box for one hour at room temperature followed by three x1 PBST washes five minutes apart. The cross-section samples were then incubated in a humidified box with primary antibodies (Table 2.3) overnight at room temperature. The second day of the process was commenced by washing the sections with 1x PBST three times 5 minutes apart. The sections were then incubated with secondary antibodies (Table 2.3) that were labelled against the primary antibodies. The sections were incubated at room temperature in a dark humidified box for two hours before washing them three times with 1xPBST five minutes apart. After the third PBST wash, the sections were incubated with 4'6-diamidine-2'-phenylindole dihydrochloride (DAPI) (D1306, Life Technologies,

Australia) for 1 minute. The sections were washed again two times with 1xPBST washes and then mounted with fluorescent mounting medium DAKO (Agilent Technologies, Australia). The glass slides that contained the cross-sections were covered with coverslips and they were left in a dark place dry overnight before imaging the next day.

2.3.6.3 Imaging

Nikon Eclipse Ti laser scanning microscope (Nikon, Japan) was utilized to take three-dimensional images of wholemount preparations and cross-sectional preparations of the samples. Wholemount preparations of the distal colon segments were observed under the microscope, and 8 randomly selected images were taken using x40 objective and the images were processed using NIS Element Software (Nikon, Japan). The cross sections were observed under the microscope, and eight randomly chosen images were captured with 20x objective per distal colon sample. Z-series images were taken to analyse the complete image at a step size of 1.75 μ m (1600 \times 1200 pixels). Images were analysed by the variation of fluorescence in each image in comparison to the relative fluorescence of each area of the image. The images were then analysed by using Image J software.

2.3.7 Morphometric Analysis of Tumours and Tumour Metastasis

Tumour growth in the caecum and colon was assessed *ex vivo* macroscopically as well as histologically. The freshly resected caecum was weighted, and the number of tumours and polyps were counted where applicable. Then the caecum was placed in PBS and cut along the mesenteric border to expose the content. Caecum tissues were then pinned down mucosal side up and flushed out the content. Fresh Caecum samples were snap-frozen for Western Blot experiments. The size, number, weight of the tumours, and tumour metastasis were analysed on the day of the tissue collection.

Table 2.2 Primary and Secondary Antibodies Used in Wholmount Preparations

Antibody	Species	Dilution	Source
Primary antibodies			
Pan neuronal marker anti-PGP9.5 antibody	Rabbit, polyclonal	1:500	Abcam, Australia
Apurinic/aprimidinic endonuclease-1 anti-APE1/Ref-1 (APE1/REF-1) antibody	Mouse, monoclonal	1:1000	A gift from Prof. M. Kelley, Indiana University, Indianapolis, Indiana, US
Cholinergic neuronal marker anti-Choline Acetyltransferase (ChAT) antibody	Goat, monoclonal	1:500	Abcam, Australia
Cholinergic fibre marker anti-Vesicular Acetylcholine Transporter (VAChT) antibody	Goat, monoclonal	1:500	Abcam, Australia
Secondary antibodies			
Alexa Flour 488	Anti-mouse	1:300	Jackson ImmunoResearch laboratories, United States
Alexa Flour 594	Anti-rabbit	1:300	
Alexa Flour 647	Anti-rabbit	1:300	
Alexa Flour 594	Anti - goat	1:300	
Alexa Flour 647	Anti - goat	1:300	

Table 2.3 Primary and Secondary Antibodies Used in Cross-sections

Antibody	Species	Dilution	Source
Primary antibodies			
Pan neuronal fibre marker anti- β -Tubulin III antibody	Chicken, monoclonal	1:500	Abcam, Australia
Pan leukocyte marker anti-CD45 antibody	Rabbit, polyclonal	1:500	Abcam, Australia
Neutrophil marker anti-myeloperoxidase (MPO) antibody	Rabbit, monoclonal	1:500	Cell signalling, Australia
Secondary antibodies			
Alexa Flour 594	Anti - chicken	1:300	Jackson ImmunoResearch laboratories, United States
Alexa Flour 488	Anti-rabbit	1:300	
Alexa Flour 647	Anti-rabbit	1:300	

2.3.8 Western Blot Analysis

Freshly harvested segments of distal colon samples were washed with 1×PBS solution to flush off its content and snaped frozen until the following day. The following day the frozen tissue samples were homogenized with a Polytron homogenizer (Kinematica AG, Lucerne, Switzerland) for 20 seconds in ice-cold Radioimmunoprecipitation Assay (RIPA) solution containing protease and phosphatase inhibitors cocktails (1:100 protease inhibitor, 1:100 phosphatase inhibitor) (Bio-Rad). Then the homogenate was centrifuged, and the lysate samples were preserved in a -80°C freezer for further analysis. The exact protein concentration of each lysate sample was determined by the detergent compatible protein assay (DC protein assay) kit (Bio-Rad Laboratories, Hercules, CA, USA). To make Western blot working samples, equal amounts of protein samples will be taken from each lysate sample based on their protein concentration and they were dissolved in 25µL of Laemmli buffer, and the rest of the volume was filled with RIPA Buffer to make 100µL of WB working samples. Prepared working samples were subjected to electrophoretic separation on sodium dodecyl sulfate-polyacrylamide gel electrophoresis (SDS-PAGE) acrylamide gels to determine the expression of different target proteins. The protein expression was evaluated following electrophoretic separation, the proteins were transferred to a polyvinylidene difluoride (PVDF) membrane and then blocked with 5% skim milk (Tris Buffered Saline containing 0.1% Tween, TBST) for 1 hour followed by 4 x 5 mins TBST washes. The membranes were incubated overnight in a platform shaker at 40rpm speed with primary antibodies (Table 2.4) based on the target of interest at -4°C. Primary antibodies were prepared in 1% Bovine Serum Albumin (BSA) (TBST, BSA, 0.01% Sodium Azide) and 1:1000 primary antibody concentration was used throughout the study. Membranes were washed 4 x 5 mins washes with TBST on the following day and probed with horseradish peroxidase (HRP)-conjugated secondary antibodies (Table 2.4) in 5% skim milk solution for 2 hours at room temperature. Membranes were then washed with 4x 5mins TBST washes the blots were developed using ECL Prime Reagent (Amersham, Piscataway, NJ, USA) followed by imaging in a DARQ CCD camera mounted to a fusion FX Imaging system (Silver Lourmat, Germany). Densitometric measurements of the protein of

interest were performed employing Fusion CAPT Advance software (Viber Lourmat, Germany). The signal intensity of the target protein was normalised to the signal intensity of the total protein loaded. The proteins extracted from distal colon segments from each animal were evaluated for the expression of Inflammatory markers, signal transducer and activator of transcription 3 (STAT3), phosphorylated STAT3 (pSTAT3) and vascular endothelial growth factor (VEGF).

2.3.9 Data and Statistical Analysis

Image J Software (National Institute of Health, Bethesda, MD, USA) was used to convert images from RGB to greyscale 8-bit binary. Images were then analysed to attain the percentage area of immunoreactivity. All immunohistochemistry images and Western Blot images were quantified as per above and statistical analysis was performed with Prism (version 9.0v, Graph Pad Software, La Jolla, CA, USA). All values were represented as mean +/- standard error of the mean (S.E.M.) except the changes in body weight (%) during the 14-day period that was presented as mean +/- standard deviation of the mean (S.D.). One-way ANOVA followed by the Tukey-Kramer post hoc test for multiple group comparison was used to analyse the differences between all groups. $P < 0.05$ was considered significant.

Table 2.4 Primary and Secondary Antibodies Used for Western Blot Experiments

Antibody	Species	Dilution	Source
Primary antibodies			
Apurinic/aprimidinic endoneuclease-1 anti-APE1/Ref-1 (APE1/Ref-1) antibody	Mouse, monoclonal	1:1000	Abcam, Australia
Vascular endothelial growth factor marker anti-VEGF antibody	Rabbit, polyclonal	1:1000	Abcam, Australia
Nuclear factor kappa-light-chain-enhancer of activated B cells marker anti-NF-kB antibody	Rabbit, monoclonal	1:1000	Cell Signaling, Australia
Signal transducer and activator of transcription 3 marker anti-STAT3 antibody	Rabbit, monoclonal	1:1000	Cell Signaling, Australia
Phospho specific signal transducer and activator of transcription 3 marker anti-pSTAT3 antibody	Rabbit, monoclonal	1:1000	Cell Signaling, Australia
Secondary antibodies			
Horseradish peroxidase (HRP) IgG (H+L)	Anti-mouse	1: 5000	Abcam, Australia
Horseradish peroxidase (HRP) IgG (H+L)	Anti-rabbit	1: 5000	Abcam, Australia

2.4 Results

2.4.1 Effects of Treatments on Clinical Symptoms

2.4.1.1 Effect of Treatments on Body Weights

Mice without cancer were weighed throughout the experimental period to assess their general health and wellbeing as well as to detect any adverse effects of the IRI and APX3330 treatments on body weight. Mice without CRC were randomly allocated into three groups that received treatments for 2 weeks following 3 days of the acclimatisation period (**Table 2.1**). Untreated mice without cancer continued to gain weight throughout the experimental period with $11.9 \pm 0.5\%$, $P < 0.01$ weight gain at day 15 from the start of the treatment compared to day 1 (**Figure 2.2A**). APX3330-treated mice without CRC also gained weight during the treatment period with an average weight gain of $7.9 \pm 0.1\%$, $P < 0.01$ at day 15 compared to day 1. IRI-treated mice did not gain weight throughout the treatment period with an average weight loss of $-1.75 \pm 0.8\%$, $P < 0.05$ at day 15 compared to day 1. The average body weight of IRI-treated mice ($22.8 \pm 0.7\text{g}$) was significantly lower at day 15 of treatment compared to untreated ($27.0 \pm 0.8\text{g}$, $P < 0.01$) and APX3330-treated ($26.1 \pm 0.7\text{g}$, $P < 0.05$) mice ($n=5$ mice/group) (**Figure 2.2B**).

Tumour-bearing mice were randomly divided into 4 groups that received treatments for 14 days starting on day 6 post CRC induction surgery (**Table 2.1**). Mice treated with two vehicles gradually gained weight during the treatment period with $8.1 \pm 1.3\%$, $P < 0.01$ weight gain at day 15 compared to day 1 (**Figure 2.3A**). Repeated *in vivo* administration of IRI did not gain weight like other groups in CRC-induced mice after a 14-day treatment period compared to day 1 ($-1.2 \pm 1.8\%$, $P < 0.05$). APX3330 + VEH-treated mice with CRC gained weight by $4.4 \pm 1.2\%$, $P < 0.01$ at day 15. A combination of IRI and APX3330 treatment increased body weight by $3.4 \pm 0.6\%$ ($P < 0.01$) at day 15 compared to day 1. The average body weight of IRI-treated mice with CRC at day 15 was $22.2 \pm 0.5\text{g}$, which was lower than VEH + VEH-treated

mice ($26.8 \pm 0.5\text{g}$, $P < 0.0001$), APX3330 + VEH-treated mice (25.3 ± 0.4 , $P < 0.01$) and combination of APX3330 + IRI-treated mice ($24.8 \pm 0.5\text{g}$, $P < 0.01$) (**Figure 2.3B**). The body weight of APX3330 + VEH-treated mice was lower compared to VEH + VEH-treated mice ($P < 0.05$). VEH + VEH-treated mice demonstrated significantly higher average body weight at day 15 due to rapid growth of tumours in the abdominal cavity ($n=4-5$ mice/group).

2.4.1.2 Effect of Treatments on the Faecal Water Content

To define the faecal water content, as a measurement of symptoms of diarrhoea or constipation, fresh faecal pellets were collected from untreated, IRI-treated and APX3330-treated mice before the initiation of the treatment (day 0), at day 7 and day 14 of treatment. Faecal water content was calculated as the percentage difference between wet and dry pellet weight to wet pellet weights. Before the start of the treatment at day 0, no differences were found in the wet and dry faecal weights and, therefore, faecal water content was not different between all three groups (untreated: $52.4 \pm 2.0\%$, IRI-treated: $51.6 \pm 1.5\%$ and APX3330-treated: $52.8 \pm 1.0\%$, respectively, $n=5$ mice/group) (**Figure 2.4A**). Wet faecal pellet weight was significantly higher in IRI-treated mice ($86.4 \pm 5.5\text{mg}$) in comparison with untreated mice without cancer ($51.5 \pm 6.5\text{mg}$, $P < 0.01$) and APX3330-treated mice ($53.6 \pm 3.5\text{mg}$, $P < 0.01$) at day 7. Dry faecal pellet weight was also significantly higher in IRI-treated mice ($29.2 \pm 1.1\text{mg}$) compared to untreated mice without cancer ($23.0 \pm 1.8\text{mg}$, $P < 0.05$) and APX3330-treated mice ($23.4 \pm 1.1\text{mg}$, $P < 0.05$) at day 7 of the treatment. The mean faecal water content was significantly higher at day 7 of the treatment in the IRI-treated group ($70.0 \pm 2.1\%$) compared to untreated $53.2 \pm 3.7\%$ ($P < 0.01$) and APX3330-treated $52.4 \pm 1.1\%$ ($P < 0.01$) groups ($n=5$ mice/group) (**Figure 2.4B**). At day 14, the wet faecal weight was considerably increased in IRI-treated mice without cancer ($97.6 \pm 3.3\text{mg}$), compared to untreated mice ($52.7 \pm 3.4\text{mg}$, $P < 0.0001$) and APX3330-treated mice ($54.3 \pm 2.6\text{mg}$, $P < 0.0001$). Dry faecal pellet weight was also significantly higher in IRI-treated mice at day 14 ($29.8 \pm 1.2\text{mg}$) in comparison with untreated mice ($23.9 \pm 1.6\text{mg}$, $P < 0.05$)

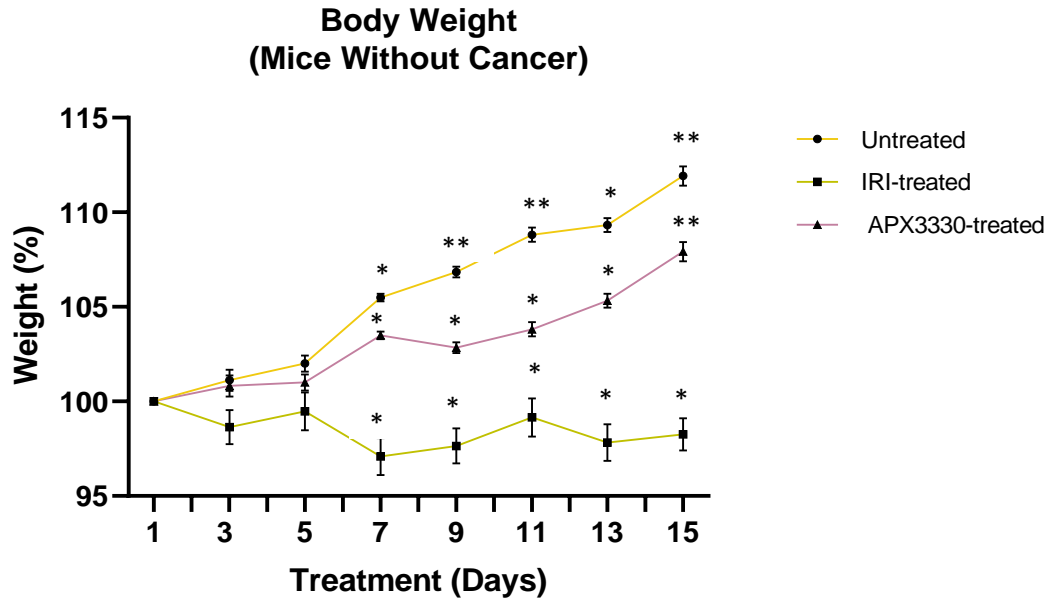
and APX3330-treated mice ($22.6 \pm 1.5\text{mg}$, $P < 0.01$). At day 14, the IRI-treated group maintained a higher level of faecal water content $72.5 \pm 5.8\%$ compared to untreated ($54.0 \pm 4.1\%$, $P < 0.05$) and APX3330-treated mice without cancer ($54.2 \pm 1.9\%$, $P < 0.05$) ($n=5$ mice/group) (**Figure 2.4C**). Thus, faecal water content was significantly higher in IRI-treated mice throughout the 14-day treatment period indicating chronic diarrhoea.

Similarly, no difference in the faecal water content was found before the start of the treatment in mice with CRC: VEH + VEH-treated ($60.3 \pm 3.0\%$), IRI + VEH ($51.5 \pm 3.3\%$), APX3330 + VEH ($51.7 \pm 2.3\%$) and combination of APX3330 + IRI-treated ($53.0 \pm 2.5\%$) mice ($n=4-5$ mice/group) (**Figure 2.5A**). At day 7, wet faecal weight was significantly higher in IRI + VEH-treated mice ($99.7 \pm 2.2\text{mg}$) when compared to VEH VEH-treated mice ($63.7 \pm 3.4\text{mg}$, $P < 0.0001$), APX3330 + VEH-treated mice ($52.2 \pm 2.8\text{mg}$, $P < 0.0001$) and combination treatment of APX3330 + IRI ($60.1 \pm 3.5\text{mg}$, $P < 0.0001$). In line with wet faeces weight, dry faeces weight was also significantly high in IRI-treated mice ($34.8 \pm 1.7\text{mg}$) compared to VEH + VEH-treated mice ($24.1 \pm 1.1\text{mg}$, $P < 0.01$) and APX3330 + VEH-treated mice ($27.4 \pm 1.8\text{mg}$, $P < 0.05$) but not combination treatment of APX3330 + IRI ($29.0 \pm 1.8\text{mg}$). Faecal water content in IRI + VEH-treated mice ($65.1 \pm 2.3\%$) was similar to VEH + VEH-treated mice ($62.1 \pm 3.4\%$) at day 7 of treatment conforming that both groups had diarrhoea. Treatment with APX3330 + VEH and APX3330 + IRI reduced faecal water content ($47.7 \pm 2.5\%$ and $52.1 \pm 2.6\%$ respectively, $P < 0.001$ and $P < 0.01$ compared to IRI + VEH-treated group and $P < 0.01$ and $P < 0.05$ compared to VEH + VEH-treated group, $n=4-5$ mice/group) (**Figure 2.5B**). At day 14, wet faecal weight was significantly higher in IRI + VEH-treated mice ($99.8 \pm 3.7\text{mg}$) when compared with VEH + VEH-treated mice ($64.1 \pm 2.6\text{mg}$), APX3330 + VEH-treated mice ($54.9 \pm 2.8\text{mg}$) and combination treatment of APX3330 + IRI mice ($57.4 \pm 3.6\text{mg}$) ($P < 0.0001$ for all). Similarly, the dry faecal weight was also significantly higher in IRI + VEH-treated mice ($35.6 \pm 1.6\text{mg}$) at day 14 as opposed to VEH + VEH-treated mice ($25.4 \pm 1.6\text{mg}$, $P < 0.01$), APX3330 + VEH-treated mice ($28.9 \pm 1.4\text{mg}$, $P < 0.05$) but not different compared to the APX3330 + IRI-treated group ($29.3 \pm 1.7\text{mg}$). At day 14, the water content in the faecal pellets was similar in IRI + VEH-treated (64.3

$\pm 1.7\%$) and VEH + VEH-treated ($60.4 \pm 3.9\%$) mice but significantly lower in APX3330 + VEH ($47.4 \pm 2.5\%$) and APX3330 + IRI ($49.0 \pm 2.6\%$) compared to VEH + VEH ($P < 0.05$ for both) and IRI + VEH ($P < 0.01$ for both) treated mice ($n = 4-5$ mice/group) (**Figure 2.5C**). Thus, the water content was significantly higher in the faeces collected from IRI-treated mice on both days 7 and 14 of treatment, indicating chronic diarrhoea.

Figure 2.2 Effect of IRI and APX3330 treatment on body weight of mice without CRC. (A) Changes in body weight (%) during the 14-day period in mice treated with Irinotecan (green), APX3330 (pink), and untreated (yellow). Data at all time points were compared to the starting body weight at day 1, which was considered as 100%. All values were presented as mean and \pm S.D. * P <0.05, ** P <0.01, n =5 mice/group. (B) Body weight of IRI and APX3330-treated mice at day 15 compared to untreated mice. All values were presented as mean and \pm S.E.M. * P <0.05, ** P <0.01, n =5 mice/group.

A



B

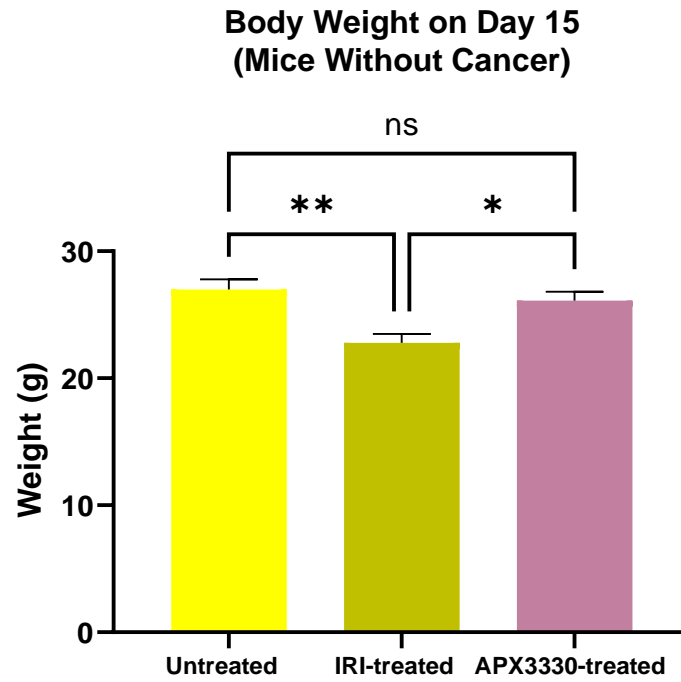
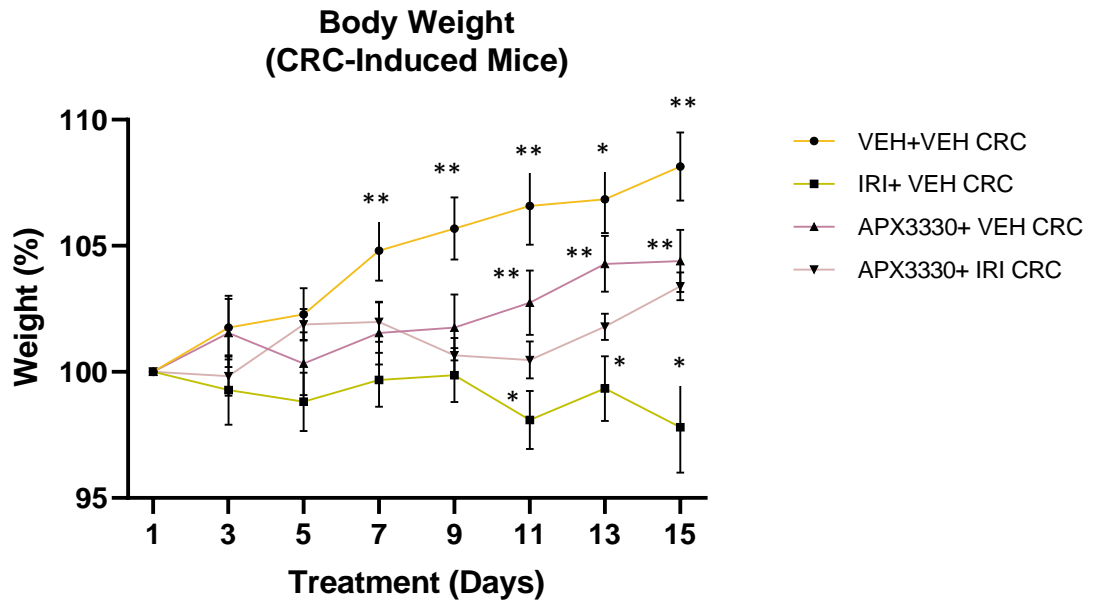


Figure 2.3 Average body weight following 14 days of treatments in CRC-induced mice. (A) Changes in body weight (%) during a 14-day treatment (starting at day 6 post-CRC-induction surgery) with two vehicles (a vehicle for Irinotecan plus a vehicle for APX3330) (yellow), Irinotecan plus a vehicle for APX3330 (green), APX3330 plus a vehicle for Irinotecan (purple) and APX3330 plus Irinotecan (pink). Data at all time points were compared to the starting body weight at day 1, which was considered as 100%. All values were presented as mean and \pm S.D. * P <0.05, ** P <0.01, n =5 mice/group. (B) The body weight of mice from all treatment groups was measured at day 15. All values were presented as mean and \pm S.E.M. * P <0.05, ** P <0.01, **** P <0.0001, n =4-5 mice/group.

A



B

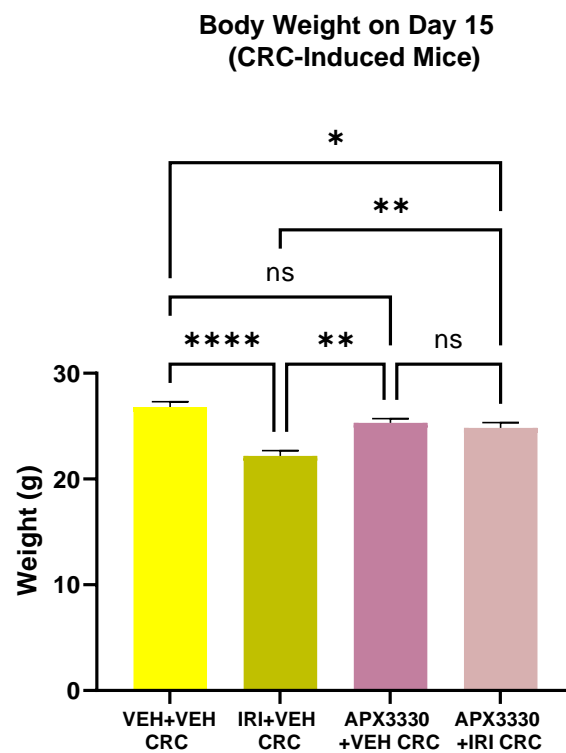
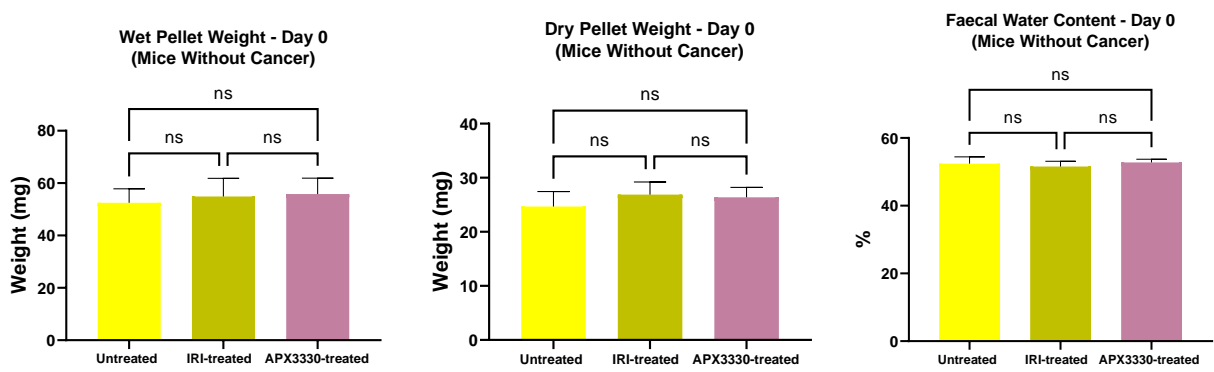
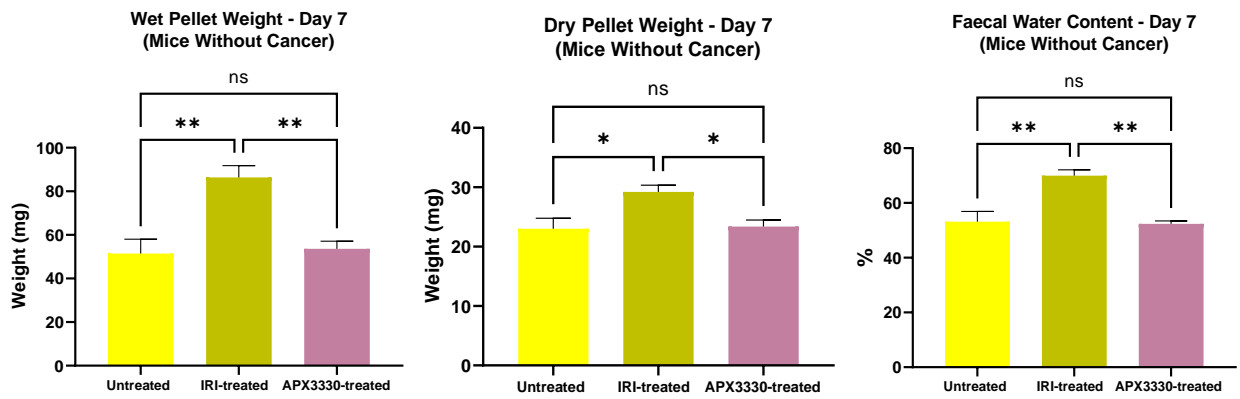


Figure 2.4 Effects of Irinotecan and APX3330 treatment on the faecal water content compared to untreated mice. The wet and dry weight of the faecal pellets (mg) and the faecal water content (the difference between wet and dry pellet weights, %) before the commencement of the treatment (A), after 7 days of treatment (B), after 14 days of treatment (C). Data presented as mean \pm S.E.M. * P <0.05, ** P <0.001, **** P <0.0001, n=5 mice/group.

A



B



C

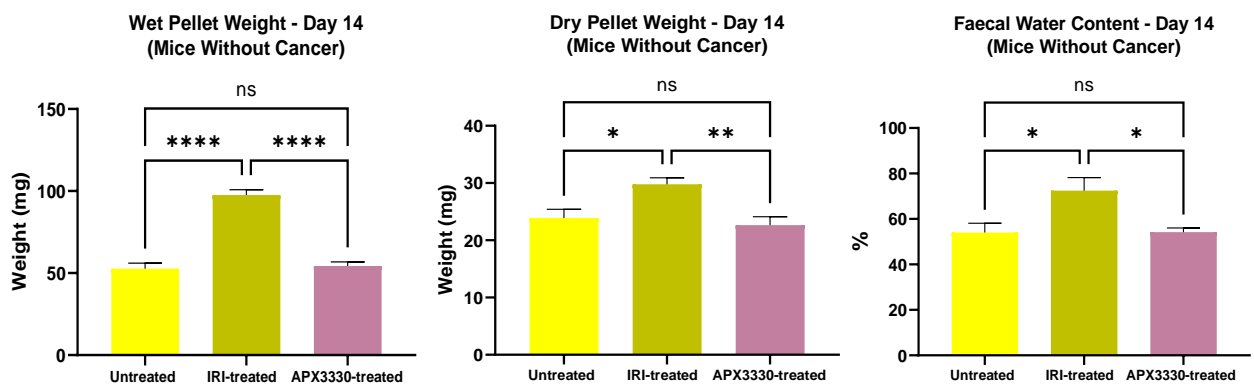
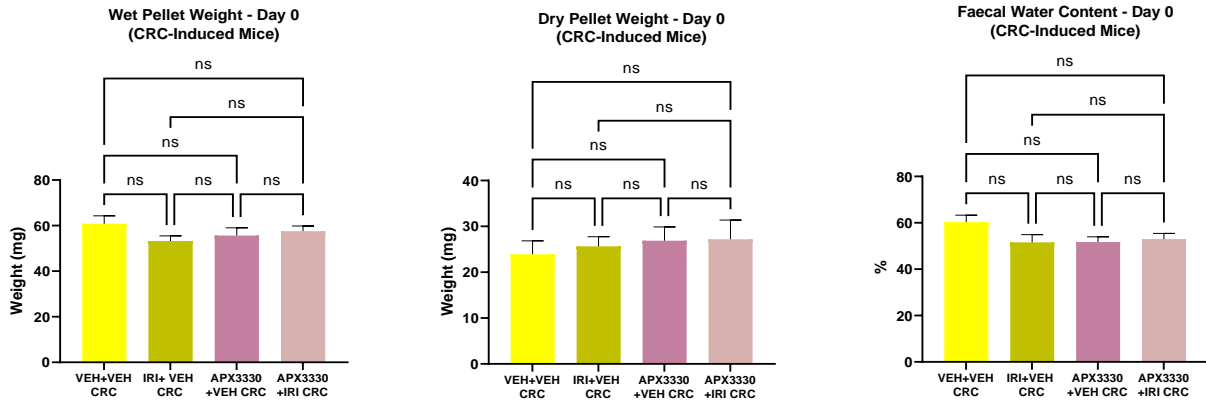
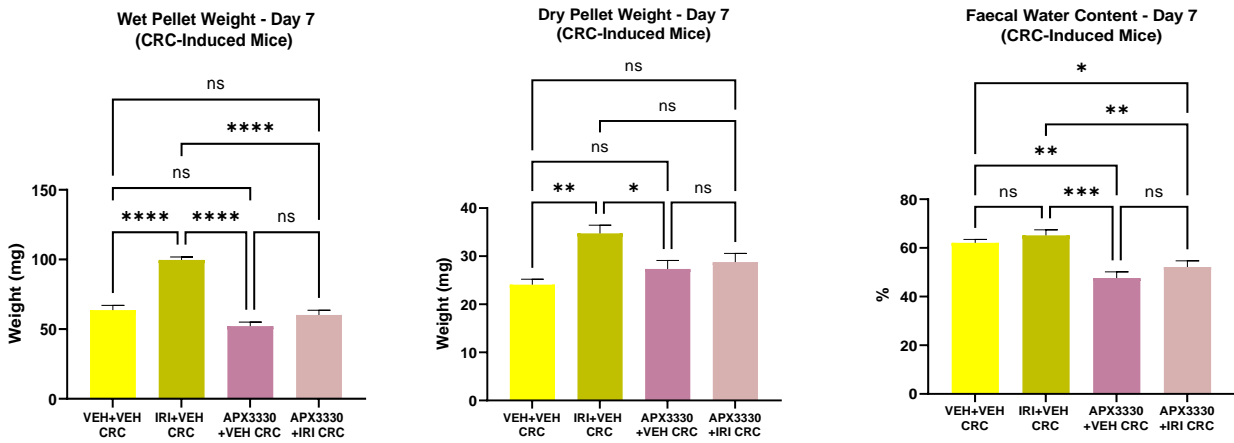


Figure 2.5 Effects of the treatments on the faecal water content in CRC-induced mice. The wet and dry weight of the faecal pellets (mg) and the faecal water content (the difference between wet and dry pellet weights, %) before the commencement of the treatment (A), after 7 days of treatment (B), after 14 days of treatment (C). Data presented as mean \pm S.E.M. * P <0.05, ** P <0.001, *** P <0.001, **** P <0.0001, n=4-5 mice/group.

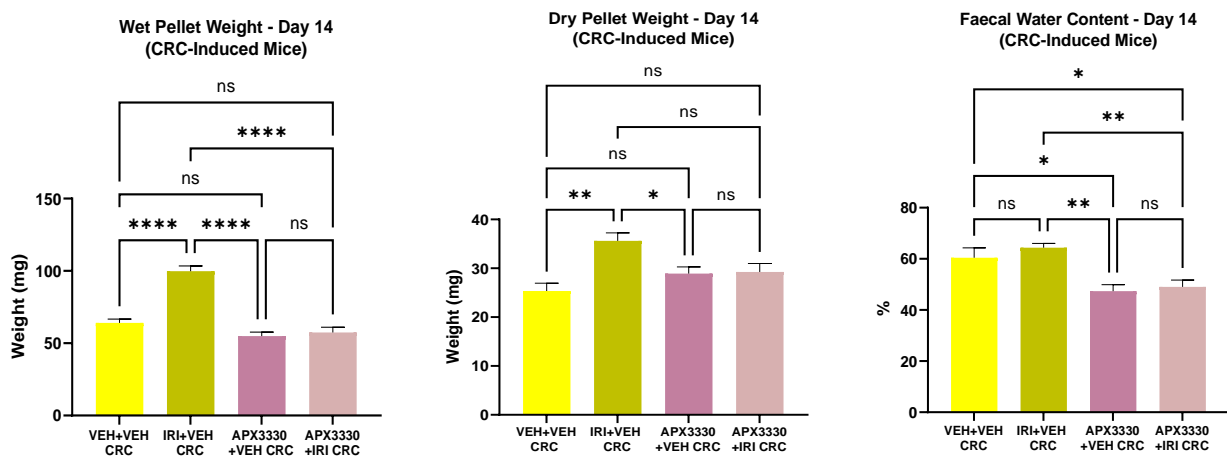
A



B



C



2.4.2 Anti-Inflammatory and Neuroprotective Properties of APX3330

2.4.2.1 Effects of Treatments on Faecal Lipocalin-2 Levels

The concentration of neutrophil gelatinase-associated protein, lipocalin-2 (LCN-2), a highly sensitive biomarker of intestinal inflammation and it has been used as a reliable biomarker to assess intestinal inflammation in auto-immune diseases that affect the central nervous system (Bachman et al., 2009, Chassaing et al., 2012, Yadav et al., 2022). The level of LCN-2 in the faecal matter has been used as a biomarker to assess the disease severity of spontaneous colitis development in IL-10 deficient mice (Chassing et al., 2012, Yadav et al., 2022). Faecal LCN-2 level was assessed in the faeces to investigate immune cell infiltration and inflammation in the gastrointestinal tract. Faecal LCN-2 levels did not show significant difference at day 0 of the treatment in IRI-treated mice without cancer (356.3 ± 7.4 pg/mL) compared to untreated mice (371.0 ± 2.0 pg/mL) and APX3330-treated mice (344.9 ± 7.2 pg/mL) (n=5 mice/group) (**Figure 2.6A**). Faecal LCN-2 level was significantly higher at day 7 of the treatment with an average of 440.8 ± 5.0 pg/mL in IRI-treated mice compared to untreated mice without cancer (374.7 ± 4.8 pg/mL, $P < 0.001$) and APX3330-treated mice (358.8 ± 11.3 pg/mL, $P < 0.0001$) (n=5 mice/group) (**Figure 2.6B**). Faecal LCN-2 level was increased at day 14 of the treatment in IRI-treated mice with an average level of 476.0 ± 6.6 pg/mL compared to untreated mice (372.0 ± 3.0 pg/mL, $P < 0.0001$) and APX3330-treated mice (340.0 ± 7.1 pg/mL, $P < 0.0001$) (n=5 mice/group) (**Figure 2.6C**). APX3330-treated mice had the lowest LCN-2 level at day 14 of treatment indicating the anti-inflammatory effects of the treatment.

In comparison to mice without CRC, all treatment groups of mice with CRC had significantly high levels of LCN-2 at day 0: 660.9 ± 32.7 pg/mL in VEH + VEH-treated CRC mice, 654.1 ± 20.8 pg/mL in IRI + VEH-treated CRC mice, 644.7 ± 33.9 pg/mL in APX3330 + VEH-treated CRC mice and 611.7 ± 21 pg/mL in IRI + APX3330-treated CRC mice indicating immune response to cancer development

(Figure 2.7A). Faecal LCN-2 levels of VEH + VEH-treated (562.7 ± 15.8 pg/mL) and IRI + VEH-treated (559.2 ± 23.8 pg/mL) mice with CRC showed higher values of LCN-2 at day 7 of the treatment that were not statistically different between these groups indicating elevated intestinal inflammation associated with cancer pathology **(Figure 2.7B).** Treatment with APX3330 + VEH and APX3330 + IRI reduced the LCN-2 levels to 469.8 ± 17.3 pg/mL and 460.6 ± 23.7 pg/mL, respectively, compared to IRI + VEH-treated and VEH + VEH-treated groups ($p < 0.05$ for all). At day 14, VEH + VEH-treated (577.3 ± 26.5 pg/mL) and IRI + VEH-treated (553.7 ± 23.6 pg/mL) CRC mice showed significantly higher LCN-2 levels compared to other treatment groups indicating elevated intestinal inflammation associated with CRC. APX3330 + VEH (421.8 ± 30.4 pg/mL) and APX3330 + IRI (429.0 ± 32.6 pg/mL) treatments reduced intestinal inflammation at day 14, compared to IRI + VEH (553.7 ± 23.6 pg/mL, $p < 0.05$ for both) and VEH + VEH-treated (577.3 ± 26.5 pg/mL, $p < 0.01$ for both) mice denoting the anti-inflammatory properties of the treatment (n=4-5 mice/group) **(Figure 2.7C).** Results indicate that Irinotecan-treated cancer-free mice had elevated faecal LCN-2 level on day 7 and 14 indicating a correlation between Irinotecan-induced intestinal inflammation. Regardless of the treatment group, CRC-induced mice had elevated levels of faecal LCN-2, indicating cancer pathology-related intestinal inflammation. Furthermore, VEH + VEH-treated and IRI + VEH-treated CRC-induced mice had significantly higher faecal LCN-2 levels compared to APX3330 + VEH-treated and APX3330 + IRI-treated tumour bearing mice. Significant changes in faecal LCN-2 level between treatment groups in both cancer-free and tumour-bearing mice provides biologically significant information regarding intestinal inflammation associated with different treatments as well as the disease pathology and severity.

2.4.2.2 Assessment of Leukocyte Accumulation and Nerve Fibre Density

To investigate immune cell infiltration into the distal colon, a pan leukocyte marker, anti-CD45 antibody, was used to label the cross-sections of the distal colon after 14 days of administration of IRI and APX3330 in mice without CRC. The total number

of CD45 positive cells was counted within the 0.4mm² area (**Figure 2.8**). To evaluate the density of the neuronal processes, cross-sections of the colon were labelled with anti- β -tubulin III antibody. The proportion of CD45+ immune cells to the density of β -tubulin III immunoreactive (IR) fibres was calculated. IRI treatment resulted in a significantly higher number of CD45+ cells in the distal colon (49.0 ± 3.6 cells/area) compared to untreated mice without cancer (19.1 ± 1.5 cells/area) and APX3330-treated mice (20.1 ± 1.5 cells/area) ($P < 0.0001$ for both) denoting elevated immune cell infiltration in the colons from IRI-treated mice (**Figure 2.8 A-A'', D**). On the contrary, the density of neuronal processes was considerably reduced in IRI-treated mice (2.0 ± 0.1 a.u) compared to untreated mice without cancer (3.0 ± 0.1 a.u) and APX3330-treated mice (3.0 ± 0.1 a.u) ($P < 0.0001$ for both) indicating damage to neuronal processes induced by IRI treatment (**Figure 2.8 B-B'', E**). The proportion of β -tubulin III-IR fibres to CD45+ cells in the distal colon was notably decreased in IRI-treated mice ($4.4 \pm 0.3\%$) compared to untreated ($18.5 \pm 1.6\%$) and APX3330-treated ($19.0 \pm 2.7\%$) ($P < 0.001$ for both) mice without cancer (n=5 mice/group) (**Figure 2.8 C-C'', F**).

Analysis of the immune cell infiltration into the colon in tumour-bearing mice at day 15 post-treatment showed that the number of CD45+ cells was significantly higher in both IRI + VEH-treated mice (78.0 ± 5.8 cells/area) and VEH + VEH-treated mice (69.4 ± 2.6 cells/area) which might be due to cancer progression. Treatment with APX3330 + VEH and APX3330 + IRI reduced the number of CD45+ cells in the colon to 24.5 ± 5.0 cells/area and 29.3 ± 3.5 cells/area compared to IRI + VEH and VEH + VEH-treated mice ($P < 0.0001$ for all) (**Figure 2.9 A-A'', D**). The density of neuronal processes in the distal colon were significantly lower in IRI + VEH-treated mice (2.3 ± 0.1 a.u) in comparison with VEH + VEH-treated mice (3.1 ± 0.1 a.u, $P < 0.01$), APX3330 + VEH-treated mice (4.4 ± 0.2 a.u, $P < 0.0001$) and APX3330 + IRI (3.6 ± 0.1 a.u, $P < 0.0001$) (**Figure 2.9 B-B'', E**). The density of β -tubulin III-IR fibres in APX + VEH-treated mice was higher compared to VEH + VEH treated ($P < 0.0001$) and APX3330 + IRI-treated ($P < 0.01$) groups. The proportions of β -tubulin III-IR fibres to CD45+ cells in IRI + VEH-treated mice ($3.2 \pm 0.3\%$) was similar to VEH + VEH-treated mice ($4.8 \pm 0.2\%$) but significantly lower compared to

APX3330 + VEH-treated ($19.0 \pm 2.7\%$, $P < 0.001$) and APX3330 + IRI-treated ($14.3 \pm 2.6\%$, $P < 0.01$) mice ($n=5$ mice/group) (**Figure 2.9 C-C''', F**). The proportion of β -tubulin III-IR fibres to CD45+ cells in both APX3330 + VEH and APX3330 + IRI groups was higher compared to VEH + VEH-treated group ($P < 0.001$ and $P < 0.05$, respectively) ($n=4-5$ mice/group).

2.4.2.3 Assessment of the Level of Myeloperoxidase

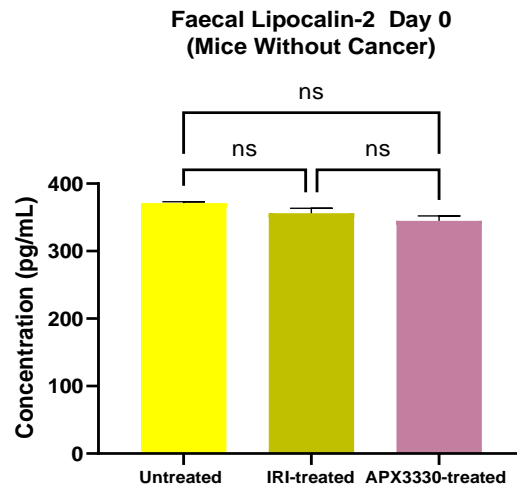
Myeloperoxidase (MPO) activation is a reliable marker of active inflammation. Cross-sectional preparations of the distal colon segments were labelled with an anti-MPO antibody to investigate the level of MPO within the 0.4mm^2 area (**Figure 2.10**). To evaluate the density of the neuronal processes, cross-sections of the colon were labelled with anti- β -tubulin III antibody. The proportion of β -tubulin III immunoreactive (IR) fibres to the level of MPO was calculated. IRI treatment resulted in a significantly higher level of MPO in the distal colon (3.1 ± 0.2 a.u) compared to untreated (1.4 ± 0.1 a.u, $P < 0.0001$) and APX3330-treated (1.9 ± 1.1 a.u, $P < 0.01$) mice without cancer (**Figure 2.10 A-A'', D**) confirming inflammation in the distal colons of IRI-treated mice. The density of neuronal processes was considerably reduced in IRI-treated mice (1.0 ± 0.1 a.u) compared to untreated (2.7 ± 0.1 a.u, $P < 0.0001$) and APX3330-treated (2.3 ± 0.3 a.u, $P < 0.001$) mice without cancer indicating damage to neuronal processes caused by IRI treatment (**Figure 2.10 B-B'', E**). The ratio of MPO levels in the distal colon to β -tubulin III-IR fibres was notably increased in IRI-treated mice (3.4 ± 0.6) when compared with untreated (0.5 ± 0.1 , $P < 0.0001$) and APX3330-treated (0.9 ± 0.1 , $P < 0.001$) mice without cancer ($n=5$ mice/group) (**Figure 2.10 C-C'', F**).

Analysis of the MPO levels in the colons of CRC-induced mice demonstrated significantly higher levels of MPO in both IRI + VEH-treated (4.8 ± 0.3 a.u) and VEH + VEH-treated (4.0 ± 0.2 a.u) mice (**Figure 2.11 A-A''', D**), which is consistent with the data on the CD45+ immune cell infiltration in the colon of CRC mice (**Figure**

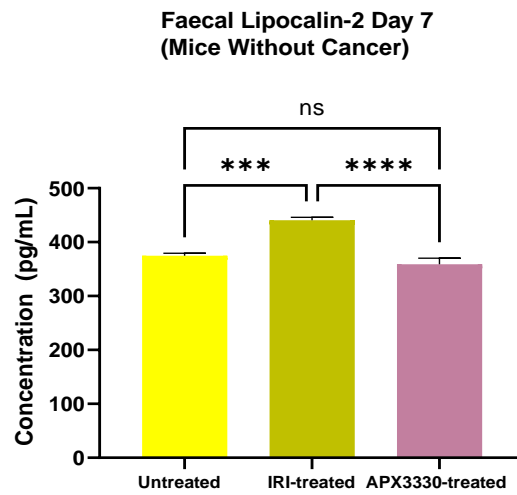
2.9). APX3330 + VEH-treated (1.3 ± 0.1 a.u) and APX3330 + IRI-treated (2.1 ± 0.3 a.u) CRC-induced mice showed significantly reduced MPO levels in the colon compared to VEH + VEH ($P < 0.0001$ and $P < 0.001$) and IRI + VEH ($P < 0.0001$) treated mice indicating anti-inflammatory properties of the treatments. The density of the neuronal processes in the distal colon was significantly lower in IRI-treated mice (2.0 ± 0.1 a.u) in comparison with VEH + VEH (3.2 ± 0.1 a.u), APX3330 + VEH (3.0 ± 0.1 a.u) and APX3330 + IRI (3.8 ± 0.1 a.u) treated mice ($P < 0.0001$ for all) **(Figure 2.11 B-B''', E)**. The ratio of MPO level to β -tubulin III-IR fibres was higher in IRI + VEH-treated mice (2.3 ± 0.1) and VEH + VEH-treated mice (1.3 ± 0.1) indicating increased damage to the neuronal processes in both groups. Treatment with APX3330 + VEH and APX3330 + IRI decreased the ratio of MPO level to β -tubulin III-IR fibres (0.4 ± 0.1 and 0.6 ± 0.1 , respectively) compared to VEH + VEH-treated ($P < 0.0001$ and $P < 0.001$, respectively) and IRI + VEH-treated ($P < 0.0001$ for both) groups (n=4-5 mice/group) **(Figure 2.11 C-C''', F)**.

Figure 2.6 Neutrophil gelatinase-associated protein lipocalin-2 levels measured in the faeces from untreated, IRI-treated, and APX3330-treated mice without CRC. Faecal lipocalin-2 levels before treatment (A), at day 7 (B), and day 14 (C) of IRI and APX3330 administration compared to untreated mice. Data presented as mean \pm S.E.M. * P <0.05, *** P <0.001, **** P <0.0001, n =5 mice/group.

A



B



C

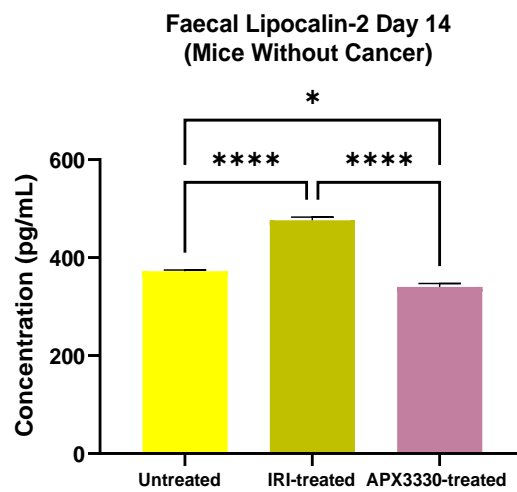
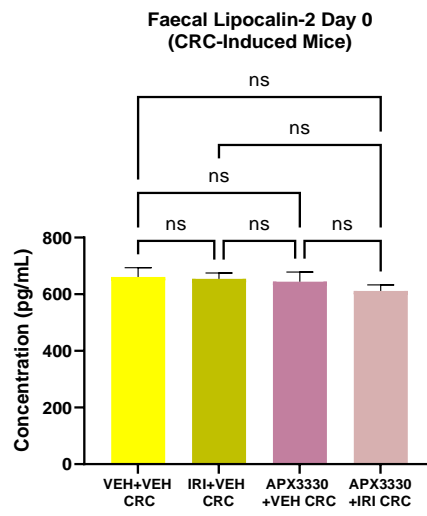
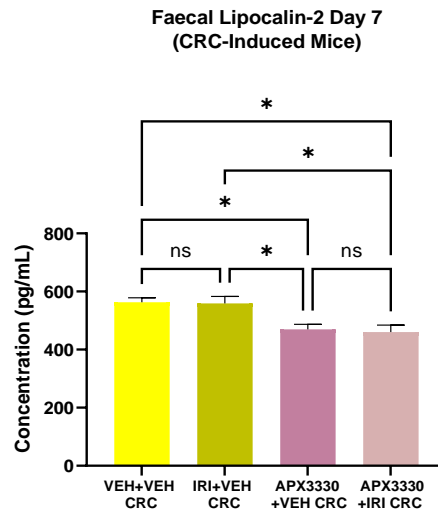


Figure 2.7 Neutrophil gelatinase-associated protein lipocalin-2 levels measured in CRC-induced mice. Faecal Lipocalin-2 levels before treatment (A), on day 7 (B), and day 14 (C). Data presented as \pm S.E.M. * P <0.05, ** P <0.001, n=4-5 mice/group.

A



B



C

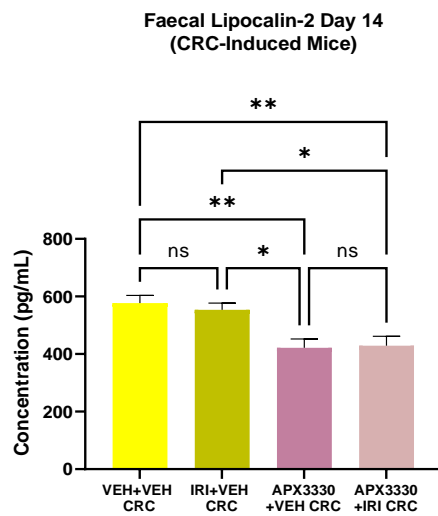


Figure 2.8 Effects of treatments on the number of CD45+ immune cells and β -Tubulin III-immunoreactive (IR) neuronal fibre density in the distal colon of mice without cancer. Cross-sectional preparations of the distal colon (20 μ m/section) from untreated (A), IRI-treated (A'), and APX3330-treated (A'') mice without CRC were labelled with a pan leukocyte marker anti-CD45 antibody (yellow) to label immune cells. Neuronal fibre density is labelled with a neuronal marker anti- β Tubulin III antibody (magenta) (B-B'') in cross-sectional preparations of the distal colon. Merged images of CD45+ and β -Tubulin III immunolabeling (C-C''). Scale bar = 100 μ m. Quantitative analysis of the number of CD45+ cells in the distal colon cross-sections (D), the density of β -Tubulin-IR nerve fibres of the distal colon cross-sections (arbitrary units, a.u) (E), the proportion of β -Tubulin III immunoreactive fibres to CD45+ cells (F). The total number of CD45+ immune cells and the density of neuronal processes within a 0.4mm² area were quantified. Data presented as mean \pm S.E.M. *** P <0.001 **** P <0.0001, n=5 mice/group.

CD45+ / β -Tubulin III / Merged

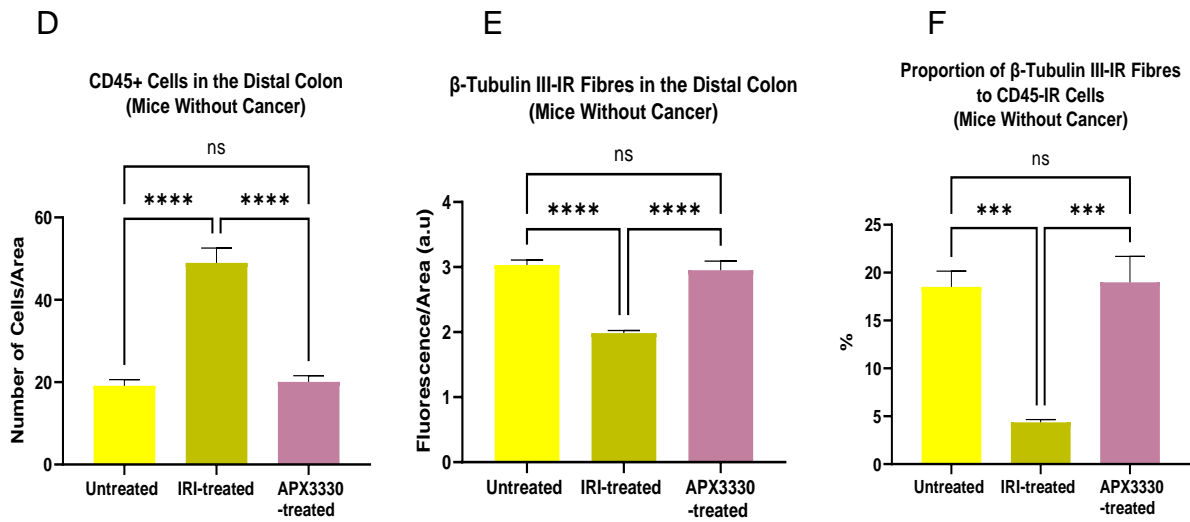
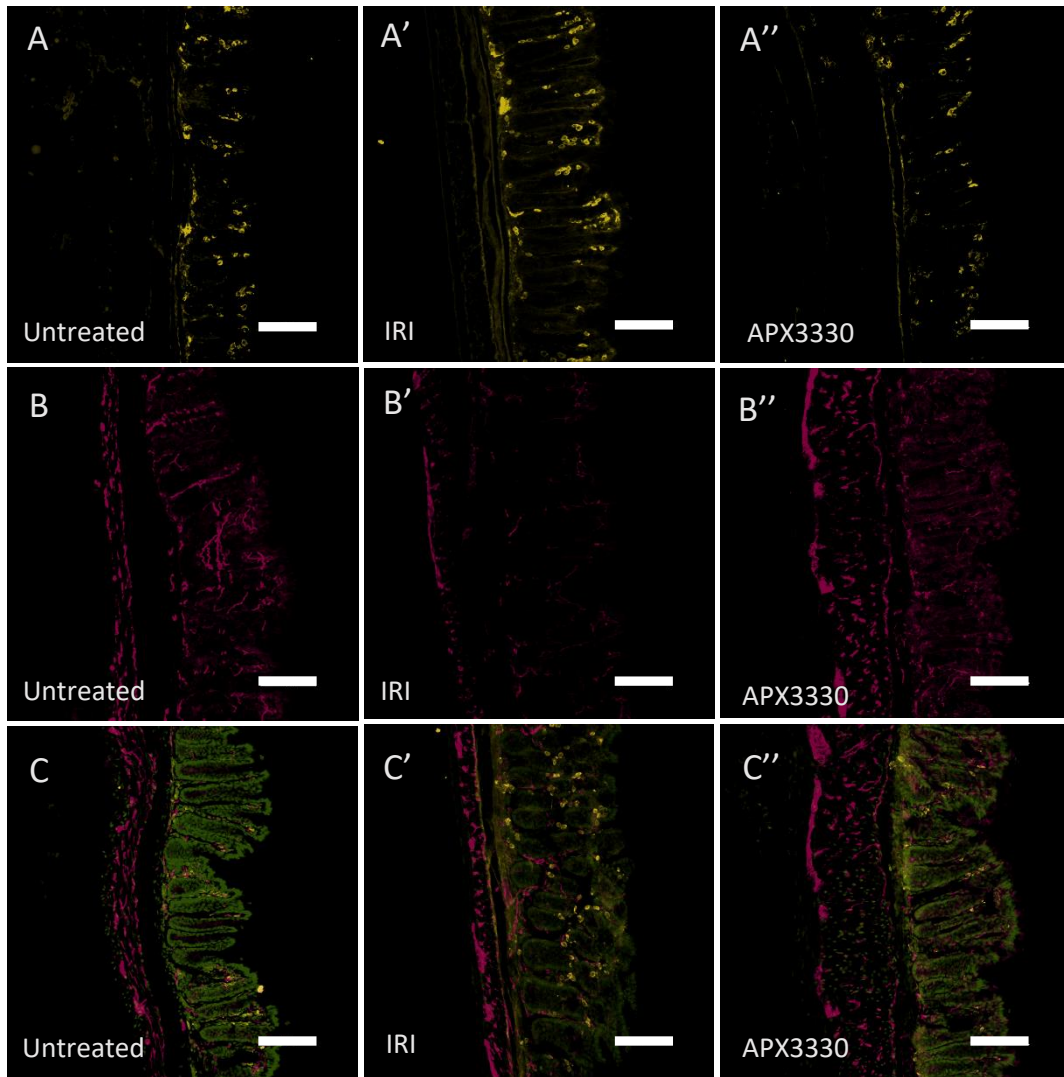
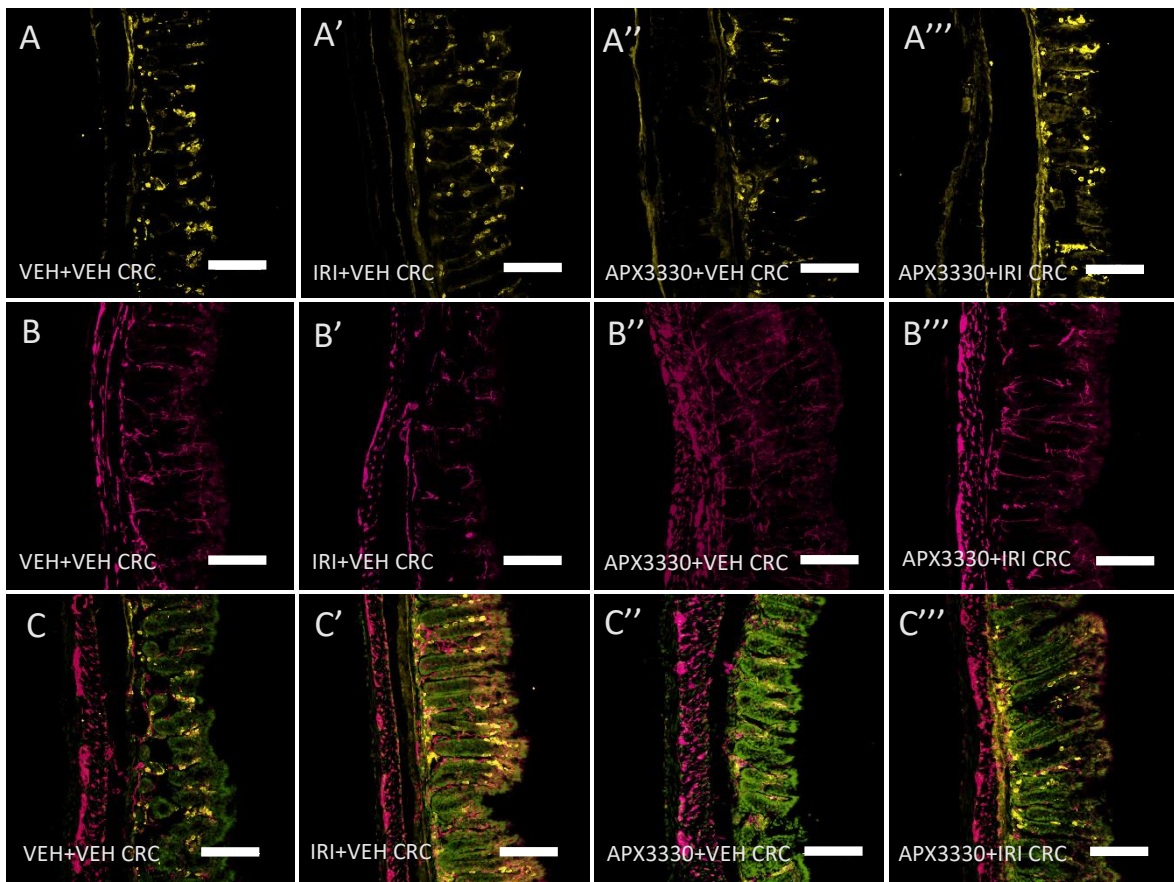
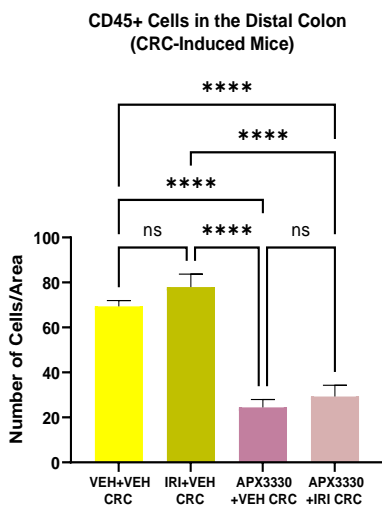


Figure 2.9 The number of CD45+ immune cells and neuronal fibre density in the distal colon of CRC-induced mice. Cross-sectional preparations of the distal colon (20µm/section) from vehicle (A), IRI+VEH-treated (A'), APX3330+VEH-treated (A''), and combination therapy of APX3330 + IRI treated (A''') mice with CRC labelled with a pan leukocyte marker anti-CD45 antibody (yellow). Neuronal fibre density in cross-sectional preparations of the distal colon labelled with a neuronal marker anti-β Tubulin III antibody (magenta) (B-B'''). Merged images of CD45+ and β-Tubulin III Immunolabelling (C-C'''). Scale bar = 100µm. Quantitative analysis of the number of CD45+ cells in the distal colon cross-sections (D), the density of β-Tubulin-IR nerve fibres in the distal colon cross-sections (arbitrary units, a.u) (E), and the proportion of β-Tubulin III immunoreactive fibres to CD45+ cells (F). The total number of CD45+ immune cells and the density of neuronal fibres were quantified within a 0.4mm² area. Data presented as mean ± S.E.M. **P*<0.05, ***P*<0.01, ****P*<0.001, *****P*<0.0001, n=4-5 mice/group.

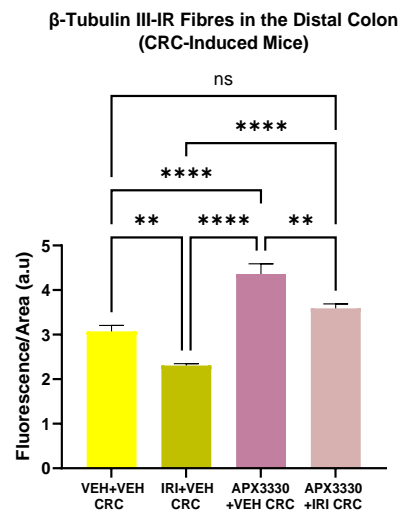
CD45+ / β -Tubulin III / Merged



D



E



F

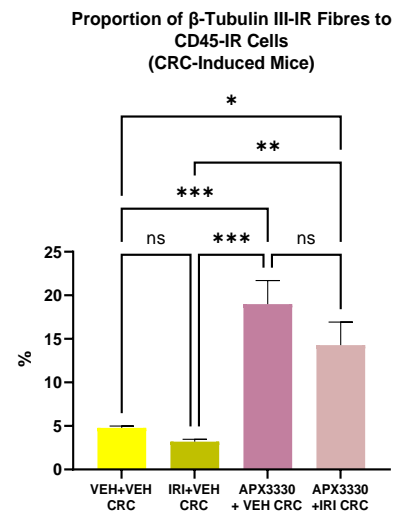


Figure 2.10 The level of myeloperoxidase (MPO) and neuronal fibre density in the distal colon of mice without cancer. Cross-sectional preparations of the distal colon (20µm/section) from untreated (A), IRI-treated (A'), and APX3330-treated (A'') mice labelled with an anti-MPO antibody (yellow). The neuronal fibres labelled with a neuronal marker, anti-β Tubulin III antibody (purple) (B-B''). Merged images of MPO and β-Tubulin III immunoreactivity (C-C''). Scale bar = 100µm. Quantitative analysis of the MPO level in the distal colon cross-sections (D), the density of β-Tubulin-IR nerve fibres of the distal colon cross-sections (arbitrary units, a.u) (E), and the proportion of β-Tubulin III immunoreactive fibres to MPO level (F). The level of MPO and the density of fibres were quantified within a 0.4mm² area. Data presented as mean ± S.E.M. ***P*<0.01, *** *P*<0.001, *****P*<0.0001, n=5 mice/group.

MPO/ β -Tubulin III/ Merged

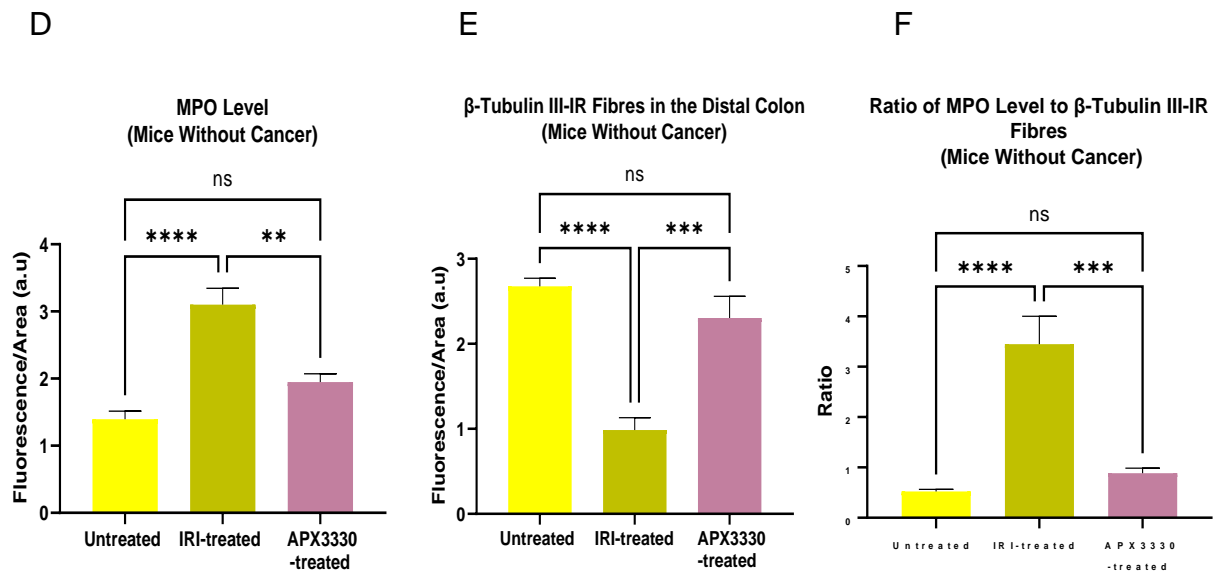
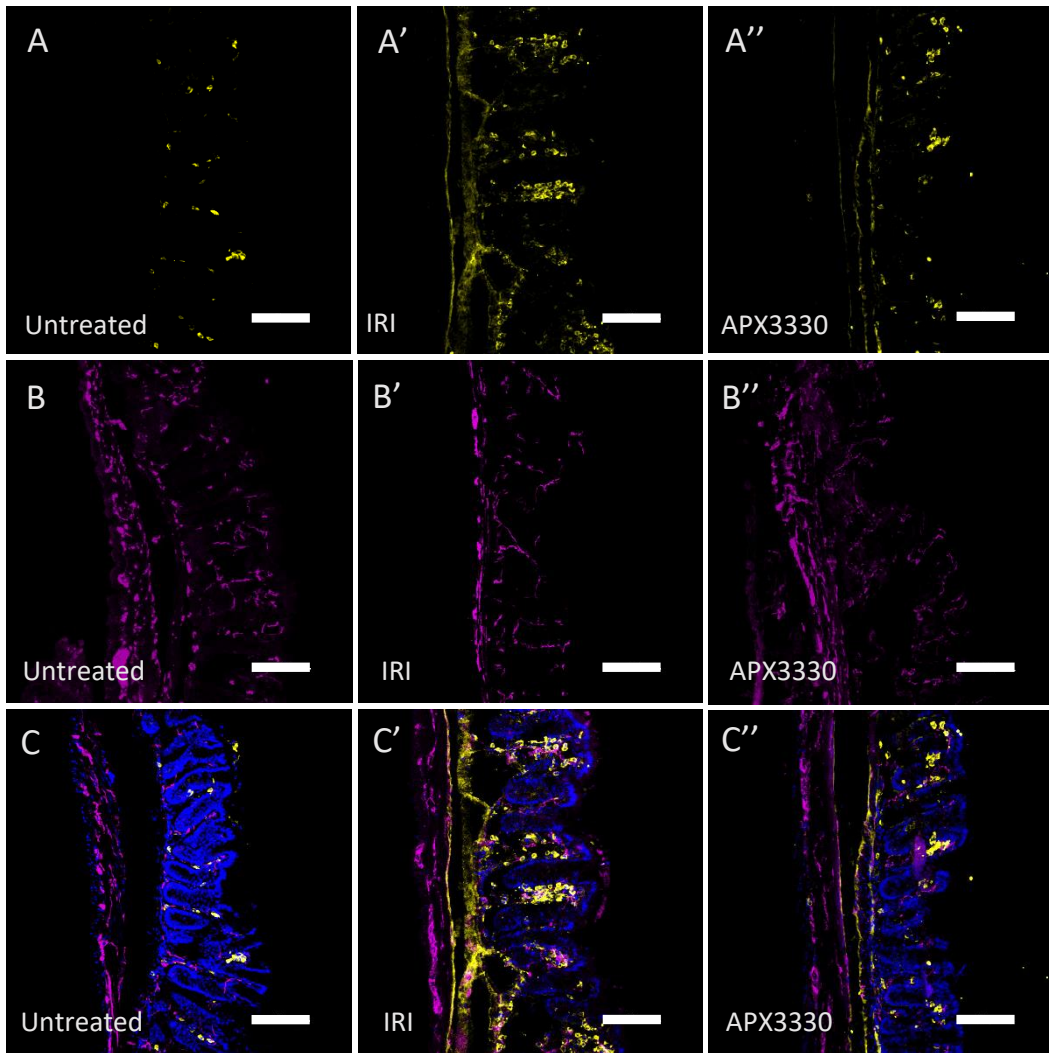
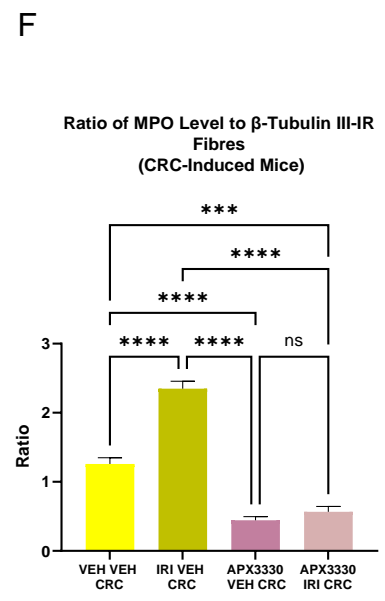
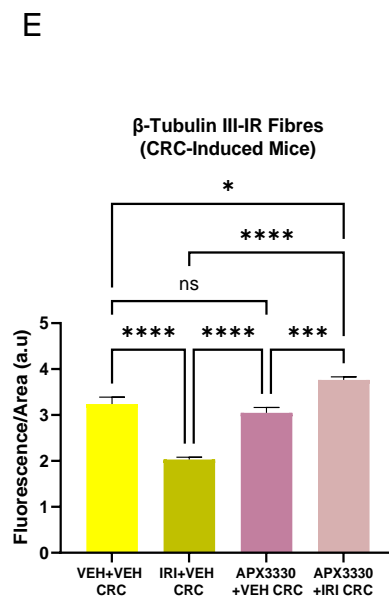
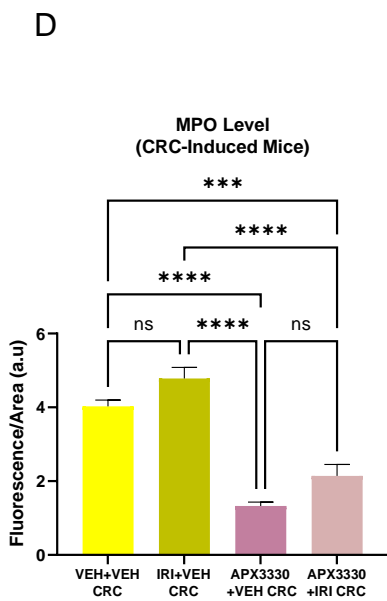
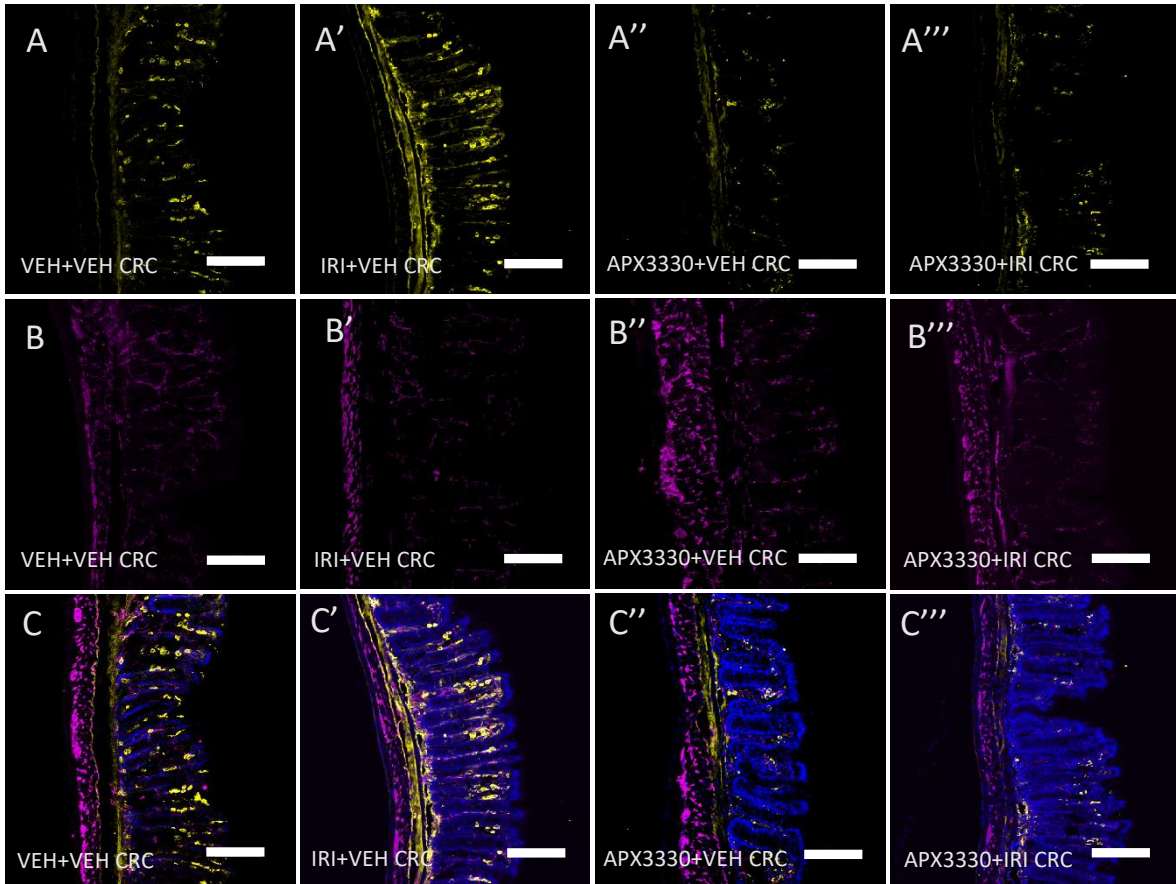


Figure 2.11 The level of myeloperoxidase (MPO) and neuronal fibre density in the distal colon of CRC-induced mice. Cross-sectional preparations of the distal colon (20µm/section) from vehicle-treated (A), IRI-treated (A'), APX3330-treated (A''), and combination therapy APX3330 + IRI-treated (A''') mice labelled with an anti-MPO antibody (yellow). The neuronal fibres labelled with a neuronal marker, anti-β Tubulin III antibody (purple) (B-B'''). Merged images of MPO+ and β-Tubulin III Immunoreactivity (C-C'''). Scale bar = 100µm. Quantitative analysis of the MPO level in the distal colon cross-sections (D), the density of β-Tubulin-IR nerve fibres of the distal colon cross-sections (arbitrary units, a.u) (E), and the proportion of β-Tubulin III immunoreactive fibres to MPO level (F). The level of MPO and the density of neuronal fibres were quantified within a 0.4mm² area. Data presented as mean ± S.E.M. **P*<0.05, ****P*<0.001, *****P*<0.0001, n=4-5 mice/group.

MPO/ β -Tubulin III/ Merged



2.4.3 Effect of the Treatments on the Total Number of Myenteric Neurons, a Subpopulation of Cholinergic Neurons, and Cholinergic Fibres

2.4.3.1 Effect of Treatments on the Total Number of Myenteric Neurons and Cholinergic Neurons

The enteric nervous system contains inhibitory and excitatory neurons that can be identified through their expression of neuronal nitric oxide synthase (nNOS) and choline acetyltransferase (ChAT), respectively (Furness, 2012). These excitatory and inhibitory enteric neurons predominately regulate gastrointestinal functions. Several studies have found that long-term intestinal inflammation has been identified as the main contributor to the damage to the enteric nervous system, including possible myenteric neuronal loss of up to 50% (Nurgali et al., 2007, Nurgali et al., 2011, Boyer et al., 2005), which may contribute to gastrointestinal dysfunction in the long-term. Acetylcholine is a major excitatory neurotransmitter in the gastrointestinal system that controls circular and smooth muscle contraction (Furness, 2012) and gastric secretion (Cooke, 2000). Previous research has found that chronic Irinotecan administration caused a significant increase in the proportion of ChAT-immunoreactive (IR) neurons and vesicular choline acetyltransferase (VACHT)-IR fibres in mice. Cholinergic neurons and cholinergic nerve fibres play an essential aspect in the excitatory motor innervation of the gut (Furness, 2012). VACHT-IR fibres facilitate essential GI tract functions such as mucus production, the vasomotor tone, and intestinal motility (Cervi et al., 2014).

To investigate the changes in the total number of myenteric neurons in the distal colon, wholemount preparations of the distal colon were labelled with a pan-neuronal marker anti-protein gene product 9.5 (PGP9.5) antibody to count neurons within a 0.4 mm² area (**Figure 2.12 A-A'**). In line with our previous findings (McQuade et al., 2017), our data demonstrate that repeated administration of IRI caused a significant reduction of myenteric neurons (60.0 ± 3.5 neurons/area)

compared to untreated (87.0 ± 6.6 neurons/area, $P < 0.01$) and APX3330-treated (80.8 ± 3.5 neurons/area, $P < 0.05$) groups. APX3330 treatment prevented the damage to myenteric neurons in the distal colon of mice without cancer ($n=5$ mice/group) (**Figure 2.12 A-A'', E**).

Our previous studies demonstrated a significant increase in a sub-population of choline acetyltransferase (ChAT)-positive neurons following IRI treatment (McQuade et al., 2017). To determine if APX3330 treatment modulates these changes, wholemount preparations of the distal colon were labelled with an anti-ChAT antibody. The average number of ChAT-IR neurons was higher in the IRI-treated group (49.7 ± 2.5 neurons/area) compared to the untreated (37.9 ± 2.0 neurons/area, $P < 0.05$) and APX3330-treated (32.1 ± 2.8 neurons/area, $P < 0.001$) groups (**Figure 2.12 B-B'', F**). The proportion of ChAT-IR cells to the total number of PGP9.5-IR neurons in the myenteric plexus was higher in the IRI-treated group ($84.8 \pm 5.6\%$) compared to the untreated ($45.6 \pm 1.7\%$) and APX3330-treated ($41.1 \pm 3.7\%$) groups ($P < 0.0001$ for both) ($n=5$ mice/group) (**Figure 2.12 D-D'', G**).

In CRC-induced cohort, IRI treatment caused significant reduction in myenteric neurons (62.6 ± 3.0 neurons/area) compared to APX3330 + VEH treatment (94.7 ± 3.2 neurons/area, $P < 0.0001$), APX3330 + IRI treatment (88.1 ± 4.9 neurons/area, $P < 0.001$) and VEH + VEH treatment groups (84.3 ± 3.3 neurons/area, $P < 0.01$, $n=5$ mice/group) (**Figure 2.13 A-A''', E**). The number of ChAT-IR neurons in the myenteric ganglia of VEH + VEH-treated and IRI + VEH-treated mice was similar (60.5 ± 2.2 neurons/area and 56.7 ± 2.7 neurons/area, respectively). Treatments with APX3330 + VEH and APX3330 + IRI significantly reduced the number of ChAT-IR neurons (35.0 ± 0.7 neurons/area and 36.6 ± 2.0 neurons/area compared to VEH + VEH-treated and IRI + VEH-treated groups) ($P < 0.0001$ for all) (**Figure 2.13 B-B''', F**). The proportion of ChAT-IR cells to the total number of PGP9.5-IR neurons in the myenteric plexus was the highest in the IRI + VEH-treated group ($90.5 \pm 0.6\%$) compared to VEH + VEH-treated ($72.0 \pm 1.8\%$), APX3330 + VEH-treated ($37.4 \pm 1.0\%$) and APX3330 + IRI-treated ($41.8 \pm$

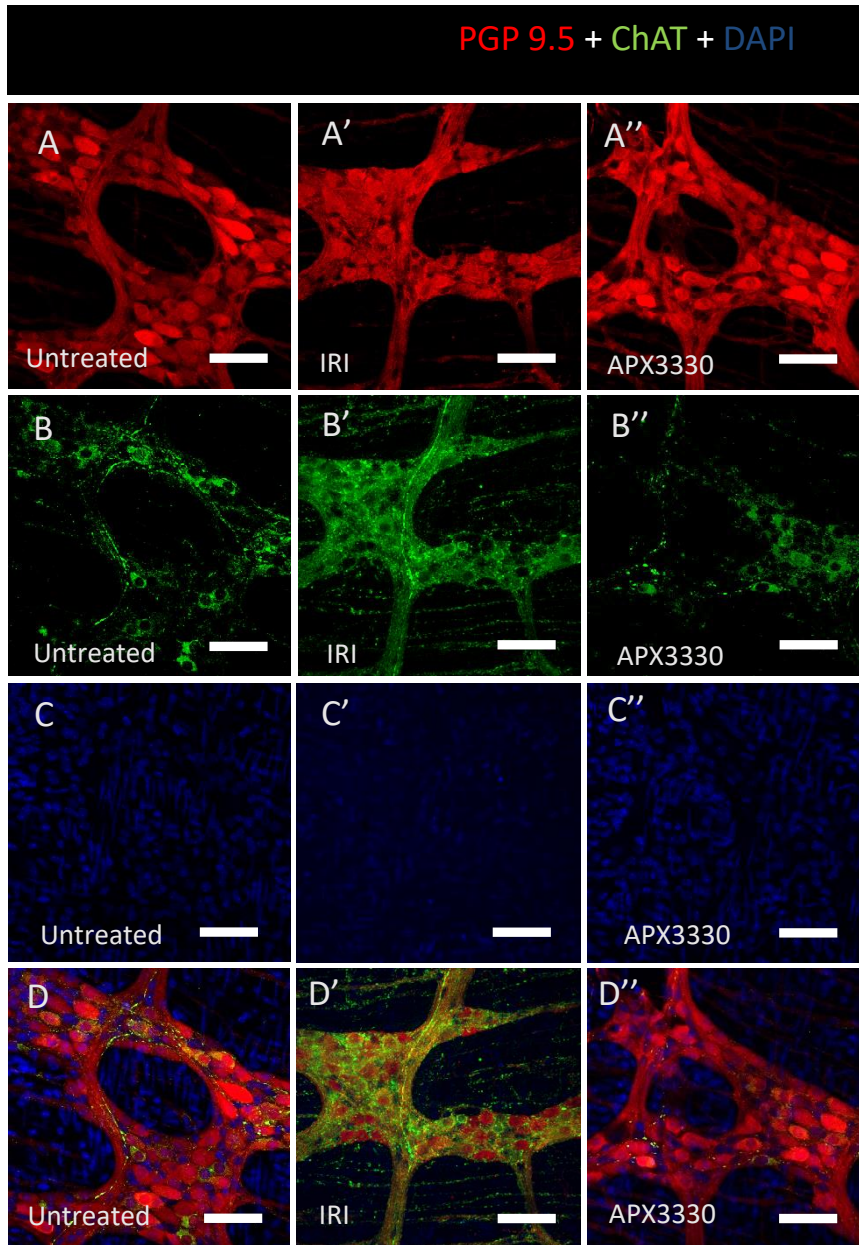
1.1%) groups ($P < 0.0001$ for all). The proportion of ChAT-IR neurons in the APX3330 + VEH-treated and APX3330 + IRI-treated mice was significantly lower compared to VEH + VEH-treated mice ($P < 0.0001$ for both) ($n = 4-5$ mice/group) (**Figure 2.13 D-D''', G**).

2.4.3.2 Effect of the Treatments on Cholinergic Nerve Fibres

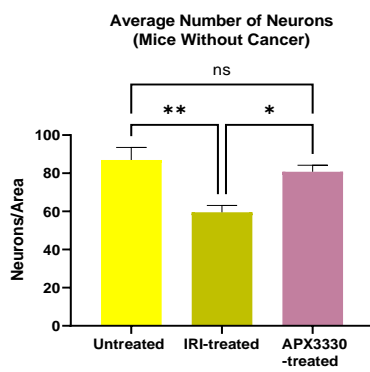
To determine whether IRI treatment caused changes in the cholinergic fibres within the myenteric plexus, the wholemount preparations of the distal colon from mice without cancer were labelled with anti-vesicular acetylcholine transporter (VACHT) antibody (**Figure 2.14 A-A''**). The effect of repeated *in vivo* administration of IRI and APX3330 on the density of VACHT-IR cholinergic fibres in the myenteric plexus was assessed within a 0.4mm^2 area. The density of VACHT-IR fibres was higher in the IRI-treated group (27.7 ± 0.8 a.u) compared to untreated (10.9 ± 1.2 a.u) and APX3330-treated (9.1 ± 0.4 a.u) groups ($P < 0.0001$ for both) ($n = 5$ mice/group) (**Figure 2.14 B**).

Similarly, the density of VACHT-IR fibres in mice with CRC was higher in the IRI + VEH-treated group (21.4 ± 1.0 a.u) compared to the VEH + VEH-treated (16.8 ± 1.1 a.u, $P < 0.01$), APX3330 + VEH-treated (14.8 ± 0.1 a.u, $P < 0.001$), and APX3330 + IRI-treated (14.6 ± 0.4 a.u, $P < 0.0001$) groups ($n = 4-5$ mice/group) (**Figure 2.15 A-A''', B**).

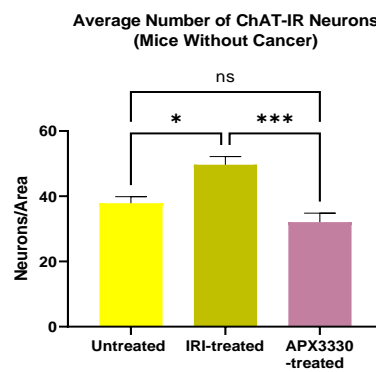
Figure 2.12 Effect of *in vivo* treatments on ChAT-IR neurons in mice without cancer. Wholemout preparations of the myenteric ganglia from the distal colon of untreated, IRI-treated, APX3330-treated mice following 14-day of *in vivo* treatment labelled with a pan-neuronal marker anti-PGP9.5 antibody (red) (A-A''), a cholinergic neuronal marker, choline acetyltransferase (ChAT) (green) (B-B'') and DAPI (C-C''). Merged images (D-D''). Scale bar = 50µm. Quantitative analysis of the average number of myenteric neurons immunoreactive for PGP9.5 (E), the average number of ChAT-immunoreactive cholinergic neurons (F), and the proportion of ChAT-IR neurons to the total number of PGP9.5-IR neurons (G) in the myenteric ganglia within 0.4 mm² area. Data presented as mean ± S.E.M. **P*<0.05, ***P*<0.01, ****P*<0.001 *****P*<0.0001, n=5 mice/group.



E



F



G

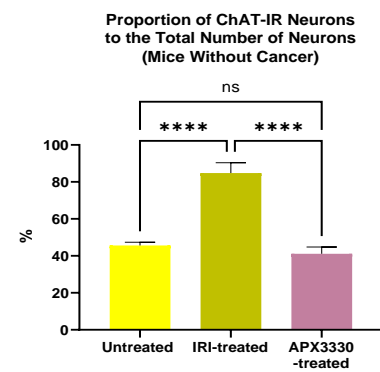


Figure 2.13 Effect of *in vivo* treatments on ChAT-IR neurons in mice with CRC.

Wholemount preparations of the myenteric ganglia from the distal colon of CRC-induced mice treated with two vehicles, IRI plus vehicle for APX3330, APX3330 plus vehicle for IRI, and a combination of APX3330 and IRI for 14 days labelled with a pan-neuronal marker anti-PGP9.5 antibody (red) (A-A'''), a cholinergic neuronal marker, choline acetyltransferase (ChAT) (green) (B-B''') and DAPI (C-C'''). Merged images (D-D'''). Scale bar = 50µm. Quantitative analysis of the average number of myenteric neurons immunoreactive for PGP9.5 (E) average number of ChAT-immunoreactive cholinergic neurons (F), the proportion of ChAT-IR neurons to the total number of PGP9.5-IR neurons (G) in the myenteric ganglia within 0.4 mm² area. Data presented as mean ± S.E.M. ***P*<0.01, ****P*<0.001 *****P*<0.0001, n=4-5 mice/group.

PGP 9.5 + ChAT + DAPI

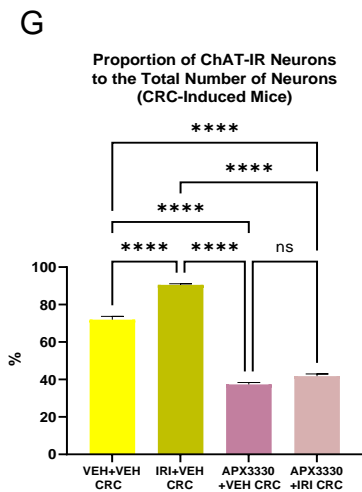
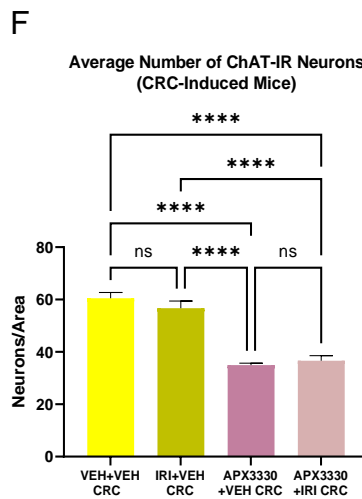
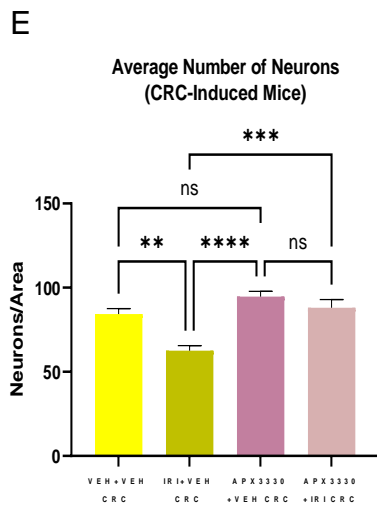
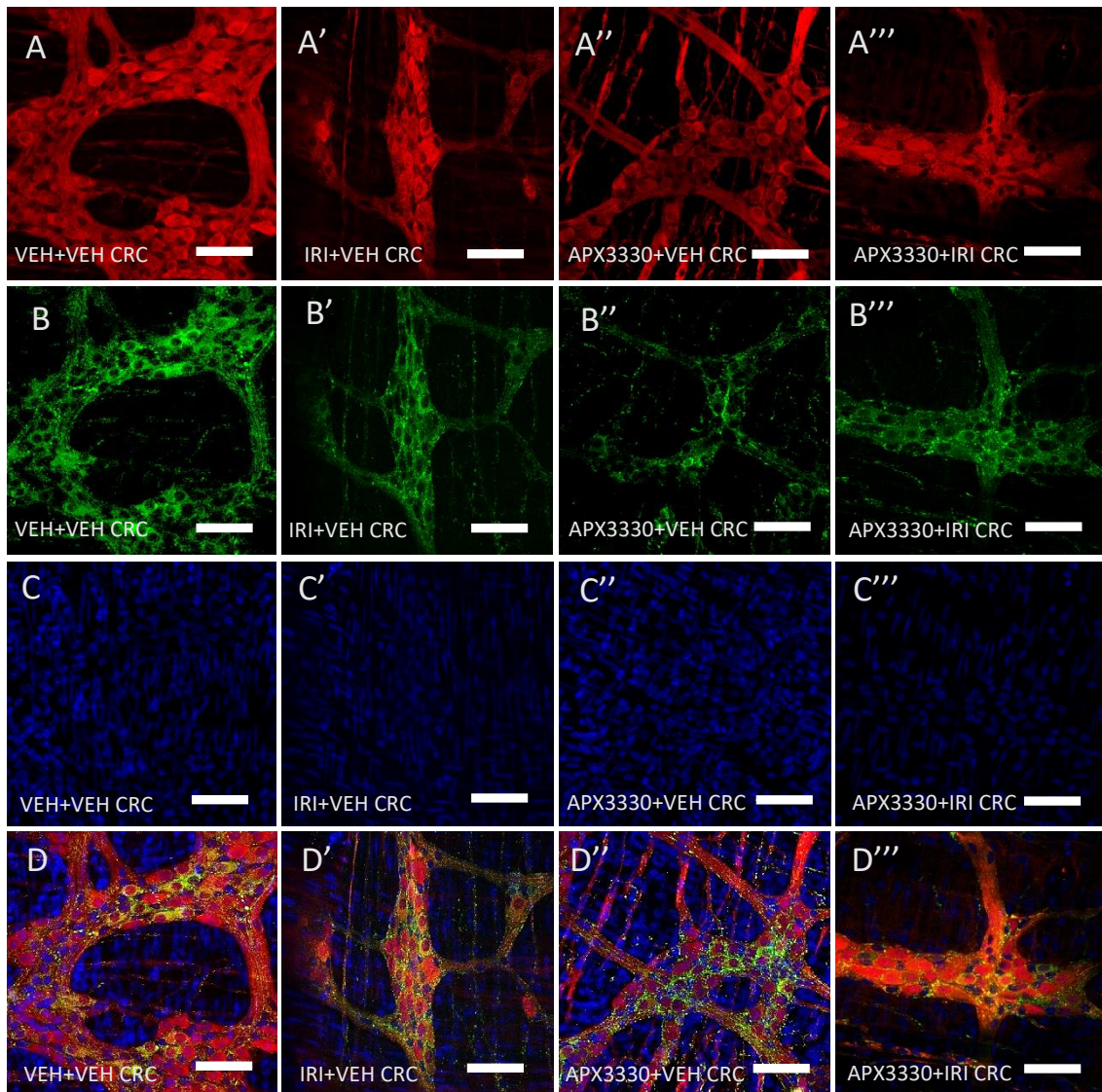
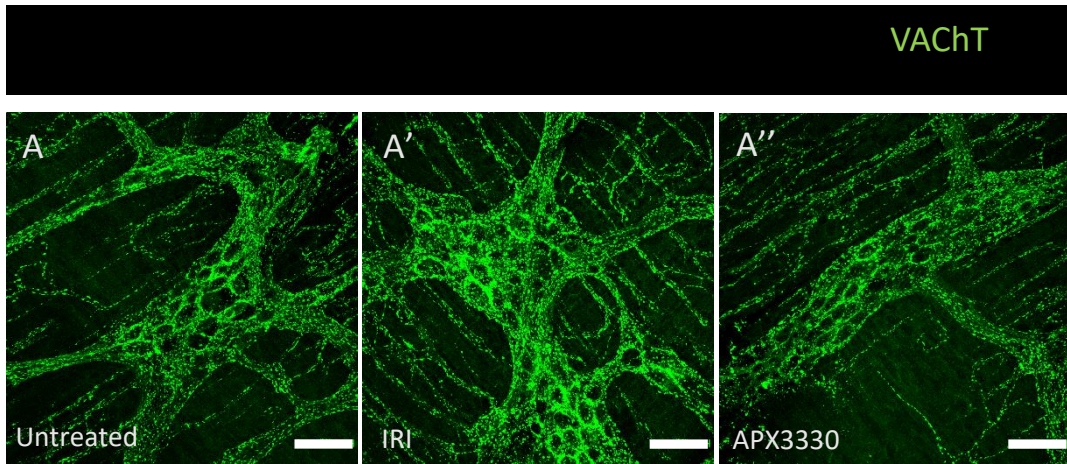


Figure 2.14 Effect of the treatments on the density of cholinergic fibres in mice without cancer. Wholemout preparations of the myenteric ganglia from the distal colon of untreated, IRI-treated, APX3330-treated mice following 14-day *in vivo* treatment labelled with a cholinergic nerve fibre marker anti-vesicle acetylcholine transferase (VACHT), antibody (green) (A-A''). Scale bar = 50µm. Quantitative analysis of the density of cholinergic nerve fibres immunoreactive to anti-VACHT antibody in the myenteric ganglia (B) within a 0.4mm² area. Data presented as mean ± S.E.M. *****P*<0.0001, *n*=5 mice/group.



B

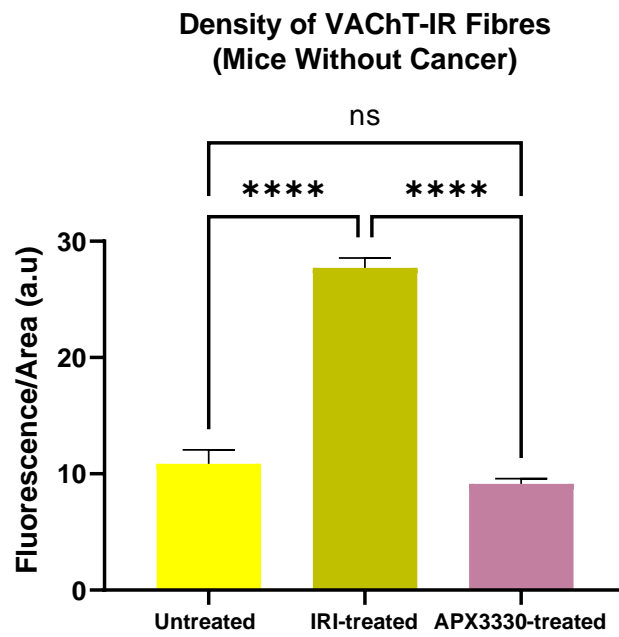
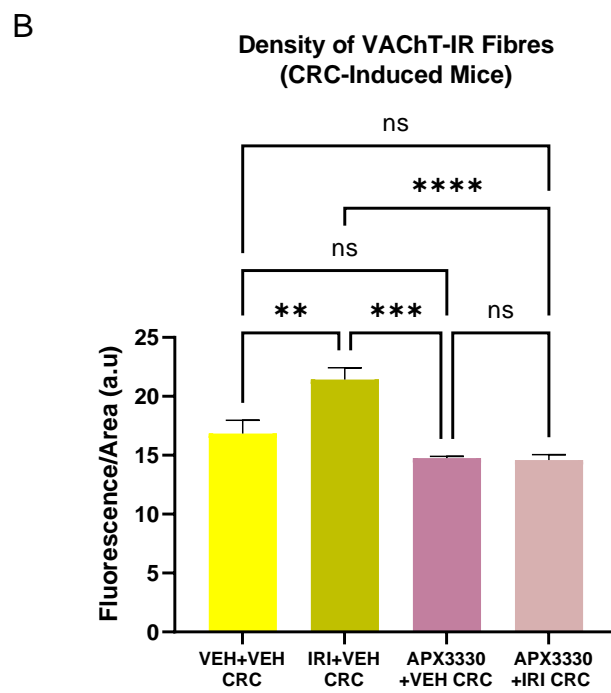
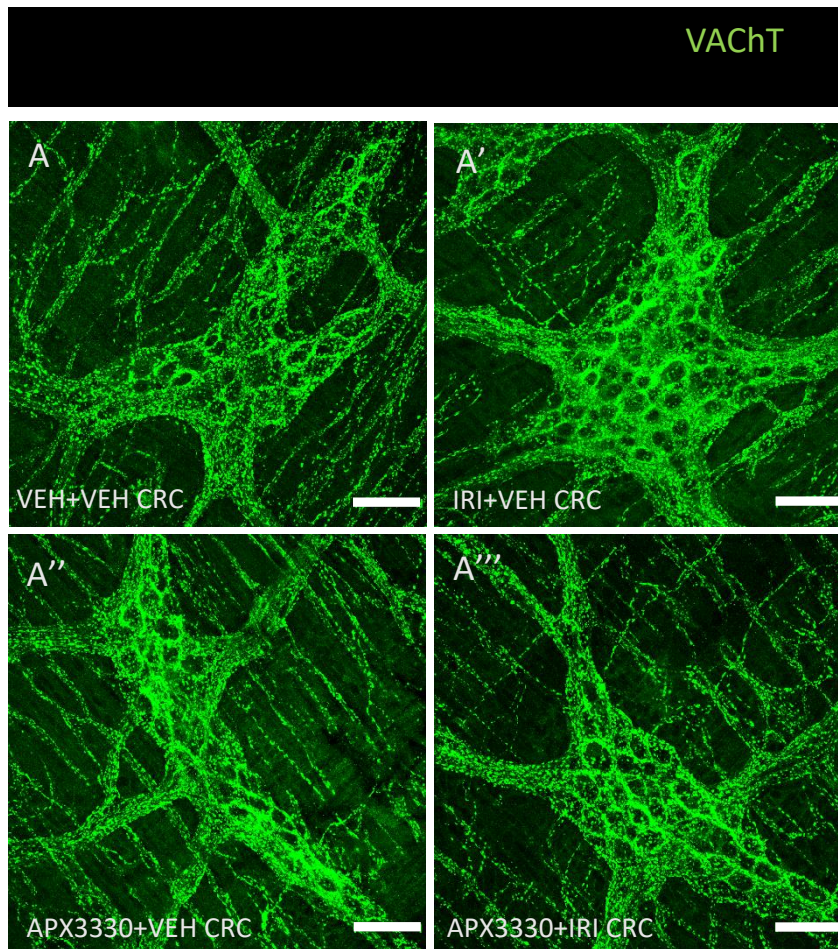


Figure 2.15 Changes in the density of cholinergic fibres in mice with CRC.

Wholemout preparations of the myenteric ganglia from the distal colon of mice treated with two vehicles, IRI plus vehicle for APX3330, APX3330 plus vehicle for IRI, and a combination of APX3330 and IRI for 14 days labelled with a cholinergic nerve fibre marker, anti-vesicle acetylcholine transferase (VACht) (green) (A-A'''). Scale bar = 50µm. Quantitative analysis of the density of cholinergic nerve fibres immunoreactive to anti-VACht antibody in the myenteric ganglia (B) within a 0.4mm² area. Data presented as mean ± S.E.M. ***P*<0.01, ****P*<0.001, *****P*<0.0001, n=4-5 mice/group.



2.4.4.1 Effect of the Treatments on APE1/Ref-1 Expression in Mice Without Cancer

In most cells APE1/Ref-1 is found in the nucleus of the cell including cancer cells as well as in neurons. As a result of disease or disease progression the protein becomes more cytosolic than residing in the nucleus. APE1/Ref-1 abundantly spread throughout the intracellular space to regulate many proteins that are involved with cell growth, survival, metastasis, and angiogenesis. In this study we have found that factors such as the pathological condition of cancer as well as IRI-induced inflammation can overstimulate the expression of APE1/Ref-1 in the cell. We used APX3330 as a single agent treatment as well as in combination of IRI for the treatment of CRC. APX3330 functions as a dual functioning molecule that has a redox regulation site and a DNA repair active site (Long et al., 2021, Mijit et al., 2022). We believe that APX3330 mitigate the adverse changes that occurred in the cell as result of hyper-activated APE1/Ref-1 due to pathological condition of cancer as well as a side effect of chemotherapy via several regulatory pathways. Once the damaged sites are removed by various glycosylases, the repair active site of APE1/Ref-1 nicks the DNA backbone creating a hydroxyl and 5'dRp group aiding repair of the single-strand DNA damage induced by reactive oxygen species (ROS) (Malfatti et al., 2021). When APE1/Ref-1 proteins' redox-active site is inhibited by APX3330, it prevents the activation of transcription factors such as AP-1, NFkB, and STAT3 (Shah et al., 2017). Thus, preventing cancer proliferation, migration, survival, angiogenesis, and inflammation. On the other hand, endonuclease activity of APX3330 prevents neuronal DNA damage and apoptosis (Heisel et al., 2021). Despite the positive outcomes of OXL and IRI in cancer treatment, these chemotherapeutic agents induce vast amounts of ROS that may contribute as a significant factor for DNA damage or cytotoxicity. Previous studies have found that OXL treatment causes the changes in APE1/Ref-1 in DRG neurons (Kelley et al., 2016). To determine if IRI treatment is associated with changes in the APE1/Ref-1 expression in the myenteric plexus of the distal colon, anti-Apurinic/aprimidinic endonuclease-1 (APE1/Ref-1) antibody was used (**Figure 2.16 A-A''**). The number of APE1/Ref-1 immunoreactive cells was significantly higher in the IRI-treated

group compared to untreated and APX3330-treated groups indicative of increased activation of the APE1/Ref-1. IRI treatment increased the number of APE1/Ref-1-IR cells (59.3 ± 2.1 cells/area) compared to untreated (37.7 ± 1.6 cells/area) and APX3330-treated mice (40.6 ± 1.8 cells/area) ($P < 0.0001$ for both) following 14 days of *in vivo* treatment. APX3330 treatment reduced the number of APE1/Ref-1 immunoreactive cells in the distal colon myenteric ganglia of mice without cancer, similar to untreated mice (n=5 mice/group) (**Figure 2.16 B**).

Quantitative analysis of the APE1/Ref-1 level of fluorescence in the distal colon myenteric ganglia is presented in **Figure 2.17**. The effect of *in vivo* IRI and APX3330 treatment on the APE1/Ref-1 expression per ganglia (**Figure 2.17A**), APE1/Ref-1 expression per area (0.4mm^2 area) (**Figure 2.17B**), and the proportion of APE1/Ref-1-IR cells to PGP9.5 neurons per ganglion (**Figure 2.17C**) was assessed in cancer-free mice. APE1/Ref-1 expression per ganglion was significantly higher in IRI-treated group (17.0 ± 1.1 a.u) compared to both untreated (10.0 ± 0.5 a.u) and APX3330-treated (12.7 ± 0.4 a.u) groups ($P < 0.0001$ for both). APX3330-treated mice also showed significantly higher APE1/Ref-1 expression per ganglion (12.7 ± 0.4 a.u) compared to untreated mice (10.0 ± 0.5 a.u, $P < 0.01$). Similarly, APE1/Ref-1 expression per area was also significantly higher in the IRI-treated group (6.5 ± 0.1 a.u) compared to both untreated (4.7 ± 0.2 a.u) and APX3330-treated (4.9 ± 0.2 a.u) ($P < 0.0001$ for both) groups indicating a higher distribution of APE1/Ref-1 protein expression following IRI treatment. Data revealed that the IRI-treated group had the highest proportion of APE1/Ref-1: PGP 9.5 ($88.1 \pm 3.6\%$) compared to both untreated ($32.3 \pm 1.8\%$) and APX3330-treated ($39.2 \pm 1.8\%$) mice ($P < 0.0001$ for both) (n=5 mice/group).

To assess the amount of APE1/Ref-1 protein expression in the distal colon of cancer-free mice, western blot analysis was performed using anti-APE1/Ref-1 antibody (**Figure 2.18**). An image of the membrane merged with the ladder after the protein transfer step has been included in supplementary data (**Figure S2.1A**). A higher level of APE1/Ref-1 expression is an indication of increased cellular

oxidative stress induced by IRI treatment. Data revealed that IRI-treated mice exhibited the highest level of APE1/Ref-1 protein expression (1.38 ± 1.2 a.u) compared to untreated (0.8 ± 0.1 a.u, $P < 0.01$) and APX3330-treated (0.9 ± 0.1 a.u, $P < 0.05$) mice (n=5 mice/group).

2.4.4.2 Effect of Treatments on the APE1/Ref-1 Expression in CRC-Induced Mice

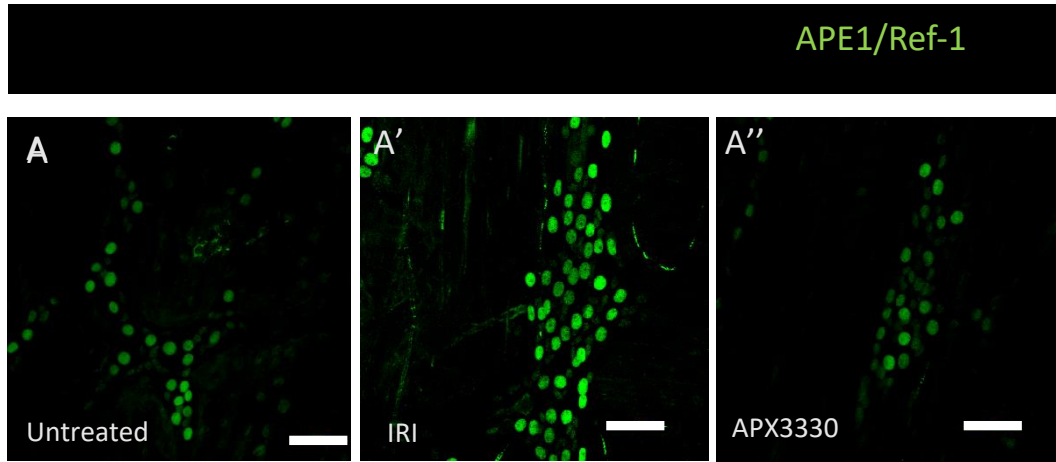
APE1/Ref-1 expression in the myenteric plexus of the distal colon was assessed following 14-day *in vivo* administration of two vehicles (VEH + VEH), APX3330 + VEH, IRI + VEH, and a combination of APX3330 + IRI (**Figure 2.19 A-A''**, **B**). The number of APE1/Ref-1 immunoreactive cells in APX3330 + VEH treatment (52.8 ± 1.7 cells/area) was the lowest compared to IRI + VEH (72.9 ± 3.0 cells/area, $P < 0.001$) and VEH + VEH (66.8 ± 3.0 cells/area, $P < 0.01$) treated groups, but not statistically significant to APX3330 + IRI-treated group (54.9 ± 1.5 cells/area) (n=4-5 mice/group).

The quantitative analysis of the level of myenteric neurons and APE1/Ref-1 immunofluorescence is presented in **Figure 2.20**. The effect of *in vivo* treatment with APX3330 + VEH, IRI + VEH, VEH + VEH, and combination of APX3330 + IRI on the APE1/Ref-1 level of fluorescence per ganglion (**A**), APE1/Ref-1 expression per area (0.4mm^2) (**B**), and the proportion of APE1/Ref-1-IR cells to PGP9.5 neurons per ganglion (**C**) was assessed in CRC-induced mice. VEH + VEH-treated mice exhibited the highest APE1/Ref-1-IR expression per ganglia (21.4 ± 1.0 a.u) compared to APX3330 + VEH (12.7 ± 0.9 a.u, $P < 0.01$) and APX3330 + IRI (14.5 ± 2.0 a.u, $P < 0.01$) treated mice. IRI + VEH-treated mice also exhibited significantly higher APE1/Ref-1-IR expression per ganglia (20.6 ± 0.9 a.u) compared to APX3330 + VEH (12.7 ± 0.9 a.u, $P < 0.01$) and APX3330 + IRI (14.5 ± 2.0 a.u, $P < 0.05$) treated mice. Similarly, IRI + VEH-treated mice exhibited the highest APE1/Ref-1 expression per area (7.9 ± 0.3 a.u) compared to APX3330 + VEH (3.4 ± 0.2 a.u, $P < 0.0001$) and APX3330 + IRI (4.1 ± 0.7 a.u, $P < 0.001$) treated groups.

VEH + VEH-treated mice also exhibited significantly higher APE1/Ref-1 expression per area (6.7 ± 0.5) compared to APX3330 + VEH (3.4 ± 0.2 a.u, $P < 0.001$) and APX3330 + IRI (4.1 ± 0.7 a.u, $P < 0.01$) treated mice. IRI + VEH-treated mice had the highest proportion of APE1/Ref-1-IR cells to PGP9.5-IR neurons per ganglion ($85.5 \pm 2.2\%$) compared to VEH + VEH-treated ($55.3 \pm 3.4\%$), APX3330 + VEH-treated ($34.9 \pm 2.9\%$) and APX3330 + IRI-treated ($51.9 \pm 2.8\%$) ($P < 0.0001$ for all) groups. In contrary, APX3330 + VEH-treated mice showed the lowest proportion of APE1/Ref-1-IR cells to PGP9.5-IR neurons per ganglion ($34.9 \pm 2.9\%$) compared to VEH + VEH ($55.3 \pm 3.4\%$, $P < 0.001$) and APX3330 + IRI ($51.9 \pm 2.8\%$, $P < 0.01$) treated mice (n=4-5 mice/group).

Western Blot analysis of the distal colon samples that were taken from CRC-induced mice following 14-treatments revealed that VEH + VEH-treated mice exhibited the highest protein expression of APE1/Ref-1 (2.6 ± 0.2 a.u) compared to APX3330 + IRI (1.4 ± 0.1 a.u, $P < 0.01$), APX3330 + VEH (1.2 ± 0.1 a.u, $P < 0.001$) and IRI + VEH (1.7 ± 0.2 a.u, $P < 0.01$) treated groups (n=4-5 mice/group) (**Figure 2.21**). An image of the membrane merged with the ladder after the protein transfer step has been included in supplementary data (**Figure S2.1B**).

Figure 2.16 APE1/Ref-1 expression in the distal colon following 14-day treatment with Irinotecan and APX3330. APE1/Ref-1 immunoreactive cells in the myenteric ganglia of the distal colon labelled with anti- APE1/Ref-1 antibody (green) from untreated (A), Irinotecan-treated (A'), APX3330-treated (A'') mice. Scale bar = 50µm. Quantitative analysis of the number of APE1/Ref-1-IR cells (B). The number of APE1/Ref-1-IR cells in the distal colon were counted per 0.4 mm² area. Data presented as mean ± S.E.M., *****P*<0.0001, n=5 mice/group.



B

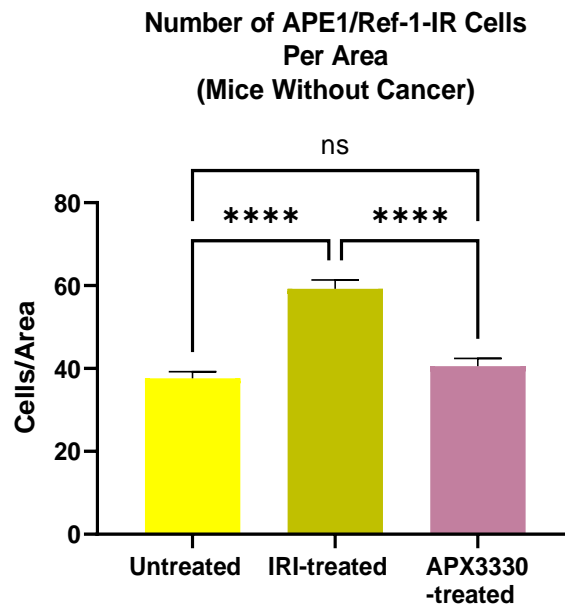
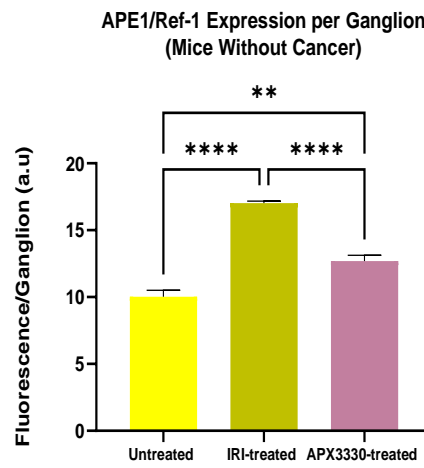
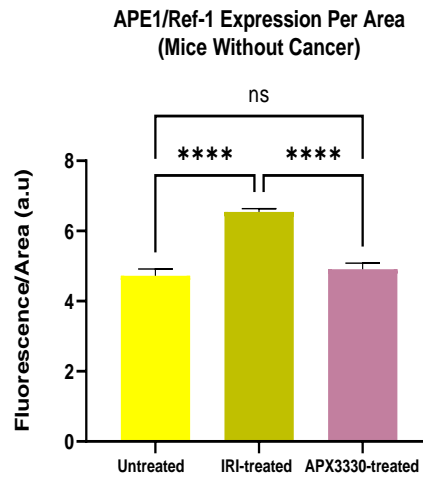


Figure 2.17 Quantitative analysis of the APE1/Ref-1 expression in the distal colon myenteric ganglia of mice without cancer. APE1/Ref-1 expression per ganglion (A), APE1/Ref-1 expression per 0.4mm² area (B), the proportion of APE1/Ref-1 cells to PGP 9.5-IR cells per ganglia (C) following 14 days of *in vivo* treatment with IRI and APX3330 compared to untreated mice. Data presented as mean \pm S.E.M. ** $P < 0.01$, **** $P < 0.0001$, n=5 mice/group.

A



B



C

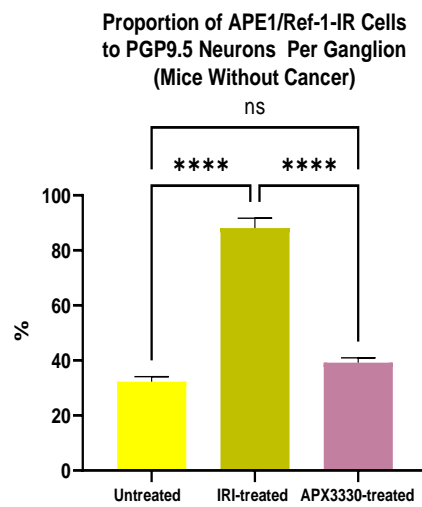
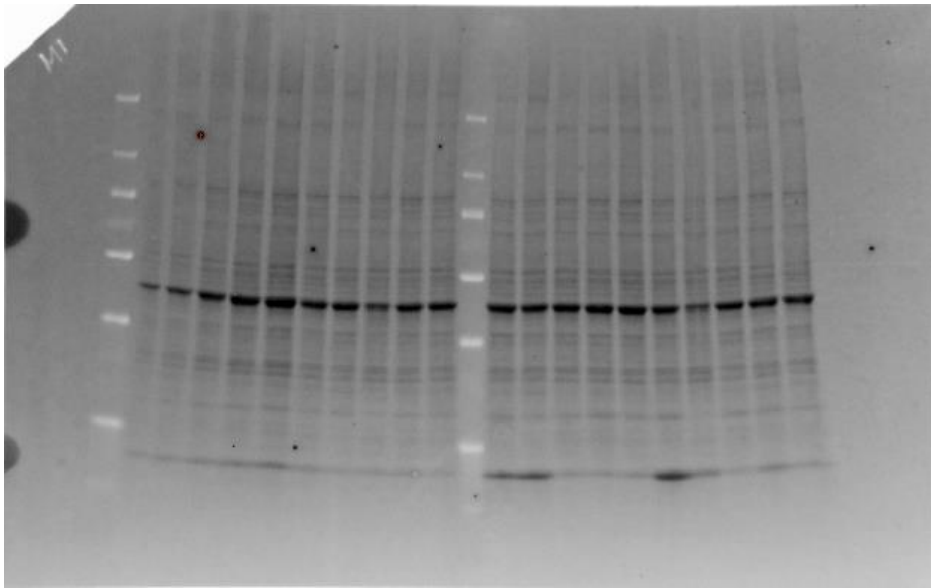
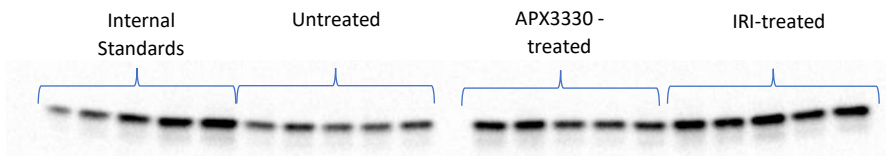


Figure 2.18 APE1/Ref-1 protein expression in the distal colon. APE1/Ref-1 protein (35 kDa) expression in the distal colon from mice without cancer following 14 days of *in vivo* treatment with Irinotecan and APX3330 compared to untreated mice. An image of the membrane with the total protein loading (A), An image of the membrane with the target protein (B), quantitative analysis of the APE1/Ref-1 protein expression normalised to the total protein values (C). Data presented as mean \pm S.E.M. * P <0.05, ** P <0.01, n=5 mice/group.

A



B



C

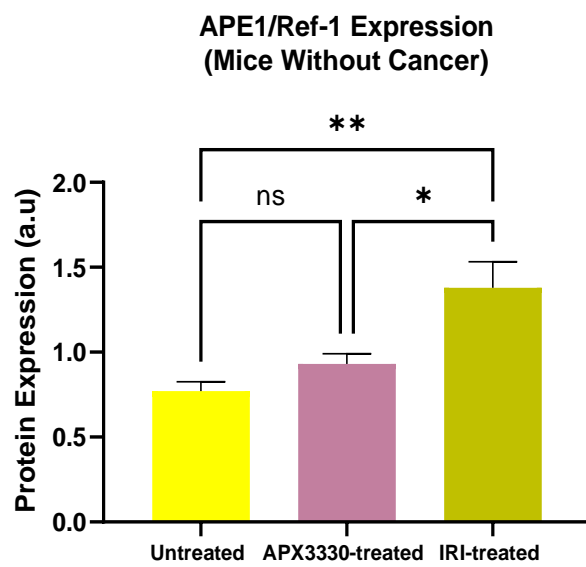
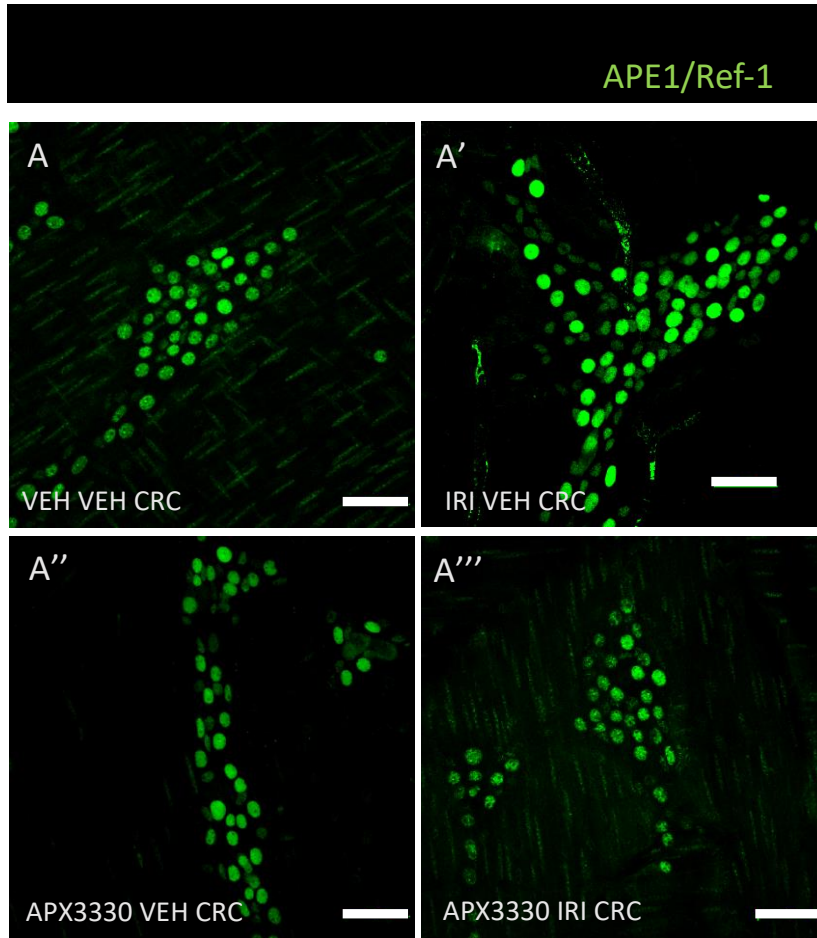


Figure 2.19 APE1/Ref-1 expression in the distal colon following 14-day treatments in CRC-induced mice. Wholemout preparations of the myenteric ganglia in the distal colon from mice treated with 2 vehicles (A), IRI plus vehicle for APX3330 (A'), APX3330 plus vehicle for IRI (A''), and a combination of APX3330 + IRI (A''') labelled with anti-APE1/Ref-1 antibody (green) to label APE1/Ref-1 immunoreactive cells. Scale bar = 50µm. Quantitative analysis of the number of APE1/Ref-1-IR cells (B) in the distal colon wholemout preparations was counted per 0.4 mm² area. Data presented as mean ± S.E.M. **P*<0.05, ***P*<0.01, ****P*<0.001, n=4-5 mice/group.



B

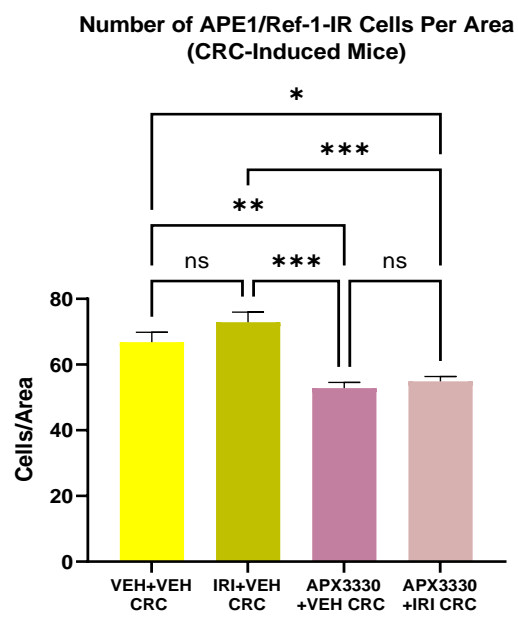
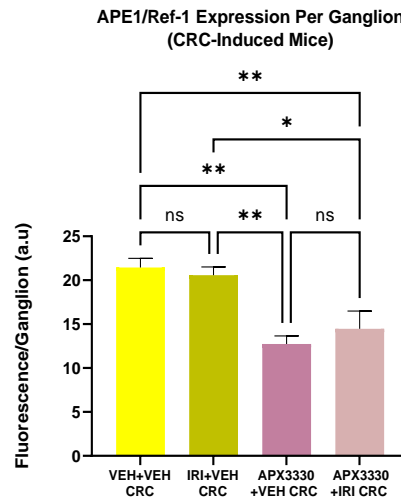
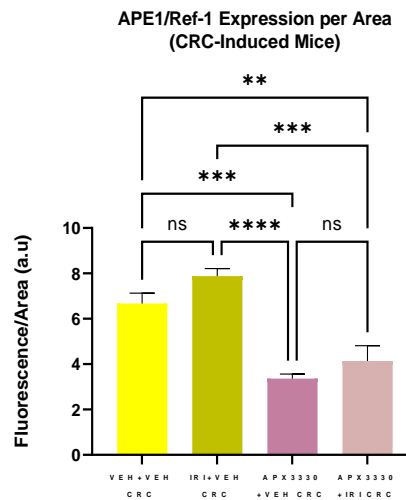


Figure 2.20 Quantitative analysis of the APE1/Ref-1 expression in the distal colon myenteric ganglia of CRC-induced mice. APE1/Ref-1 expression per ganglion (A), APE1/Ref-1 expression per 0.4mm² area (B), the proportion of APE1/Ref-1-IR cells to PGP 9.5-IR cells per ganglia (C) following 14 days of *in vivo* treatment with two vehicles, IRI plus vehicle for APX3330, APX3330 plus vehicle for IRI and a combination of APX3330 + IRI. Data presented as mean ± S.E.M. **P*<0.05, ***P*<0.01, ****P*<0.001 *****P*<0.0001, n=4-5 mice/group.

A



B



C

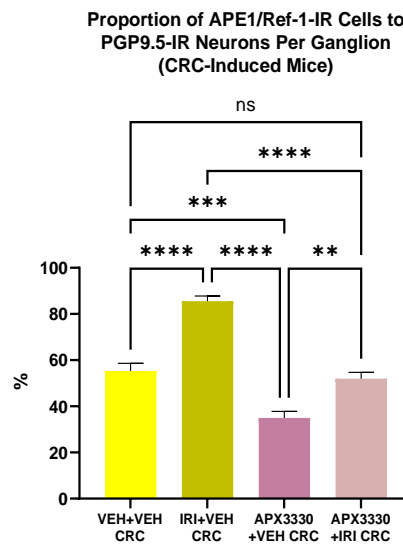
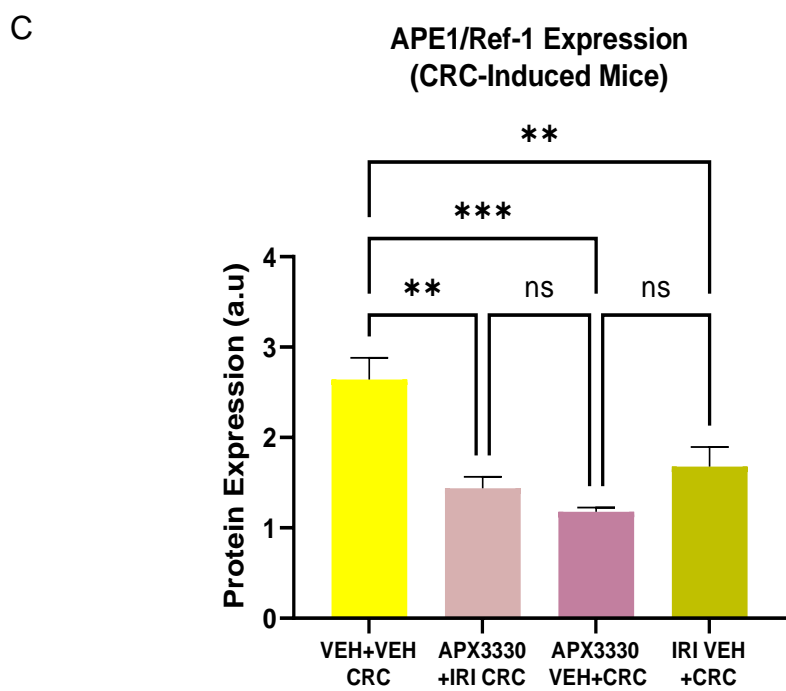
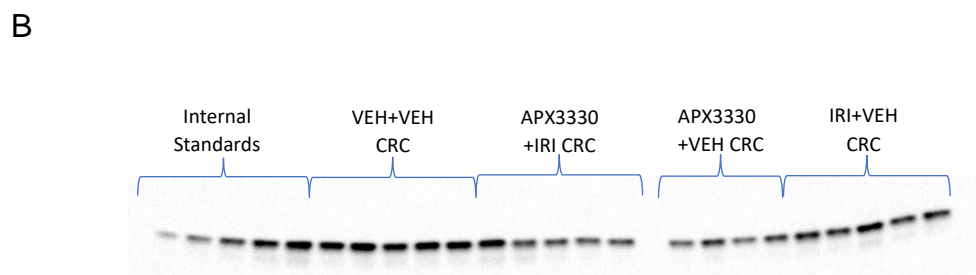
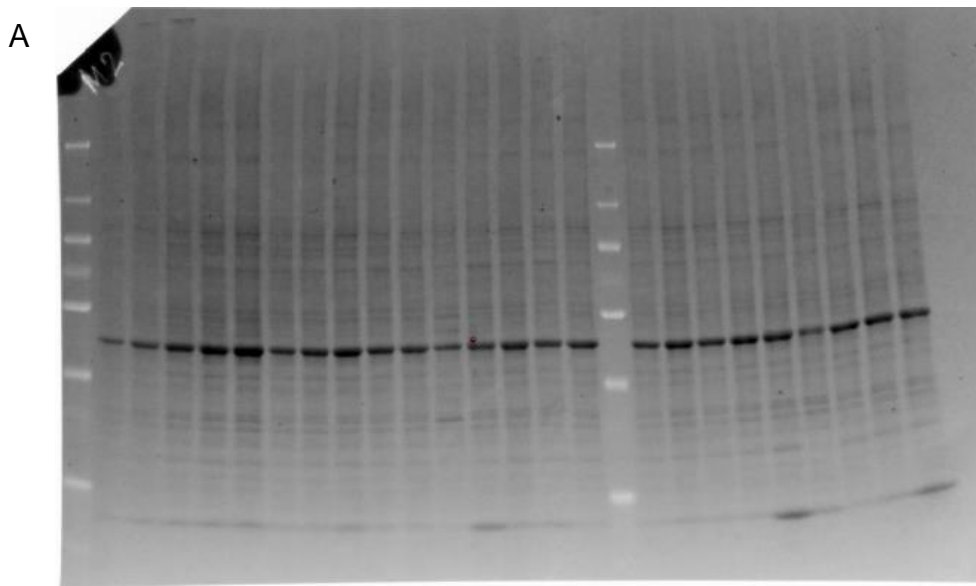


Figure 2.21 APE1/Ref-1 protein expression in the distal colon of mice with CRC. APE1/Ref-1 protein (35 kDa) expression in the distal colon from CRC-induced mice following 14-day of *in vivo* treatment with 2 vehicles, Irinotecan plus vehicle for APX3330, APX3330 plus vehicle for IRI, and combination therapy of APX3330 + IRI. An image of the membrane with the total protein loading (A), An image of the membrane with the target protein (B), quantitative analysis of the APE1/Ref-1 protein expression normalised to the total protein values (C). Data presented as mean \pm S.E.M. ** $P < 0.01$, *** $P < 0.001$, n=4-5 mice/group.



2.4.5 Effect of the Treatments on Transcription Factors

2.4.5.1 NF- κ B Expression

To investigate changes in nuclear factor kappa-light-chain-enhancer of activated B cells (NF- κ B) protein expression following *in vivo* treatment with IRI and APX3330 compared to untreated mice, the distal colon samples were assessed by Western blot experiments using anti-NF- κ B antibody. An image of the membrane with the total protein loading (**Figure 2.22 A**). Data revealed that the level of NF κ B protein expression was significantly higher in IRI-treated mice (2.4 ± 0.03 a.u) compared to APX3330-treated (1.1 ± 0.1 a.u) and untreated (0.8 ± 0.1 a.u) mice ($P < 0.0001$ for both) signifying elevated inflammation in the GI tract following IRI treatment (**Figure 2.22 B, C**). The level of NF- κ B expression in APX3330-treated mice was relatively close to untreated group data denoting the anti-inflammatory properties of APX3330 treatment (n=5 mice/group). An image of the membrane merged with the ladder after the protein transfer step has been included in supplementary data (**Figure S2.2A**).

An image of the membrane with the total protein loading (**Figure 2.23 A**). NF- κ B protein expression in mice with CRC indicated that IRI + VEH-treated mice had significantly higher protein expression of NF- κ B (3.2 ± 0.1 a.u) compared to VEH + VEH (2.1 ± 0.3 a.u, $P < 0.01$), APX3330 + VEH (0.6 ± 0.1 a.u, $P < 0.0001$) and APX3330 + IRI (0.6 ± 0.1 a.u, $P < 0.0001$) treated mice (n=4-5 mice/group) (**Figure 2.23 B, C**). Thus, indicating the anti-inflammatory properties of APX3330 as well as the effectiveness of the combination treatment. An image of the membrane merged with the ladder after the protein transfer step has been included in supplementary data (**Figure S2.2B**).

2.4.5.2 STAT3 and pSTAT3 Expression in Mice Without Cancer

To investigate changes in signal transducer and activator of transcription 3 (STAT3) protein expression following *in vivo* treatment with IRI and APX3330 compared to untreated mice, the STAT3 protein expression of distal colon samples was assessed by Western blot experiments using anti-STAT3 antibody. An image of the membrane with the total protein loading (**Figure 2.24 A**). Western blot analysis of the distal colon samples from mice without cancer revealed that, APX3330-treated group had the highest STAT3 protein expression (3.0 ± 0.1 a.u) compared to untreated (2.3 ± 0.1 a.u, $P < 0.01$) and IRI-treated (1.2 ± 0.1 a.u, $P < 0.0001$) groups (n=5 mice/group) (**Figure 2.24 B, C**). The IRI-treated group had the lowest expression of STAT3 in the cancer-free cohort suggesting the possibility of phosphorylation of STAT3 in the system. An image of the membrane merged with the ladder after the protein transfer step has been included in supplementary data (**Figure S2.3A**).

To investigate changes in the phosphorylated signal transducer and activator of transcription 3 (pSTAT-3) protein expression we performed Western blot experiments on the distal colon of mice without cancer following 14-day *in vivo* treatments using anti-pSTAT3 antibody. The rabbit monoclonal antibody used in the experiment was specifically made to bind at the Tyr705 phosphorylated site of the STAT3 protein. An image of the membrane with the total protein loading (**Figure 2.25 A**). Data revealed that IRI-treated group had significantly higher protein expression of pSTAT3 (3.6 ± 0.1 a.u) compared untreated (1.4 ± 0.2 a.u) and APX3330-treated (1.2 ± 0.1 a.u) ($P < 0.0001$ for both) mice indicating increased activation of STAT3 protein into pSTAT3 state (n=5 mice/group) (**Figure 2.25 B, C**). An image of the membrane merged with the ladder after the protein transfer step has been included in supplementary data (**Figure S2.3B**).

2.4.5.3 STAT3 and pSTAT3 Expression in CRC-Induced Mice

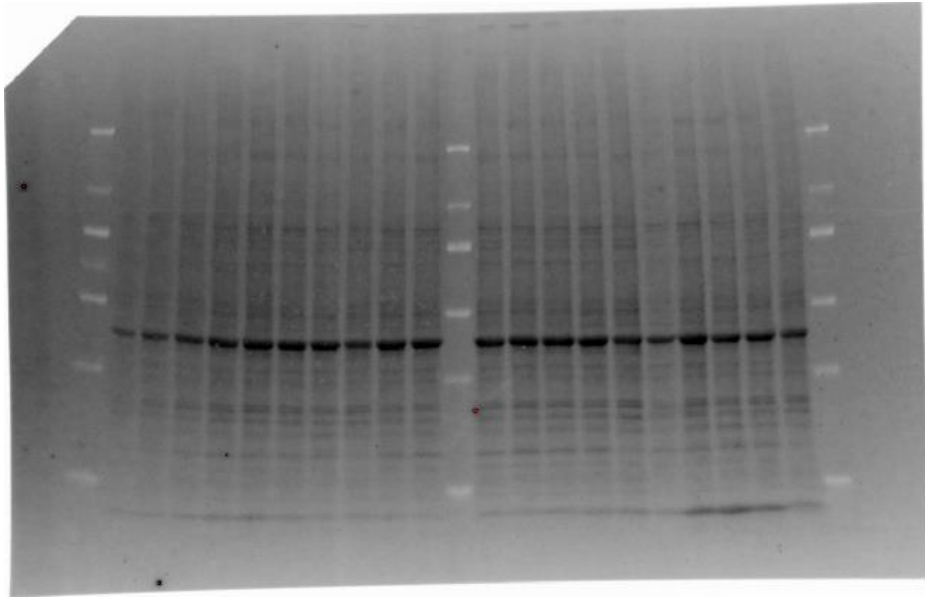
An image of the membrane with the total protein loading (**Figure 2.26 A**). Western

blot analysis of the distal colon samples from CRC-induced mice revealed that IRI + VEH (0.5 ± 0.1 a.u) and VEH + VEH (0.8 ± 0.1 a.u) treated groups showed significantly lower expression of STAT3 compared to APX3330 + IRI-treated (1.5 ± 0.2 a.u, $P < 0.01$, $P < 0.05$) and APX3330 + VEH-treated (2.1 ± 0.2 a.u, $P < 0.0001$, $P < 0.001$) groups (n=4-5 mice/group) (**Figure 2.26 B, C**). IRI + VEH and VEH + VEH-treated groups showed the lowest expression of STAT3 protein expression indicating increased activation of the protein. An image of the membrane merged with the ladder after the protein transfer step has been included in supplementary data (**Figure S2.4A**).

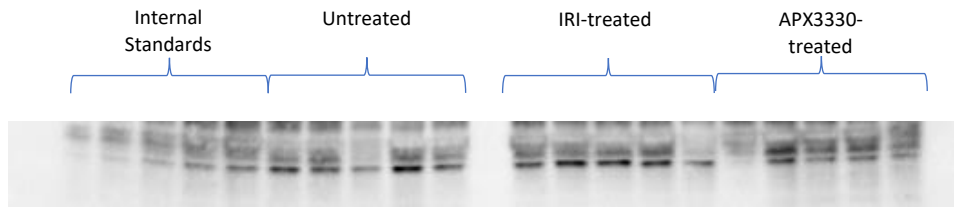
An image of the membrane with the total protein loading (**Figure 2.27 A**). In CRC-induced cohort, APX3330 + VEH-treated mice exhibited the lowest expression of pSTAT3 (0.9 ± 0.2 a.u) compared to IRI + VEH-treated (2.1 ± 0.3 a.u, $P < 0.01$) and VEH + VEH-treated (1.7 ± 0.2 a.u, $P < 0.05$) but not statistically significant compared to APX3330 + IRI-treated (1.0 ± 0.2 a.u) group indicating that APX3330 treatment inhibited increased activation of STAT3 protein into its active phosphorylated state pSTAT3 (n=4-5 mice/group) (**Figure 2.27 B, C**). An image of the membrane merged with the ladder after the protein transfer step has been included in supplementary data (**Figure S2.4B**).

Figure 2.22 NF- κ B protein expression in the distal colon of mice without cancer. NF- κ B protein expression (60 kDa) in the distal colon from mice following 14-day *in vivo* treatment with Irinotecan and APX3330 compared to untreated without cancer mice. An image of the membrane with the total protein loading (A), An image of the membrane with the target protein (B), quantitative analysis of the APE1/Ref-1 protein expression normalised to the total protein values (C). Data presented as mean \pm S.E.M. **** $P < 0.0001$, n=4-5 mice/group.

A



B



C

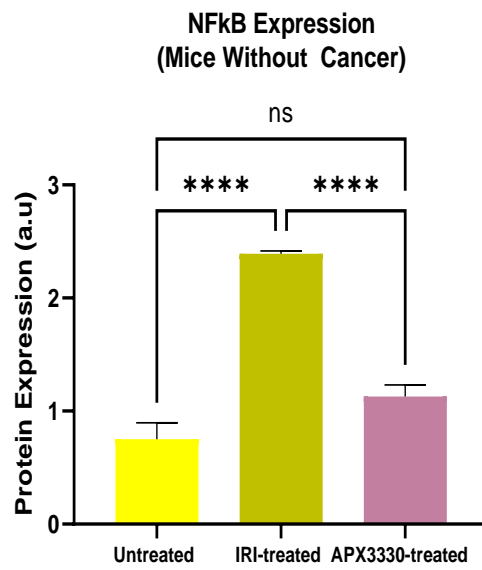
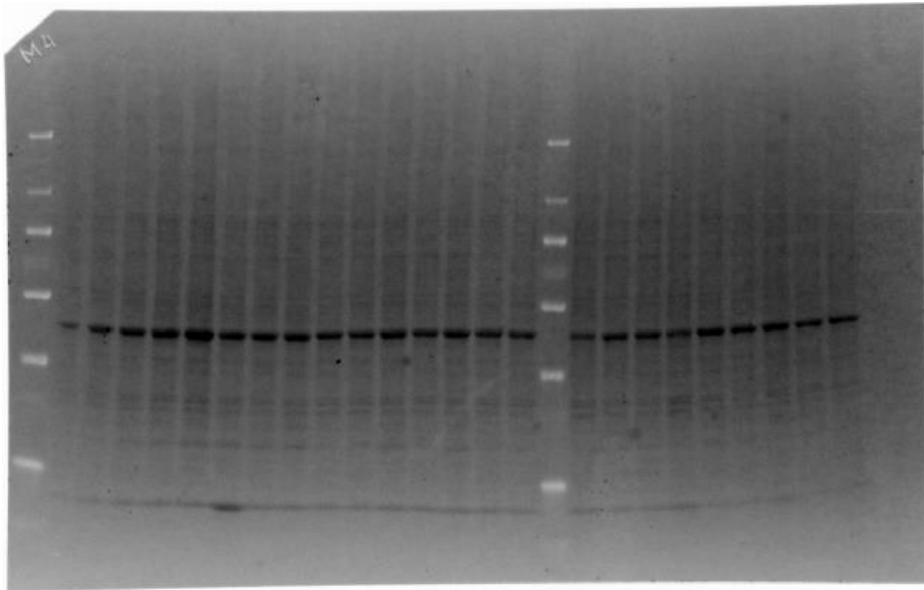


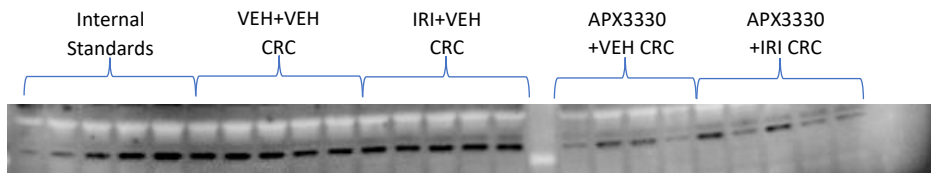
Figure 2.23 NF- κ B protein expression in the distal colon of CRC-induced mice.

NF- κ B protein expression (60 kDa) in the distal colon from CRC-induced mice following 14-day *in vivo* treatment with 2 vehicles, Irinotecan plus vehicle for APX3330, APX3330 plus vehicle for IRI, and combination therapy of APX3330 + IRI. An image of the membrane with the total protein loading (A), An image of the membrane with the target protein (B), quantitative analysis of the NF- κ B protein expression normalised to the total protein values (C). Data presented as mean \pm S.E.M. ** P <0.01, *** P <0.001, **** P <0.0001, n=4-5 mice/group.

A



B



C

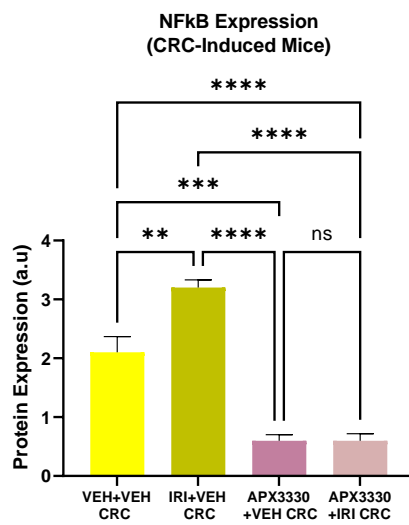
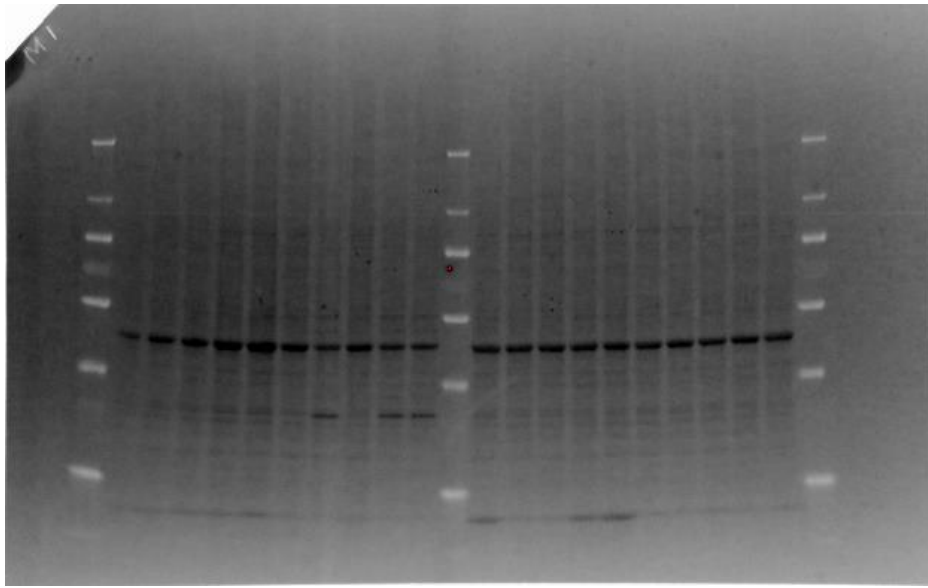
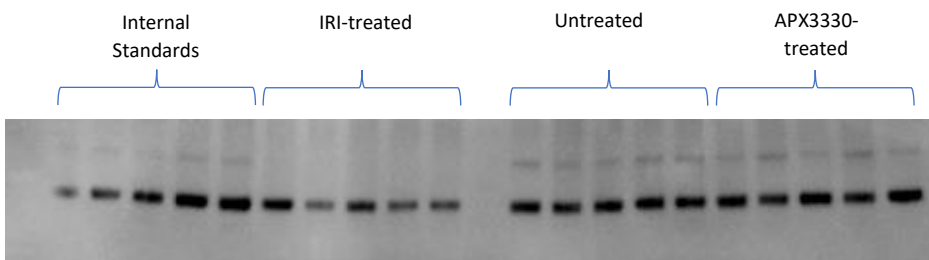


Figure 2.24 Signal transducer and activator of transcription 3 (STAT3) protein expression in the distal colon of mice without cancer. STAT3 protein (88 kDa) expression in the distal colon from mice following 14-day *in vivo* treatment with Irinotecan and APX3330 compared to untreated mice. An image of the membrane with the total protein loading (A), An image of the membrane with the target protein (B), quantitative analysis of the STAT3 protein expression normalised to the total protein values (C). Data presented as mean \pm S.E.M. ** $P < 0.01$, *** $P < 0.001$, **** $P < 0.0001$, $n = 5$ mice/group.

A



B



C

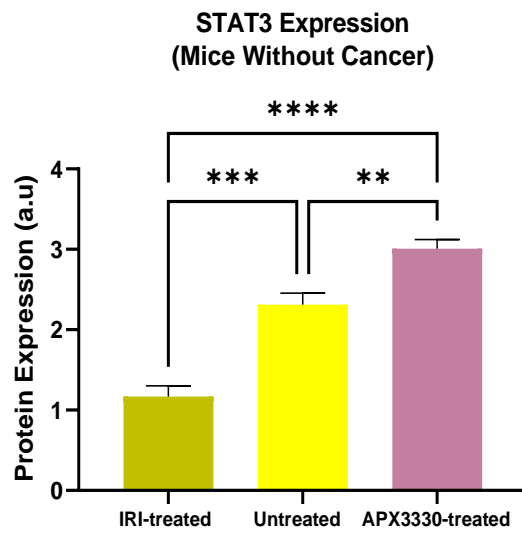
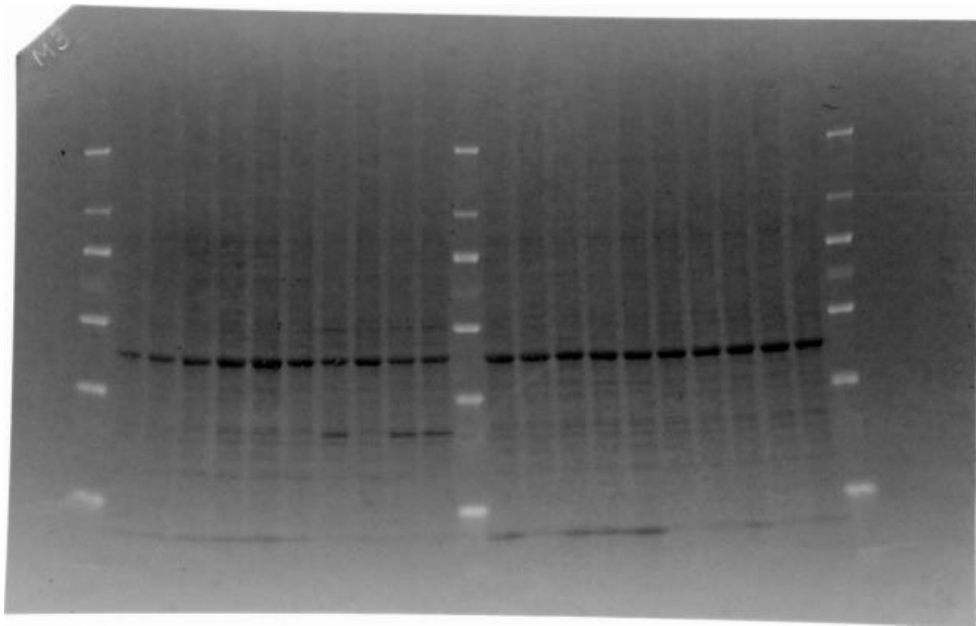
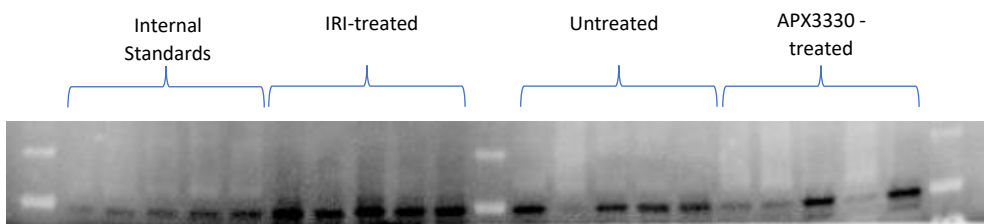


Figure 2.25 Phosphorylated signal transducer and activator of transcription 3 (pSTAT3) protein expression in the distal colon of mice without cancer. pSTAT3 protein (88 kDa) expression in the distal colon from mice following 14-day *in vivo* treatment with Irinotecan and APX3330 compared to untreated mice. An image of the membrane with the total protein loading (A), An image of the membrane with the target protein (B), quantitative analysis of the pSTAT3 protein expression normalised to the total protein values (C). Data presented as mean \pm S.E.M. **** $P < 0.0001$, n=5 mice/group.

A



B



C

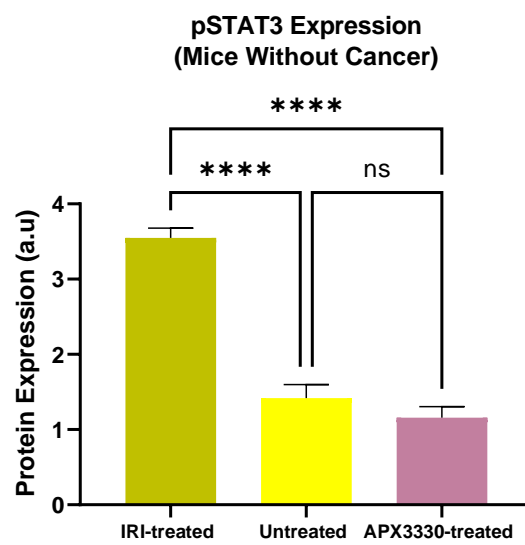
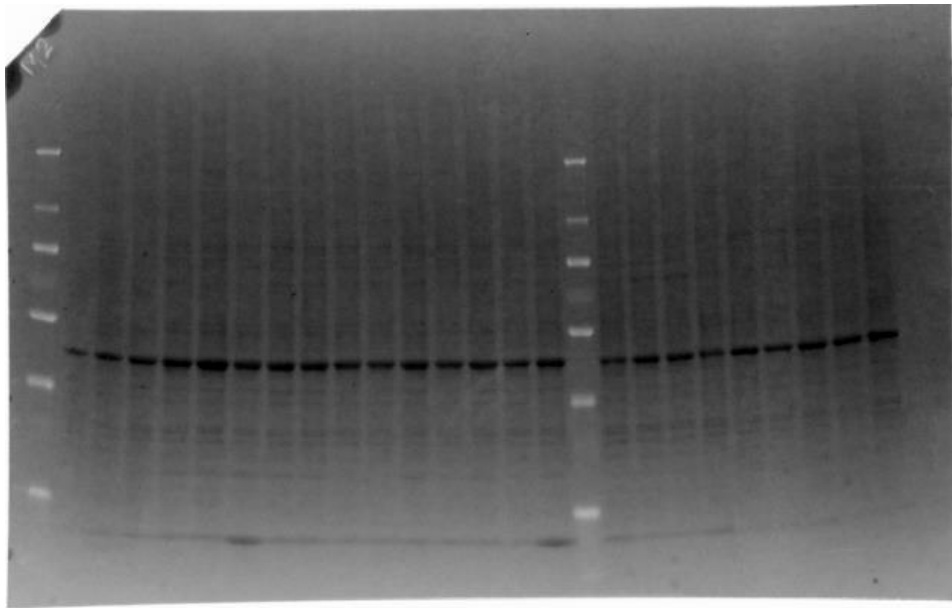
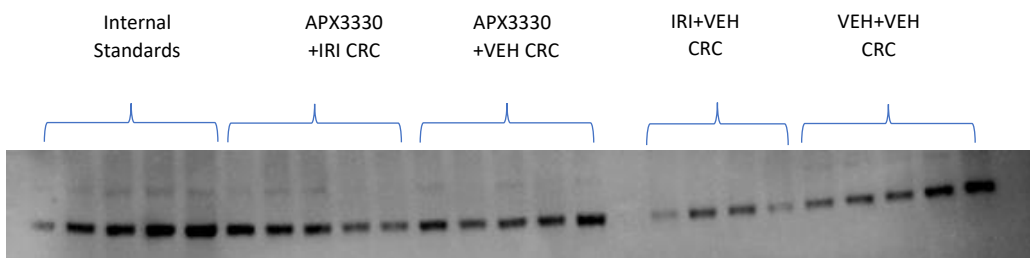


Figure 2.26 Signal transducer and activator of transcription 3 (STAT3) protein expression in the distal colon of mice with CRC. STAT3 protein (88 kDa) expression in the distal colon from CRC-induced mice following 14-day *in vivo* treatment with 2 vehicles, Irinotecan plus vehicle for APX3330, APX3330 plus vehicle for IRI, and a combination of APX3330 + IRI. An image of the membrane with the total protein loading (A), An image of the membrane with the target protein (B), quantitative analysis of the STAT3 protein expression normalised to the total protein values (C). Data presented as mean \pm S.E.M. * P <0.05, ** P <0.01, *** P <0.001, **** P <0.0001, n=4-5 mice/group.

A



B



C

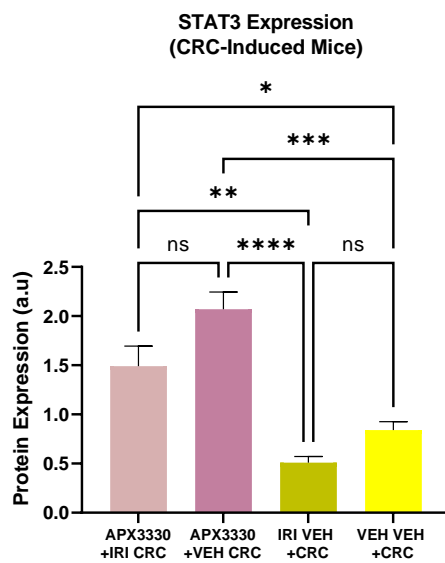
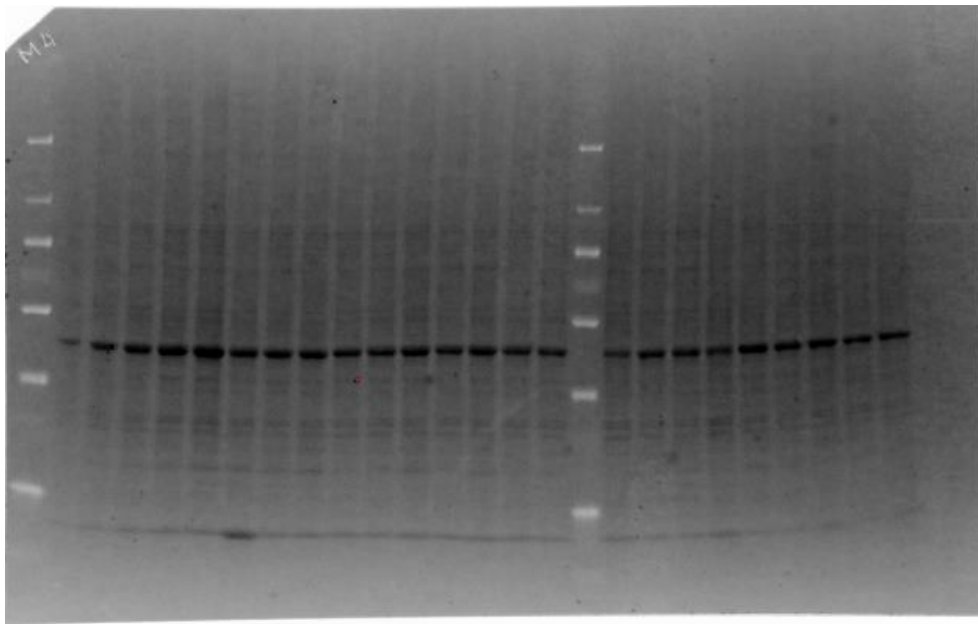
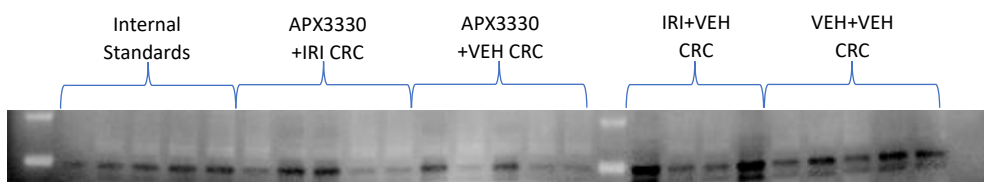


Figure 2.27 Phosphorylated signal transducer and activator of transcription 3 (pSTAT3) protein expression in the distal colon of mice with CRC. pSTAT3 protein (88 kDa) expression in the distal colon from mice following 14-day *in vivo* treatment with 2 vehicles, Irinotecan plus vehicle for APX3330, APX3330 plus vehicle for IRI, and a combination of APX3330 + IRI treated CRC-induced mice. An image of the membrane with the total protein loading (A), An image of the membrane with the target protein (B), and quantitative analysis of the pSTAT3 protein expression was normalised to the total protein values (C). Data presented as mean \pm S.E.M. * P <0.05, ** P <0.01, n=4-5 mice/group.

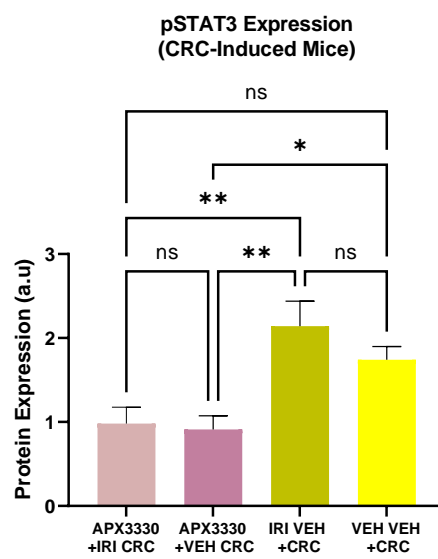
A



B



C



2.4.6 Effect of the Treatments on Tumour Growth and Metastasis in the Colon

2.4.6.1 Assessment of the Caecum Size, and Number of Tumours Following Treatments in CRC-Induced Mice

The freshly resected caecums were weighed as soon as they were taken out from the mice to determine the variation between the sizes of the caecum between treatment groups. The average caecum weight of VEH + VEH-treated mice was significantly higher ($3.2 \pm 0.3\text{g}$) compared to IRI + VEH-treated ($2.0 \pm 0.1\text{g}$, $P < 0.01$), APX3330 + VEH-treated ($1.7 \pm 0.03\text{g}$, $P < 0.001$) and APX3330 + IRI-treated ($1.9 \pm 0.1\text{g}$, $P < 0.01$) mice (**Figure 2.28 A-D, E**). Since VEH + VEH-treated group did not receive any treatments, data indicated that these mice had much larger caecums compared to other groups APX3330 treatment significantly reduced the caecum size due to inhibited growth of tumours indicative of anti-tumour properties of APX3330 treatment (n=4-5 mice/group).

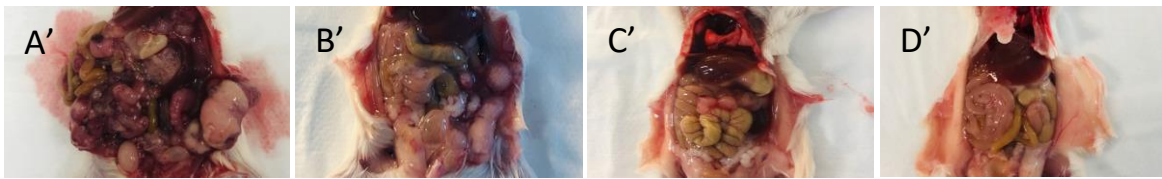
To assess the efficacy of different treatment regimens, the tumour diameter and the number of tumours were quantified. VEH + VEH-treated mice had the biggest tumour diameter ($27.0 \pm 1.2\text{mm}$) compared to IRI + VEH ($17.3 \pm 1.3\text{mm}$), APX3330 + VEH ($5.12 \pm 0.5\text{mm}$) and APX3330 + IRI ($0 \pm 0\text{mm}$) ($P < 0.0001$ for all) treated mice (**Figure 2.28, A-D, F**). Their caecums were completely consumed by multiple tumours by day 21 post-surgery and a many secondary tumours were present in the abdominal cavity. The secondary spread of the tumours was observed in other organs including the spleen, liver, large intestine, small intestine, as well as the stomach wall (**Figure 2.28, A'-D'**). The number of tumours present in the abdominal cavity were significantly higher in VEH + VEH-treated mice (70.8 ± 5.4 tumours/mouse) compared to IRI + VEH (12.6 ± 0.9 tumours/mouse), APX3330 + VEH (1.6 ± 0.8 tumours/mouse) and APX3330 + IRI (0 ± 0 tumours/mouse) treated mice ($P < 0.0001$ for all) (**Figure 2.28, A'-D', G**). The number of tumours was not statistically significant between APX3330 + VEH ($1.6 \pm$

0.8 tumours/mouse) and APX3330 + IRI (0 ± 0 tumours/mouse) treated groups (n=4-5 mice/group).

2.4.6.2 Effect of the Treatments on VEGF Expression

We have observed the secondary spread of tumours into the colon in VEH + VEH, IRI + VEH, and APX3330 + VEH-treated mice whereas mice treated with APX3330 + IRI did not show any signs of secondary spread of tumours following 14-days of *in vivo* treatment (**Figure 2.29**). The antiangiogenic potential of different treatment options was evaluated by the Western blot analysis of the protein expression of vascular endothelial growth factor (VEGF) in the distal colon by using an anti-VEGF antibody. An image of the membrane with the total protein loading (**Figure 2.30 A**). VEGF protein expression was significantly higher in VEH + VEH-treated mice (2.6 ± 0.1 a.u) compared to IRI + VEH (2.1 ± 0.1 a.u, $P < 0.01$), APX3330 + VEH (0.4 ± 0.1 a.u, $P < 0.0001$) and APX3330 + IRI (0.8 ± 0.1 a.u, $P < 0.0001$) treated mice indicating increased tumour vascularisation in the VEH + VEH-treated group (**Figure 2.27 B, C**). VEGF expression in the colons from IRI + VEH-treated group was also significantly higher compared to APX3330 + VEH and APX3330 + IRI treated mice, indicating high susceptibility of developing new blood vessels in tumours thus increasing tumour metastasis. APX3330 + VEH-treated and APX3330 + IRI-received mice with CRC had the lowest level of VEGF protein expression compared to other groups indicating anti-angiogenic and anti-tumour effectiveness of APX3330 by itself as well as a combination therapy with IRI (n=4-5 mice/group). An image of the membrane merged with the ladder after the protein transfer step has been included in supplementary data (**Figure S2.5**).

Figure 2.28 Effects of the treatments on tumour growth. Tumours in the caecums and abdominal cavity from mice treated with two vehicles (A-A'), Irinotecan plus vehicle for APX3330 (B-B'), APX3330 plus vehicle for IRI (C-C'), and a combination of APX3330 + Irinotecan (D-D''). The average weight of the caecum in grams (E), the average tumour diameter (F), and the average number of tumours in the abdominal cavity (G) at day 21 post-surgery. Data presented as mean \pm S.E.M. * P <0.05, ** P <0.01, *** P <0.001, **** P <0.0001, n=4-5 mice/group.



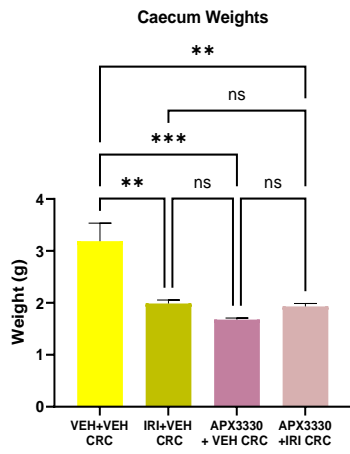
VEH+VEH CRC

IRI+VEH CRC

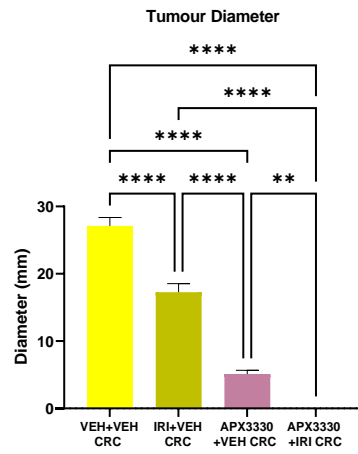
APX3330+VEH CRC

APX3330+IRI CRC

E



F



G

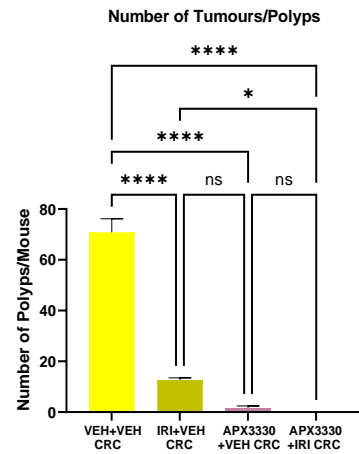


Figure 2.29 Tumour metastasis in the distal colon. Tumours in the colon from mice treated with two vehicles (A), Irinotecan plus vehicle for APX3330 (B), APX3330 plus vehicle for IRI (C), and APX3330 + Irinotecan (D). Scale bar = 100µm.

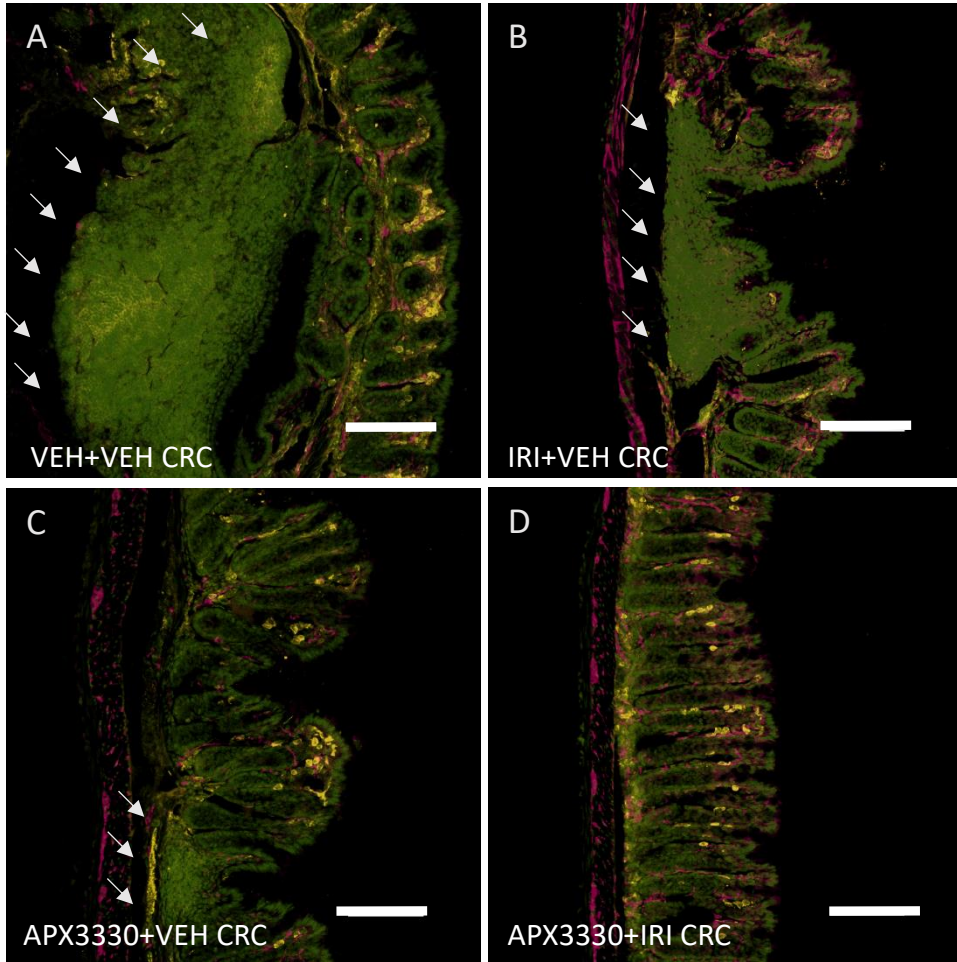
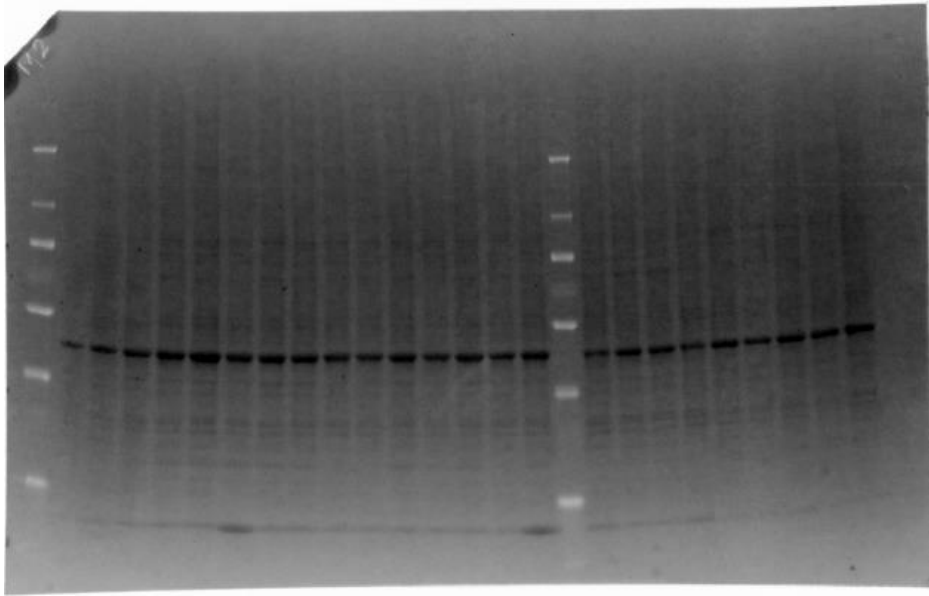
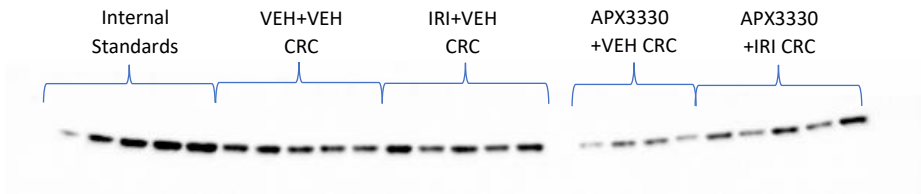


Figure 2.30 Vascular endothelial growth factor (VEGF) protein expression following treatments in mice with CRC. VEGF protein (38-44 kDa) expression in the distal colon from CRC-induced mice treated with two vehicles, Irinotecan plus vehicle for APX3330, APX3330 plus vehicle for IRI, and combination therapy of APX3330 + Irinotecan for 14 days. An image of the membrane with the total protein loading (A), An image of the membrane with the target protein (B), quantitative analysis of the VEGF protein expression normalised to the total protein values (C). Data presented as mean \pm S.E.M. * P <0.05, ** P <0.01, **** P <0.0001, n=4-5 mice/group.

A

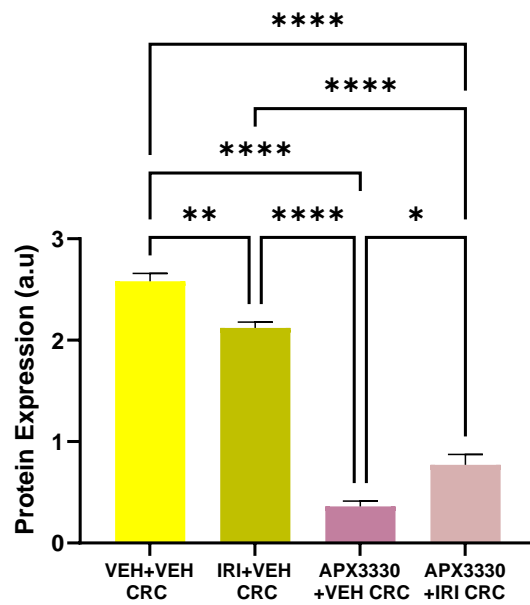


B



C

VEGF Expression in the Distal Colon (CRC-Induced Mice)



2.5 Discussion

This study is the first to investigate the efficacy of APX3330 as a treatment for IRI-induced enteric neuropathy. We analysed the effects of *in vivo* administration of IRI and APX3330 on the colon myenteric plexus neurons that control GI tract motility. We also investigated the anti-tumour efficacy of APX3330 by itself as well as in combination with IRI for the treatment of colorectal cancer. IRI-induced intestinal inflammation and anti-inflammatory properties of APX3330 were also assessed as a part of the study. The results show that repeated IRI administration causes intestinal inflammation leading to severe diarrhoea in mice with and without cancer evidenced by increased levels of faecal LCN-2, and the number of CD45+ and MPO+ cells in the colon. APX3330 given in combination with IRI alleviated intestinal inflammation and chronic diarrhoea in CRC-induced mice and APX3330 treatment also exhibited aforementioned properties when treated with mice without cancer. IRI treatment caused severe weight loss in mice throughout the treatment duration and APX3330 treatment caused weight gain in mice similar to healthy mice at the same age. IRI but not APX3330 induced myenteric neuronal loss in the distal colon but increased the number and proportion of cholinergic ChAT-IR neurons and VAcHT-IR nerve fibres. APX3330 treatment did not affect the number of neurons and changes in cholinergic neurons when administered alone in mice without CRC. APX3330 treatment was able to reduce the number of ChAT-IR neurons and VAcHT-IR fibres in IRI-treated CRC-induced mice. IRI treatment was also associated with changes in APE/Ref-1 expression in the myenteric plexus of the distal colon. Wholmount preparations of the distal colon segments expressed fewer APE1/Ref-1-IR cells in the myenteric plexus following APX3330 and APX3330 + IRI combination treatment. APX3330 treatment exhibited anti-tumour properties by reducing/diminishing tumour growth and secondary tumour spread in CRC-induced mice compared to two vehicles-treated and IRI-treated mice. VEH + VEH-treated mice had the highest number of tumours because they did not receive any cancer treatments. Combination treatment of APX3330 + IRI exhibited the most successful outcome among all the treatment groups by completely getting rid of secondary tumours following 14 days of *in vivo* treatment. IRI-treated and vehicle-

treated groups exhibited higher protein expression of NF- κ B, VEGF, and pSTAT3 and lower expression of STAT3, indicating tumour thriving microenvironment. Western blot data revealed decreased expression of NF- κ B, VEGF, STAT3, and pSTAT3 after APX3330 and combination therapy, providing evidence that APX3330 acts via modulation of APE1/Ref-1 regulated transcription factors associated with inflammation, tumour progression, metastasis, and angiogenesis.

IRI treatment is associated with gastrointestinal mucositis, a common chemotherapy-related side-effect, that causes a debilitating impact on patients' general wellbeing (Okunaka et al., 2021, Smith et al., 2020, O'Reilly et al., 2020, Avritscher et al., 2004). Irinotecan causes intestinal mucositis that arises as inflammation, epithelial degradation, and epithelial ulceration leading to acute and chronic diarrhoea, and causing severe weight loss in patients (McQuade et al., 2020, Thorpe et al., 2013, Duncan and Grant, 2003, Sonis et al., 2004, Stringer et al., 2009d). Even though the occurrence and the severity of intestinal mucositis are mainly dependent on the patient and the treatment regimen, roughly 87% of patients reported IRI-induced acute and chronic diarrhoea (Boeing et al., 2021, Krishnamurthi et al., 2019, Mego et al., 2015, Rougier et al., 1998, Avritscher et al., 2004). Our results from faecal LCN-2 analysis show that IRI causes acute and chronic diarrhoea in both cohorts of mice with and without cancer. Data showed that IRI treatment caused significantly higher faecal water content at days 7 and 14 in both CRC-induced and mice without cancer indicating acute and chronic diarrhoea. APX3330 and combination treatment reversed IRI-induced acute and chronic diarrhoea following 14 days of *in vivo* administration. It is believed that crypt cell death is associated with acute intestinal toxicity which is caused by anti-cancer treatments such as IRI that triggers mucosal inflammation and breakdown of the mucosal barrier. However, the direct link to the phenomena is still unclear to a point whether the origin of intestinal mucositis arises as a result of direct cytotoxicity of IRI treatment, or it is mediated by a series of intermediate events that eventually lead to mucosal inflammation and damage (Sonis et al., 2004). Our data revealed that APX3330 treatment exhibited anti-inflammatory properties by reducing inflammation in CRC-induced mice.

Initiation and the progression of gastrointestinal mucositis can be subdivided into five sequential phases namely, initiation, upregulation, message generation, signalling and amplification, ulceration, and inflammation followed by the healing process (Sougiannis et al., 2021, Thomsen et al., 2018, Sonis, 2009, Sonis et al., 2004, Lee et al., 2014). Previous research findings show that the healing phase takes approximately two weeks post-treatment to complete the proliferation and differentiation of gastrointestinal epithelium (Mahendran et al., 2018, Bertoglio et al., 2012, Sultani et al., 2012, Sonis et al., 2004, Lee et al., 2014). Nevertheless, even though the histopathological damages are shown to be recovered within a shorter period post-treatment, long term side-effects of IRI such as diarrhoea can last up to 10 years after cessation of the treatment (Hino et al., 2022, Lu et al., 2022, Di Fiore et al., 2009, Denlinger and Barsevick, 2009, Schneider et al., 2007, Numico et al., 2015). Similar results have been found in other studies that were conducted in pelvic radiation therapy where they found intestinal permeability and mucosal damage highest halfway through the treatment period and it starts to gradually improve the GI tract damage while adverse side effects of the treatment such as nausea, diarrhoea and abdominal pain remain throughout the treatment period causing severe weight loss in patients (Carratu et al., 1998, Hovdenak et al., 2000). Research data support the hypothesis that crypt cell death associated with radiation therapy is partially triggered by apoptotic endothelial lesions (Paris et al., 2001) whereas the intestinal dysfunction may arise as a direct or indirect consequence of changes in non-epithelial tissues (Sonis et al., 2004) such as GI muscle and nerve supply by the enteric nervous system.

Acute and chronic diarrhoea is one of the main GI side effects caused by IRI treatment and plenty of research supports the hypothesis that IRI-related diarrhoea is mainly caused by inflammation and mucosal damage (Sun et al., 2020, Gunasegaran et al., 2020, Okunata et al., 2021, Boeing et al., 2021, Stringer et al., 2007, Stringer et al., 2008, Stringer et al., 2009a, Stringer et al., 2009d, Gibson et al., 2003, Logan et al., 2008). Our data revealed that IRI treatment caused chronic inflammation in the gut by significantly high CD45+ Immune cells and neutrophil accumulation in the gut following the 14-day treatment period. Pro-inflammatory

cytokines such as Interleukin-1 (IL-1) and tumour necrosis factor α (TNF- α) (Khandia and Munjal, 2020, Mantovani et al., 2010, Rajput and Wilber, 2010, Lawrence, 2009, Tahara, 2008) activate transcription factors such as nuclear factor- κ B (NF- κ B) that is closely related to inflammatory cascades that affect GI function. Previous studies have found a significant increase in NF- κ B and pro-inflammatory cytokines in the colon between 2-12 h duration following IRI administration coinciding with the initiation of histological changes in the gut and the appearance of diarrhoea (Logan et al., 2008). Similarly, studies research conducted in rats have found that IRI treatment significantly upregulates the expression of pro-inflammatory cytokines such as interferon- γ (IFN- γ) and TNF- α indicating acute intestinal inflammation (Pathak et al., 2015, Hu et al., 2006). Co-treatment with St. John's wort significantly reduced the expression of TNF- α -mRNA in the intestine which was also correlated with improved intestinal lesions as well as a reduction in diarrhoea (Pathak et al., 2015, Hu et al., 2006), signifying the importance of IRI-induced inflammatory response in the manifestation of diarrhoea. The results of our study demonstrate that APX3330 and APX3330 + IRI combination treatment alleviated IRI-induced diarrhoea in CRC-induced mice following 14 days of *in vivo* administration suggesting APX3330's anti-inflammatory properties. CD45+ immune cell infiltration and neutrophil accumulation in the distal colon were also significantly reduced by the APX3330 treatment further supporting its anti-inflammatory properties. The anti-inflammatory effects of APX3330 treatment also evidenced by reduced LCN-2 levels in faeces from mice receiving APX3330 and combination treatment.

It is believed that acute symptoms of chemotherapy-related GI side effects are due to mucosal damage, whereas long-term GI dysfunction and chronic diarrhoea are caused by the damage to the neurons that control gastric secretion and motility (Zaiss et al., 2021, Laforgia et al., 2021, Li et al., 2021, Addington and Fremier, 2016, McQuade et al., 2016, McQuade et al., 2017). Previous studies done by our lab have demonstrated that repeated *in vivo* administration of IRI caused enteric neuronal death up to 16% from day 7 to day 14 (McQuade et al., 2017). Since IRI exerts its anti-tumour efficacy by inhibiting DNA topoisomerase 1, it is

believed that it does not target or damage post mitotic cells such as enteric neurons that have completed the cell division and differentiation process. However, the accumulation of its active metabolite SN-38 in the intestinal mucosa is responsible for neurotoxicity and enterotoxicity (Soveri, 2019). IRI's analogue camptothecin, that also inhibits DNA topoisomerase 1, was found to induce cortical neuronal death via apoptosis (Matosevic and Bosak, 2020). Camptothecin treatment induces chromatin condensation, plasma membrane blebbing, cytoplasmic shrinking and fragmentation of DNA that is consistent with the activation of the apoptotic cascade (Morris and Geller, 1996). Chemotherapy-induced myenteric neuronal loss in mice following Oxaliplatin and Cisplatin administration correlated with changes in colonic motility and GI transit (Wafai et al., 2013, Vera et al., 2011, Pini et al., 2016). Enteric neuronal damage and loss significantly contribute to long-term chemotherapy-induced GI side-effects, and it is crucial to find an alternative treatment that has no or minimal damage to the enteric system neurons. APX3330 by itself or in combination with IRI showed neuroprotective effects in both cohorts of mice with and without cancer. It has increased the number of myenteric neurons in the distal colon when administered with IRI in CRC-induced mice. Considering the anti-inflammatory and neuroprotective aspects, APX3330 makes a viable candidate to address the IRI-induced neuronal damage and mucositis.

In the enteric nervous system, cholinergic neurons play a vital part in excitatory motor innervation in the gut (Furness, 2012, Uchiyama et al., 2021, Lake et al., 2013, Fung et al., 2020, Fleming et al., 2020). IRI treatment causes phenotypic changes in the myenteric neurons especially the cholinergic excitatory ChAT-IR neurons that may contribute to acute and chronic GI side effects such as diarrhoea. Previous studies from our lab have found that IRI treatment cause changes in the subpopulations of myenteric neurons immunoreactive for ChAT as early as 3 days and it can increase the proportion of ChAT-IR neurons up to 17% throughout the treatment duration followed by post-treatment (McQuade et al., 2017) in mice without cancer. In line with our previous findings, our data revealed that IRI caused the increase in the number of ChAT-IR neurons in the distal colon following 14 days of *in vivo* treatment in both mice with and without cancer. Our

data also revealed that APX3330 treatment alone and in combination with IRI could reduce the number of ChAT-IR neurons in the distal colon following 14 days of treatment. ChAT functions as a catalytic enzyme in the process of synthesising acetylcholine (Okuda and Huga, 2003, von Rosenvinge et al., 2013, Wessler and Kirkpatrick., 2020). Acetyl and choline are utilised intracellularly to produce acetylcholine and the reuptake of choline from extracellular space is mainly controlled by the rate-limiting factor. Choline uptake is mainly dependent on three different transport systems, namely, high-affinity choline transporter 1 (CHT1), choline transporter-like1 (CTL1 and organic cation transporters (OCTs) such as OCT1, OCT2, and OCT3. High-affinity choline transporter-1 and organic cation transporter -1 have been studied in the myenteric and submucosal plexus as well as in the mucosal epithelium in the larger and small intestines (Chen et al., 2001, Harrington et al., 2010). Studies conducted in the human intestine following IRI treatment have revealed that various organic cation transporters are involved in absorbing anti-cancer medications including IRI (Shnitsar et al., 2009, Koepsell, 2015). The researchers have also observed an increased expression of those transporters found in kidney carcinoma cells lymphoma cells that have an impact on the chemo receptivity in patients (Gupta et al., 2012, Shnitsar et al., 2009). However, the role of OCTs expressed in enteric neurons in IRI and APX3330 has yet to be explored. Our findings suggest that IRI causes increased expression in ChAT-IR neurons in the myenteric plexus and APX3330 treatment decrease the number of ChAT-IR neurons suggesting IRI treatment's involvement in synthesising or induced reuptake of choline via OCTs. The role of APX3330 in choline-binding with the OCTs and choline transport into the neurons needs to be further investigated.

IRI binds to the active site of acetylcholinesterase and inhibits the breakdown of more stable acetylcholine enzymes. Therefore, more acetylcholinesterase level was evident due to increased cholinergic activity of IRI leading to functional inhibition of the enzyme (Uchiyama et al., 2021, Elbeddini et al., 2020, Harel et al., 2005, Dodds and Rivory, 1999). In the intracellular space, once acetylcholine is synthesised via the assistance of the acetylcholinesterase enzyme, it is enclosed

into vesicles and then transferred towards axons into the synaptic clefts so the neurotransmitters can be released at the axon terminals. VACHT is the transporter that is responsible for acetylcholine transport into the vesicles before sending it towards the axon terminal to signal transmission. We observed that IRI treatment induced a significantly high density of VACHT-IR fibres in the myenteric plexus following 14 days of *in vivo* treatment. Our findings showed that APX3330 reduces the expression of VACHT-IR fibres in the distal colon in both cohorts of mice with and without cancer. APX3330 treatment by itself also exhibited a reduced density of VACHT-IR fibres and it also significantly reduced the VACHT fibre density in CRC-induced mice. Therefore, our findings suggest that the IRI treatment causes cholinergic syndrome that leads to excessive amounts of acetylcholine in the enteric neurons that affects the physiological functions of the gut. Acetylcholine is a major neurotransmitter in the enteric nervous system that controls the contractions of circular and smooth muscle cells in the gut (Furness, 2012, Knauf et al., 2020, McQuilken et al., 2021, Yelleswarapu, 2021). It is also responsible for mucosal secretion (Cooke, 2000, Herath et al., 2020) and collectively, the acute diarrhoea induced by IRI treatment is mainly caused by the cholinergic syndrome in colorectal cancer patients (De Lisa et al., 2020, Glimelius et al., 2002, Hecht, 1998). However, a delayed onset and long-term diarrhoea is believed to be multifactorial and mainly due to the damages to the enteric neurons as well as changes in secretory mechanism (McQuade et al., 2014, van Heerden et al., 2021, Saliba et al., 1998, Bleiberg and Cvitkovic, 1996).

Western blot data of APE1/Ref-1 protein expression revealed that IRI treatment caused increased expression of APE1/Ref-1 and APX3330 treatment decreased APE1/Ref-1 expression. NFkB expression was also significantly higher in IRI-treated mice suggesting increased inflammation. APX3330 and combination therapy were able to reverse/reduce IRI-induced inflammation in CRC-induced mice. Redox inhibition of APX3330 was assessed by evaluating the expression of STAT3 and pSTAT3 protein expression. IRI treatment caused decreased expression of STAT3 and increased expression of pSTAT3 indicating downstream transcriptional activation of the number of cytosolic proteins that regulate

inflammation, tumour growth, metastasis, and angiogenesis. APX3330 treatment showed increased STAT3 expression and decreased pSTAT3 expression suggesting decreased activation of transcriptional factors associated with inflammation, tumour progression, and survival.

Assessment of the effects of the treatments on tumour growth and metastasis was performed in mice with cancer. CT-26 colorectal cancer cells were injected into the cecum as the primary cancer induction site. Mice in the VEH + VEH-treated group had much larger caecum size and weight compared to IRI + VEH-treated, APX3330 + VEH-treated and APX3330 + IRI-treated mice. Visible tumours were also present in the primary tumour induction site of IRI + VEH-treated mice. In both APX3330 + VEH-treated and APX3330 + IRI-treated mice, the tumours in the caecum were barely visible. The size and the weight of the caecum were not significantly affected in these groups due to inhibited growth of tumours indicative of anti-tumour properties of APX3330 treatment.

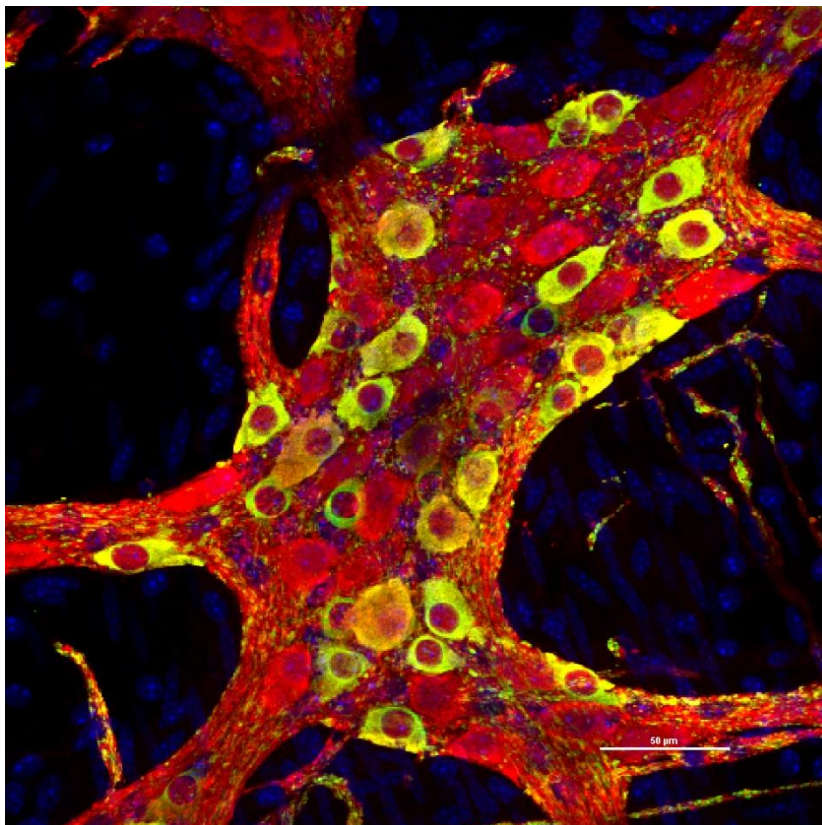
The efficacy of different treatment regimens was also assessed by measuring the tumour diameter and the average number of tumours following treatments. VEH + VEH-treated mice had the largest tumour diameter compared to IRI + VEH, APX3330 + VEH and APX3330 + IRI treated mice. Multiple tumours were present in the abdominal cavity by day 21 post-surgery. The secondary spread of the tumours was observed in other organs, including the spleen, liver, large intestine, small intestine, as well as the stomach wall. The number of tumours present in the abdominal cavity was significantly higher in VEH + VEH-treated mice due to not receiving anti-tumour medications compared to other treatment groups. Therefore, our data demonstrated APX3330's antitumor properties by itself and in combination therapy with IRI for the treatment of colorectal cancer.

2.6 Conclusion

Our study demonstrates that IRI induces intestinal inflammation that may contribute to myenteric neuronal loss and phenotypic changes in subpopulations in myenteric neurons. APX3330 treatment on the other hand was able to reverse the neuronal damages caused by IRI treatment and it also exhibited neuroprotective properties when used as a combination therapy in CRC-induced mice. IRI-induced GI dysfunction may associate with the increased number of cholinergic neurons and fibres in the colon that leads to alterations in colonic motor activity. APX3330 reduced the number of cholinergic neurons and the density of fibres in the distal colon exhibiting anti-inflammatory properties of the treatment. Western blot data also revealed that APX3330 downregulates the expression of NFkB, and pSTAT3, as a part of redox inhibition of APE1/Ref-1 protein. This study demonstrates the neuroprotective and anti-tumour efficacy of APX3330 in combination with IRI for the treatment of IRI-induced GI side-effects in a preclinical model of CRC.

3

INVESTIGATING THE NEUROPROTECTIVE AND ANTI-CANCER EFFICACY OF APX3330 IN COMBINATION WITH OXALIPLATIN IN THE MURINE MODEL OF CRC



Wholemount preparation of the myenteric ganglia from the distal colon of OXL+VEH-treated mouse with CRC labelled with a pan-neuronal marker anti-PGP9.5 antibody (red), an inhibitory neuronal marker, neuronal nitric oxide synthase (green) and DAPI (blue) (Scale bar = 50μm)

3.1 Summary

Oxaliplatin is a third-generation platinum-based chemotherapeutic medication used as a first-line treatment for advanced colorectal cancer (CRC). Since the medication is associated with gastrointestinal side effects it often results in dose limitations and, in severe cases, complete cessation of the treatment. Oxaliplatin disrupts DNA replication and transcription by forming DNA adducts that results in ceasing the cell cycle (Devanabanda and Kasi, 2022, Banca et al., 2021). Moreover, Oxaliplatin treatment is also associated with inducing high levels of oxidative stress that leads to DNA damage and myenteric neuronal death in the ENS (Lee and Wen, 2021, Bae et al., 2021). The enteric nervous system (ENS), that governs gastric motility, is drastically affected by Oxaliplatin treatment and the side-effects cause by the drug last in the gastrointestinal system for up to 10 years post-treatment. Apurinic/apyrimidinic endonuclease 1/reduction-oxidation (redox) effector factor-1 (APE1/Ref-1) is a multifunctional cytosolic protein that comprises a redox active site and a DNA repair active site that exerts several intracellular functions such as DNA damage repair caused by oxidative stress, ionising radiation, and alkylating agents as well as redox regulation of transcription factors that are crucial for cancer cell proliferation, survival, and cell growth (Kelley et al., 2019). The expression of APE1/Ref-1 protein has shown to be significantly increased in various cancers such as prostate cancer, breast cancer, pancreatic cancer, gastric cancer etc. including treatment-resistant tumours (Hainaut et al., 1993, Chen et al., 1994, Madhusudan et al., 2005, Hanson et al., 2005, Koshiji et al., 2005, Langie et al., 2007, Shahda et al., 2011, Gamplala et al., 2020, Mijit et al., 2021, Long et al., 2021). Targeting and inhibiting APE1/Ref-1 protein's redox function provides an avenue to control inflammation, angiogenesis, and cellular growth in cancer. APX3330 [(2E)-2-[(4,5-dimethoxy-2-methyl-3,6-dioxo-1,4-cyclohexadien-1-yl) methylene]-undecanoic Acid, targets APE1/Ref-1 protein's redox activity by binding to its redox-active site via two active sites of the protein (Kelley et al., 2012, Caston et al., 2021). Recent studies demonstrated that APX3330 exerts anti-inflammatory, neuroprotective, and tumour suppressive effects in dorsal root ganglion (DRG) neurons (Kelley and Fehrenbacher, 2017). The focus of this study is to investigate the neuroprotective

and anti-tumour efficacy of APX3330 against Oxaliplatin-induced damage to the myenteric neurons of the ENS and to investigate the molecular mechanisms of APX3330 that modulate its neuroprotective and anti-tumour properties. We also aimed to evaluate if APX3330 can reduce the side effects caused by Oxaliplatin when it is used as a combination therapy. In this study, we tested if APX3330 can decrease enteric neuronal damage caused by chronic Oxaliplatin treatment and the anti-tumour efficacy of APX3330 to reduce tumour progression. CT-26 murine colorectal cell line was used to induce cancer in the mouse caecum. The caecum was exteriorised and ~1 million CT-26 cancer cells were injected between the inner and outer serosal layers of the caecum. Once the visible bulla formation occurs the caecum was returned to the abdomen and the abdominal muscles were restitched. Treatment started at day 6 post-surgery. APX3330 (25mg/kg/d) and Oxaliplatin (3mg/kg/d) were administered *in vivo* for two weeks. APX3330 was injected intraperitoneally two times a day with a 12-hours interval for 14 consecutive days and Oxaliplatin was injected every second day with a maximum of three injections a week for two weeks. Combination treatment was executed as per the above treatment schedule. Thus, the mice received both treatments during the treatment period. Vehicle for Oxaliplatin (sterile water, x3 times a week for two weeks) and vehicle for APX3330 (2% Cremophor: 2% EtOH and 96% sterile water, x2 times daily for two weeks) were injected into sham-treated mice intraperitoneally and combination therapy mice received three Oxaliplatin injections a week for two weeks and APX3330 treatment twice daily for two weeks. Final experiments took place on day 14 of treatments. Faecal samples were collected to measure the water content of the faeces to determine the signs of constipation or diarrhoea. Anti-tumour efficacy of APX3330 treatment was assessed by evaluation of the size, the number of tumours and the secondary spread of tumours into the colon. The structural changes in the myenteric neurons were assessed by performing immunohistochemistry experiments on wholemount and cross-sectional preparations. Oxaliplatin-induced neuronal loss was assessed by counting the total number of neurons labelled with anti-protein gene product 9.5 (PGP9.5) antibody in the myenteric ganglia. The wholemount preparations were co-labelled with anti-APE1/Ref-1 antibody to count the number of APE1/Ref-1-immuno-reactive (IR) cells per area. To count the number of inhibitory myenteric neurons, the

whollemount preparations of the myenteric ganglia were labelled with anti-neuronal nitric oxide synthase (nNOS) antibody and co-labelled with a pan neuronal marker, PGP9.5. Western blot experiments were performed to investigate the possible alterations of the regulatory molecular pathways, as well as to assess cytochrome c levels in the distal colon. We further evaluated protein expression of signal transducer and activator of transcription 3 (STAT3), phospho specific signal transducer and activator of transcription 3 (pSTAT3) and vascular endothelial growth factor (VEGF) proteins in the distal colon that directly interfere with cancer survival, metastasis, and angiogenesis via Western blot experiments. The results of our study demonstrated that Oxaliplatin-treated mice lost weight throughout the treatment, and they had less faecal water content exhibiting constipation. APX3330-treated and combination therapy mice gained weight after 14 days of treatment and they did not show any signs of constipation. Two vehicles-treated mice with CRC gained weight throughout the treatment period due to the rapidly growing tumours in the abdominal cavity. Two vehicles-treated group had the highest number and the weight of tumours in the CRC-induced cohort followed by the Oxaliplatin-treated group. APX3330-treated mice had small tumours at the tumour induction site and the combination treatment group did not have any tumours or secondary spread other than the visible small polyp formation at the primary tumour induction site. Chronic *in vivo* administration of Oxaliplatin resulted in an elevated level of cytochrome c, and increased apoptosis in the distal colon. Oxaliplatin treatment resulted in the loss of myenteric neurons and an increased number of neuronal nitric oxide synthase-immuno-reactive (nNOS-IR) neurons indicating elevated levels of oxidative stress. Vehicle-treated mice with CRC also showed high expression of nNOS-IR neurons indicating oxidative stress due to the pathological condition of cancer. APX3330 treatment and combination treatment alleviated the adverse side-effects of Oxaliplatin by increasing the number of myenteric neurons and decreasing the expression of nNOS-IR neurons indicating decreased oxidative stress. Western Blot data showed that mice treated with APX3330 and combination of APX3330 with Oxaliplatin treatment had the lowest amount of cytochrome c expression, lower expression of VEGF and pSTAT3 and higher expression of STAT3. Cytochrome c expression was much higher in Oxaliplatin + VEH-treated and VEH + VEH-treated groups with CRC. Our study is the first to provide evidence

that APX3330 protects myenteric neurons from OXL-induced damage in the murine model of CRC. Furthermore, our study experimentally evaluates and supports the hypothesis of APE1/Ref-1 redox inhibition by APX3330, demonstrating the changes in the downstream transcription proteins of APE1/Ref-1. We have also demonstrated the APX3330's anti-tumour efficacy by inhibiting tumour progression and metastasis in the murine CRC model.

3.2 Introduction

Oxaliplatin is a platinum-based chemotherapeutic medication that is usually administered by itself or with 5-fluorouracil as a first-line treatment for tumours that are resistant to the first and second-generation platinum-based chemotherapeutics, namely carboplatin and cisplatin (Raymond et al., 1998, Salat, 2020, Cavaletti and Marmioli, 2020, Schoch et al., 2020, Dembic, 2020). When Oxaliplatin is used with other chemotherapeutic drugs it showed enhanced therapeutic efficacy than using Oxaliplatin alone (Mani et al., 2000, Andre et al., 2004, De Gramont et al., 2007, Cremolini et al., 2020, Ramasubbu et al., 2021, Avellone et al., 2021).

Oxaliplatin exerts its therapeutic potential by binding to cellular DNA, forming cross-links that results in inhibiting DNA replication, transcription and arrest of the cell cycle causing cell death (Devanabanda and Kasi, 2022, Sehgal, 2016, Al-Batran et al., 2019). Oxaliplatin forms platinum-DNA adducts that bind to the unwinding DNA strands in the mitotic cells which trigger the suspension of the cell cycle and lead dividing cells to the apoptotic pathway (Graham et al., 2000, Chou et al., 2002, Goodisman et al., 2006). Recent studies have found that the accumulation of these platinum adducts is associated with damage to sensory neurons (Chou et al., 2000, Gros et al., 2004, Al-Batran et al., 2019, Abraham et al., 2021). Even though Oxaliplatin treatment is cytotoxic it is less toxic to the newly generating blood cells and the renal system compared to cisplatin and carboplatin treatments (Raymond et al., 1998). Nevertheless, Oxaliplatin induces acute and

delayed peripheral neuropathies along with gastrointestinal dysfunctions (Stojanovska et al., 2014, Shigematsu et al., 2020, Bouchenaki et al., 2021).

Oxaliplatin induces severe gastrointestinal side effects including nausea, vomiting, constipation, and /or diarrhoea, and stomach cramps. These side-effects are the predominant cause of dose limitation, and in severe cases, the treatment. Patients undergoing high-dose chemotherapy and roughly 40% of patients undergoing standard-dose chemotherapy experience bloating, ulceration, pain, vomiting, diarrhoea, and/or constipation across the duration of the treatment (McQuade et al., 2014, McQuade et al., 2020). Therefore, finding an efficient and tolerable treatment presents itself as a challenging factor for advanced stage and treatment-resistant cancers (Verstappen et al., 2003, McQuade et al., 2014, Kawai et al., 2021).

Chemotherapy-induced peripheral neuropathy (CIPN) is a serious side effect that can lead to the dose reduction and, thereby, affects the efficacy of the treatment. Patients usually experience numbness and tingling sensations, increased sensitiveness to touch and cold, decreased tendon reflexes, and loss of proprioception, especially in the hands and feet due to the damage to peripheral sensory neurons. A larger portion of patients undergoing chemotherapy, experiences tabbing, burning, and electrical sensations (Seretny et al., 2014, Argyriou et al., 2020). Among other chemotherapeutic medications, Oxaliplatin has dose-dependent toxicity on the nervous system (Alcindor and Beauger, 2011, Devanabanda and Kasi, 2022). It can cause acute and chronic peripheral neuropathy. Oxaliplatin-induced peripheral neuropathy presents with paraesthesia, dysesthesias, or allodynia that usually occurs around the mouth and the throat while the patient is receiving the treatment or after the treatment, which can also be triggered by being exposed to the cold. The acute symptoms usually resolve within a few hours to days following treatment. Paraesthesia, dysesthesia, hypoesthesia and decreased proprioception that develop in the distal extremities are among the common chronic peripheral neuropathy symptoms of Oxaliplatin treatment that is

seen in patients who received a cumulative dose of 780 mg/m² (9 doses, 10%) and the patients who received 1170 mg/m² (13 doses, 50%). Current anti-cancer treatments are limited by a lack of preventative or therapeutic options (Hershman et al., 2014, Stone et al., 2016, Hu et al., 2019, Salat, 2020). Several studies support the hypothesis that DNA damage induced by platinum-based drugs is a major contributing factor to CIPN. In addition to forming platinum-DNA adducts that cause neural toxicity (Ta et al., 2006, Dzagnideze et al., 2007, Kang et al., 2021, Velasco et al., 2021, Shou et al., 2021), platinum-based chemotherapeutics are also correlated with the increased formation of reactive oxygen species (ROS) that contributes to oxidative DNA damage and neurotoxicity (Siomek et al., 2006, Preston et al., 2009, Shah et al., 2017, Kelley et al., 2017, Kleith et al., 2017, Park et al., 2019, Cruz-Bermudez et al., 2019, Xue et al., 2020).

The diverse nature of cancer reduces the treatment efficacy of many cancer-killing treatments including Oxaliplatin. Thus, the treatments that hold the most effective outcomes are the ones that target multiple signalling pathways to isolate and diminish tumour survival pathways. APE1/Ref-1 (Apurinic/Apyrimidinic endonuclease 1/ Redox factor 1) is an intracellular protein that activates multiple transcription factors involved in cancer cell survival adding the tumour growth and metastasis (Tell et al., 2005, Kelley et al., 2018, Frossi et al., 2019, Caston et al., 2021). APE1/Ref-1 is involved in multiple signalling pathways and blocking or controlling its activity provides the avenue to block multiple cancer survival pathways (Kelley et al., 2012, Codrich et al., 2019, Heisel, 2021, Li et al., 2021). APE1/Ref-1's wide-ranging functions make it an attractive therapeutic target in cancer therapy (Kelley et al., 2019, Caston et al., 2021). In the DNA repair realm, APE1/Ref-1 exerts its activity via the Base Excision Repair pathway (BER) to mitigate DNA damage due to oxidative stress induced by either disease pathology such as cancer or by treatments such as chemotherapeutics (Kelley et al., 2019, Roychoudhury, 2019). APE1/Ref-1 protein controls intracellular redox function by regulating several transcription factors such as NF- κ B, AP-1, and STAT3 (Gampala et al., 2021, Caston et al., 2021, Kepenu and Kelley, 2021). These transcription factors are responsible for inflammation, and angiogenesis which in turn are

important factors in cancer growth and survival (Kelley et al., 2019, Kepenu and Kelley, 2021). Recently, the redox modulation of APE1/Ref-1 has been defined as a key player in disease pathology and as a target for novel therapeutic approach for several diseases (Caston et al., 2021). In the scope of cancer, APE1/Ref-1 plays a critical role in cancer cell metabolism, chemotherapy-induced peripheral neuropathy as well as cancer-associated inflammation (Mahmut et al., 2021). APE1/Ref-1 protein has been initially studied for its endonuclease capacity to repair damaged DNA via the BER pathway (Caston et al., 2021). In recent years, it has shed the light on APE1/Ref-1 in the regulation of key cellular functions including redox homeostasis (Chen et al., 2010, El Hadri et al., 2012, Sriramajayam et al., 2021), inflammatory responses (Sahakian et al., 2020), mitochondrial metabolism (Gampala et al., 2021, Silpa et al., 2021), as well as neovascularization. APE1/Ref-1 protein functions both in the cytoplasm as well as in the nucleus (Tell et al., 2005, Di Maso et al., 2007), and research have also identified its function outside of the cell to induce pro-inflammatory cytokine IL-6 (Nath et al., 2017). APE1/Ref-1 serum levels have been used as an important biomarker for several cancers including bladder, hepatocellular, and oral squamous cell carcinoma (Shin et al., 2015, Choi et al., 2016, Pascut et al., 2019, Lee et al., 2020).

APE1/Ref-1's endonuclease activity involves repairing DNA damage caused by oxidative stress, alkylating agents, and ionizing radiation (Vasko et al., 2011, de Pontes Santos et al., 2020, Caston et a., 2021). APE1/Ref-1 is also involved in DNA damage repair caused by ROS (Gampala et al., 2021, Silpa et al., 2021). If the damage is beyond repair, genetic instability drives the cells to programmed cell death by activating the apoptotic cascade (Sahakian et al., 2020, Curtis et al., 2021). APE1/Ref-1 also influences the DNA repair activities via redox modulation of several transcription factors.

APE1/Ref-1 is the main regulator of both ubiquitous and tissue-specific transcription factors such as AP-1, NF-kB, Egr-1, p53, HIF1- α , CREB and PAX-5, PAX- 8, TTF-1, PEBP-2 (Xanthoudakis et al., 1992, Huang et al., 1993, Akamatsu

et al., 1997, Hirota et al., 1999, Ueno et al., 1999, Lando et al., 2000, Tell et al., 2000, El Hadri et al., 2012, Stone et al., 2016, Hu et al., 2018, Al-Zwaini et al., 2020, Tang et al., 2021, Caston et al., 2021). Some of these transcription factors are directly involved in tumour growth, survival, metastasis, and angiogenesis. For instance, AP-1, NF- κ B, PAX, HIF1- α , HLF, and p53 have a direct influence on cancer progression, and targeting APE1/Ref-1, stands a greater chance of effective therapeutic outcomes for the disease progression. NF- κ B, AP-1, STAT3, and HIF1- α are four main transcription factors that are under APE1/Ref-1's direct control (Evans et al., 2000, Fishel et al., 2007, Ray et al., 2009, Luo et al., 2010, Nagoya et al., 2014, Zhao et al., 2021, Hartman et al., 2021) and they have been identified as main driving forces in pancreatic cancer progression, treatment resistance and metastatic potential (Shin et al., 2009, Yang et al., 2009, Fishel et al., 2015, Fishel et al., 2016, Babu et al., 2018).

Angiogenesis is one of the main factors influencing cancer progression; it falls under the APE1/Ref-1 redox regulation umbrella that is controlled by several transcription factors such as HIF1- α , NF- κ B, and AP-1 (Maulik et al., 2002, Luo et al., 2012, Nagoya et al., 2014, Zhao et al., 2021). Recent research has identified the therapeutic potential of APX3330 and its analogues due to its anti-angiogenic properties (Nyland et al., 2010, Kelley et al., 2011, Kelley et al., 2014, Shahda et al., 2019, Gampala et al., 2021).

Several small-molecule inhibitors that can selectively and precisely target APE1/Ref-1 protein's different functional sites have been introduced in the pre-clinical setting. APE1/Ref-1 redox inhibitor, APX3330, has completed Phase I clinical trial as an anti-cancer drug for solid tumours with a good safety profile, verified target engagement, and approved to continue the trial to Phase II with a daily dose of 600mg (Caston et al., 2021). APX3330 is a novel small molecule compound that selectively inhibits only the redox function of APE1/Ref-1 protein. In this study, we aimed to investigate the efficacy of APX3330 to protect the enteric neurons from Oxaliplatin-induced damage and to potentiate the anti-tumour

effectiveness in combination with Oxaliplatin in an orthotopic model of CRC. This project is mainly focused on the reduction of GI side-effects associated with OXL and the anti-tumour efficacy of APX3330. We hypothesised that APX3330 will reduce inflammation-induced damage to the enteric nervous system (ENS) and gastrointestinal dysfunctions in the murine model of colorectal cancer (CRC). Furthermore, we hypothesised that the impediment of the APE1/Ref-1 redox signalling pathway will alleviate DNA damage as well as inflammation-related cellular damage. With regards to the above hypothesis, the neuroprotective and anti-cancer efficacy of APX3330 in combination with Oxaliplatin for the treatment of CRC in the murine model was further investigated as the aim of the chapter.

3.3 Methods

3.3.1 Animals

Male *Balb/c* mice (n=35) were purchased from the Animal Resources Centre (Perth, Australia) and housed in groups of 5 per cage at the Western Centre for Health Research and Education (WCHRE) for the duration of the project. The animals were kept in a temperature-controlled environment at approximately 22°C with a 12-hour day/night cycle with free access to food and water. The mice were allowed to acclimatise 3-5 days before experiments. All experiments were approved by the Victoria University Animal Experimentation Ethics Committee (Ethics number AEC19-010) and performed according to the guidelines of the National Health and Medical Research Council (NHMRC) Code of Practice for the Care and Use of Animals for Scientific Purposes.

3.3.2 Cell Culture

Murine colorectal cell line CT-26 cells were used to induce cancer in *Balb/c* mice at 9 weeks of age. CT-26 cells were cultured in Roswell Park Memorial Institute

(RPMI) 1640 culture medium (Sigma-Aldrich, Castle Hill, Australia). Culture medium was supplemented with 10% Foetal Bovine Serum (FBS), 1% penicillin-streptomycin, and 1% glutamine. The cells were cultured in 5% CO₂ and 95% air atmosphere at 37°C. Cells were grown in 75cm² flasks and once they grow into confluent or semi-confluent monolayers, they were further passaged or used for the study. The passaged cells were washed with 1x PBS (Phosphate Buffered Saline) before passaging and the cells were seeded by using 0.25% trypsin. Once the cells reached 80-90% confluency in the flask they were separated from the bottom of the flask and centrifuged to obtain the condensed cells for the preparation of injections. Cell pellet was suspended in 1mL PBS. One part of cell suspension was mixed with 1 part of 0.4% trypan blue and the mixture was incubated for 3 minutes in room temperature. A drop of cell/ trypan blue mixture was added to a hemacytometer and cells were counted within 3-5 minutes. Trypan Blue dye was used to determine the number of cells in each vial. The viability of the cells was determined by observing the blue colour hue on the cell surface and they were counted under a light microscope and used a cell counting formula to calculate the total number of viable cells in 1mL of media. The condensed cell lysate was mixed with 100µL of media and 200 µL of Matrigel to prepare for injections. 1x10⁶ cells were mixed with 25µL Matrigel per injection with >95% viability defined by trypan blue exclusion.

3.3.3 Orthotopic Implantation of CT-26 Tumour Cells

The cancer induction was performed by implanting murine CT-26 colorectal cancer cells into the mice caecum. Briefly, mice have received anaesthetics before surgeries using xylazine (10mg/kg) and ketamine (80mg/kg). The level of anaesthesia was checked constantly by performing paw pinch reflex tests especially before and during the surgery. The surgeries were performed in an aseptic environment and the mice were placed on a heat mat (30-36°C) during surgeries to prevent heat loss. The surgical instruments were autoclaved before the surgeries and only opened on the operating table under an aseptic environment during surgeries. The abdominal area of the mice was shaved and swabbed with

70% ethanol followed by covering with sterile film to prepare the mice for the procedure. A small abdominal incision was made along the midline to exteriorise the caecum and the caecum was placed on sterile gauze during the procedure. One million (1×10^6) CT-26 murine colorectal tumour cells, that were suspended in 25 μ L of Matrigel with >95% viability, was injected into the caecum using an insulin needle. The tumour cells were injected into the outer layer of the caecum and a visible bulla formation was observed. The injections were carried out in a way to prevent any extra-caecal fluid leakage to complete the criteria for successful injection. The caecum was returned to the abdominal cavity, the abdominal muscles were sutured using polygalaceous suture and the skin was sutured using surgical silk or dissolvable skin sutures. The incision area in the abdomen was swabbed with saline followed by sterilising with Iodine to aid the recovery process. After the surgery, the mice were given an analgesic, Temgesic/buprenorphine (0.05mg/kg) subcutaneously. After returning to the recovery cage, the mice were closely monitored for 1-2 hours until they were conscious and moving around the cage and they were returned to the animal house, and they remained there until the end of the treatment period.

3.3.4 Treatments

Mice without CRC (n=15/cohort) were randomly divided into three groups untreated (n=5), Oxaliplatin-treated (n=5), and APX3330-treated (n=5) received treatments twice as per the treatment plan (Table 3.1). Following CRC-induction surgery mice with cancer (n=18/cohort) were randomly divided into four groups including a two vehicles-treated group (n=5), Oxaliplatin plus vehicle for APX3330-treated (n=5), APX3330 plus vehicle for Oxaliplatin (OXL)-treated (n=4) and a combination of Oxaliplatin plus APX3330 (n=4) group (Table 3.1). All groups received treatments for two weeks starting from day 6 post-surgery. In the cancer-free cohort, the untreated group (n=5) did not receive any treatments and were subjected to final experiments on day 15. Oxaliplatin-treated without cancer mice received treatments every second day with a maximum of 3 injections per week for 14 days and

APX3330-treated cancer-free mice received treatments twice a day with 12 hours duration for 14 days. CRC-induced, two vehicles-treated (vehicle for Oxaliplatin plus vehicle for APX3330), Oxaliplatin plus vehicle for APX3330-treated, APX3330 plus vehicle for Oxaliplatin-treated, and a combination of Oxaliplatin with APX3330-treated mice received treatments twice daily with 12-hours interval. Details of the treatment groups and treatment regimens are outlined in Table 3.1. Mice received intraperitoneal injections (IP) of Oxaliplatin (OXL) (Tocris Bioscience, UK) (3 mg/kg/dose) (3 times a week, 2 weeks) via a 30 ½ gauge needle. OXL was dissolved in sterile water to make stock solutions and they were refrigerated at -20°C until they were further diluted to make working solutions for the intraperitoneal injections (McQuade et al., 2016). The dose of the Oxaliplatin was calculated to achieve a cumulative dose corresponding to an average human dose (Reagan-Shaw et al., 2008, Kohne et al., 2012). APX3330 (25 mg/kg) dose was given to mice 2x daily with 12 h intervals for 14 days via intraperitoneal injections starting on the same day as OXL. APX3330 was dissolved in 2% Cremophor, 2% Ethanol, and 96% sterile water, due to the poor dissolvability of APX3330. APX3330 dose was based on our previous study that showed neuroprotective and anti-inflammatory effects in mice with chronic intestinal inflammation (Sahakian et al., 2021). The volumes for all injections were calculated to the animal's body weight every day with less than 200 µL per injection (Table 3.1).

3.3.5 Clinical Parameters

3.3.5.1 Body Weights

Mice were weighed daily before the treatments starting three days after acclimatisation. They were weighed throughout the treatment period until the day of the final experiments. Bodyweight data were used as an indicator of their general health and wellbeing.

Table 3.1 Treatment Regimens

Treatment Group	Number of Mice	Treatment
Mice without CRC		
Untreated	n=5	No Treatment
Oxaliplatin-treated	n=5	OXL: 3 mg/kg/dose (dissolved in sterile water) 3 times a week, 2 weeks
APX3330-treated	n=5	APX3330: 25 mg/kg/dose (dissolved in 2% EtOH and 96% sterile water) 2x daily with 8 h interval, 2 weeks
Mice with CRC		
Vehicle 1 + Vehicle 2-treated	n=5	Vehicle 1: sterile water 3 times a week, 2 weeks Vehicle 2: 2% Cremophor: 2% EtOH and 96% sterile water 2x daily with 8 h interval, 2weeks
APX3330 + Vehicle-treated	n=4	APX3330: 25 mg/kg/dose 2x daily with 8 h interval, 2 weeks Vehicle 1: sterile water 3 times a week, 2 weeks
Oxaliplatin + Vehicle-treated	n=5	OXL: 3 mg/kg/dose 3 times a week, 2 weeks Vehicle 2: 2% Cremophor: 2% EtOH and 96% sterile water 2x daily with 8 h interval, 2weeks
Oxaliplatin + APX3330-treated	n=4	OXL: 30 mg/kg/dose 3 times a week, 2 weeks APX3330: 25 mg/kg/dose 2x daily with 8 h interval, 2 weeks

3.3.5.2 Faecal Water Content

Faecal water content was calculated by analysing the difference between wet and dry faecal weights. The wet weight of the faecal pellets was measured immediately after the sample collection. Samples were placed in a 60°C oven overnight and then the dry weights of the samples were measured. Faecal water content was analysed before the commencement of the treatment (day 0), middle (day7), and the end of the treatment (day 14). Faecal water content was calculated by analysing the percentage difference between wet and dry faecal weights to wet pellet weights using the following formula:

$$\text{Faecal water content (\%)} = \frac{\text{Wet pellet weight} - \text{Dry pellet weight}}{\text{Wet pellet weight}} \times 100$$

3.3.6 Tissue Collection

On day 6 post-surgery the mice started receiving Oxaliplatin, APX3330, Vehicle, or a combination of treatments for 14 days. After the treatments mice were culled by giving a lethal injection of phenobarbital. The caecum was exteriorised and examined for tumour growth. Samples of the caecum, distal colon, and secondary spread of tumour samples in the abdominal cavity were immediately snap-frozen in liquid nitrogen for Western blot analysis. Fresh colon samples were collected and processed for immunohistochemistry experiments as described below.

3.3.6.1 Immunohistochemistry in Wholemout Preparations

Immunohistochemistry was performed as described in Robinson et al. (2014) and

Wafai, et al. (2013). The distal colon tissue samples from each animal were collected and placed in oxygenated phosphate-buffered saline (PBS, pH7.2) that contained nicardipine (3 μ M) for 20 minutes to inhibit smooth muscle contractions. Wholmount preparation sample tissues were maximally stretched and pinned flat with the mucosal side up into the dish. Then the tissue samples were fixed with Zamboni's fixative (2% formaldehyde containing 0.2 % picric acid) overnight at 4°C. The next day, the tissue sections were washed with dimethyl sulfoxide (DMSO, Sigma-Aldrich, Australia) three times 10 minutes apart to clear off the fixative followed by three times ten-minute washes of phosphate-buffered saline (PBS). Tissue samples of the distal colon that were prepared for Immunohistochemistry wholmounts were then placed in 10mL of PBS+0.01g of Sodium Azide solution and stored at 4°C for long-term storage.

The tissues processed for wholmount preparations were then washed (2x5 mins) with phosphate-buffered saline with 0.01% Triton X 100 (PBST) and then peeled the mucosal layer, submucosal muscle layer, and the circular muscle layer off to visualise the myenteric plexus of the colon. Once the longitudinal muscle-myenteric plexus (LMMP) of the wholmount preparation is neatly dissected, the tissues were incubated in a humidified box with 10% normal donkey serum (Chemicon, USA) for 1 hour at room temperature. The tissues were then washed (3 x 5 mins) with PBST followed by incubating with primary antibodies (Table 3.2) overnight at room temperature. The following day, the tissue preparations were washed in PBST (3x10 min) before incubation with species-specific secondary antibodies (Table 3.2) that were developed to detect and bind to the primary antibody. The tissue sections were incubated in a dark humidified box for two hours at room temperature before washing in (3x10 min) PBST. After the third PBST wash, the sections were incubated with 4'6-diamidine-2'-phenylindole dihydrochloride (DAPI) (D1306, Life Technologies, Australia) for 1 minute which serves as a fluorescent nucleic acid stain. Tissues were then further subjected to PBST washes (2x10 min) and then mounted on glass slides using fluorescent mounting medium (DAKO).

Table 3.2 Primary and Secondary Antibodies Used in Wholemout Preparations

Antibody	Species	Dilution	Source
Primary antibodies			
Pan neuronal marker anti-PGP9.5 antibody	Rabbit, polyclonal	1:500	Abcam, Australia
Apurinic/aprimidinic endoneuclease-1 anti-APE1/Ref-1 (APE-1) antibody	Mouse, monoclonal	1:1000	A gift from Prof. M. Kelley, Indiana University, Indianapolis, Indiana, US
Neuronal nitric oxide synthase anti-nNOS antibody	Goat, monoclonal	1:500	Abcam, Australia
Secondary antibodies			
Alexa Flour 488	Anti-mouse	1:300	Jackson ImmunoResearch laboratories, United States
Alexa Flour 594	Anti-rabbit	1:300	
Alexa Flour 647	Anti - goat	1:300	

3.3.6.2 Imaging

Nikon Eclipse Ti laser scanning microscope (Nikon, Japan) was utilized to take three-dimensional images of wholemount preparations of the samples. Wholemount preparations of the distal colon segments were observed under the microscope, and 8 randomly selected images were taken using x40 objective and the images were processed using NIS Element Software (Nikon, Japan). Z-series images were taken to analyse the complete image at a step size of 1.75 μ m (1600 \times 1200 pixels). Images were analysed by the variation of fluorescence in each image in comparison to the relative fluorescence of each area of the image. The images were then analysed by using Image J software.

3.3.7 Morphometric Analysis of Tumours and Metastasis

Tumour growth in the caecum and colon was assessed *ex vivo* macroscopically as well as histologically. The freshly resected caecum was weighted, and the number of tumours and polyps were counted where applicable. Then the caecum was placed in PBS and cut along the mesenteric border to expose the content. Caecum tissues were then pinned down mucosal side up and flushed out the content. Fresh caecum samples were snap-frozen for Western Blot experiments. The size, number, and weight of the tumours, tumour metastasis were analysed on the day of the tissue collection.

3.3.8 Western Blot Analysis

Freshly harvested segments of distal colon samples were washed with 1 \times PBS solution to flush off its content and snap frozen until the following day. The following day the frozen tissue samples were homogenized with a Polytron

homogenizer (Kinematica AG, Lucerne, Switzerland) for 20 seconds in ice-cold Radioimmunoprecipitation Assay (RIPA) solution containing protease and phosphatase inhibitors cocktails (1:100 protease inhibitor, 1:100 phosphatase inhibitor) (Bio-Rad). Then the homogenate was centrifuged, and the lysate samples were preserved in a -80°C freezer for further analysis. The exact protein concentration of each lysate sample was determined by the detergent compatible protein assay (DC protein assay) kit (Bio-Rad Laboratories, Hercules, CA, USA). To make Western blot working samples, equal amounts of protein samples will be taken from each lysate sample based on their protein concentration and they were dissolved in $25\mu\text{L}$ of Laemmli buffer and the rest of the volume was filled with RIPA Buffer to make $100\mu\text{L}$ of WB working samples. Prepared working samples were subjected to electrophoretic separation on sodium dodecyl sulfate-polyacrylamide gel electrophoresis (SDS-PAGE) acrylamide gels to determine the expression of different target proteins. The protein expression was evaluated following electrophoretic separation, the proteins were transferred to a polyvinylidene difluoride (PVDF) membrane and then blocked with 5% skim milk (Tris Buffered Saline containing 0.1% Tween, TBST) for 1 hour followed by 4 x 5 mins TBST washes. The membranes were incubated overnight in a platform shaker at 40rpm speed with primary antibodies (Table 3.4) based on the target of interest at -4°C . Primary antibodies were prepared in 1% Bovine Serum Albumin (BSA) (TBST, BSA, 0.01% Sodium Azide) and 1:1000 primary antibody concentration was used throughout the study. Membranes were washed 4 x 5 mins washes with TBST on the following day and probed with horseradish peroxidase (HRP)-conjugated secondary antibodies (Table 3.4) in 5% skim milk solution for 2 hours at room temperature. Membranes were then washed with 4x 5mins TBST washes the blots were developed using ECL Prime Reagent (Amersham, Piscataway, NJ, USA) followed by imaging in a DARQ CCD camera mounted to a fusion FX Imaging system (Silver Lourtmat, Germany). Densitometric measurements of the protein of interest were performed employing Fusion CAPT Advance software (Viber Lourtmat, Germany). The signal intensity of the target protein was normalised to the signal intensity of the total protein loaded. The proteins extracted from distal colon segments from each animal were evaluated for the expression of APE1/Ref-1,

cytochrome c, signal transducer and activator of transcription 3 (STAT3), phosphorylated STAT3 (pSTAT3) and vascular endothelial growth factor (VEGF).

3.3.9 Data and Statistical Analysis

Image J Software (National Institute of Health, Bethesda, MD, USA) was used to convert images from RGB to greyscale 8-bit binary. Images were then analysed to attain the percentage area of immunoreactivity. All immunohistochemistry images and Western Blot images were quantified as per above and statistical analysis was performed with Prism (version 9.0v, Graph Pad Software, La Jolla, CA, USA). All values were represented as mean +/- standard error of the mean except the changes in body weight (%) during the 14-day period that was presented as mean +/- standard deviation of the mean (S.D.). One-way ANOVA followed by the Tukey-Kramer post hoc tests for multiple group comparison test was used to analyse the differences between all groups. $P < 0.05$ was considered significant.

Table 3.3 Primary and Secondary Antibodies Used for Western Blot Experiments

Antibody	Species	Dilution	Source
Primary antibodies			
Apurinic/aprimidinic endoneuclease-1 anti-APE1/Ref-1 (APE1/Ref-1) antibody	Mouse, monoclonal	1:1000	Abcam, Australia
Vascular endothelial growth factor marker anti-VEGF antibody	Rabbit, polyclonal	1:1000	Abcam, Australia
Cytochrome c	Rabbit, polyclonal	1:1000	Abcam, Australia
Signal transducer and activator of transcription 3 marker anti-STAT3 antibody	Rabbit, monoclonal	1:1000	Cell signalling, Australia
Phospho specific signal transducer and activator of transcription 3 marker anti-pSTAT3 antibody	Rabbit, monoclonal	1:1000	Cell signalling, Australia
Secondary antibodies			
Horseradish peroxidase (HRP) IgG (H+L)	Anti-mouse	1: 5000	Abcam, Australia
Horseradish peroxidase (HRP) IgG (H+L)	Anti-rabbit	1: 5000	Abcam, Australia

3.4 Results

3.4.1 Effects of Treatments on Clinical Symptoms

3.4.1.1 Effects of Treatments on Body Weights

Mice without cancer were weighed throughout the experiment period to assess their general health and wellbeing as well as to detect any adverse side effects of the OXL and APX3330 treatments on body weight. Mice without CRC were randomly allocated into three groups that received treatments for 2 weeks following 3 days of the acclimatisation period (**Table 3.1**). Untreated mice without cancer continued to gain weight throughout the experimental period with $11.9 \pm 0.5\%$, $P < 0.01$ weight gain at day 15 from the start of the treatment compared to day 1 (**Figure 3.1A**). APX3330-treated mice without CRC also gained weight during the treatment period with an average weight gain of $7.9 \pm 0.1\%$, $P < 0.01$ at day 15 compared to day 1. OXL-treated mice did not gain weight throughout the treatment period with an average weight loss of $-1.3 \pm 1.3\%$, $P < 0.05$ at day 15 compared to day 1. The average body weight of OXL-treated mice ($22.0 \pm 0.7\text{g}$) was significantly lower at day 15 of treatment compared to untreated ($26.9 \pm 0.7\text{g}$, $P < 0.001$) and APX3330-treated ($25.1 \pm 0.6\text{g}$, $P < 0.01$) mice ($n=5$ mice/group) (**Figure 3.1B**).

Tumour-bearing mice were randomly divided into 4 groups that received treatments for 14 days starting on day 6 post CRC induction surgery (**Table 3.1**). Mice treated with two vehicles gradually gained weight during the treatment period with $8.1 \pm 1.3\%$, $P < 0.01$ weight gain at day 15 compared to day 1 (**Figure 3.2A**). Repeated *in vivo* administration of OXL caused significant weight loss in CRC-induced mice after a 14-day treatment period compared to day 1 ($-3.3 \pm 0.4\%$, $P < 0.01$). APX3330 + VEH-treated mice with CRC gained weight by $4.4 \pm 1.3\%$, $P < 0.05$ at day 15. A combination of OXL and APX3330 treatment increased body weight by $3.3 \pm 0.6\%$ ($P < 0.05$) at day 15 compared to day 1. The average body weight of OXL-treated mice with CRC at day 15 was $21.4 \pm 0.5\text{g}$, which was lower

than VEH + VEH-treated mice ($26.8 \pm 0.5\text{g}$, $P<0.0001$), APX3330 + VEH-treated mice (25.3 ± 0.4 , $P<0.001$) and combination of APX3330 + OXL-treated mice ($24.3 \pm 0.6\text{g}$, $P<0.01$) (**Figure 3.2B**). The body weight of APX3330 + VEH-treated mice was lower compared to VEH + VEH-treated mice ($P<0.05$). VEH + VEH-treated mice demonstrated significantly higher average body weight at day 15 due to rapid growth of tumours in the abdominal cavity ($n=4-5$ mice/group).

3.4.1.2 Effects of Treatments on Faecal Water Content

To define the faecal water content, as a measurement of symptoms of diarrhoea or constipation, fresh faecal pellets were collected from untreated, OXL-treated, and APX3330-treated mice before the initiation of the treatment (day 0), at day 7 and day 14 of treatment. Faecal water content was calculated as the percentage difference between wet and dry pellet weight to wet pellet weights. Before the start of the treatment at day 0, no differences were found in the wet and dry faecal weights and, therefore, faecal water content was not different between all three groups (untreated: $52.9 \pm 2.0\%$, OXL-treated: $54.5 \pm 1.2\%$ and APX3330-treated: $52.8 \pm 0.9\%$, respectively, $n=5$ mice/group) (**Figure 3.3A**). Wet faecal pellet weight was significantly lower in OXL-treated mice ($31.9 \pm 2.3\text{mg}$) in comparison with untreated mice without cancer ($51.5 \pm 2.5\text{mg}$, $P<0.001$) and APX3330-treated mice ($53.6 \pm 3.5\text{mg}$, $P<0.001$) at day 7. Dry faecal pellet weight was also significantly lower in OXL-treated mice ($21.6 \pm 1.1\text{mg}$) compared to untreated mice without cancer ($29.0 \pm 2.2\text{mg}$, $P<0.05$) and APX3330-treated mice ($30.4 \pm 2.4\text{mg}$, $P<0.05$) at day 7 of the treatment. The mean faecal water content was significantly lower at day 7 of the treatment in the OXL-treated group ($32.5 \pm 1.2\%$) compared to untreated $43.2 \pm 2.8\%$ ($P<0.01$) and APX3330-treated $43.4 \pm 1.1\%$ ($P<0.01$) groups ($n=5$ mice/group) (**Figure 3.3B**). At day 14, the wet faecal weight was considerably decreased in OXL-treated mice without cancer ($29.8 \pm 4.0\text{mg}$), compared to untreated mice ($52.7 \pm 1.4\text{mg}$, $P<0.001$) and APX3330-treated mice ($54.3 \pm 2.6\text{mg}$, $P<0.001$). Dry faecal pellet weight was also significantly lower in OXL-treated mice at day 14 ($21.5 \pm 1.3\text{mg}$) in comparison with untreated mice ($29.9 \pm 2.6\text{mg}$, $P<0.05$)

but not significantly different from APX3330-treated mice ($22.6 \pm 1.5\text{mg}$) compared to OXL-treated mice. At day 14, the OXL-treated group maintained a lower level of faecal water content $27.7 \pm 1.2\%$ compared to untreated ($43.2 \pm 3.1\%$, $P < 0.001$) and APX3330-treated mice without cancer ($51.0 \pm 1.9\%$, $P < 0.0001$) ($n=5$ mice/group) (**Figure 3.3C**). Thus, faecal water content was significantly lower in OXL-treated mice throughout the 14-day treatment period indicating chronic constipation.

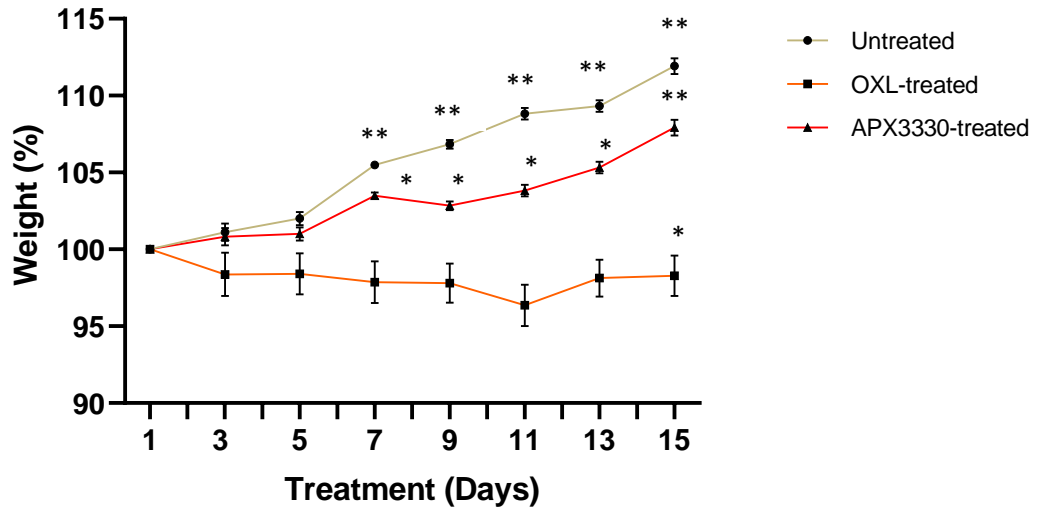
Similarly, no difference in the faecal water content was found before the start of the treatment in mice with CRC: VEH + VEH-treated ($45.9 \pm 3.0\%$), OXL + VEH ($51.3 \pm 2.2\%$), APX3330 + VEH ($46.3 \pm 3.3\%$) and combination of APX3330 + OXL-treated ($47.1 \pm 1.4\%$) mice ($n=5$ mice/group) (**Figure 3.4A**). At day 7, wet faecal weight was significantly lower in OXL + VEH-treated mice ($30.0 \pm 1.7\text{mg}$) when compared to VEH + VEH-treated mice ($59.9 \pm 2.4\text{mg}$, $P < 0.0001$), APX3330 + VEH-treated mice ($51.2 \pm 2.8\text{mg}$, $P < 0.0001$) and combination treatment of APX3330 + OXL ($49.5 \pm 2.5\text{mg}$, $P < 0.001$). In line with wet faeces weight, dry faeces weight was also significantly lower in OXL-treated mice ($21.5 \pm 1.1\text{mg}$) compared to APX3330 + VEH-treated mice ($31.4 \pm 1.8\text{mg}$, $P < 0.01$) and combination treatment of APX3330 + IRI ($30.4 \pm 2.6\text{mg}$, $P < 0.05$) but not VEH + VEH-treated mice ($28.0 \pm 1.4\text{mg}$, $P < 0.01$). Faecal water content in OXL + VEH-treated mice ($28.5 \pm 1.5\%$) was lower compared to VEH + VEH ($53.4 \pm 2.4\%$, $P < 0.0001$), APX3330 + VEH ($38.8 \pm 1.5\%$, $P < 0.01$) and APX3330 + OXL ($38.6 \pm 1.9\%$, $P < 0.01$) treated mice indicating constipation in OXL-treated mice ($n=5$ mice/group) (**Figure 3.4B**). At day 14, wet faecal weight was significantly lower in OXL + VEH-treated mice ($29.8 \pm 3.0\text{mg}$) when compared with VEH + VEH-treated mice ($59.1 \pm 1.6\text{mg}$), APX3330 + VEH-treated mice ($58.9 \pm 1.8\text{mg}$) and combination treatment of APX3330 + OXL mice ($49.5 \pm 2.5\text{mg}$) ($P < 0.0001$ for all). Similarly, the dry faecal weight was also significantly lower in OXL + VEH-treated mice ($22.2 \pm 1.7\text{mg}$) at day 14 as opposed to VEH + VEH-treated mice ($31.4 \pm 1.6\text{mg}$, $P < 0.05$), APX3330 + VEH-treated mice ($32.9 \pm 2.4\text{mg}$, $P < 0.01$) but not different compared to the APX3330 + OXL-treated group ($23.7 \pm 1.6\text{mg}$). At day 14, the water content in the faecal pellets was significantly lower in OXL + VEH-treated mice ($25.5 \pm 2.5\%$) compared to VEH +

VEH ($46.9 \pm 2.9\%$), APX3330 + VEH ($44.1 \pm 1.5\%$) and APX3330 + OXL ($52.2 \pm 1.3\%$) ($P < 0.0001$ for all) treated mice ($n=4-5$ mice/group) (**Figure 3.4C**). Thus, the water content was significantly lower in the faeces collected from OXL-treated mice on both days 7 and 14 of treatment, indicating chronic constipation.

Figure 3.1 Effect of OXL and APX3330 treatment on body weight of mice without cancer. (A) Changes in body weight (%) during 14-day treatment period of mice treated with Oxaliplatin (orange), APX3330 (red), and untreated (green). Data at all time points were compared to the starting body weight at day 1, which was considered as 100%. All values were presented as mean and \pm S.D. * P <0.05, ** P <0.01, n =5 mice/group. (B) Body weight of OXL and APX3330-treated mice at day 15 compared to untreated mice. All values were presented as mean and \pm S.E.M. ** P <0.01, *** P <0.001 n =5 mice/group.

A

Body Weight (Mice Without Cancer)



B

Body Weight on Day 15 (Mice Without Cancer)

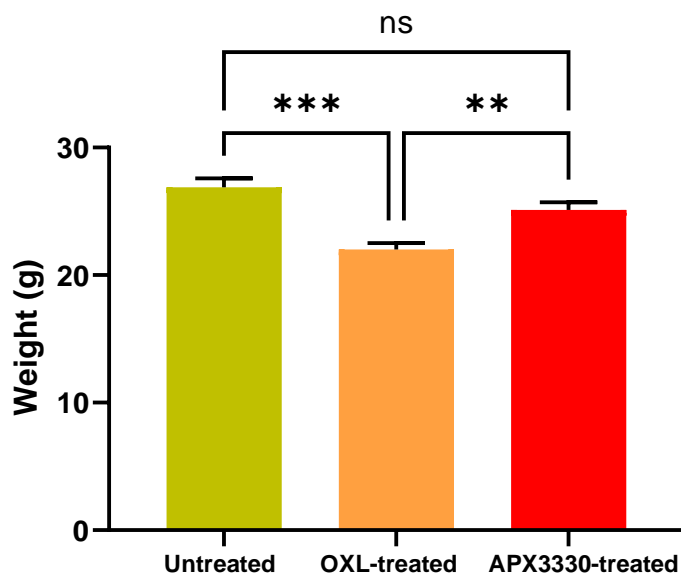
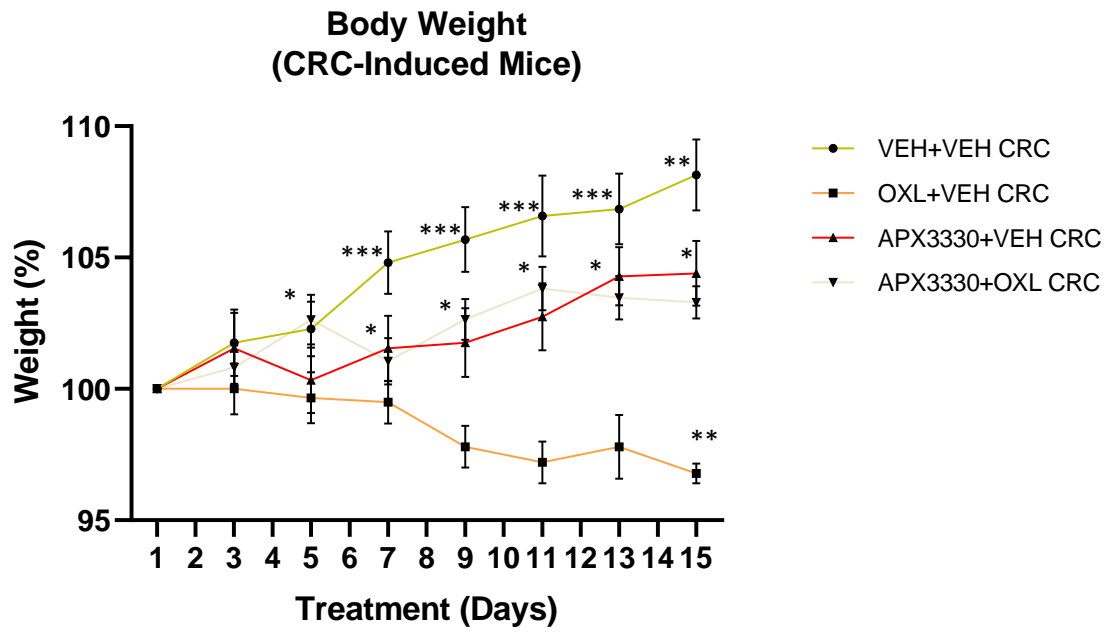


Figure 3.2 Average body weight following 14 days of treatments in CRC-Induced mice. (A) Changes in body weight (%) during 14-day treatment starting at day 6 post CRC-induction surgery with a vehicle for APX3330 plus a vehicle for OXL (green), Oxaliplatin plus a vehicle for APX3330 (orange), APX3330 plus a vehicle for OXL (red) and a combination of APX3330 plus OXL (yellow). Data at all time points were compared to the starting body weight at day 1, which was considered as 100%. All values were presented as mean and \pm S.D. * P <0.05, ** P <0.01, *** P <0.001, n =5 mice/group. (B) The body weight of mice from all treatment groups measured at day 15. All values were presented as mean and \pm S.E.M. * P <0.05, ** P <0.01, *** P <0.001, **** P <0.0001, n =4-5 mice/group.

A



B

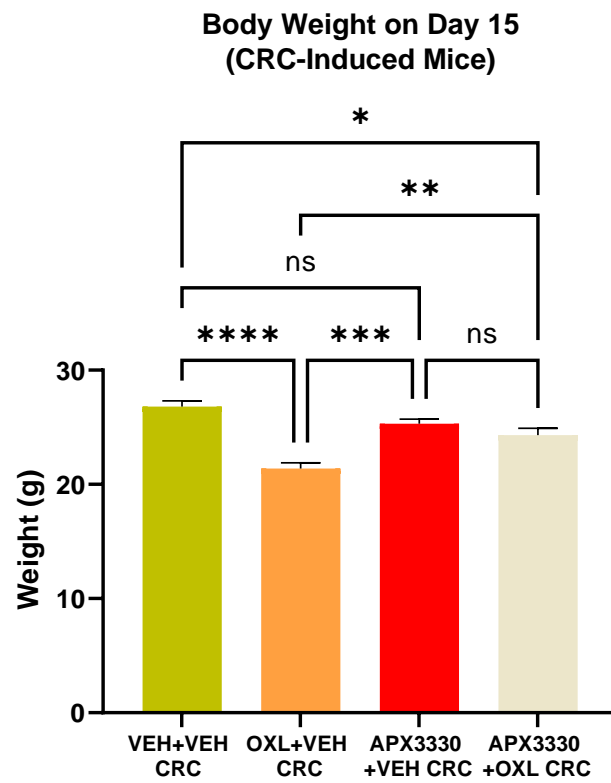
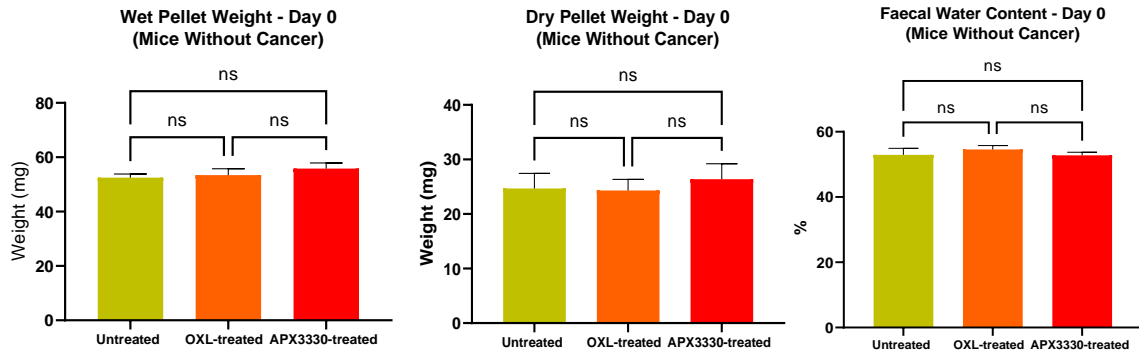
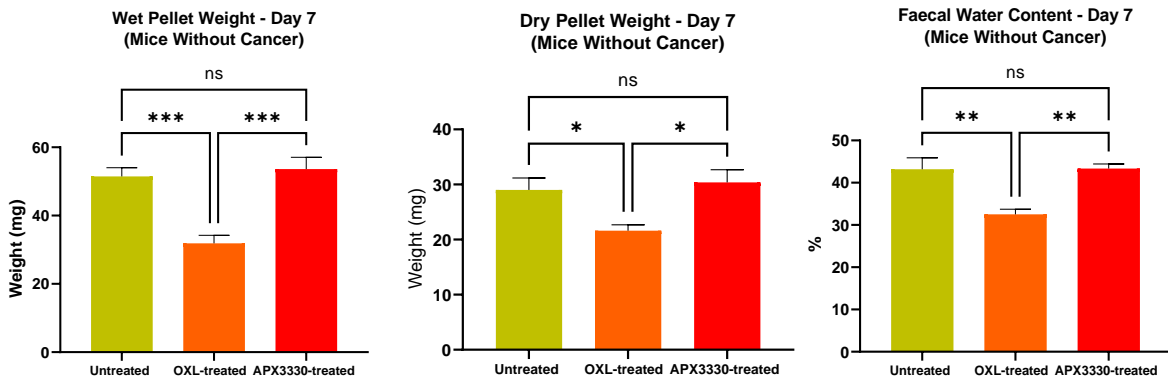


Figure 3.3 Effects of Oxaliplatin and APX3330 treatment on faecal water content of mice without cancer. The wet and dry weight of the faecal pellets (mg) and the faecal water content (the difference between wet and dry pellet weights, %) before the commencement of the treatment (A), after 7 days of treatment (B), after 14 days of treatment (C). Data presented as mean \pm S.E.M. * P <0.05, ** P <0.01, *** P <0.001, **** P <0.0001, $n=5$ mice/group.

A



B



C

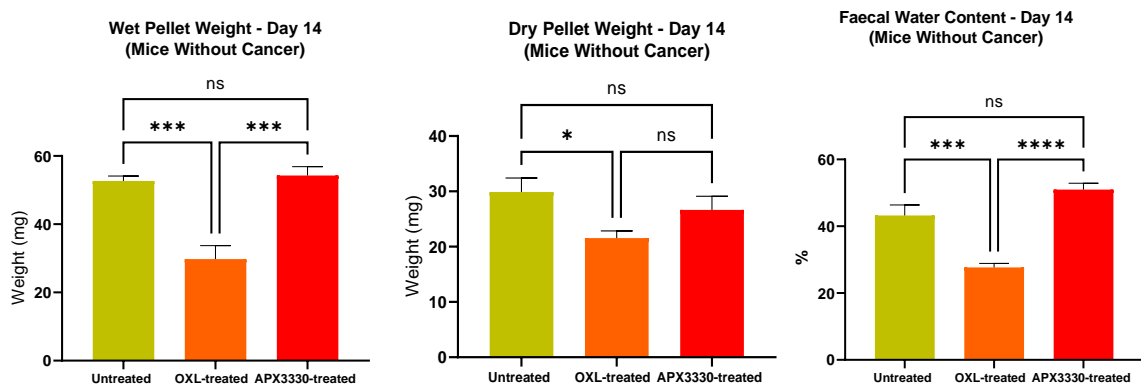
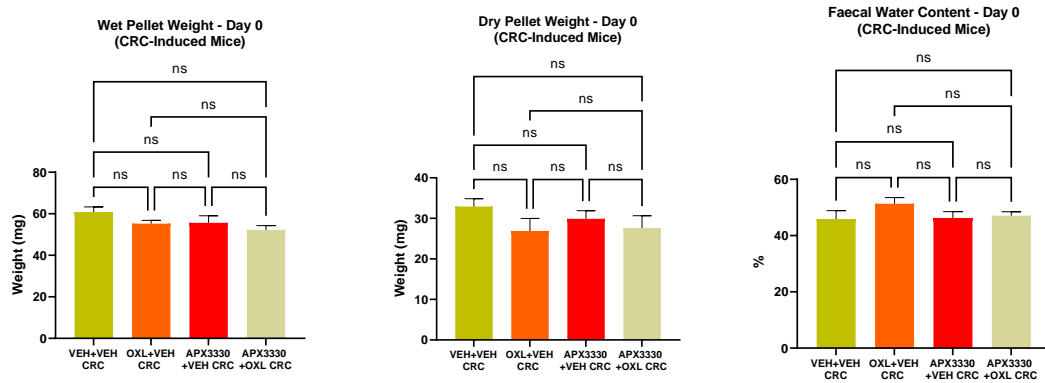
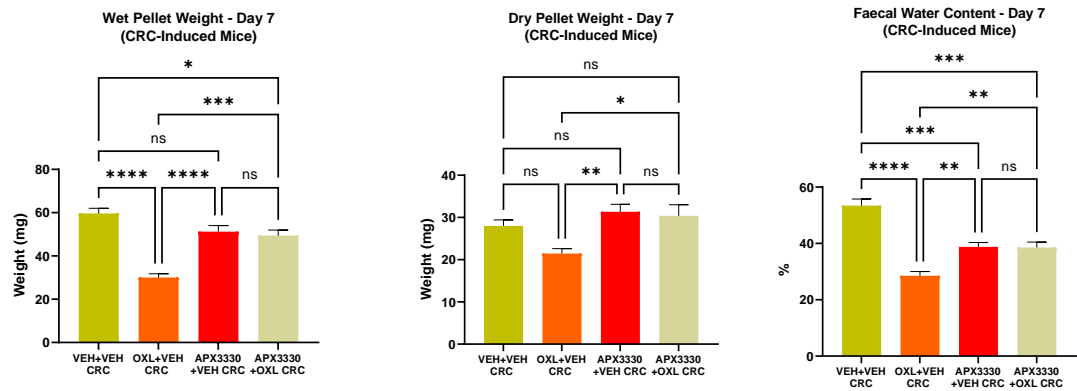


Figure 3.4 Effects of the treatments on faecal water content in CRC-induced mice. The wet and dry weight of the faecal pellets (mg) and the faecal water content (the difference between wet and dry pellet weights, %) before the commencement of the treatment (A), after 7 days of treatment (B), after 14 days of treatment (C). Data presented as mean \pm S.E.M. * P <0.05, ** P <0.001, *** P <0.001, **** P <0.0001, n=4-5 mice/group.

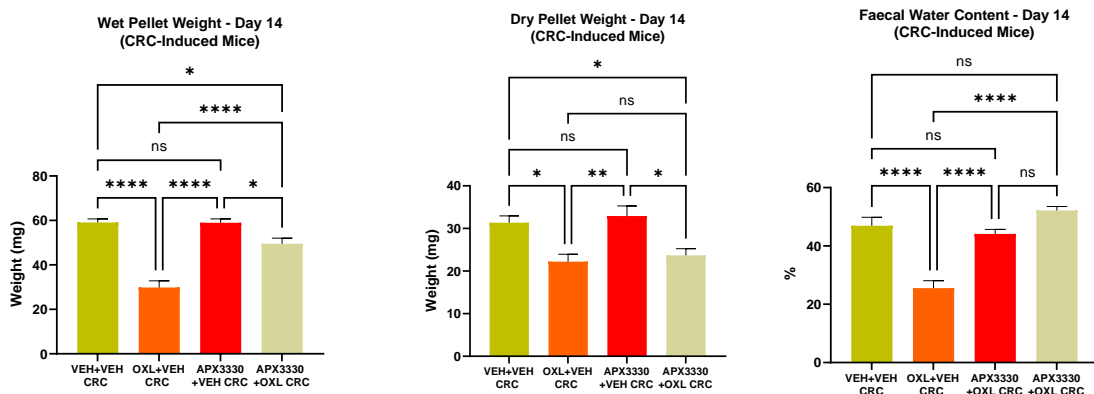
A



B



C



3.4.2 Effect of the Treatments on the Total Number of Myenteric Neurons and Inhibitory Neurons

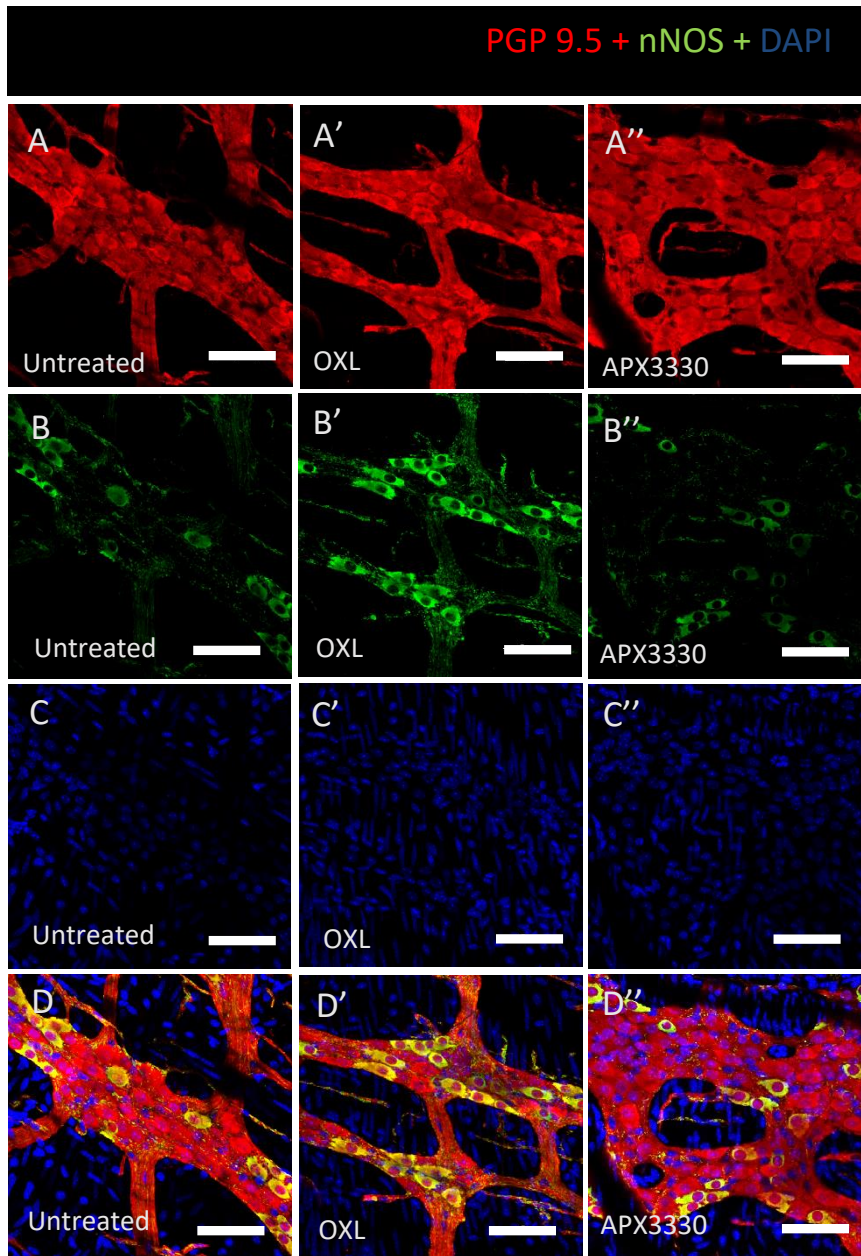
To investigate the changes in the total number of myenteric neurons in the distal colon, wholemount preparations of the distal colon were labelled with pan-neuronal marker anti-protein gene product 9.5 (PGP9.5) antibody to count neurons within a 0.4 mm² area (**Figure 3.5 A-A''**). Data revealed that repeated administration of Oxaliplatin caused myenteric neuronal loss and APX3330 treatment caused less damage to myenteric neurons in the distal colon in mice that did not have cancer (**Figure 3.5 E**). Repeated *in vivo* administration of Oxaliplatin induced myenteric neuronal loss in the distal colon (49.0 ± 2.3 neurons/area) compared to untreated (88.5 ± 1.9 neurons/area) and APX3330-treated mice (88.0 ± 4.5 neurons/area) ($P < 0.0001$ for both) (n=5 mice/group).

To investigate changes in subpopulations of myenteric inhibitory muscle motor neurons and interneurons immunoreactive for nNOS, wholemount preparations of the distal colons were labelled with a neuronal nitric oxide synthase specific anti-nNOS antibody (**Figure 3.5 B-B''**) and cell nuclei marker DAPI (**Figure 3.5 C-C''**). Neurons within 0.4mm² areas were counted. The number of nNOS immunoreactive neurons was the highest in Oxaliplatin-treated mice (26.8 ± 1.5 neurons/area) compared to untreated (15.0 ± 1.5 neurons/area, $P < 0.001$) and APX3330-treated (16.0 ± 2.0 neurons/area, $P < 0.01$) mice. The proportion of nNOS-immunoreactive neurons to the total number of PGP9.5-immunoreactive neurons was the highest in Oxaliplatin-treated mice (54.7 ± 1.3 %) compared to untreated (17.0 ± 1.8 %) and APX3330-treated (18.2 ± 2.8) ($P < 0.0001$ for both) (n=5 mice/group).

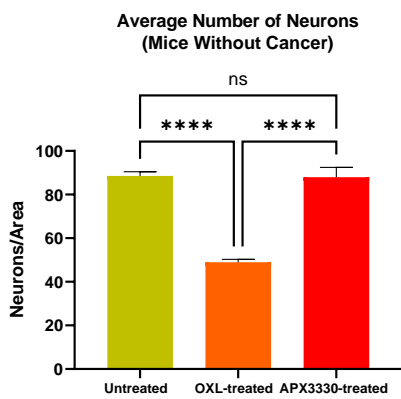
With regards to CRC-induced mice, wholemount preparations of the distal colon sections were labelled with PGP9.5 (**Figure 3.6 A-A'''**) and anti-nNOS (**Figure 3.6 B-B'''**) antibodies and counterstained with DAPI (**Figure 3.6 C-C'''**) to investigate changes in the total number of myenteric neurons, changes in

subpopulations of myenteric inhibitory muscle motor and interneurons immunoreactive for nNOS with 14 days *in vivo* administration of the treatments. Oxaliplatin treatment caused significant reduction of myenteric neurons (48.1 ± 2.5 neurons/area) compared to VEH + VEH-treated (70.4 ± 2.2 neurons/area), APX3330 + VEH (78.4 ± 1.2 neurons/area) and combination treatment of APX3330 + OXL (88.4 ± 1.7 neurons/area) treated groups ($P < 0.0001$ for all) (**Figure 3.6 E**). The number of nNOS-IR neurons was the highest in the OXL + VEH-treated group (27.8 ± 1.3 neurons/area) compared to VEH + VEH (20.6 ± 1.5 neurons/area, $P < 0.05$), APX3330 + VEH (11.3 ± 1.3 neurons/area, $P < 0.0001$) and combination of APX3330 + OXL (14.8 ± 1.9 neurons/area, $P < 0.0001$) treated CRC mice (**Figure 3.6 F**). The proportion of nNOS: PGP9.5 was the highest in OXL + VEH-treated mice ($57.9 \pm 2.5\%$) compared to VEH + VEH-treated ($29.9 \pm 0.8\%$), APX3330 + VEH-treated ($14.5 \pm 1.7\%$) and combination of APX3330 + OXL received ($16.8 \pm 0.9\%$) tumour-bearing mice ($P < 0.0001$ for all) ($n = 4-5$ mice/group) (**Figure 3.6 G**).

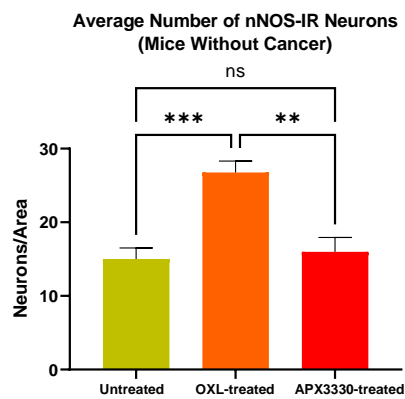
Figure 3.5 Effect of *in vivo* treatments on neuronal nitric oxide synthase (nNOS)-immunoreactive neurons in mice without cancer. Wholemout preparations of the myenteric ganglia from the distal colon of untreated, OXL-treated, APX3330-treated mice following 14-day of *in vivo* treatment labelled with a pan-neuronal marker anti-PGP9.5 antibody (red) (A-A''), an inhibitory neuronal marker, neuronal nitric oxide synthase (green) (B-B'') and DAPI (C-C''). Merged images (D-D''). Scale bar = 50µm. Quantitative analysis of the average number of myenteric neurons immunoreactive for PGP9.5 (E), the average number of nNOS-immunoreactive inhibitory neurons (F), the proportion of nNOS-IR neurons to the total number of PGP9.5-IR neurons (G) in the myenteric ganglia within 0.4 mm² area. Data presented as mean ± S.E.M. ***P*<0.01, ****P*<0.001, *****P*<0.0001, n=5 mice/group.



E



F



G

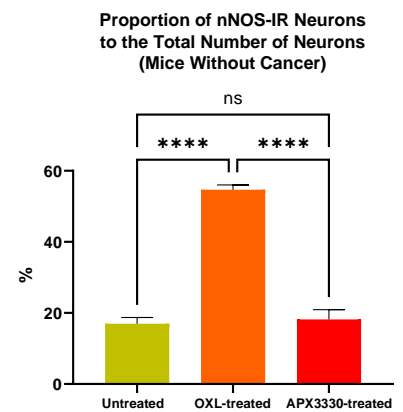
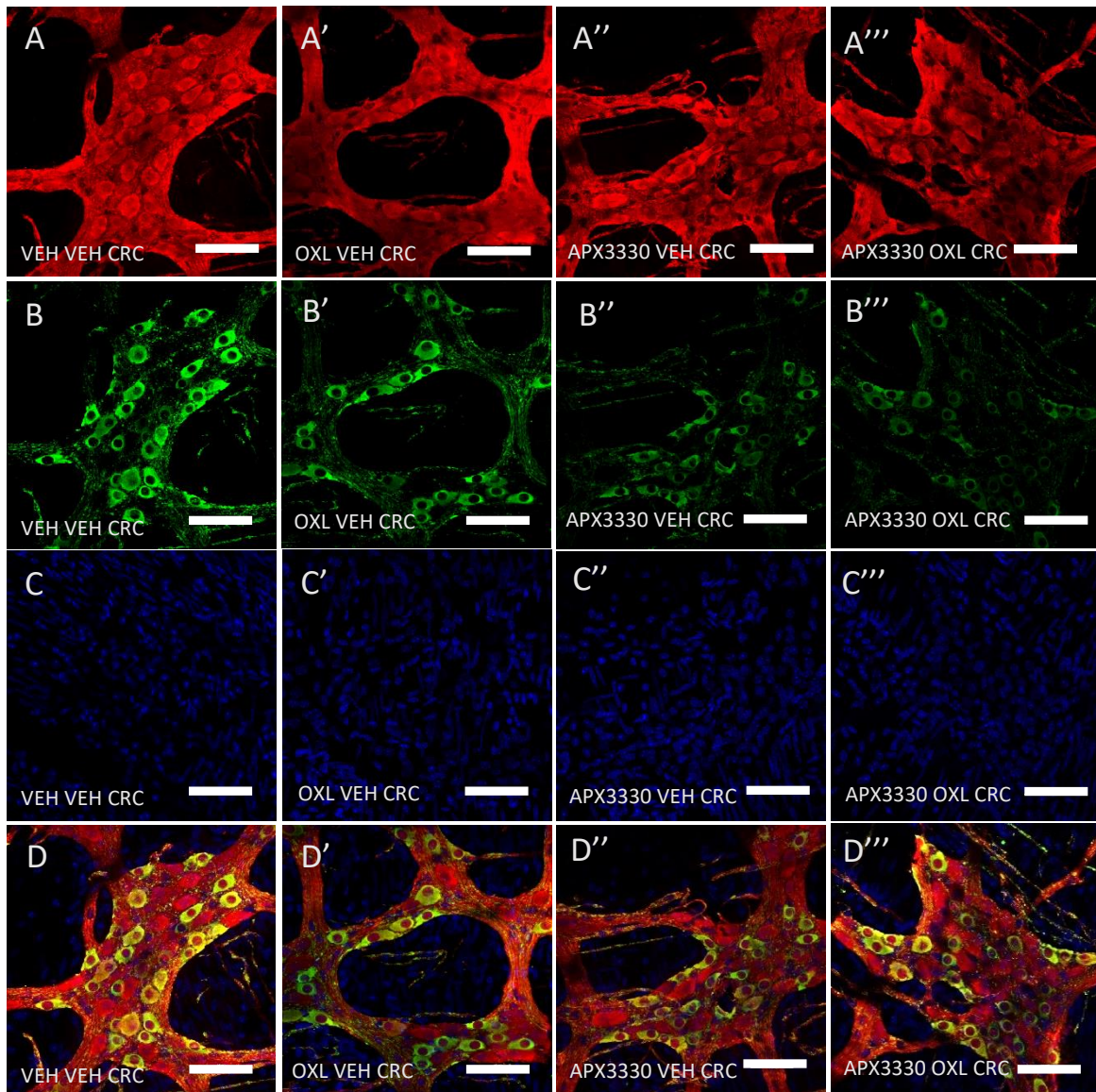
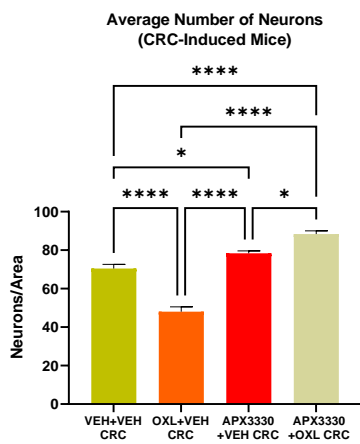


Figure 3.6 Effect of *in vivo* treatments on nNOS-IR neurons in CRC-induced mice. Wholemount preparations of the myenteric ganglia from the distal colon of mice treated with 2 vehicles, Oxaliplatin plus vehicle for APX3330, APX3330 plus vehicle for OXL, and a combination of APX3330 + OXL following 14 days of *in vivo* treatment labelled with a pan-neuronal marker anti-PGP9.5 antibody (red) (A-A'''), an inhibitory neuronal marker neuronal nitric oxide synthase (green) (B-B''') and DAPI (C-C'''). Merged images (D-D'''). Scale bar = 50µm. Quantitative analysis of the average number of myenteric neurons immunoreactive for PGP9.5 (E), the average number of nNOS-immunoreactive neurons (F), the proportion of nNOS-IR inhibitory neurons to the total number of PGP9.5-IR neurons (G) in the myenteric ganglia within 0.4 mm² area. Data presented as mean ± S.E.M. **P*<0.05, ***P*<0.01, ****P*<0.001, *****P*<0.0001, n=4-5 mice/group.

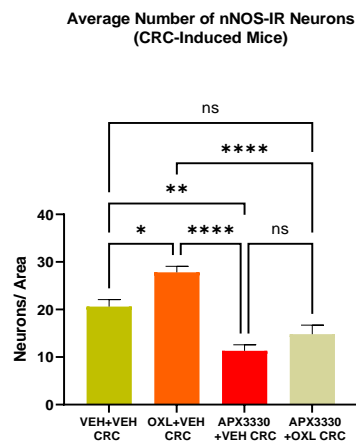
PGP 9.5 + nNOS + DAPI



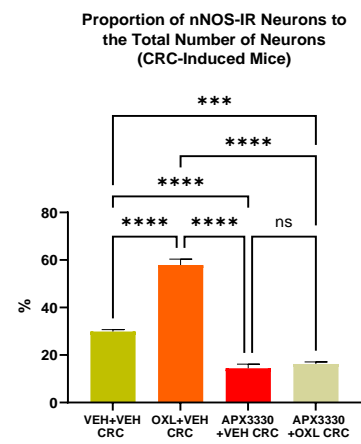
E



F



G



3.4.3.1 Effect of the Treatments on APE1/Ref-1 Expression in Mice Without Cancer

To determine if Oxaliplatin treatment is associated with changes in the APE1/Ref-1 expression in the myenteric plexus of the distal colon, an anti-Apurinic/aprimidinic endonuclease-1 (APE1/Ref-1) antibody was used (**Figure 3.7 A-A''**). Data revealed that APX3330 treatment reduced the number of APE1/Ref-1 immunoreactive cells in the myenteric ganglia while OXL increased the number of APE1/Ref-1-IR cells following 14 days of *in vivo* treatment in mice without cancer. Increased expression of APE1/Ref-1 in the myenteric ganglia was found in OXL-treated mice (79.0 ± 1.0 cells/area) compared to both untreated (45.4 ± 2.2 cells/area) and APX3330-treated (52.1 ± 1.9 cells/area) mice ($P < 0.0001$ for both) ($n = 5$ mice/group) (**Figure 3.7 B**).

Quantitative analysis of the APE1/Ref-1 immunofluorescence in the distal colon myenteric ganglia is presented in **Figure 3.8**. The effect of *in vivo* OXL and APX3330 treatment on the APE1/Ref-1 expression per ganglia (**Figure 3.8A**), APE1/Ref-1 expression per area (**Figure 3.8B**), and the proportion of APE1/Ref-1: PGP9.5 per ganglion (**Figure 3.8C**) was assessed in cancer-free mice. Data revealed a significantly higher expression of APE1/Ref-1 per ganglion in OXL-treated group (23.3 ± 0.5 a.u.) compared to both untreated (10.0 ± 0.5 a.u.) and APX3330-treated group (12.7 ± 0.4 a.u.) ($P < 0.0001$ for both). Similarly, the expression of APE1/Ref-1 per area was also significantly higher in OXL-treated mice (7.7 ± 0.6 a.u.) compared to untreated (4.7 ± 0.2 a.u., $P < 0.001$) and APX3330-treated (6.3 ± 0.3 a.u., $P < 0.05$) mice at day 15 of treatments. Data revealed that the proportion of APE1/Ref-1: PGP9.5-IR cells was the highest in the OXL-treated group ($98.7 \pm 2.6\%$) due to having a higher number of APE1/Ref-1 expressing cells reactive to the number of neurons in the myenteric ganglia compared to both untreated ($38.9 \pm 1.5\%$) and APX3330-treated ($50.2 \pm 2.4\%$) mice ($P < 0.0001$ for both) ($n = 5$ mice/group).

To assess the amount of APE1/Ref-1 protein expression in the distal colon of cancer-free mice, western blot analysis was performed using anti-APE1/Ref-1 antibody (**Figure 3.9**). An image of the membrane merged with the ladder after the protein transfer step has been included in supplementary data (**Figure S3.1A**). Western blot data of APE1/Ref-1 protein expression of the distal colon revealed that OXL treatment significantly increased the expression of APE1/Ref-1 protein in the distal colons of OXL-treated mice and a higher level of APE1/Ref-1 expression is an indication of increased cellular oxidative stress-induced as a side-effect of the OXL treatment. Western blot data revealed that APE1/Ref-1 protein expression was significantly lower in untreated (1.4 ± 0.1 a.u) mice compared to OXL-treated ($2.1 \text{ a.u} \pm 0.1 \text{ a.u}$, $P < 0.01$) and APX3330-treated ($1.9 \text{ a.u} \pm 0.2 \text{ a.u}$, $P < 0.05$) mice (n=5 mice/group).

3.4.3.2 Effect of the Treatments on the APE1/Ref-1 Expression in CRC-Induced Mice

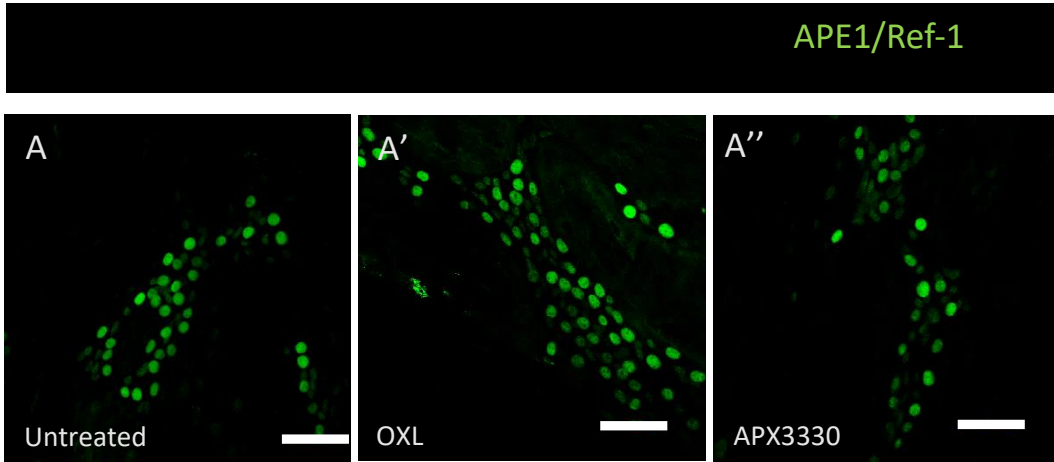
APE1/Ref-1 expression in the myenteric plexus of the distal colon was assessed following 14-day *in vivo* administration of two vehicles (VEH + VEH), APX3330 + VEH, OXL + VEH, and a combination of APX3330 + OXL treated CRC-induced mice (**Figure 3.10 A-A''', B**). The number of APE1/Ref-1 immunoreactive cells in APX3330 + VEH treated CRC-mice was lower (52.8 ± 1.7 neurons/area) compared to VEH + VEH (73.6 ± 2.5 neurons/area), OXL + VEH (76.6 ± 1.6 neurons/area) treated mice ($P < 0.0001$ for both) but not significantly different compared to APX3330 + OXL-treated mice (56.7 ± 2.4 neurons/area) (n=4-5 mice/group).

The quantitative analysis of the level of myenteric neurons and APE1/Ref-1 immunofluorescence in CRC-induced mice is presented in **Figure 3.11**. OXL + VEH-treated mice exhibited the highest APE1/Ref-1 expression per ganglia (26.0 ± 1.8 a.u) compared to VEH + VEH (17.4 ± 1.0 a.u, $P < 0.01$), APX3330 + VEH (12.7 ± 0.9 a.u, $P < 0.0001$) and APX3330 + OXL (14.9 ± 1.0 a.u, $P < 0.0001$) treated mice

(**Figure 3.11A**). Similarly, OXL + VEH-treated mice exhibited the highest APE1/Ref-1 expression per area (8.7 ± 0.2 a.u) compared to VEH + VEH (6.7 ± 0.5 a.u, $P < 0.001$), APX3330 + VEH (5.4 ± 0.1 a.u, $P < 0.0001$) and APX3330 + OXL (5.9 ± 0.3 a.u, $P < 0.0001$) treated groups (**Figure 3.11B**). VEH + VEH-treated mice exhibited significantly higher APE1/Ref-1 expression per area compared to OXL + VEH APX3330 + VEH-treated mice. OXL + VEH-treated mice had the highest proportion of APE1/Ref-1-IR cells to PGP9.5-IR neurons per ganglion ($98.5 \pm 2.6\%$) compared to VEH + VEH-treated ($80.2 \pm 2.7\%$, $P < 0.001$), APX3330 + VEH-treated ($57.7 \pm 2.9\%$, $P < 0.0001$) and APX3330 + OXL-treated ($68.9 \pm 2.1\%$, $P < 0.0001$) groups (**Figure 3.11C**). In contrary, APX3330 + VEH-treated mice showed the lowest proportion of APE1/Ref-1-IR cells to PGP9.5-IR neurons per ganglion compared to VEH + VEH ($P < 0.0001$), OXL + VEH ($P < 0.0001$) and APX3330 + OXL ($P < 0.05$) treated mice (n=4-5 mice/group).

Western Blot analysis of the distal colon samples that were taken from CRC-induced mice following 14-day treatments revealed that APX3330 + VEH and APX3330 + OXL treatments significantly decreased the expression of APE1/Ref-1 protein compared to other treatment groups suggesting its capacity of reducing the oxidative stress and therefore, less expression of APE1/Ref-1 (**Figure 3.12**). An image of the membrane merged with the ladder after the protein transfer step has been included in supplementary data (**Figure S3.1B**). Data revealed that VEH + VEH-treated mice (1.4 ± 0.2 a.u) showed higher APE1/Ref-1 protein expression compared to APX3330 + VEH (0.8 ± 0.2 a.u, $P < 0.001$) and combination of APX3330 + OXL (0.8 ± 0.1 a.u, $P < 0.001$) treated groups but not statistically significantly different to OXL + VEH-treated mice (1.2 ± 0.2 a.u) (n=4-5 mice/group).

Figure 3.7 APE1/Ref-1 expression in the distal colon following 14-day treatment with Oxaliplatin and APX3330. APE1/Ref-1 immunoreactive cells in the myenteric ganglia of the distal colon labelled with anti-APE1/Ref-1 antibody (green) from untreated (A), Oxaliplatin-treated (A'), APX3330-treated (A'') mice. Scale bar = 50µm. Quantitative analysis of the number of APE1/Ref-1-IR cells (B). The number of APE1/Ref-1-IR cells in the distal colon was counted per 0.4 mm² area. Data presented as mean ± S.E.M. *****P*<0.0001, n=5 mice/group.



B

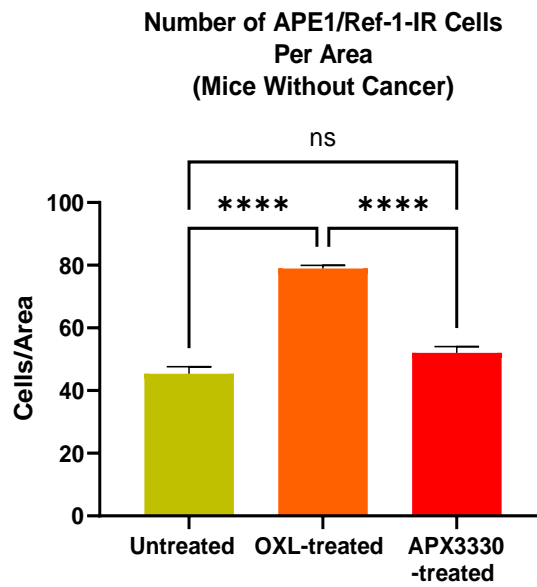
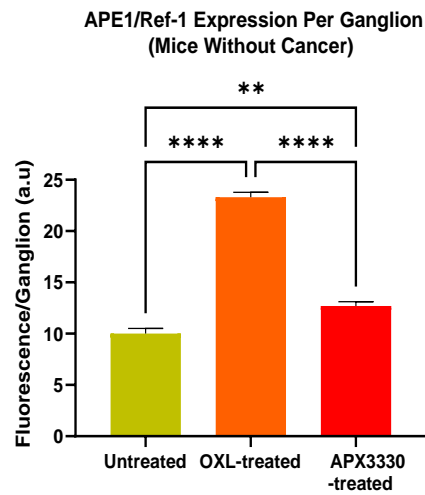
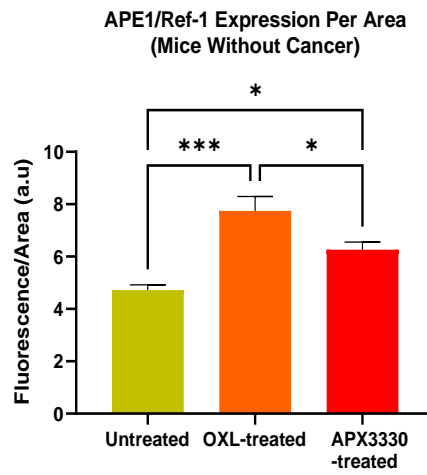


Figure 3.8 Quantitative analysis of the APE1/Ref-1 expression in the distal colon myenteric ganglia of mice without cancer. APE1/Ref-1 expression per ganglion (A), APE1/Ref-1 expression per 0.4mm² area (B), the proportion of APE1/Ref-1-IR cells to PGP9.5-IR cells per ganglia (C) following 14 days of *in vivo* treatment with OXL and APX3330 compared to untreated mice. Data presented as mean \pm S.E.M. * P <0.05, ** P <0.01, *** P <0.001 **** P <0.0001, n=5 mice/group.

A



B



C

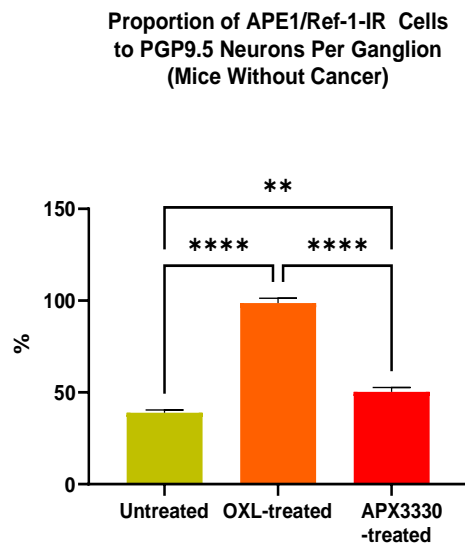
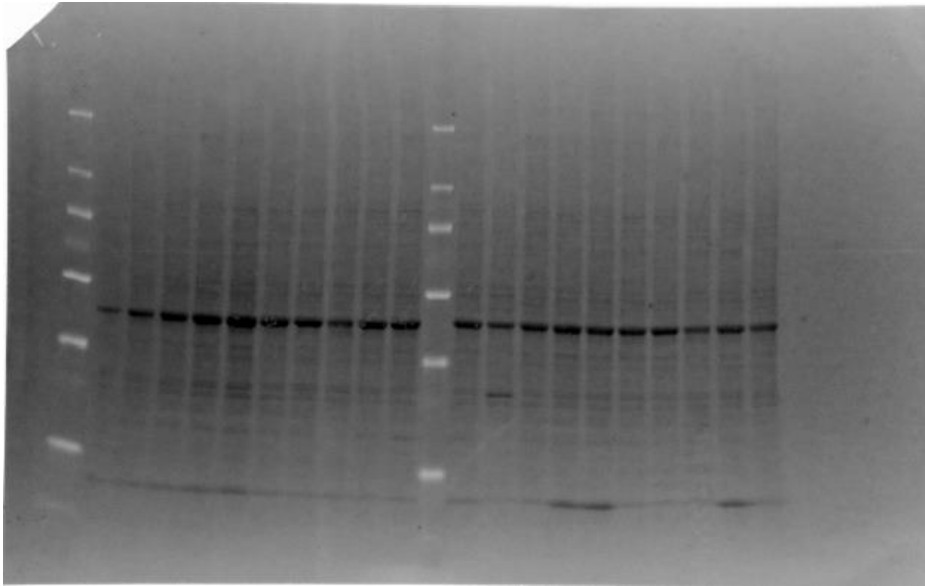
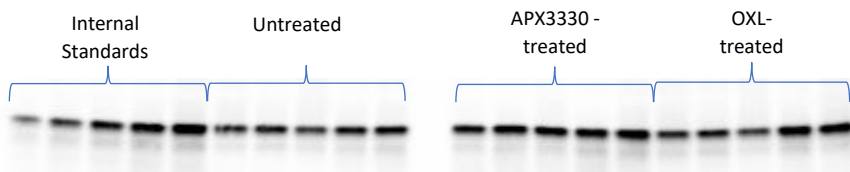


Figure 3.9 APE1/Ref-1 protein expression in the distal colon of mice without cancer. APE1/Ref-1 protein (35 kDa) expression in the distal colon from mice without cancer following 14-day of *in vivo* treatment with Oxaliplatin and APX3330 compared to untreated mice. An image of the membrane with the total protein loading (A), An image of the membrane with the target protein (B), quantitative analysis of the APE1/Ref-1 protein expression normalised to the total protein values (C). Data presented as mean \pm S.E.M. * P <0.05, ** P <0.01, n=5 mice/group.

A



B



C

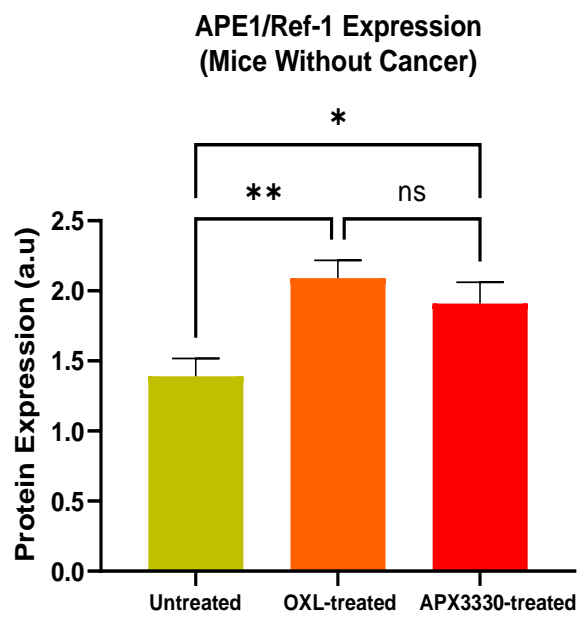
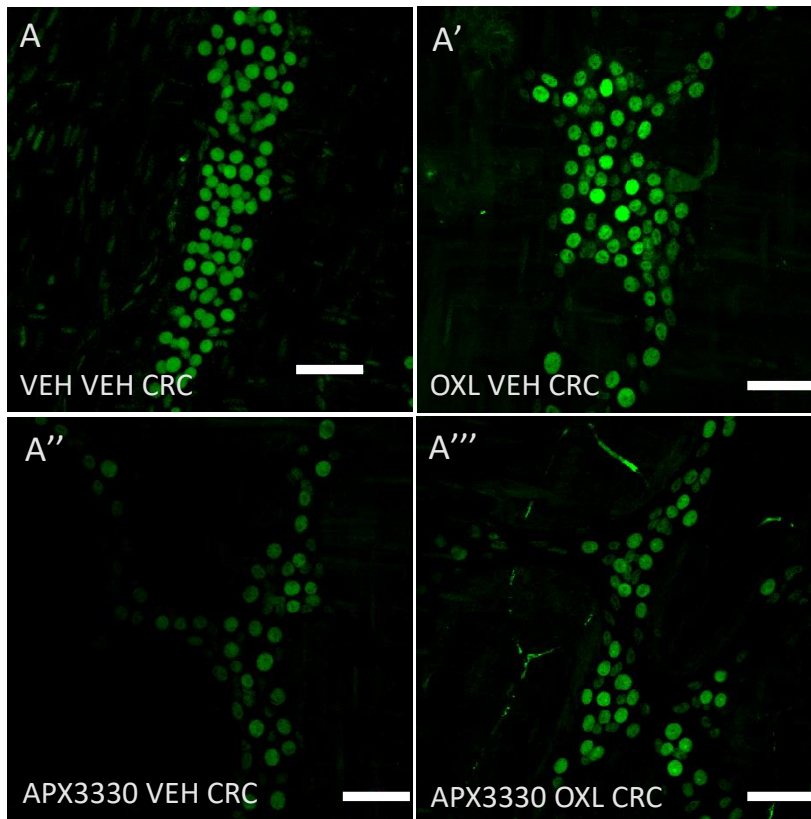


Figure 3.10 APE1/Ref-1 expression in the distal colon following 14-day treatments in CRC-induced mice. APE1/Ref-1 immunoreactive cells in the myenteric ganglia of the distal colon labelled with anti-APE1/Ref-1 antibody (green) from mice treated with 2 vehicles (A), Oxaliplatin plus vehicle for APX3330 (A'), APX3330 plus vehicle for OXL (A''), and a combination of APX3330 + OXL (A'''). Scale bar = 50 μ m. Quantitative analysis of the number of APE1/Ref-1-IR cells (B) in the distal colon wholemount preparations. The number of APE1/Ref-1-IR cells in the distal colon was counted per 0.4 mm² area. Data presented as mean \pm S.E.M. *** P <0.001 **** P <0.0001, n=4-5 mice/group.

APE1/Ref-1



B

Number of APE1/Ref-1-IR Cells Per Area
(CRC-Induced Mice)

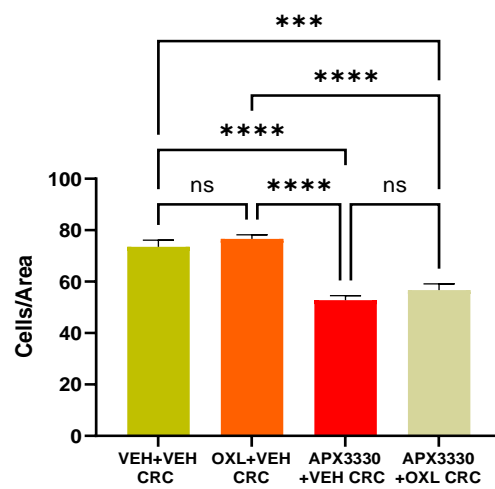
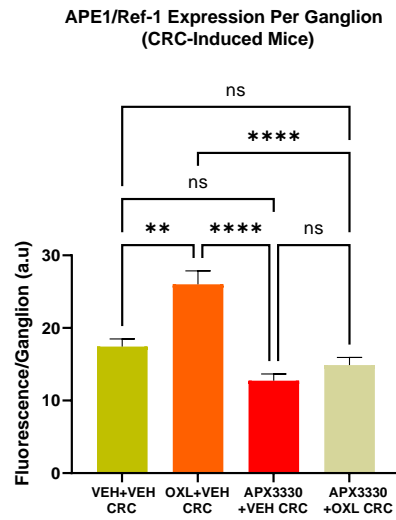
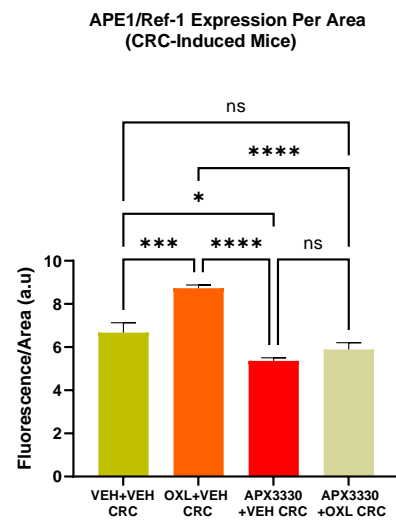


Figure 3.11 Quantitative analysis of the APE1/Ref-1 expression in the distal colon myenteric ganglia of CRC-induced mice. APE1/Ref-1 expression per ganglion (A), APE1/Ref-1 expression per 0.4mm² area (B), the proportion of APE1/Ref-1-IR cells to PGP 9.5-IR cells per ganglion (C) following 14 days of *in vivo* treatment with 2 vehicles, Oxaliplatin plus vehicle for APX3330, APX3330 plus vehicle for OXL, and a combination of APX3330 + OXL. Data presented as mean \pm S.E.M. * P <0.05, ** P <0.01, *** P <0.00, **** P <0.0001, n=4-5 mice/group.

A



B



C

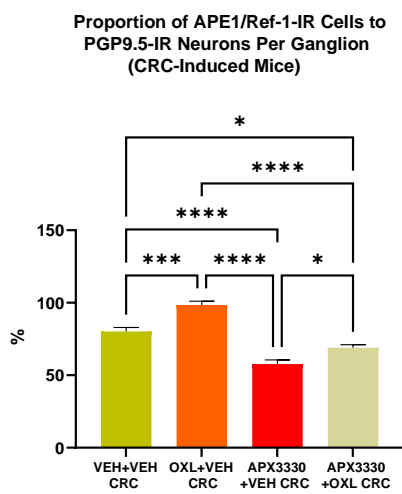
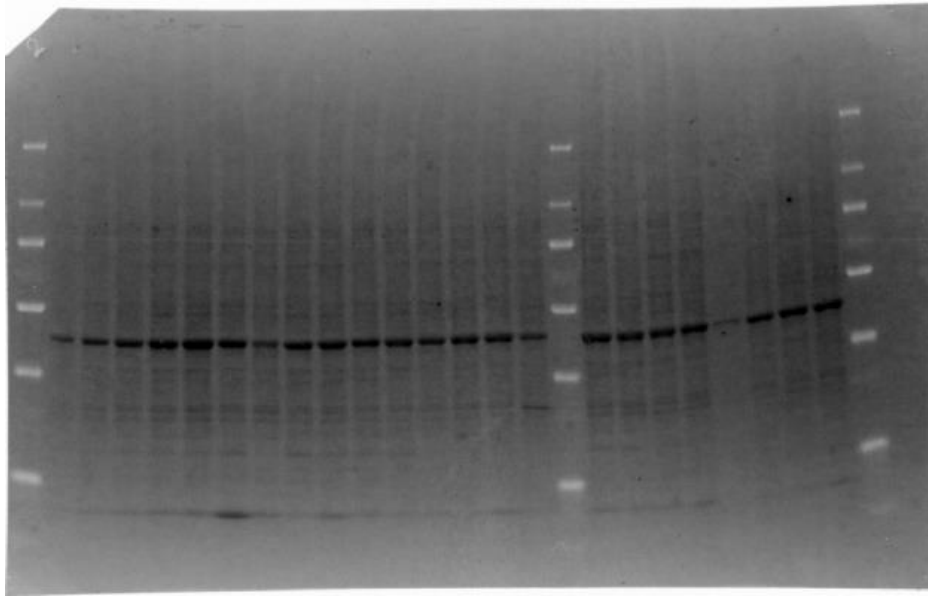
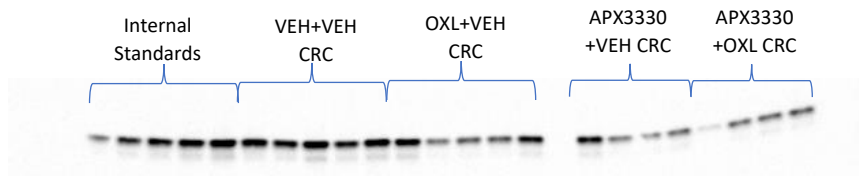


Figure 3.12 APE1/Ref-1 protein expression in the distal colon of mice with CRC. APE1/Ref-1 protein (35 kDa) expression in the distal colon from CRC-induced mice following 14-day of *in vivo* treatment with 2 vehicles, Oxaliplatin plus vehicle for APX3330, APX3330 plus vehicle for OXL, and a combination of APX3330 + OXL. An image of the membrane with the total protein loading (A), An image of the membrane with the target protein (B), quantitative analysis of the APE1/Ref-1 protein expression normalised to the total protein values (C). Data presented as mean \pm S.E.M. ** $P < 0.01$, *** $P < 0.001$, n=4-5 mice/group.

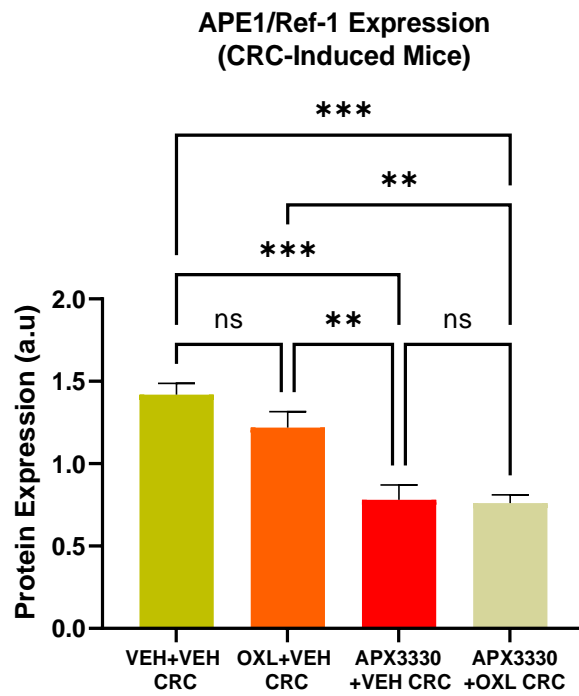
A



B



C



3.4.4 Effect of the Treatments on Cytochrome c and STAT3 Expression

3.4.4.1 Cytochrome c Expression

To investigate changes in cytochrome c protein expression following *in vivo* treatment of OXL and APX3330 compared to untreated mice, the distal colon samples were assessed by Western blot experiments using an anti-cytochrome c antibody. An image of the membrane with the total protein loading (**Figure 3.13 A**). An image of the membrane merged with the ladder after the protein transfer step has been included in supplementary data (**Figure S3.2A**). Data revealed that cytochrome c protein expression was significantly higher in OXL-treated mice (2.3 ± 0.1 a.u) compared to APX3330-treated (1.0 ± 0.1 a.u, $P < 0.0001$) and untreated (1.7 ± 0.1 a.u, $P < 0.05$) mice signifying elevated oxidative stress in the GI tract following OXL treatment (**Figure 3.13 B, C**). Cytochrome c expression was significantly lower in Untreated and APX3330-treated mice compared to OXL-treated mice ($P < 0.001$) (n=5 mice/group).

An image of the membrane with the total protein loading (**Figure 3.14 A**). Cytochrome c expression in CRC-induced group indicated that OXL + VEH-treated mice had significantly higher protein expression of cytochrome c (3.4 ± 0.3 a.u), compared to APX3330 + VEH-treated (1.5 ± 0.1 a.u, $P < 0.001$) and combination of APX3330 + OXL-treated mice (0.9 ± 0.1 a.u, $P < 0.0001$) but not statistically significant between VEH + VEH-treated (2.9 ± 0.3 a.u) and OXL + VEH-treated mice (**Figure 3.14 B, C**). Thus, indicating the oxidative stress-buffering properties of APX3330 as well as the effectiveness of the combination treatment of APX3330 + OXL. An image of the membrane merged with the ladder after the protein transfer step has been included in supplementary data (n=4-5 mice/group) (**Figure S3.2B**).

3.4.4.2 STAT3 and pSTAT3 Protein Expression in the Distal Colon of Mice Without Cancer

To investigate changes in signal transducer and activator of transcription 3 (STAT3) protein expression following *in vivo* treatment with OXL and APX3330 compared to untreated mice, the STAT3 protein expression of distal colon samples was assessed by Western blot experiments using an anti-STAT3 antibody. An image of the membrane with the total protein loading (**Figure 3.15 A**). An image of the membrane merged with the ladder after the protein transfer step has been included in supplementary data (**Figure S3.3A**). Western blot analysis of the colons from mice without cancer revealed that OXL-treated group had the lowest protein expression of STAT3 (0.7 ± 0.1 a.u), compared to APX3330 (2.0 ± 0.1 a.u) and untreated (1.8 ± 0.2 a.u) ($P < 0.001$ for both) groups (n=5 mice/group) (**Figure 3.15 B, C**).

To investigate changes in the phosphorylated signal transducer and activator of transcription 3 (pSTAT-3) protein expression we performed Western blot experiments on the distal colon of mice without cancer following 14-day *in vivo* treatments using an anti-pSTAT3 antibody. An image of the membrane with the total protein loading (**Figure 3.16 A**). An image of the membrane merged with the ladder after the protein transfer step has been included in supplementary data (**Figure S3.3B**). Data revealed that OXL-treated group had significantly higher protein expression of pSTAT3 (3.2 ± 0.3 a.u) compared to untreated (0.5 ± 0.1 a.u, $P < 0.0001$) and APX3330-treated (1.1 ± 0.3 a.u, $P < 0.001$) mice indicating increased activation of STAT3 protein into pSTAT3 state (n=5 mice/group) (**Figure 3.16 B, C**).

3.4.4.3 STAT3 and pSTAT3 Protein Expression in the Distal Colon of CRC-Induced Mice

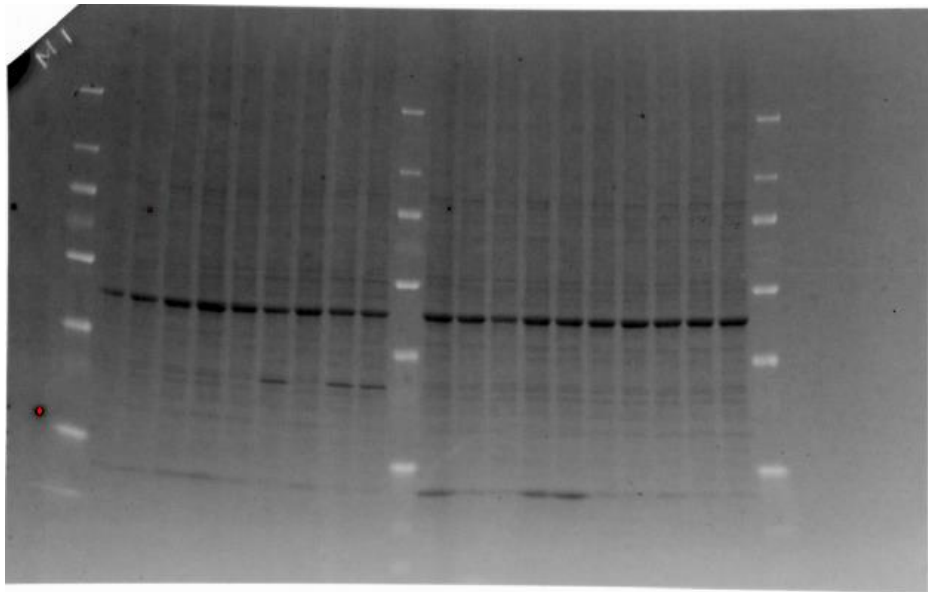
An image of the membrane with the total protein loading (**Figure 3.17 A**). Western blot analysis of the protein expression of STAT3 in the distal colon samples of CRC-induced mice revealed that VEH + VEH-treated group showed the lowest protein expression of STAT3 (0.8 ± 0.1 a.u) compared to APX3330 + VEH (3.4 ± 0.4 a.u,

$P < 0.0001$) and combination of APX3330 + OXL (3.1 ± 0.4 a.u., $P < 0.001$) treated groups but not statistically significant compared to OXL + VEH-treated group (1.7 ± 0.2 a.u) (**Figure 3.17 B, C**). An image of the membrane merged with the ladder after the protein transfer step has been included in supplementary data (**Figure S3.4A**). OXL + VEH and VEH + VEH-treated groups showed the lowest expression of STAT3 protein indicating increased activation of the protein to execute downstream activation of target proteins (n=4-5 mice/group).

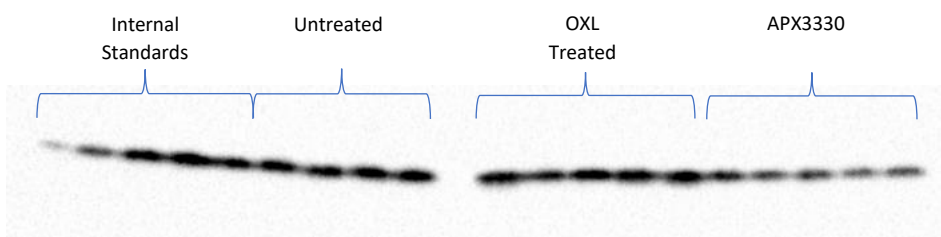
An image of the membrane with the total protein loading (**Figure 3.18 A**). In CRC-induced cohort, APX3330 + VEH-treated mice exhibited the lowest expression of pSTAT3 (0.8 ± 0.1 a.u) compared to OXL + VEH- treated (3.0 ± 0.3 a.u, $P < 0.0001$), and VEH + VEH-treated (2.1 ± 0.3 a.u, $P < 0.01$) groups but not statistically significant compared to the combination of APX3330 + OXL-treated group (1.2 ± 0.1 a.u) indicating decreased activation of STAT3 protein into its active phosphorylated state pSTAT3 with APX3330 treatment (n=4-5 mice/group) (**Figure 3.18 B, C**). An image of the membrane merged with the ladder after the protein transfer step has been included in supplementary data (**Figure S3.4B**).

Figure 3.13 Cytochrome c protein expression in the distal colon from mice without cancer. Cytochrome c protein (14 kDa) expression in the distal colon from mice without cancer following 14-day *in vivo* treatment with Oxaliplatin and APX3330 compared to untreated mice. An image of the membrane with the total protein loading (A), An image of the membrane with the target protein (B), quantitative analysis of the cytochrome c protein expression normalised to the total protein values (C). Data presented as mean \pm S.E.M. * P <0.05, *** P <0.001, **** P <0.0001, n=5 mice/group.

A



B



C

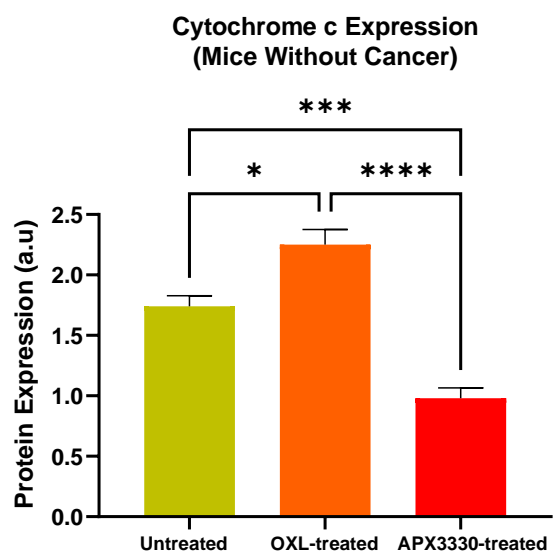
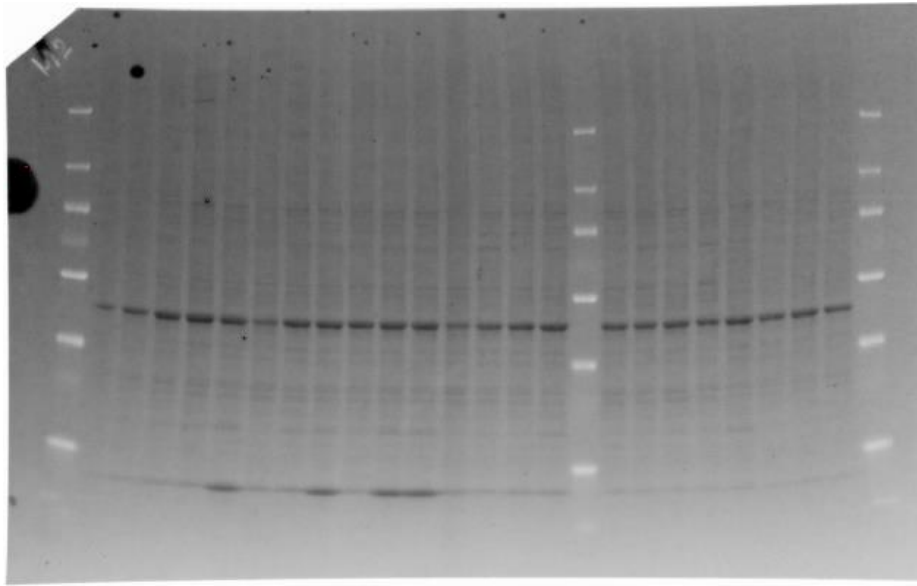
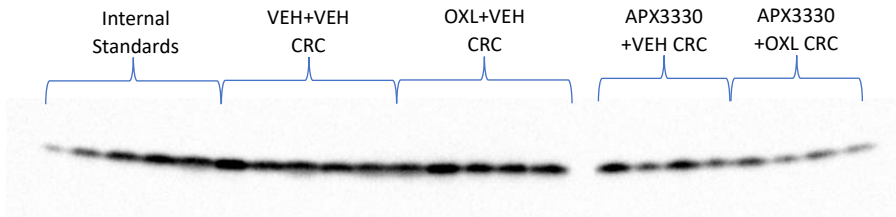


Figure 3.14 Cytochrome c protein expression in the distal colon from mice with CRC. Cytochrome c protein (14 kDa) expression in the distal colon from mice with CRC following 14-day *in vivo* treatment with 2 vehicles, Oxaliplatin plus vehicle for APX3330, APX3330 plus vehicle for OXL, and a combination of APX3330 + OXL treated CRC-induced mice. An image of the membrane with the total protein loading (A), An image of the membrane with the target protein (B), quantitative analysis of the cytochrome c protein expression normalised to the total protein values (C). Data presented as mean \pm S.E.M. ** $P < 0.01$, *** $P < 0.001$, **** $P < 0.0001$, $n = 5$ mice/group.

A



B



C

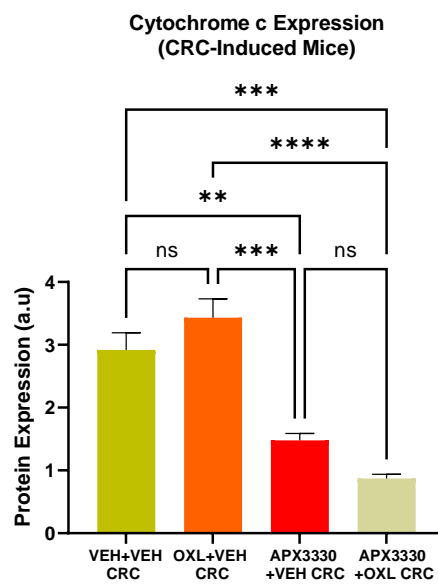
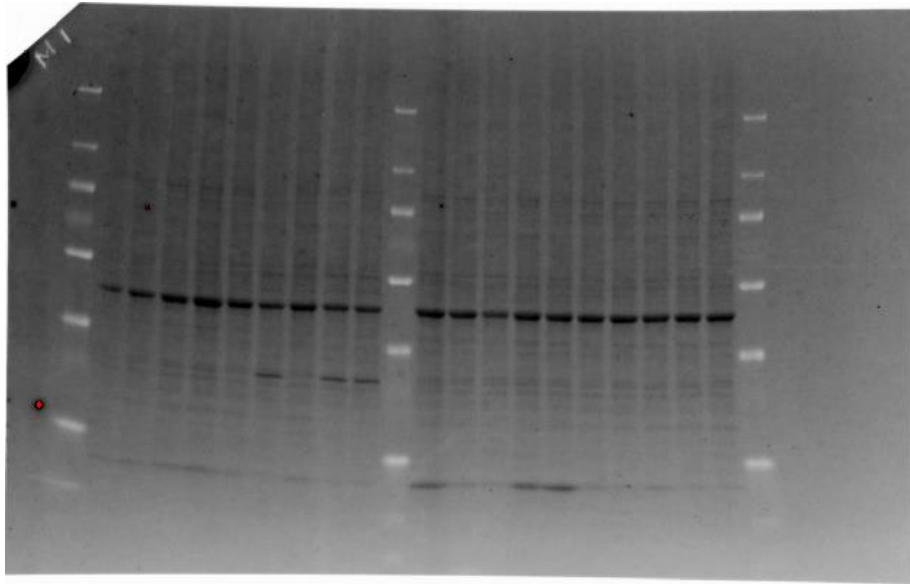
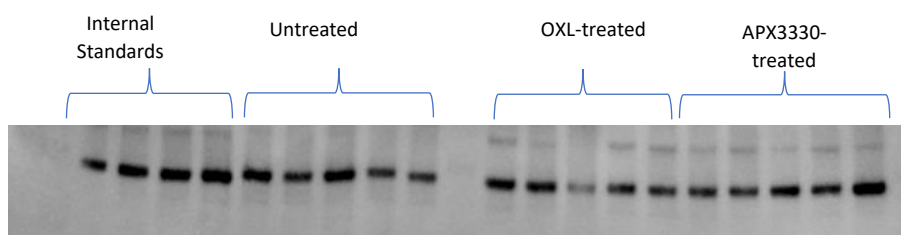


Figure 3.15 Signal transducer and activator of transcription 3 (STAT3) protein expression in the distal colon of mice without cancer. STAT3 protein (88 kDa) expression in the distal colon from mice following 14-day *in vivo* treatment with Oxaliplatin and APX3330 compared to untreated without cancer mice. An image of the membrane with the total protein loading (A), An image of the membrane with the target protein (B), quantitative analysis of the STAT3 protein expression normalised to the total protein values (C). Data presented as mean \pm S.E.M. *** $P < 0.001$, n=5 mice/group.

A



B



C

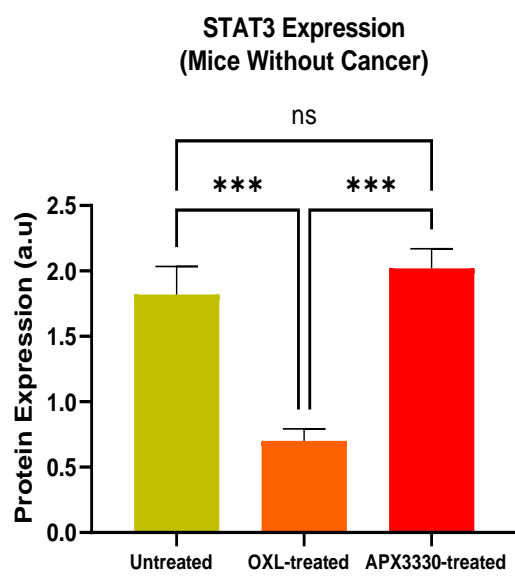
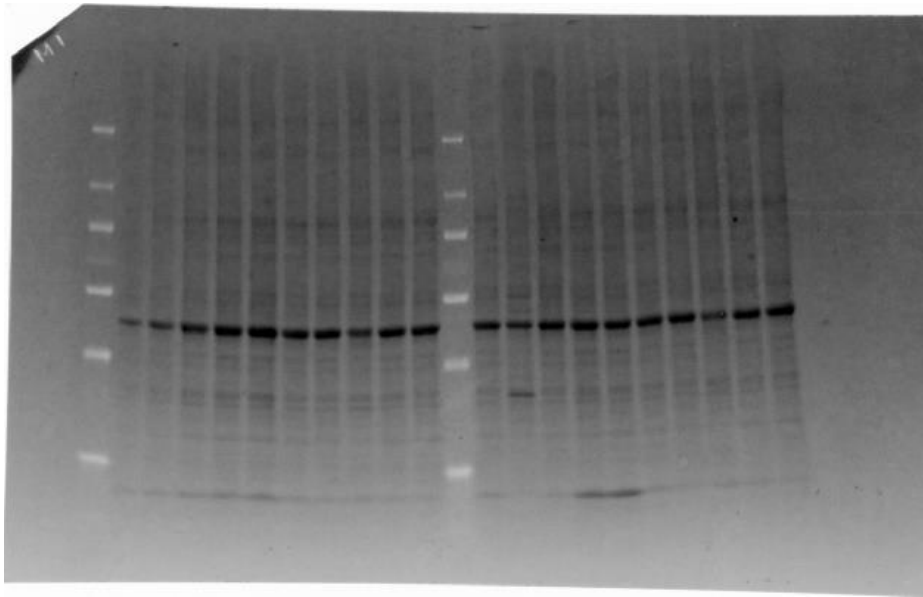
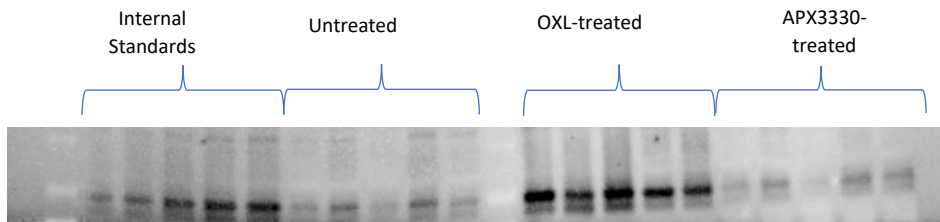


Figure 3.16 Phosphorylated signal transducer and activator of transcription 3 (pSTAT3) protein expression in the distal colon of mice without cancer. pSTAT3 protein (88 kDa) expression in the distal colon from mice following 14-day *in vivo* treatment with Oxaliplatin and APX3330 compared to untreated without cancer mice. An image of the membrane with the total protein loading (A), An image of the membrane with the target protein (B), quantitative analysis of the pSTAT3 protein expression normalised to the total protein values (C). Data presented as mean \pm S.E.M. *** $P < 0.001$, **** $P < 0.0001$, $n = 5$ mice/group.

A



B



C

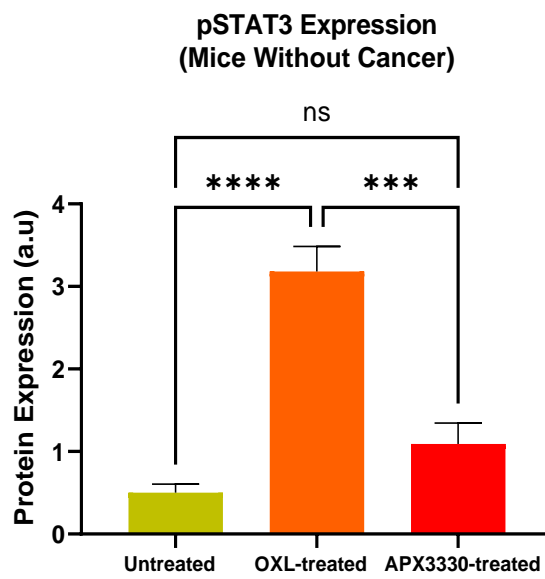
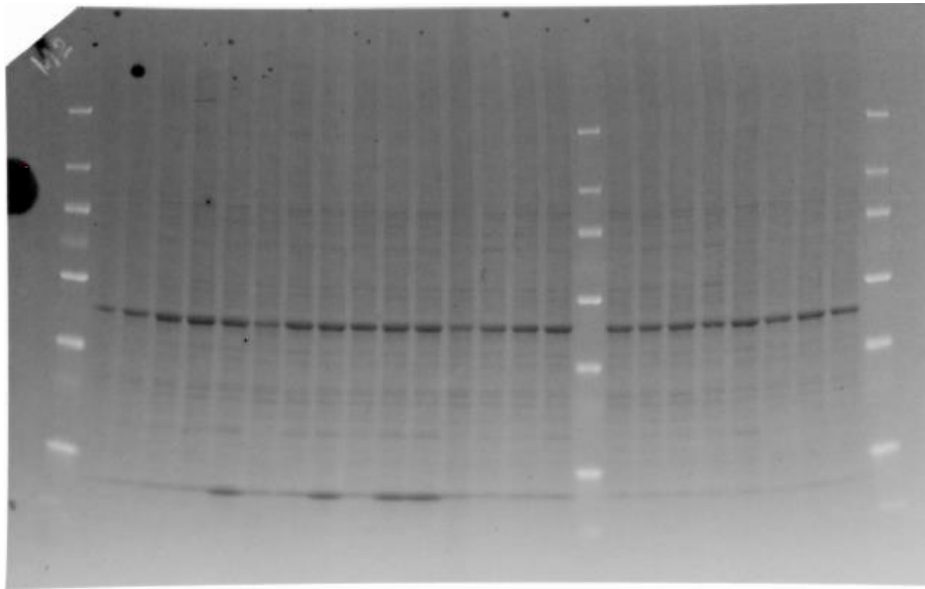
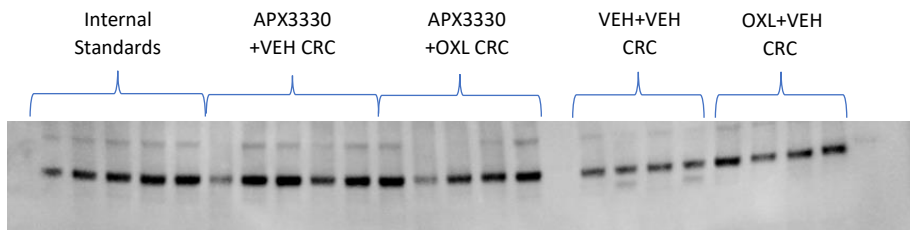


Figure 3.17 Signal transducer and activator of transcription 3 (STAT3) protein expression in the distal colon of CRC-induced mice. STAT3 protein (88 kDa) expression in the distal colon from CRC-induced mice following 14-day *in vivo* treatment with 2 vehicles, Oxaliplatin plus vehicle for APX3330, APX3330 plus vehicle for OXL, and a combination of APX3330 + OXL. An image of the membrane with the total protein loading (A), An image of the membrane with the target protein (B), quantitative analysis of the STAT3 protein expression normalised to the total protein values (C). Data presented as mean \pm S.E.M. * P <0.05, *** P <0.001, **** P <0.0001, n=4-5 mice/group.

A



B



C

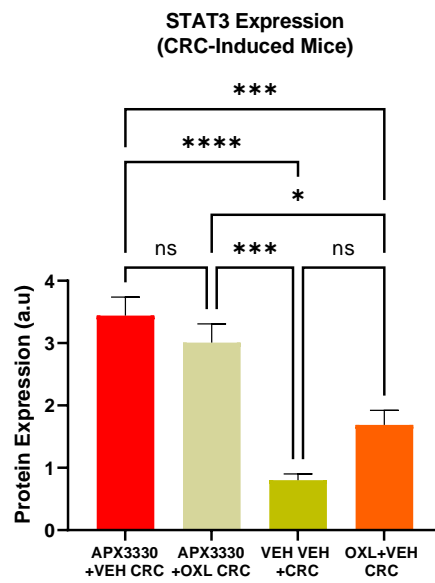
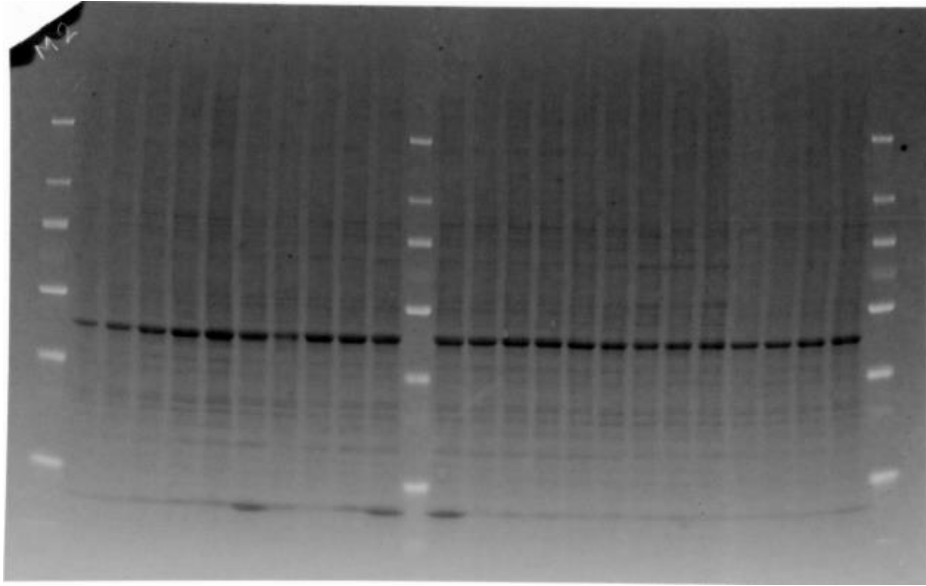
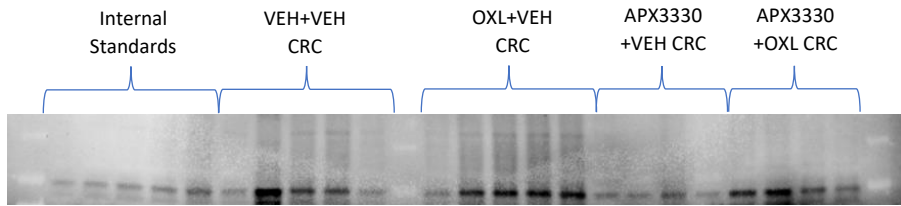


Figure 3.18 Phosphorylated signal transducer and activator of transcription 3 (pSTAT3) protein expression in the distal colon of CRC-induced mice. pSTAT3 protein (88 kDa) expression in the distal colon from mice following 14-day *in vivo* treatment with 2 vehicles, Oxaliplatin plus vehicle for APX3330, APX3330 plus vehicle for OXL, and a combination of APX3330 + OXL treated CRC-induced mice. An image of the membrane with the total protein loading (A), An image of the membrane with the target protein (B), quantitative analysis of the pSTAT3 protein expression normalised to the total protein values (C). Data presented as mean \pm S.E.M. * P <0.05, ** P <0.01, *** P <0.001, **** P <0.0001, n=4-5 mice/group.

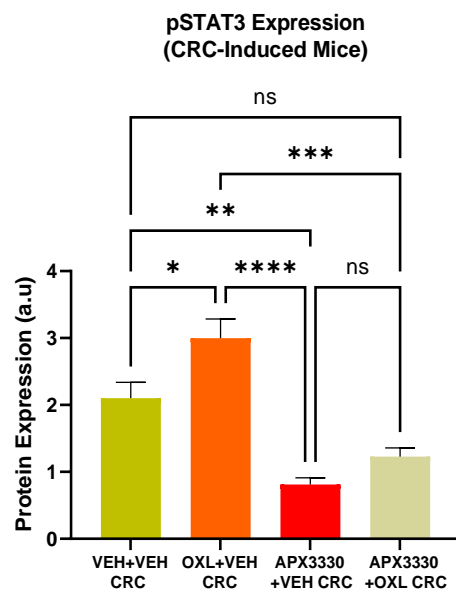
A



B



C



3.4.5 Effect of the Treatments on Tumour Growth and Metastasis

3.4.5.1 Assessment of the Caecum Size, and Number of Tumours Following Treatments in CRC-Induced Mice

The freshly resected caecums were weighed as soon as they were taken out from the mice to determine the variation between the sizes of the caecum between treatment groups (**Figure 3.19 A-D'**). The average caecum weight of VEH + VEH-treated mice was significantly higher ($3.2 \pm 0.3\text{g}$) compared to OXL + VEH-treated ($1.7 \pm 0.3\text{g}$), APX3330 + VEH-treated ($1.4 \pm 0.1\text{g}$), and APX3330 + OXL-treated ($1.4 \pm 0.1\text{g}$) mice ($P < 0.001$ for all) (**Figure 3.19 E**). Since the VEH + VEH-treated group did not receive any treatments, data indicated that those mice had larger caecums compared to other groups. OXL + VEH, APX3330 + VEH and combination of APX3330 + OXL treatments showed significantly smaller average caecum size due to inhibited growth of tumours ($n=4-5$ mice/group).

To assess the efficacy of different treatment regimens, the tumour diameter and the number of tumours were quantified. VEH + VEH-treated mice had the largest tumour diameter ($34.1 \pm 1.7\text{mm}$) compared to OXL + VEH ($22.3 \pm 1.3\text{mm}$), APX3330 + VEH ($10.1 \pm 1.3\text{mm}$) and APX3330 + OXL ($0 \pm 0\text{mm}$) treated mice ($P < 0.0001$ for all) (**Figure 3.19, A-D, F**). The caecums of VEH + VEH-treated mice were completely consumed by multiple tumours by day 21 post-surgery and a many secondary tumours were present in the abdominal cavity. The secondary spread of the tumours was observed in other organs including the spleen, liver, large intestine, small intestine, as well as the stomach wall (**Figure 3.19, A'-D'**). The number of tumours present in the abdominal cavity were significantly higher in VEH + VEH-treated mice (70.8 ± 5.4 tumours/mouse) compared to OXL + VEH (14.8 ± 1.0 tumours/mouse), APX3330 + VEH (1.6 ± 0.6 tumours/mouse) and APX3330 + OXL (0 ± 0 tumours/mouse) treated mice ($P < 0.0001$ for all) (**Figure 3.19, G**). The number of tumours was not statistically significant between APX3330 + VEH and APX3330

+ OXL-treated groups. Combination treatment of OXL + APX3330 exhibited the most successful outcome among all treatment groups by completely getting rid of secondary tumours following 14 days *in vivo* treatment (n=4-5 mice/group). We have observed the secondary spread of tumours into the colon in VEH + VEH, OXL + VEH, and APX3330 + VEH-treated mice whereas mice treated with APX3330 + OXL did not show any signs of secondary spread of tumours following 14-days of *in vivo* treatment (**Figure 3.20**).

3.4.5.2 Effect of the Treatments on VEGF Expression

The antiangiogenic potential of different treatment options was evaluated by the Western blot analysis of the protein expression of vascular endothelial growth factor (VEGF) in the distal colon by using an anti-VEGF antibody. An image of the membrane with the total protein loading (**Figure 3.21 A**). VEGF protein expression was significantly higher in VEH + VEH-treated mice (2.3 ± 0.2 a.u) compared to APX3330 + VEH (1.1 ± 0.1 a.u, $P < 0.001$) and APX3330 + OXL (1.1 ± 0.1 a.u, $P < 0.001$) treated mice but not statistically significant between VEH + VEH and OXL + VEH (2.1 ± 0.1 a.u) treated groups indicating increased tumour vascularisation in the VEH + VEH and OXL + VEH-treated groups (**Figure 3.21 B, C**). VEGF expression in the colons from OXL + VEH-treated group was also significantly higher compared to APX3330 + VEH and APX3330 + OXL treated mice, indicating high susceptibility of developing new blood vessels in tumours thus increasing tumour metastasis. APX3330 + VEH-treated and APX3330 + OXL-received mice with CRC had the lowest level of VEGF protein expression compared to other groups indicating anti-angiogenic and anti-tumour effectiveness of APX3330 by itself as well as a combination therapy with OXL (n=4-5 mice/group). An image of the membrane merged with the ladder after the protein transfer step has been included in supplementary data (**Figure S2.5**).

Figure 3.19 Effects of the treatments on tumour growth. Tumours in the caecums and abdominal cavity from mice treated with 2 vehicles (A-A'), Oxaliplatin plus vehicle for APX3330 (B-B'), APX3330 plus vehicle for OXL (C-C'), and a combination of APX3330 + OXL (D-D'). The average weight of the caecum in grams (E), the average tumour diameter (F), the average number of tumours in the abdominal cavity (G) at day 21 post-surgery. Data presented as mean \pm S.E.M. * P <0.05, *** P <0.01, **** P <0.0001, n=4-5 mice/group.

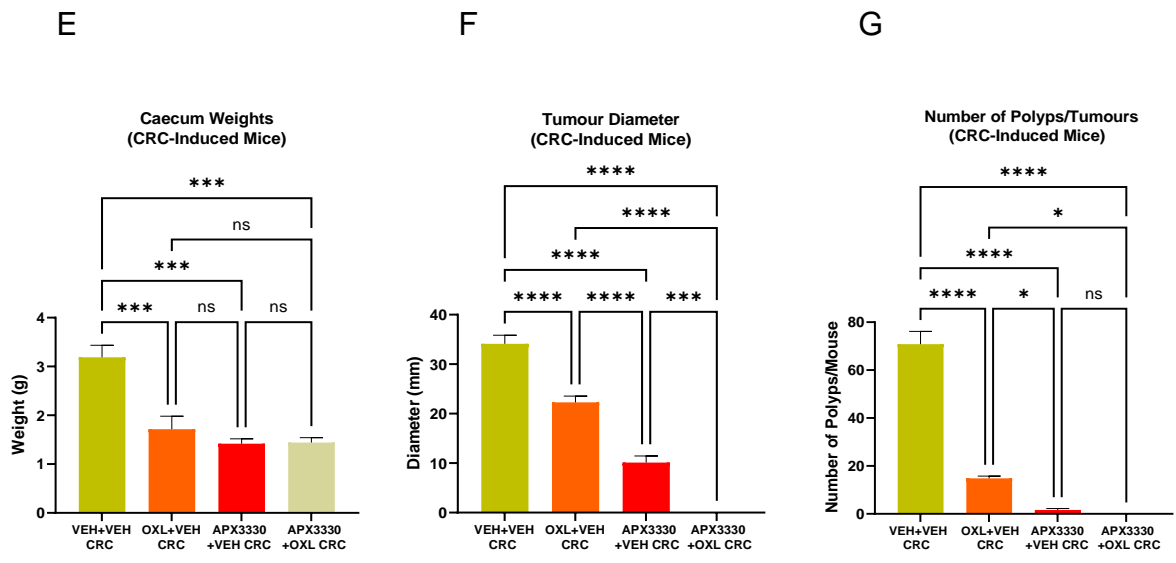
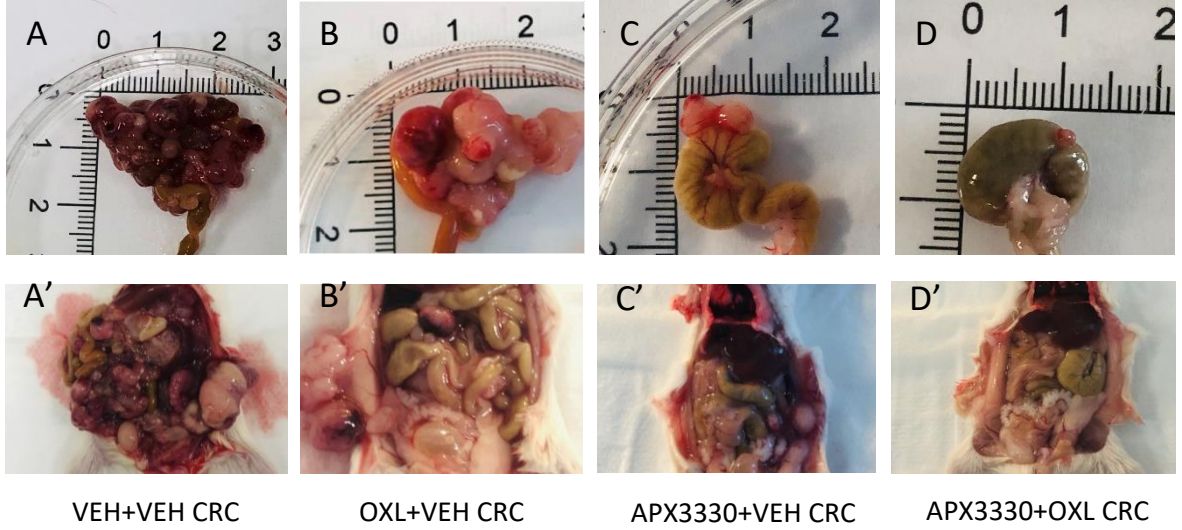


Figure 3.20 Tumour metastasis in the distal colon. Tumours in the colon from mice treated with 2 vehicles (A), Oxaliplatin plus vehicle for APX3330 (B), APX3330 plus vehicle for OXL (C), and a combination of APX3330 + OXL (D). Scale bar = 100µm.

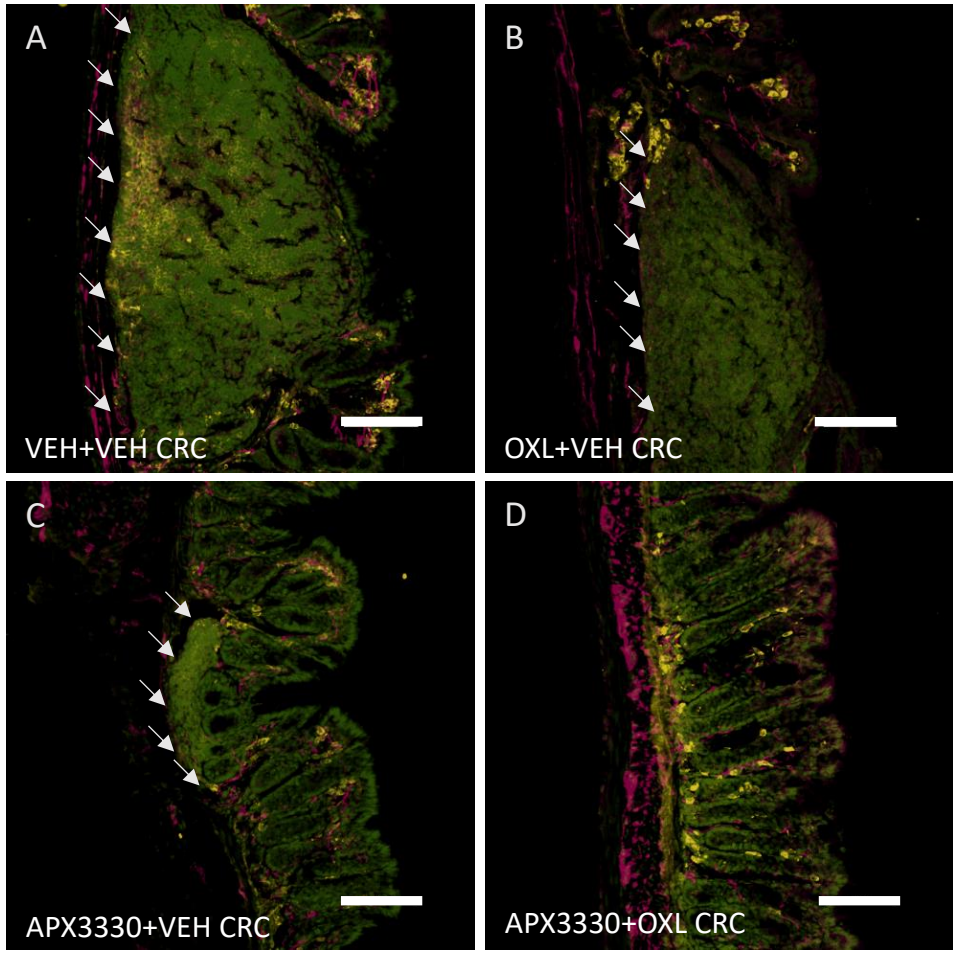
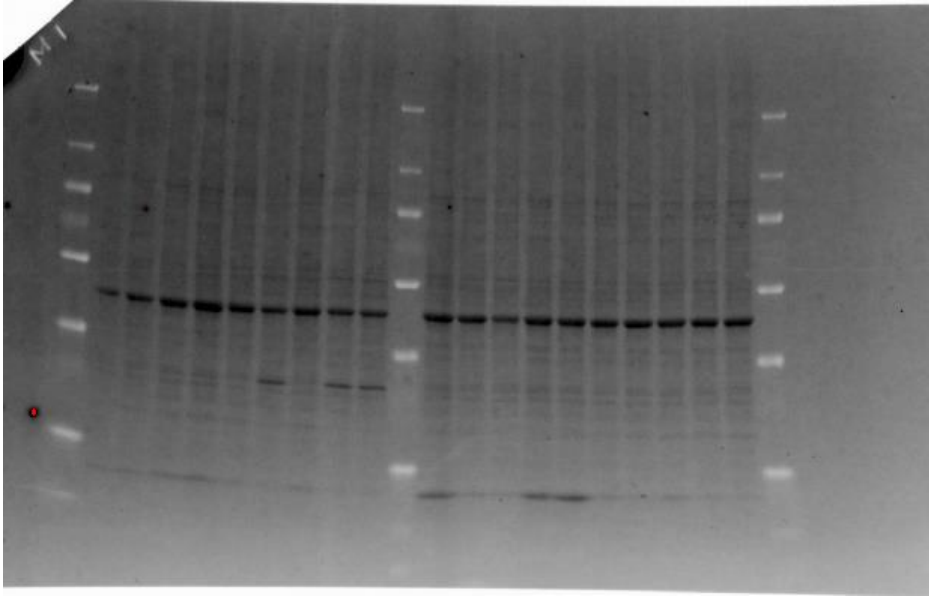
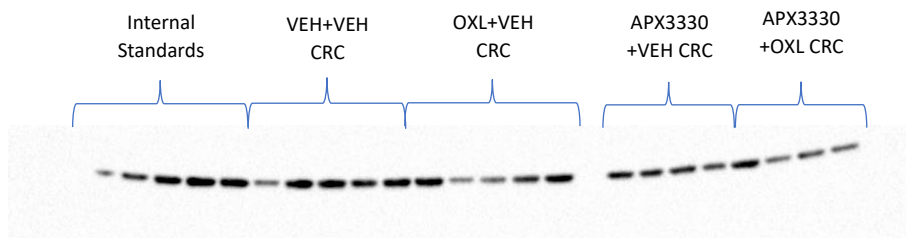


Figure 3.21 Vascular endothelial growth factor (VEGF) protein expression following treatments in mice with CRC. VEGF protein (38-44 kDa) expression in the distal colon from CRC-induced mice treated with 2 vehicles, Oxaliplatin plus vehicle for APX3330, APX3330 plus vehicle for OXL, and a combination of APX3330 + OXL for 14 days. An image of the membrane with the total protein loading (A, An image of the membrane with the target protein (B), quantitative analysis of the VEGF protein expression normalised to the total protein values (C). Data presented as mean \pm S.E.M. ** $P < 0.01$, *** $P < 0.001$, n= 4-5 mice/group

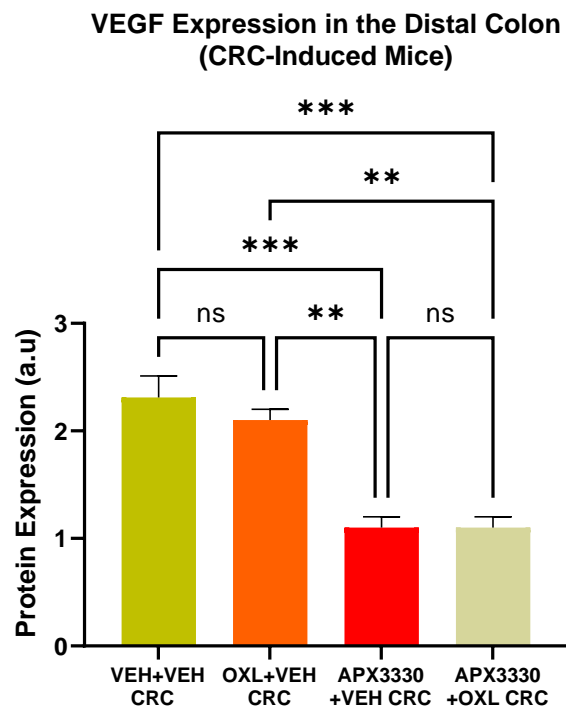
A



B



C



3.5 Discussion

This study is the first to demonstrate the efficacy of APX3330 for the treatment of OXL-induced enteric neuropathy in mice with and without colorectal cancer. Our study has also demonstrated for the first time, redox inhibition of APE1/Ref-1 protein by using APX3330 can protect myenteric neurons from OXL-induced damage. Based on the immunohistochemistry data that assessed the effect of the treatments on the total number of myenteric neurons, a reduction in the total number of neurons following Oxaliplatin treatment was observed in both cancer and cancer-free mice. Our data from western blot experiments demonstrated that cancer pathology and Oxaliplatin treatment caused increased levels of cytochrome c in the distal colon compared to other treatment groups. The release of cytochrome c might be due to oxidative stress-induced depolarisation of the mitochondrial membrane and might lead to the activation of apoptotic pathways. This requires further investigation. Our results showed that APX3330 alleviates chemotherapy-induced myenteric neuronal death, and decreases the release of cytochrome c in the distal colons of mice with and without cancer. Our study demonstrated that APX3330 inhibits the redox activation of APE1/Ref-1, STAT3 and VEGF that promote tumour progression. Our study showed that APX3330 treatment can reduce OXL-related constipation. Our data has also demonstrated that APX3330 + VEH and combination of APX3330 + OXL have shown normal faecal water content, similar to healthy cohort exhibiting positive outcomes for OXL-induced constipation.

In the clinical setting, one of the side-effects related to OXL treatment is the severe weight loss of patients due to GI-related complications (Kawai et al., 2021). Patients suffer from the loss of appetite that leads to weight loss that negatively impacts their general wellbeing. Our data showed that untreated mice continued to gain weight throughout the treatment period while OXL-treated cancer free mice lost weight by the end of 14 days treatment period indicating OXL associated GI side-effects. APX3330 treated cancer free mice, on the other hand, gained weight during the treatment period indicating positive outcomes of the treatment. Repeated *in vivo* administration of APX3330 and combination APX3330 + OXL caused steady

weight gain throughout the treatment duration in CRC-induced cohort indicating APX3330's ability to alleviate OXL-induced GI side-effects. Repeated *in vivo* administration of OXL caused severe weight loss in mice after 14-day treatment and, on the other hand, VEH + VEH-treated CRC group gradually gained weight during the treatment period due to the rapid growth of tumours in the abdominal cavity. The weight gain of APX3330-treated mice was steady, and they did not have large tumours or secondary spread of tumours contributing to their weight gain indicating its efficacy as an anti-cancer agent.

To define the clinical symptoms resulting from different treatment options, fresh faecal pellets were collected from day 0, day 7, and day 14 from the experimental groups for further analysis. Data showed significantly lower faecal water content in the OXL-treated group compared to untreated and APX3330-treated groups in the healthy treatment cohort indicating severe constipation in OXL-treated mice. Considering the CRC-induced cohort, the mean percentage difference between wet and dry faeces weight was significantly lower in OXL-treated group compared to VEH + VEH, APX3330 + VEH and APX3330 + OXL-treated groups indicating OXL-induced constipation. Data also showed positive outcomes for APX3330 + VEH-treated group and combination of APX3330 + OXL treated groups by having higher water percentage in faecal matter indicating APX3330's capacity to alleviate the symptoms.

Several research has found that chronic accumulation of oxidative stress can lead to neuronal loss, a decline in neural function, mutilating short-term and long-term gastrointestinal tract function (Chandrasekaran et al., 2011). We observed increased expression of nNOS-IR neurons following chronic OXL treatment. Even though, neuronal nitric oxide is essential sphincter relaxation and generation of complex gastrointestinal motor patterns, which in turn are utilised for propulsion of food in the GI tract (Sarna et al., 1993, Roberts et al., 2007, Roberts et al., 2008). Since OXL treatment is closely associated with severe constipation, altered levels of NO could be an indication of malfunction of GI tract peristaltic activity which leads to

retaining digestive contents longer than usual and it may lead to constipation. According to recent research, altered levels of nNOS in the enteric nervous system have been linked to several pathological conditions elevated levels of nNOS in the ENS could be indicative of oxidative stress (Rivera et al., 2011a). This hypothesis was supported by our findings. APX3330 treatment resulted in increased myenteric neuron protection, decreased the number of nNOS-immunoreactive inhibitory muscle motor and interneurons, and their proportion in the myenteric ganglia after 14 days treatment.

Our study exhibited for the first time, APX3330 treatment encompasses neuroprotective and causes less damage to the myenteric neurons, decreased expression of APE1/Ref-1 immunoreactive cells in the longitudinal myenteric preparations, as well as decreased protein expression of APE1/Ref-1 in the distal colon following APX3330 and combination treatment of APX3330 + OXL. Repeated *in vivo* administration of OXL induced myenteric neuronal loss in the distal colon whereas APX3330 treatment and combination treatment of APX3330 + OXL alleviated the neuronal survival. OXL treatment revealed higher susceptibility of myenteric neuronal loss compared to other treatment groups. Our findings indicated that APX3330 treatment has neuroprotective effects on the neurons in the myenteric plexus of the distal colon. Our findings revealed that OXL treatment was associated with changes in the APE1/Ref-1 expression in the myenteric plexus of the distal colon. OXL treatment exhibited higher expression of APE1/Ref-1 protein in the myenteric neurons, indicative of elevated oxidative stress. Comparatively, APX3330 treatment and combination of APX3330 + OXL treatment showed less expression of APE1/Ref-1 in the myenteric neurons indicating less oxidative stress in the ganglia. Immunohistochemical and Western blot data of APE1/Ref-1 protein expression of the distal colon revealed that APX3330 treatment and combination of APX3330 + OXL significantly reduced the expression of APE1/Ref-1 protein in the distal colon segments of both healthy treatment cohort and CRC-induced cohort. A higher level of APE1/Ref-1 expression is an indication of increased cellular oxidative stress due to OXL treatment and/or pathological condition of cancer. APX3330

seems to reduce the APE1/Ref-1 protein expression indicative of its capacity to alleviate oxidative stress and DNA damage.

Western blot data revealed that OXL treatment induced an increased expression in cytochrome c and APX3330 treatment significantly decreased the expression of cytochrome c within the distal colon. Elevated cytochrome c expression in the distal colon after OXL treatment indicated elevated mitochondrial damage. Data indicated that APX3330 treatment caused the least expression of cytochrome c, indicating less mitochondrial damage. Our findings also indicated that combination treatment of APX3330 + OXL significantly reduced the cytochrome c expression in the distal colon after 14 days *in vivo* administration.

Signal transducer and activator of transcription 3 (STAT3) is a cytoplasmic protein that is responsible for transmitting signals retrieved from activated cytokine and growth factor receptors in the plasma membrane to the nucleus to regulate gene transcription (Heinrich et al., 1998, Leeman et al., 2006, Quesnelle et al., 2007). STAT3 engaged in the transcription modulation of several genes that regulate cell proliferation, differentiation, metastasis, angiogenesis, inflammation as well as the immune response (Leeman et al., 2006, Frank et al., 2007, Germain et al., 2007, Jing et al., 2005). STAT3 in the tumour cells increases the expression of certain growth factors such as IL-6, IL-10, TGF β , and VEGF (Phuengkham et al., 2019). Recent findings have revealed that elevated level of pSTAT3 was correlated with poor disease prognosis (Leeman et al., 2006, Frank et al., 2007, Germain et al., 2007, Aggrawal et al., 2009). In our research, we found that the APX3330 + VEH-treated mice and combination of APX3330 + OXL-treated mice exhibited higher levels of STAT3 protein expression which in turn explains its dormant state of not being activated in the cell. In contrast, VEH + VEH-treated and OXL + VEH-treated groups exhibited lower expression of STAT3 protein. Western blot data of cancer-free cohort revealed that APX3330-treated group and untreated group exhibited higher expression of STAT3 protein, while OXL-treated group showed

lowest STAT3 protein expression indicating the possibility of activated STAT3 protein in the system.

In normal cells transient activation of phosphorylated signal transducer and activation of transcription factor 3 (pSTAT3) is predominately manifest by phosphorylation of the STAT3 protein. This process transmits transcriptional signals from cytokines and growth factor receptors on the cell surface to the plasma membrane to the nucleus of the cell (Darnell et al., 1994). STAT3 signalling pathway has long been a therapeutic target for cancer owing to its role in tumour formation, metastasis, and drug resistance (Ishibashi et al., 2018, Priego et al., 2018, Bromberg et al., 1999, Wang et al., 2018). Numerous studies have shown that hyperactivation of STAT3 can mediate tumour-induced immunosuppression that can lead to poor immune response and further enhance tumour progression and metastasis. Inhibiting STAT3 protein has several therapeutic benefits including reduced tumour cell-intrinsic proliferation, improved immunosuppressive crosstalk within the tumour microenvironment, and enhanced anti-tumour effects of tumour-infiltrating immune cells. APX3330 on the other hand is capable of inhibiting APE1/REF-1 proteins' redox activation and thus, inhibiting the activation of STAT3. Western blot data revealed that untreated and APX3330-treated groups exhibited significantly lower expression of pSTAT3 compared to OXL-treated group indicating increased activation of STAT3 protein into pSTAT3 in OXL-treated mice. Among CRC-induced cohort, APX3330 + VEH-treated, and combination of APX3330 + OXL-treated groups revealed lower expression of pSTAT3 expression compared to OXL + VEH-treated and VEH + VEH-treated groups indicating less activation of STAT3 protein into its active phosphorylated state pSTAT3.

To define the clinical symptoms resulting from different treatment options, the caecum of the mice was collected and weighed on the final experiment day. Caecum data showed that OXL-treated healthy treatment group had the highest caecum weight compared to other groups in that cohort. VEH + VEH-treated group had the largest and heaviest caecum of CRC-induced cohort because the caecum

was entirely consumed by the tumour and massive tumours were arising from the caecum. APX3330 + VEH and OXL + APX3330-treated CRC-induced mice had average size caecum indicating the efficacy of the treatment. To assess the efficacy of different treatment regimens, the average tumour diameter, the number of tumours, as well as tumour metastasis were analysed quantitatively. Tumour metastasis typically involves several important steps including local invasion, intravasation, survival in the circulation, arrest at the distant organ site and extravasation, micro metastasis formation, and metastatic colonisation (Pachmayr et al., 2017). VEH + VEH-treated mice had the largest number of tumours with a rich blood supply that were spread in the entire abdominal cavity. The secondary spread of the tumours was present in the abdomen including the spleen, liver, large intestine, small intestine as well as stomach wall. VEH + VEH-treated mice had the largest number and the size of tumours hence they have not received any cancer treatments. OXL + VEH and APX3330 + VEH treatments showed a smaller number of secondary tumours in the abdominal cavity and combination of APX3330 + OXL-treated mice did not show any secondary spread of tumours indicating the success of the treatment.

Several transcription factors that fall under the umbrella of APE1/Ref-1's redox regulation, including AP-1, NF- κ B, HIF-1 α , and p53, alongside VEGF as a transmembrane factor that are directly or/and indirectly involved in cancer survival, metastasis, and angiogenesis by producing a variety of proteins in the tumour microenvironment so cancer can thrive and grow (Heisel., 2021, Xanthoudakis et al., 1992, Xiao et al., 2002, Ema et al., 1999). VEGF is a major transcription factor that stimulates and enhances the growth of new blood vessels into newly forming tumours. By inhibiting APE1/Ref-1 proteins' redox regulation, APX3330 treatment was able to reduce the angiogenesis in CRC-induced mice. Therefore, the treatment groups that received either APX3330 + VEH or APX3330 + OXL showed significantly lower VEGF expression in the distal colon, and they showed significantly lower tumour growth and metastasis indicating a greater therapeutic potential.

Redox inhibition of APE1/Ref-1 protein via APX3330 seems to down-regulate VEGF expression that in turn decreases the capacity of forming new blood vessels in the tumours. Once the angiogenesis keeps under control in the tumour microenvironment the secondary spread of the tumour, the tumour aggressiveness, and treatment-resistance can be easily targeted by other medications. Antiangiogenic therapies such as anti-VEGF treatment have been approved for cancer treatment (Nagoya et al., 2014, McMahon et al., 2000, Zibara et al., 2015, Vasudev et al., 2014) for their therapeutic potential as an anti-tumour treatment. Our study focussed on the therapeutic anti-tumour potential of APX3330 and combination of APX3330 + OXL for the treatment of CRC compared to OXL treatment alone. It was evident that APX3330 + VEH-treated group exhibited significantly lower VEGF protein expression indicating anti-angiogenic properties of APX3330. VEGF expression in the VEH + VEH- treated group was significantly higher compared to other treatment groups indicating the higher possibility of secondary tumour spread. APX3330 treatment alone had minor secondary spread of tumours into the colon whereas the combination treatment of APX3330 + OXL did not show any signs of secondary spread of tumours indicating the higher success rate of combination therapy for the treatment of CRC.

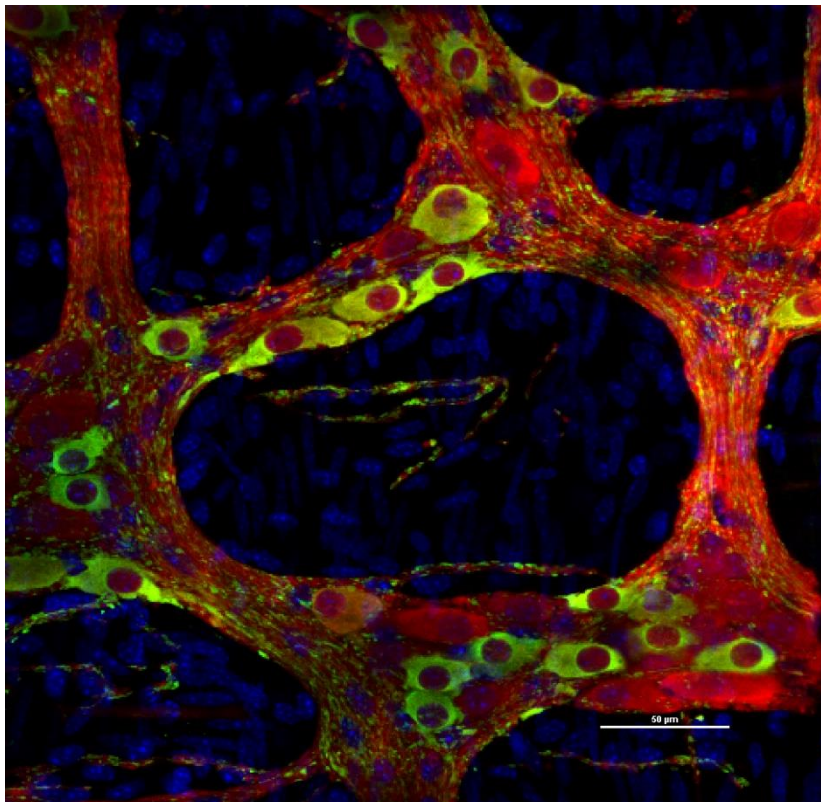
3.6 Conclusion

This study is the first to investigate the efficacy of APX3330 to protect the enteric neurons from OXL-induced damage and to potentiate the anti-tumour effectiveness of APX3330 in a combination of OXL in an orthotopic model of CRC. The results show that the impediment of the APE1/Ref-1 redox signalling pathway via APX3330 not only alleviated myenteric neuronal damage but also it exhibited anti-tumour properties that aid in attenuating tumours and diminishing tumour metastasis. The study results showed the efficacy of APX3330 given in combination with OXL, alleviated neuronal toxicity associated with OXL. The study results also exhibited anti-tumour efficacy of APX3330 in combination with OXL compared to individual chemotherapeutics. Furthermore, Western blot data showed an increase in

cytochrome c expression with OXL treatment and a significant reduction with APX3330 treatment. Cytochrome c is released from mitochondrial because of mitochondrial membrane depolarisation or increased mitochondrial membrane permeability. It is possible that OXL directly or indirectly induces/triggers mitochondrial DNA damage that results in the release of cytochrome c. APX3330 treatment and combination treatment of APX3330 + OXL on the other hand showed decreased expression of nNOS immunoreactive cells and decreased expression of cytochrome c following 14-day treatment period indicating APX3330 efficacy to ameliorate oxidative stress.

4

GENERAL DISCUSSION AND CONCLUSION



Wholemout preparation of the myenteric ganglia from the distal colon of VEH+VEH-treated mouse with CRC labelled with a pan-neuronal marker anti-PGP9.5 antibody (red), an inhibitory neuronal marker, neuronal nitric oxide synthase (green) and DAPI (blue) (Scale bar = 50μm)

4.1 General Discussion

Chemotherapy-induced GI dysfunction is a common and debilitating side-effect that reduces the efficacy of cancer treatment. Constipation and diarrhoea are among the significant side-effects of common chemotherapy medications currently used in the clinical setting as a standard treatment for cancer. Oxaliplatin and Irinotecan have been used in the clinical setting as a first-line treatment due to their anti-tumour properties in treating various cancers, including colorectal cancer. Despite their efficacy in cancer-killing properties, these chemotherapeutic medications are associated with debilitating neurotoxic and gastrointestinal side effects. These strenuous chemotherapy-induced GI side-effects usually lead to dose reductions, treatment delays, and in severe circumstances, cessation of the treatment with poor treatment outcomes. Regardless of their impact on patients' quality of life, they are still being used as a mainstay treatment due to the lack of novel therapeutic approaches in the cancer treatment milieu. Redox modulation function of APE1/Ref-1 protein and strong capacity to modulate multiple functions in the cellular environment drew the attention of current cancer research as a successful candidate to target multifactorial nature of tumour drug resistance. The recent development of APX3330, a redox inhibitor of APE1/Ref-1 protein, allowed to separately study the individual functions of APE1/Ref-1 based on repair activity, redox regulation, and other protein-protein interactions. The capacity of APX3330 to tease apart APE1/Ref-1's DNA repair and redox regulation provides the ability to identify how APE1/Ref-1 interacts in each of its sites, which provides the avenue to develop specific treatments that enhance tumour killing properties while reducing toxicities. The experiments contributing to this thesis provide insights into the therapeutic potential of APX3330 in combination with Oxaliplatin and Irinotecan to treat colorectal cancer. This study also focused on the Oxaliplatin and Irinotecan-induced gastrointestinal dysfunction and enteric neuropathy, as well as the ability of APX3330 to ameliorate adverse side-effects induced by Oxaliplatin and Irinotecan treatments. This chapter consolidates the findings presented in this thesis and acknowledges the main directions for future research.

4.2 Chemotherapy-induced Enteric Neuropathy and Gastrointestinal Dysfunction

This thesis provides novel insights into Oxaliplatin and Irinotecan-induced enteric neuropathy and neuroprotective and anti-tumour efficacy of APX3330 in healthy and CRC-induced mice. Long-term administration of Oxaliplatin and Irinotecan was associated with substantial myenteric neuronal loss. APX3330 treatment ameliorated the gastrointestinal damage caused by Oxaliplatin and Irinotecan following 14 days of *in vivo* treatment. Several pathological conditions such as slow transit constipation, irritable bowel syndrome, diabetes, diverticulitis, and inflammatory bowel disease are known to be associated with enteric neuronal loss that gives rise to a range of gastrointestinal complications (Ochoa-Cortes et al., 2016, Bernardini et al., 2012, Tornblom et al., 2002, Chandrasekharan et al., 2011, Wedel et al., 2010, Bassotti et al., 2009, Ganguli et al., 2007, Bassotti and Villanacci, 2006). The data presented in chapters 2 and 3 demonstrate Irinotecan and Oxaliplatin-induced enteric neuropathy following 14 days treatment period. Among three different medications compared in the study, Irinotecan and Oxaliplatin caused a significant myenteric neuronal loss in the distal colon following 14 days of treatment. APX3330 treatment caused neuroprotection and exhibited anti-tumour properties when used alone or as a combination treatment with Irinotecan or Oxaliplatin. APX3330 successfully reduced inflammation in Irinotecan-treated healthy and CRC-induced mice, indicating its anti-inflammatory properties. Oxaliplatin-induced side-effects plays a pivotal role in a high degree of myenteric neuronal loss following 14 days of treatment. Irinotecan treatment causes increased inflammation in the distal colon and plays a vital role in enteric neuropathy following chronic Irinotecan treatment. APX3330 has shown successful results when used alone or with Oxaliplatin and Irinotecan, indicating its efficacy in oxidative stress and inflammation induced by IRI and OXL. Redox inhibition of APE1/Ref-1 protein via small molecule inhibitor APX3330 modulates multiple regulatory pathways to reduce oxidative stress, inflammation, enteric neuroprotection, and tumour progression.

Irinotecan causes acute and chronic diarrhoea, a main side-effect of the treatment. Approximately 60-80% of patients experience acute diarrhoea within 24-hours of administration of Irinotecan (Gibson and Stringer, 2009), indicating rapid and progressive changes in GI tract function. Patients experience delayed-onset diarrhoea 24 hours after Irinotecan administration which is shared by approximately 80% of patients (Saliba et al., 1998). Several studies support the hypothesis that chronic accumulation and reactivation of SN-38 leads to long-term disruption of intestinal microflora and perpetual mucosal damage (McQuade et al., 2014, Stringer et al., 2009b, Gibson and Stringer, 2009, Javle et al., 2007), however, exact mechanisms underlying the acute and chronic onset of diarrhoea after Irinotecan administration are still unclear. Administration of atropine for acute diarrhoea attenuated the symptoms highlighting the possibility of the involvement of secretomotor cholinergic neurons (Tache et al., 2018). Damage to the enteric nervous system neurons may cause delayed onset of diarrhoea after Irinotecan administration.

Data presented in chapter 2 indicate that Irinotecan treatment significantly increased the faecal water content after 14 days of *in vivo* treatment, suggesting secretory diarrhoea. This is in line with previous research findings suggesting that Irinotecan-induced delayed and prolonged onset diarrhoea arises because of multifaceted changes in the GI tract collateral with a primarily secretory mechanism that comes from an underlying effect of inflammation (Saliba et al., 1998, Beilberg and Cvitkovic, 1996). Our data in chapter 2 support myriad research data related to Irinotecan-induced diarrhoea. Our experiment data on faecal water content revealed that Irinotecan treatment caused diarrhoea in healthy and CRC-induced mice assessed on days 7 and 14. APX3330 treatment has alleviated the symptoms by bringing the faecal water content back to a healthy range. Mucosal damage and regeneration were not studied in this research. However, previous research conducted by our lab group has found that Irinotecan treatment was associated with severe mucosal ulceration, morphological disorganisation, and crypt hyperplasia in the mouse colon following both acute and chronic Irinotecan treatment (McQuade et al., 2017). In line with these findings, several other studies have also reported

that Irinotecan treatment causes crypt ablation, epithelial atrophy, and villous blunting in the rat jejunum following Irinotecan treatment (Logan et al., 2008, Bateman et al., 2016, Wardill et al., 2016, Al-Dasooqi et al., 2017). Previous research has shown that histopathological damage caused by Irinotecan treatment resolves within days following treatment, and chronic diarrhoea persists up to 10 years post-treatment (Numico et al., 2015, Denlinger and Barsevick, 2009). The underlying delayed onset and long-term diarrhoea mechanisms are yet to be discovered. Recent research, including a previous study by our group, draws the possibility that early mucosal damage and acute intestinal inflammation can lead to the damage and death of enteric neurons leading to chronic diarrhoea and gastrointestinal dysfunction (McQuade et al., 2017).

The results of our study presented in chapter 2 demonstrated that Irinotecan treatment is closely associated with intestinal inflammation. Inflammation was confirmed by the high level of inflammatory marker neutrophil gelatinase-associated protein Lipocalin 2 (LCN-2) present in the faecal matter of Irinotecan-treated mice with and without CRC. Irinotecan-treated mice exhibited the highest LCN-2 levels throughout the treatment period assessed on days 1, 7 and 14, indicating acute and chronic inflammation in the gut following Irinotecan treatment. APX3330 seems to attenuate the inflammation by downregulating several transcription factors and stimulating endonuclease activity to repair damaged DNA (Kelley, 2020, Mijit et al., 2021).

We assessed the immune cell infiltration of CD45-positive cells and the activation of myeloperoxidase (MPO) in the distal colon following 14 days of treatment to evaluate the initiation of active inflammation. Irinotecan-induced inflammation was also confirmed by increased number of CD45-positive leukocytes in the colon from mice with and without cancer, consistent with our previous report, McQuade et al., 2017. MPO activation is a reliable marker of active inflammation. Neutrophils are one of the primary leukocytes recruited by the immune system to fight against inflammation. They are short-lived white blood cells

that contain azurophilic granules containing the enzyme MPO (Belal et al., 2021, Schroder et al., 2021). Previous research has demonstrated that high faecal and serum MPO levels are correlated with the increased disease severity of patients with chronic GI tract inflammation (Hansberry et al., 2017, Chami et al., 2018). In the presence of hydrogen peroxide and free chloride ions, MPO undergoes a halogenation cycle that yields hypochlorous acid (HOCl) and two-electron oxidants (Davies and Hawkins, 2020). HOCl acid is a potent bactericidal agent and free-electron oxidant because the chemical reaction contributes to oxidative stress by producing free radicals (Bapte et al., 2022). However, constant intestinal exposure to MPO and HOCl acid due to inflammation results in cell death, and in severe cases, it can lead to secondary host tissue injury (Belal et al., 2021). Chronic administration of Irinotecan leads to high levels of neutrophil accumulation in GI mucosa that, in return, results in perpetual intestinal inflammation.

Several previous studies have reported that *in vitro* and *in vivo* treatment with Irinotecan triggers an excessive attraction of inflammatory cells (Cottone et al., 2015, Logan et al., 2008). We found that co-administration of APX3330 with Irinotecan reduces the expression of CD45-positive cells in the distal colon of mice with and without cancer. This was also correlated with improved symptoms of diarrhoea throughout 14 days of treatment. Similarly, it has been reported that co-administration of the anti-inflammatory agent St John's Wort with Irinotecan significantly reduced the expression of pro-inflammatory markers in rat intestines (Hu et al., 2006).

Our findings and previous research suggest a strong correlation between myenteric neuronal loss and Irinotecan-induced inflammation. The enteric nervous system contains inhibitory and excitatory neurons that can be identified through their expression in nNOS and ChAT in the neurons (Ferness, 2012). These excitatory and inhibitory enteric neurons predominately regulate gastrointestinal functions. Several studies have found that long-term intestinal inflammation has been identified as the main contributor to the damage to the enteric nervous system,

including possible myenteric neuronal loss of up to 50% (Nurgali et al., 2007, Nurgali et al., 2011, Boyer et al., 2005), which may contribute to gastrointestinal dysfunction in the long-term. In this study, we found that long-term intestinal inflammation following Irinotecan treatment was correlated with significant neuronal loss in the myenteric plexus of the distal colon, whilst APX3330 treatment mitigated the inflammation and associated enteric neuronal loss following 14 days of treatment. Previous study by our group has reported that neuronal loss with Irinotecan administration has been correlated with changes in colonic and intestinal motility (McQuade et al., 2017). Our study is the first to investigate the neuroprotective effects of APX3330 and enteric neuronal survival in the models of Irinotecan-treated mice with and without CRC. The density of neuronal processes in the distal colon was also assessed using the neuronal marker β -tubulin III. Data revealed that Irinotecan treatment correlated with reduced density of neuronal processes in healthy and CRC-induced mice, indicating elevated damage of enteric neurons. APX3330 treatment prevented Irinotecan-induced damage to the nerve fibres.

Our results indicate the changes in subpopulations of the myenteric plexus in the distal colon after chronic Irinotecan treatment. Chronic Irinotecan administration caused a significant increase in the proportion of choline acetyltransferase (ChAT)-IR neurons and vesicular choline acetyltransferase (VChAT)-IR fibres in mice. Irinotecan treatment correlates with acute diarrhoea usually experienced within 24 hours post Irinotecan administration and cholinergic syndrome in CRC patients (Hecht, 1998).

Acetylcholine is a major excitatory neurotransmitter in the gastrointestinal system that controls circular and smooth muscle contraction (Furness, 2012) and gastric secretion (Cooke, 2000). Therefore, cholinergic neurons and cholinergic nerve fibres play an essential aspect in the excitatory motor innervation of the gut (Furness, 2012). VChAT-IR fibres facilitate essential GI tract innervation functions such as mucus production, the vasomotor tone in GI mucosa, and innervating

enteric ganglia as well as innervation of gastrointestinal smooth muscles that control motility, secretion, and blood flow (Cervi et al., 2014). APX3330 treatment decreased the expression of ChAT-IR neurons resulting in a low proportion of ChAT-IR cells in the myenteric plexus of the distal colon preventing muscles from hyperexcitation that leads to diarrhoea. APX3330 treatment prevented Irinotecan-induced increase in neuronal fibre density immunoreactive to VAcHT.

The results presented in chapter 2 revealed that APE1/Ref-1 expression determined by immunohistochemical, and Western blot analyses was higher in Irinotecan-treated mice with and without cancer. Increased activation of APE1/Ref-1 is concurrent with the elevated activation redox regulatory pathway via the redox active site of APE1/Ref-1 protein. In contrast, the APX3330 treatment ameliorated the increase in APE1/Ref-1 level caused by Irinotecan treatment and the cancer pathology in CRC-induced mice.

Signal transducer and activator of transcription 3 (STAT3) is a cytoplasmic protein that belongs to the mammalian STAT-3 family of seven proteins, namely STAT1, STAT2, STAT3, STAT4, STAT5a, STAT5b, and STAT6 (STATs) (Guanizo et al., 2018, Darnell et al., 1994) that mediate several intracellular signalling pathways, including cell proliferation, differentiation, survival, and angiogenesis (Hanlon et al., 2019, Rawlings et al., 2004). In normal cells, the transient activation of STAT3 is predominately manifested by protein phosphorylation. This process transmits transcriptional signals from cytokines and growth factor receptors on the cell surface to the plasma membrane to the cell's nucleus (Darnell et al., 1994). On the other hand, STAT3 protein becomes hyperactivated, especially in pathological conditions such as cancer (Johnson et al., 2018). Targeting the STAT3 signalling pathway has long been a therapeutic target for cancer owing to its role in tumour formation, metastasis, and drug resistance (Ishibashi et al., 2018, Priego et al., 2018, Bromberg et al., 1999, Wang et al., 2018). Numerous studies have shown that hyperactivation of STAT3 can mediate tumour-induced immunosuppression that can lead to poor immune response and further enhance tumour progression

and metastasis (Mittal et al., 2018, Wang et al., 2018). STAT3 remains inactive in the cytoplasm of an unstimulated cell, and it becomes activated mainly by phosphorylation at tyrosine and serine residues (Sgrignani et al., 2018). Phosphorylated STAT3 protein then translocates into the nucleus, followed by DNA binding, ultimately executing their destined nuclear function (Sgrignani et al., 2018).

STAT3 is responsible for transmitting signals retrieved from activated cytokine and growth factor receptors in the plasma membrane to the nucleus to regulate gene transcription (Lee et al., 2019, Quesnelle et al., 2007, Leeman et al., 2006, Heinrich et al., 1998). STAT3 engaged in the transcription modulation of several genes that regulate cell proliferation, differentiation, metastasis, angiogenesis, inflammation, and the immune response (Rebe and Ghiringhelli, 2019, Lee et al., 2019, Frank et al., 2007, Germain et al., 2007, Leeman et al., 2006, Jing et al., 2005). In contrast, STAT3 regulates as a point of conjunction for several oncogenic signalling pathways in tumor cells to govern the anti-tumour response (Guha et al., 2019). In cancer cells and other cells that cohabit in the cancer ecosystem, STAT3 expresses hyperactivation, which plays a vital role in tumour progression by upregulating the production of immunosuppressive factors and inhibiting the expression of crucial immune activation regulators (Rebe and Ghiringhelli, 2019). Tumour microenvironment (TME) is a complex ecosystem where several heterogeneous cells varieties such as cancer cells, endothelial cells, smooth muscle cells, tumour associated fibroblasts, and tumour infiltrating fibroblasts habitat together in the tumour microenvironment for growth, survival, proliferation, angiogenesis, and metastasis (Pearce et al., 2018, Azizi et al., 2018). Therefore, it has become challenging to achieve successful immunotherapy outcomes; hence it must combat the tumour microenvironment that mediates tumour resistance. Hyperactivated STAT3 in the tumour cells increases the expression of specific growth factors such as IL-6, IL-10, TGF β , and VEGF (Phuengkham et al., 2019). NF- κ B is another critical transcription factor that STAT3 has close links with its function. It interacts with NF- κ B to further promote the progression and aggressiveness of the tumour (Yu et al., 2009, Fan et al., 2013, Taniguchi et al., 2018). NF- κ B is a critical transcription factor that can upregulate a

spectrum of target proteins involved in inflammation and cancer initiation (Yu et al., 2009). Several studies have identified STAT3 and NF- κ B crosstalk with each other in multiple regulatory pathways. For instance, cytokines like IL-6 can activate both STAT3 and NF- κ B at the same time (Fan et al., 2013). Both transcription factors share common target proteins in cell proliferation metastasis and angiogenesis. Several recent studies support that for a significant number of cancers, elevated levels of STAT3 were correlated with poor disease prognosis (Leeman et al., 2006, Frank et al., 2007, Germain et al., 2007). STAT-3 activation initiates the activation of several genes that block apoptosis, favor cell proliferation and survival, inhibit anti-tumour response, and promote angiogenesis and metastasis (Leeman et al., 2006, Frank et al., 2007; Germain et al., 2007, Regis et al., 2008). Recent studies have taken the approach of disrupting STAT3 signalling, that leads to growth inhibition and apoptosis in tumour cell lines and can impair tumour growth in mouse Xenograft cancer models (Leeman et al., 2006, Germain et al., 2007, Jing et al., 2005, Egloff and Grandis, 2009, Boehm et al., 2008). Western blot data presented in chapter 2 revealed that Irinotecan treatment resulted in increased protein expression of NF- κ B in both healthy and CRC-induced cohorts, indicating increased inflammation. APX3330 treatment showed significantly low NF- κ B protein expression in both healthy and CRC mice demonstrating the anti-inflammatory properties of the treatment.

Other post-translational modifications such as acetylation, methylation, and SUMOylation can alter STAT3 transcriptional activity by altering STAT3 phosphorylation (Sgrignani et al., 2018). This adds more complexity to cancer pathology by adding more chances of getting STAT3 transcriptional activation, making it challenging to target inhibiting the protein. Acetylation, demethylation, methylation, phosphorylation, and sumoylation can collectively phosphorylate STAT3 and stimulate the transcriptional activation that is ultimately expressed in target gene transcription in the nucleus (Ishibashi et al., 2018). As a result of STAT3 phosphorylation, it up-regulates gene transcription of BCL-xl, Cyclin D1/D2, MCL1, MYC, Survivin, and downregulates P53 oncogene which in turn aids in cancer cell proliferation and survival (Johnson et al., 2018). Transcriptional activation of STAT3

increases the gene activation of MMP2/9, HGF, bFGF, VEGF, and HIF1 α , resulting in the decrease in the target gene activation of AKT CXCL10, IL-12, IFN- β/γ , and p53 that aids in angiogenesis of the tumour (Johnson et al., 2018). Increasing the post-translational activation of STAT3 further enhances the expression of MMP2/9, Twist1, and Vimentin, which enhance tumour metastasis (Johnson et al., 2018). IL-6/10, PD-1/PD-L1/PD-L2, TGF β , and VEGF expression have been up-regulated by STAT3 phosphorylation while CD80/86, CXCL 10, CCL5, MHC class II, TNF, IFN- β/γ and IL-12 post-transcriptional gene activation is being down-regulated the STAT3 (Johnson et al., 2018). Therefore, targeting the STAT3 signalling pathway has shown significant therapeutic potential in cancer treatment. Inhibiting STAT3 protein has several therapeutic benefits, including reduced tumour cell-intrinsic proliferation, improved immunosuppressive crosstalk within the tumour microenvironment, and enhanced anti-tumour effects of tumour-infiltrating immune cells. Data from chapter 2 revealed that Irinotecan treated cancer-free mice was associated with decreased expression of STAT3 and increased expression of pSTAT3, demonstrating activated STAT3 protein into its phosphorylated state, indicating downstream activation of several other transcription factors such as HIF1- α , AP-1, and NF-kB furthering Irinotecan induced inflammation. In CRC-induced cohort, APX3330 treated, and combination treatment of APX3330 + Irinotecan increased expression of STAT3 and decreased expression of pSTAT3, indicating less activation of STAT3 protein into its phosphorylated state resulted in reduced downstream activation of several transcription factors that support tumour growth, survival, metastasis, angiogenesis, and inflammation.

The secondary spread of the tumour depends on the type of cancer, aggressiveness, and treatments (Melzer et al., 2017). Tumour metastasis occurs when cancer cells detach from the primary site, typically entering the circulatory or lymphatic system traveling through the lymph or blood, adhering to secondary sites, and producing more tumours (Melzer et al., 2017). This process typically involves several essential steps, including local invasion, intravasation, survival in the circulation, arrest at the distant organ site and extravasation, micrometastasis formation, and metastatic colonisation (Pachmayr et al., 2017). After the cancerous

cells grow into a primary tumour, it activates matrix metalloproteins (MMPs), allowing the cancer cells to invade local tissues by degrading basement membranes. These MMPs are either produced by cancer cells themselves or stimulate the extracellular matrix to produce them (Pachmayr et al., 2017). The solitary, invading cancerous cells undergo epithelial to mesenchymal transition (EMT), allowing cells to repress E-cadherins and upregulate N-cadherins. This process is maintained via several transcription factors. It enables the cancer cells to adapt from epithelial cells to mesenchymal cell phenotype that aids its ability to intravasate into the bloodstream (Pachmayr et al., 2017). N-cadherins also have less affinity to intracellular adhesion allowing cancer cells to further local tissue invasion. Once the cells undergo EMT, they can make their way into the bloodstream through the surface of the blood vasculature. Once the cells pass through the intravasation process, they can disseminate to different sites of the body and lodge into secondary sites. Cancer cells then undergo extravasation by squeezing through the blood vessels and entering the secondary sites in the extracellular matrix, allowing them to form colonies and secondary tumours. Newly colonised tumours stimulate formation of new blood vessels called angiogenesis which is triggered by hypoxia. Angiogenesis supports further tumour growth and metastasis (Melzer et al., 2017). Most metastasised cancers have limited treatment options due to the multifactorial survival mechanisms of cancer. One possible treatment avenue is by preventing angiogenesis. Hence, preventing the cancerous cells from spreading through the circulatory system and preventing the growth of new tumours. It is essential to stop the secondary spread of the tumour as, according to recent statistics, above 90 percent of cancer-related fatalities are due to metastasis. Therefore, targeting metastasis in cancer treatment is essential since inhibition of metastasis could affectedly reduce fatality rates (Simmons, 2019). Regarding anti-tumour properties of the different treatment options, only the CRC-induced cohort was considered. Data presented in chapter 2 revealed that Vehicle + Vehicle-treated CRC-induced mice had the highest number of tumours and the largest size of caecum engorged with many tumours. At the same time, APX3330 treatment resulted in a lower number of tumours and the average diameter of caecum free from tumours and polyps.

Angiogenesis and anti-angiogenic targets stirred recent cancer treatment avenues. It is regulated by a mixture of large amounts of pro-and anti-angiogenic molecules such as Vascular Endothelial Growth Factor (VEGF), platelet-derived growth factor (PDGF), tumour necrosis factor (TNF)- α , interleukin (IL)-8, transforming growth factor (TGF)- α , transforming growth factor (TGF)- β , and angiogenin (Zhao., et al., 2015, Folkman et al., 2007). Cancer prognosis mainly depends on the amount of pro-and anti-angiogenic factors present in the tissues, which in retunes govern the aggressiveness of cancer (Nishida et al., 2006, McMahon et al., 2000). The balance between pro-and anti-angiogenic factors exhibits cast irregularities in cancer resulting in the aberrant forming of new blood vessels that supply blood to forming tumours (Folkman et al., 2007, Goel et al., 2011). Antiangiogenic therapies such as anti-VEGF treatment have been approved for cancer treatment (McMahon et al., 2000, Zibara et al., 2015, Vasudev et al., 2014). VEGF is a major factor that stimulates and enhances the growth of new blood vessels into newly forming tumours. Therefore, it is imperative to recognise significant transcription factors aiding cancer progression and survival. It is also essential to block or inhibit their function for better cancer treatment and decreased treatment resistance. In that regard, APX3330 proves a more significant potential and therapeutic target to control tumour growth. Our study focussed on the therapeutic potential of Irinotecan, Oxaliplatin, APX3330, and combination treatment to investigate the efficacy of the treatments as an anti-tumour therapy. VEGF expression was assessed in CRC-induced mice via Western blot experiments. Data revealed that Vehicle-treated CRC-induced mice had the highest VEGF protein expression suggesting high susceptibility to neovascularisation providing blood supply to newly developing tumours. On the contrary, APX3330 and combination therapy of APX3330 with Irinotecan expressed significantly lower VEGF protein expression highlighting the efficacy of APX3330 as an anti-tumour agent.

The neuroprotective and anti-tumour efficacy of APX3330 in combination with Oxaliplatin is presented in chapter 3. Oxaliplatin treatment caused severe constipation measured by faecal water content on days 1, 7, and 14 in cancer-free

mice and CRC-induced cohorts. Our study revealed that APX3330 treatment improved the weight gain and faecal water content back to their normal range, suggesting that APX3330 may alleviate the gastrointestinal side effects associated with chemotherapy. Previous research conducted by our lab group and several other studies has demonstrated that Oxaliplatin treatment caused delayed gastrointestinal transit, reduction in the total number of colonic contractions, drop in the proportion and frequency of colonic migration motor complexes (CMMCs), reduction in the frequency of short contractions (McQuade et al., 2017, McQuade et al., 2016), inhibition of CMMS in the colon following Oxaliplatin treatment (Wafai et al., 2013) and inhibition of intestinal transit following cisplatin-treated rats (Vera et al., 2011). These changes caused by Oxaliplatin treatment caused a reduction in faecal output and reduced faecal water content (McQuade et al., 2016). In Chapter 3, we have also found similar results with Oxaliplatin treatment. We have also introduced the efficacy of APX3330 to alleviate Oxaliplatin-induced constipation for the first time.

Neuronal damage and loss have been closely correlated with oxidative stress (Rojas-Gutierrez et al., 2017, Lassmann and Horssen, 2016). It has been reported in several pathologies, including Charcot-Marie neuropathy, acrylamide-induced neuropathy, diabetic neuropathy, and chemotherapy-induced peripheral neuropathy (Areti et al., 2014, Saifi et al., 2003, Chandrasekaran et al., 2011, Vincent et al., 2004). Recent research has identified the clinical importance of oxidative stress and corresponding mitochondrial damage as critical players in the emergence of oxaliplatin-induced peripheral neuropathy (Jugait et al., 2022, Kerckhove et al., 2017, Zheng et al., 2011). Recent research on Oxaliplatin-treated rats has reported that mitotoxicity is highly expressed in the sciatic nerve of the Oxaliplatin-treated cohort, resulting in a disruption in cellular respiration and ATP production associated with peripheral neuropathy following Oxaliplatin treatment (Zheng et al., 2011). Oxaliplatin-induced elevated ROS production was found to negatively affect the mitochondrial electron transport chain (mETC) leading to mitochondrial dysfunction (Joseph and Levine, 2009). Recent research conducted by Gampala and the collaborators (2021) found that Ref-1 inhibitors caused

decreased utilisation of TCA cycle substrates slowing the growth of cancer cell in co-culture spheroids as well as tumour size reduction demonstrated in the *in vivo* xenograft model (Gampala et al., 2021). Oxaliplatin-induced mitochondrial dysfunction caused the release of cytochrome c from the mitochondria into the cell leading the cells to initiate the intrinsic pathway of cell death (Waseem et al., 2017). Chapter 3 demonstrated that Oxaliplatin treatment causes neuronal damage in the distal colon. It is also associated with mitochondrial reactive oxygen species and mitochondrial dysfunction. Western blot experiments of cytochrome c expression in the distal colon revealed that Oxaliplatin treatment caused the highest level of cytochrome c expression in the distal colon following 14 days of *in vivo* treatment in both healthy and CRC-induced mice indicating elevated levels of oxidative stress associated with the treatment. APX3330 reduced cytochrome c expression after 14 days of treatment, in the CRC-induced cohort. Cytochrome c release from mitochondria triggers the downstream activation of caspase 9 and caspase 3, forming mature proteosomes to execute apoptosis via intrinsic pathways (Vince et al., 2018). A recent study conducted in neuronal cultures from dorsal root ganglia (DRG) has also found that Oxaliplatin-treated mice exhibited increased levels of mitochondrial superoxide levels (Kelley et al., 2014). Neurons are susceptible to oxidative stress and are more vulnerable to ROS-induced damage due to the widely found polyunsaturated fatty acids enriched in nerve cell membranes (Lenkiewicz et al., 2016). ROS have also been found to alter the ion transport mechanism of the cell, directly via modifying regulatory proteins or indirectly via peroxidation of membrane lipids (Angelova and Abramov, 2016). Several research has identified that elevated ROS production in the cell is associated with the destruction of several intracellular components, including mitochondria (Wei et al., 2000).

Data revealed that Oxaliplatin treatment caused a substantial myenteric neuronal loss in the distal colon following 14 days of *in vivo* treatment. Wholmount preparations of the distal colon labelled with anti-protein gene product 9.5 (PGP9.5) antibody exhibited that Oxaliplatin treatment caused the highest myenteric neuronal loss in healthy and CRC-induced cohorts. APX3330 showed neuroprotective effects on enteric neurons. When used as a combination therapy with Oxaliplatin, it could

increase the total neuronal number to Oxaliplatin treatment alone, indicating its neuroprotective properties. Elevated expression of ROS with Oxaliplatin treatment and myenteric neuronal loss in the distal colon were further associated with high expression of neuronal nitric oxide synthase (nNOS) immunoreactive (IR) neurons in the distal colon. Similar results have been reported in rats and mice treated with cisplatin and oxaliplatin, having an increased proportion of nNOS-IR neurons (Wafai et al., 2013, Vera et al., 2011). Our data from chapter 3 identified that Oxaliplatin treatment was associated with increased expression in the number and the proportion of nNOS-IR neurons in the distal colon in healthy and CRC-induced mice. On the contrary, in both healthy and CRC-induced cohorts, APX3330 treated mice were found to have decreased expression of nNOS-IR neurons in the distal colon. Nitric oxide (NO) released from nNOS-IR motor and interneurons functions as an essential neurotransmitter that controls gastrointestinal motility (Takahashi, 2003, Lecci et al., 2002). The stupendous yield of NO and concomitant nitrosylation has been associated with inhibition of dynamin-related protein 1, correlated with synaptic impairment and disruption in synaptic transmission (Savidge, 2011). McQuade et al., 2016 has also found that Oxaliplatin-induced oxidative stress causes enteric neuropathy.

Platinum accumulation and inflammation are other essential factors associated with Oxaliplatin-induced enteric neuronal loss. Concurrent existence of oxidative stress and low-grade inflammation has been reported in several diseases, including chronic kidney disease, cardiovascular disease, diabetes, alcoholic liver disease, and neurodegenerative conditions (Cachoferio et al., 2008, Biswas, 2016, Ambade and Mandrekar, 2012, Biswas et al., 2007, Onyango, 2008, Hald et al., 2007). Another research conducted by Fischer and Maier has reported that both oxidative stress and chronic inflammation can cause deleterious executes on neurons (Fischer and Maier, 2015). Thus, the researchers suggest future directions to investigate whether Oxaliplatin treatment-induced oxidative stress instigates systemic inflammation in the long haul (Stojanovska et al., 2017).

An elevated level of APE1/Ref-1 expression was reported in several cancer pathologies, including colorectal cancer, prostate cancer, breast cancer, renal cancer, gastric cancer, multiple myeloma, non-small cell lung cancer, gynaecologic cancers, pancreatic cancer, glioblastoma, germ cell tumours, head, and neck tumours and osteoblastoma (Wang et al., 2019, Zheng et al., 2012, Kelley et al., 2011, Su et al., 2011,). Chapter 3 demonstrated that Oxaliplatin treatment caused significantly high expression of APE1/Ref-1 in the myenteric plexuses neurons of the distal colon assessed by immunohistochemistry data of the wholemount preparations and in western blot experiments. Vehicle + Vehicle-treated; CRC-induced mice also had significantly high APE1/Ref-1 protein expression. Data revealed that APX3330 treatment reduces the expression of APE1/Ref-1 in both immunohistochemistry and western blot experiments.

In chapter 3, we have also assessed the downstream protein expression of STAT3 and pSTAT3 to evaluate the activation of possible regulatory pathways. Our data revealed that Oxaliplatin-treated mice exhibited the highest pSTAT3 protein expression in the cancer-free and CRC-induced cohorts indicating elevated downstream activation in the STAT3 regulatory pathway. Vehicle-treated CRC group also had elevated expression of pSTAT3, indicating increased activation of the STAT3 regulatory pathway. Activation of STAT3 indicated by high expression of pSTAT3 is associated with tumour growth, proliferation, metastasis, angiogenesis, survival, and inflammation. On the contrary, APX3330-treated, and combination treatment of Oxaliplatin + APX3330 had significantly lower expression of pSTAT3, indicating reduced activation of STAT3 regulatory pathway inhibiting tumour growth and metastasis.

Data presented in chapter 3 revealed that the Vehicle + Vehicle-treated group exhibited the largest caecum, the highest number of tumours and polyps following 14 days of treatment. Considering the anti-tumour efficacy of the treatments, Oxaliplatin treatment was effective in reducing tumour progression, however, it was not successful in the complete inhibition of the tumour growth.

APX3330 treatment, was a successful treatment by having no secondary spread of tumours following 14 days. Combination treatment of APX3330 + Oxaliplatin showed the most promising outcome among all the treatment groups by having no visible tumour formation in the primary tumour induction site as well as the absence of metastasis.

The expression of vascular endothelial growth factor (VEGF) in the distal colon segments was measured via western blot experiments to investigate the anti-angiogenic properties of different treatment options. Chapter 3 data revealed that the vehicle-treated CRC group had the highest expression of VEGF protein, followed by the Oxaliplatin + vehicle-treated group suggesting high susceptibility to neovascularisation providing blood supply to newly developing tumours. APX3330 treatment alone and the combination of APX3330 + Oxaliplatin had significantly lowered the expression of VEGF, indicative of inhibition of forming new blood vessels.

4.3 Conclusion and Future Directions

Based on our research findings and most previous research findings, it is fair to conclude that the mechanisms underlying chemotherapy-induced gastrointestinal dysfunction arise because of complex and multifaceted mechanisms. Importantly, our research presented for the first time APX3330 showed enhanced enteric neuronal survival and improved GI function following Oxaliplatin and Irinotecan treatment. APX3330 treatment reduced the severity of constipation following Oxaliplatin treatment and alleviated Irinotecan-induced diarrhoea. Therefore, the importance of further investigation of the effects of APX3330 on gut microbiota and its association with enteric neurons is highlighted in this study for future directions. Faecal water content following Oxaliplatin treatment also indicated severe constipation by having significantly low water content compared to other treatment groups. On the contrary, faecal water content following Irinotecan treatment was

considerably higher than in different treatment groups denoting chronic diarrhoea following 14 days of treatment. APX3330 treatment in both Oxaliplatin and Irinotecan chapters showed successful results by protecting enteric neurons from Oxaliplatin and Irinotecan treatment, followed by improving Oxaliplatin induced constipation and Irinotecan caused diarrhoea indicating the correlation between chemotherapy-induced enteric neuronal damage and gastrointestinal dysfunction.

This thesis has demonstrated that individual administration of Oxaliplatin and Irinotecan caused neuronal damage and substantial reduction of myenteric neurons in the distal colon, significantly correlated with gastrointestinal dysfunction. Combination therapies such as FOLFIRI, FOLFOX, and FOLFOXIRI are currently being used in the clinical setting to treat CRC (Van Cutsem et al., 2010, Grothey et al., 2004, Falcone et al., 2002, Souglakos et al., 2006). While the effects of combination chemotherapeutic treatments on the enteric nervous system have yet to be further investigated, the anti-cancer efficacy of combination chemotherapeutics such as FOLFIRI and FOLFOX have been validated in mouse models of CRC (Robinson et al., 2013). Present work on using APX3330 combined with Oxaliplatin and Irinotecan to treat CRC successfully provides the groundwork for investigating consequent enteric neuronal survival and improved gastrointestinal dysfunction.

Considering the similarities and differences between tumour bearing and non-tumour bearing mice that were treated with Oxaliplatin, Irinotecan and APX3330 non-tumour bearing mice exhibited less damage to the GI tract compared to tumour bearing mice. At the end of the treatment period at day-14, tumour bearing mice had visibly fragile GI tracts that did not have much storage life in the cool room compared to non-tumour bearing mice. Fine dissections had to be carried out carefully during immunohistochemistry experiments due to fragile nature of the GI tract of the tumour bearing mice. The cecum of the mice that received combination treatment of Oxaliplatin + APX3330 and Irinotecan + APX3330, appeared much similar to non-tumour bearing mice. Irinotecan-treated tumour

bearing mice exhibited symptoms of severe diarrhoea compared to Irinotecan-treated non-tumour bearing mice. Combination of APX3330 + Irinotecan seems to mitigate the adverse side-effects due to exhibiting milder symptoms of diarrhoea compared to other groups of tumour bearing mice. Similarly, Oxaliplatin-treated tumour bearing mice showed extreme symptoms of constipation compared to non-tumour bearing mice. With regards to the number of myenteric neurons in the distal colon, Untreated-non tumour bearing mice had the highest number of myenteric neurons compared to Oxaliplatin and Irinotecan-treated non tumour bearing mice and treatments received tumour bearing mice.

APX3330 has completed the phase I clinical trials in oncology and phase IIb in DR/DME as a single chemotherapeutic agent (Kelley et al., 2017, Boyer et al., 2022). It has been progressing on its way to use in several other cancers as a chemotherapeutic treatment. Previous research has found that APX3330, in combination with 5-FU, successfully reduces tumour growth and metastasis (Fishel et al., 2011). Given the severity of enteric neuronal loss associated with Oxaliplatin and Irinotecan treatment in chapters 2 and 3, APX3330 was administered as a single treatment and as a combination therapy with oxaliplatin and Irinotecan in healthy and CRC-induced mice to investigate the neuroprotective and anti-tumour efficacy of the treatment. Several studies conducted in chemotherapy, such as platinum compounds, taxanes, bortezomib, and vinca alkaloids treated in animal models, have found that mitochondrial dysfunction and axonal mitotoxicity contribute to neuropathic symptoms (Podratz et al., 2011, Jin et al., 2008, Zheng et al., 2011, Zheng et al., 2012). Data presented in chapter 3 and findings from previous research advocate the association of oxidative stress-related mitochondrial dysfunction in the progression of enteric neuropathy and the damage to peripheral sensory neurons (Areti et al., 2014). Since Oxaliplatin-induced mitochondrial dysfunction has been associated with enteric neuropathy, several studies suggest the potential of drugs to improve mitochondrial function as a therapeutic approach to prevent chemotherapy-associated GI side-effects (Xiao and Bennett, 2012).

Although this study is the first to investigate the neuroprotective and anticancer efficacy of APX3330 in combination with Oxaliplatin and Irinotecan in healthy and CRC-induced mice, several limitations may impact the clinical relevance of the study. This may include, but is not limited to, 1) the use of older animal models closer to relevant to human age, which has a high risk of getting CRC; 2) expand the study to investigate the changes and the association with the immune system, since it is closely related to disease pathology and chemotherapy side-effects; 3) include a group of mice that underwent a mock surgery to access the implications of an invasive procedure as well as to evaluate the effect on neurons following surgery-associated stress and healing; 4) incorporate experiments that directly measure oxidative stress and DNA damage; 5) include more studies on the expression of proteins in intrinsic and extrinsic apoptotic pathways in western blot experiments; 6) investigate the total protein expression and cleaved/phosphorylated protein expression of the same protein to see activation or inhibition of the protein with the treatment; and 7) use of human studies to validate the clinical relevance of the findings in a preclinical model of CRC

The duration of the candidature did not allow to continue experiments with sham treatment and combination treatment of APX3330 with Oxaliplatin and Irinotecan in healthy mice. Due to unforeseen circumstances of a global pandemic during most of the study period, access to the animal facility to perform live animal experiments, and to the WCHRE laboratory to perform molecular studies were limited. Hence, the number of mice used in each group had to be reduced to meet the deadlines. We considered the complex interactions between chemotherapy-induced gastrointestinal side effects in cancer-free mice, cancer/tumour-affiliated gastrointestinal dysfunction, and chemotherapy-induced GI side-effects. Previous research on human CRC studies has found significant damage to the nerves that supply large intestines during CRC invasion and changes in the neuronal fibre density of both myenteric and submucosal plexus (Godlewski, 2010). Our research had focused on the combined changes in the myenteric plexus neurons and their subpopulations in the distal colon following 14 days of administration of Oxaliplatin, Irinotecan, APX3330, and Sham in both healthy and CRC-induced mice. Future

research needs to be conducted to determine the molecular level interactions and possible regulatory pathways to a better understanding of subcellular interactions of the treatment agents and other proteins. Further, the chemotherapeutic potential of APX3330 is currently under phase II clinical trial to treat several cancers, including pancreatic and colon cancer, with promising results (Jiang et al., 2010). Using APX3330 as a chemotherapeutic agent in combination with either Oxaliplatin or Irinotecan is relatively new, and intensive research should be conducted to bring this novel therapeutic approach from bench to bedside.

The enteric nervous system contains inhibitory and excitatory neurons that can be identified through their expression of nNOS and ChAT in the cytoplasm (Furness, 2012). These excitatory and inhibitory enteric neurons predominately regulate gastrointestinal functions. APX3330 treatment caused enteric neuroprotection, reduced inflammation, and exhibited anti-tumour properties. APX3330 seems to attenuate the inflammation by downregulating several transcription factors and stimulating endonuclease activity to repair damaged DNA (Kelley, 2020, Mijit et al., 2021). In this study, we found that long-term intestinal inflammation following Irinotecan treatment was correlated with significant myenteric neuronal loss in the distal colon, whilst co-administration APX3330 mitigated the inflammation and improved symptoms of diarrhoea that change the colonic and intestinal motility (McQuade et al., 2017). APX3330 treatment prevented Irinotecan-induced damage to the nerve fibres. APX3330 treatment decreased the expression of ChAT-IR neurons and (VACht)-IR fibres resulting in a low proportion of ChAT-IR cells, and (VACht)-IR fibres in the myenteric plexus of the distal colon preventing muscles from increased contractile activity that leads to diarrhoea.

Oxaliplatin treatment caused severe constipation measured by faecal water content that has also been demonstrated in previous studies by delayed gastrointestinal transit, reduction in the total number of colonic contractions, drop in the proportion and frequency of CMMCs caused a reduction in faecal output and

reduced faecal water content (McQuade et al., 2017, McQuade et al., 2016). Oxaliplatin-induced mitochondrial dysfunction causes the release of cytochrome c from the mitochondria into the cell leading the cells to activate caspase 9 and caspase 3, forming mature proteosomes to execute apoptosis via intrinsic pathways (Waseem et al., 2017, Vince et al., 2018) that leads to neuronal damage and loss in the distal colon. Data revealed that Oxaliplatin treatment caused a substantial myenteric neuronal loss and APX3330 showed neuroprotective effects on enteric neurons by expressing the lowest cytochrome c expression. Oxaliplatin treatment was associated with increased expression in the number and proportion of nNOS-IR neurons in the distal colon. APX3330 treated mice were found to have decreased expression of nNOS-IR neurons in the distal colon. Our research has shown for the first time that the neuroprotective effects of APX330 successfully alleviate Oxaliplatin-induced damage that leads to constipation.

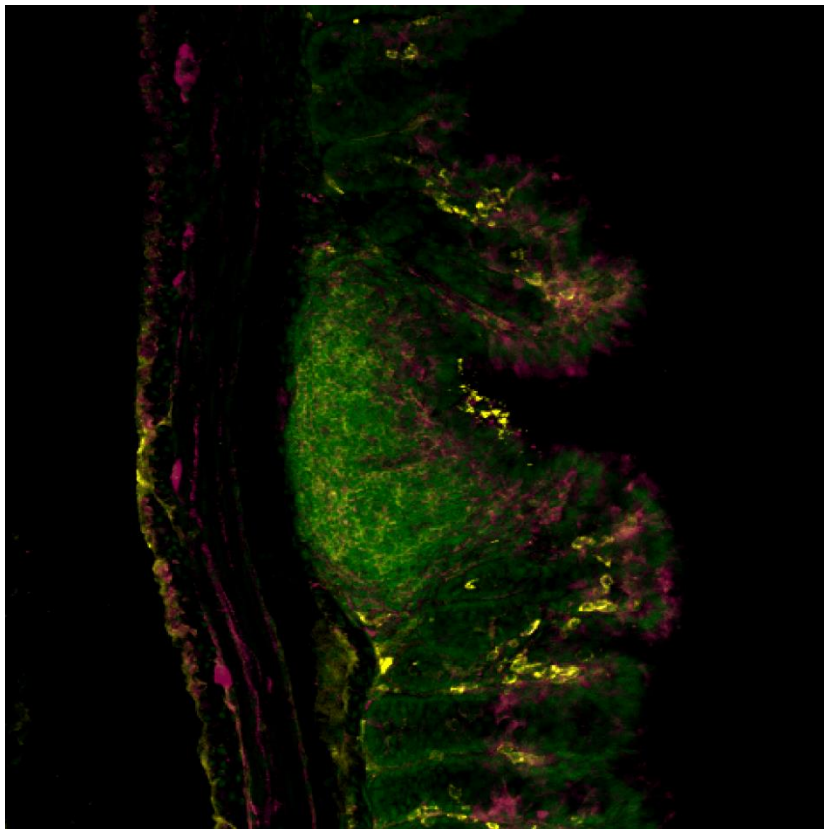
Finally, this thesis has delivered significant evidence to draw a correlation between chemotherapy-induced gastrointestinal dysfunction and enteric neuronal loss in mice; limited studies in humans have been conducted to draw definitive conclusions on chemotherapy-induced enteric neuronal loss. Previous research in human colon samples from chemo-treated patients has demonstrated the changes in electrophysiological properties in myenteric neurons (Carbone et al., 2016) and nuclear translocation of specific proteins from the cytoplasm (Carbone et al., 2016, Stojanovska et al., 2016), suggesting neuronal damage. Nevertheless, the possible regulatory molecular pathways need to be further investigated, along with the extensive analysis of the efficacy, safety, and mechanism of action of APX3330 co-treatment with other chemotherapeutic agents in CRC patients.

Regardless of the recent developments and therapeutic discoveries for the treatment of metastatic CRC, the median overall survival of patients was only improved from 12 months to 24 months over the past decade. Thus, the five-year survival expectancy of patients remains unchanged (Balko and Black., 2009, Bathe et al., 2009, Fletcher, 2009, Meyerhardt and Mayer, 2005). Even though the

discovery of a cure for cancer would be the ultimate achievement, optimization of already existing chemotherapeutic agents that are used in the clinical setting as well as the discovery of effective treatments for chemotherapy-induced side effects provides a sustainable avenue for research to bring about an improved prognostic outcome of CRC. Based on several previous research findings relevant to our research arena, as well as the research findings from our lab group indicate the importance of protecting enteric neurons from chemotherapeutic agents would hold the succession of future research in mitigating chemotherapy-induced gastrointestinal dysfunction (Wang et al., 2007, Pachman et al., 2011, Argyriou et al., 2006, Bardos et al., 2003, Jin et al., 2012, Ta et al., 2013, Melli et al., 2008, Brederson et al., 2012, Piccolo and Kolesar, 2014, Pace et al., 2010). Our research and previous findings show that pharmacologically protecting enteric neurons holds a robust future direction to alleviate chemotherapy-induced enteric neuropathy and gastrointestinal dysfunction.

5

REFERENCES



Cross-sectional preparation of the distal colon of IRI+VEH-treated mouse with CRC labelled with a pan-leukocyte marker anti-CD45 antibody (yellow), neuronal marker anti- β Tubulin III antibody (magenta) and DAPI (green) (Scale bar = 100 μ m)

- Abernethy, A. P., Herndon II, J. E., Wheeler, J. L., Day, J. M., Hood, L., Patwardhan, M., ... & Lyerly, H. K. (2009). Feasibility and acceptability to patients of a longitudinal system for evaluating cancer-related symptoms and quality of life: a pilot study of an e/ Tablet data-collection system in academic oncology. *Journal of Pain and symptom management*, 37(6), 1027-1038.
- Abernethy, A. P., Wheeler, J. L., & Zafar, S. Y. (2009). Detailing of gastrointestinal symptoms in cancer patients with advanced disease: new methodologies, new insights, and a proposed approach. *Current opinion in supportive and palliative care*, 3(1), 41-49.
- Abraham, J. P., Magee, D., Cremolini, C., Antoniotti, C., Halbert, D. D., Xiu, J., ... & Spetzler, D. B. (2021). Clinical validation of a machine-learning–derived signature predictive of outcomes from first-line oxaliplatin-based chemotherapy in advanced colorectal cancer. *Clinical Cancer Research*, 27(4), 1174-1183.
- Abu-Sbeih, H., Mallepally, N., Goldstein, R., Chen, E., Tang, T., Dike, U. K., ... & Wang, Y. (2020). Gastrointestinal toxic effects in patients with cancer receiving platinum-based therapy. *Journal of Cancer*, 11(11), 3144.
- Adelstein, B. A., Macaskill, P., Chan, S. F., Katelaris, P. H., & Irwig, L. (2011). Most bowel cancer symptoms do not indicate colorectal cancer and polyps: a systematic review. *BMC gastroenterology*, 11(1), 1-10.
- Akamatsu, Y., Ohno, T., Hirota, K., Kagoshima, H., Yodoi, J., & Shigesada, K. (1997). Redox regulation of the DNA binding activity in transcription factor PEBP2: the roles of two conserved cysteine residues. *Journal of Biological Chemistry*, 272(23), 14497-14500.
- Akbar, M., Essa, M. M., Daradkeh, G., Abdelmegeed, M. A., Choi, Y., Mahmood, L., & Song, B. J. (2016). Mitochondrial dysfunction and cell death in neurodegenerative diseases through nitroxidative stress. *Brain research*, 1637, 34-55.
- Alameddine, A. K., Conlin, F. T., Binnall, B. J., Alameddine, Y. A., & Alameddine, K. O. (2018). How do cancer cells replenish their fuel supply?. *Cancer Reports*, 1(1), e1003.
- Al-Batran, S. E., Homann, N., Pauligk, C., Goetze, T. O., Meiler, J., Kasper, S., ... & FLOT4-AIO Investigators. (2019). Perioperative chemotherapy with fluorouracil plus leucovorin, oxaliplatin, and docetaxel versus fluorouracil or capecitabine plus cisplatin and epirubicin for locally advanced, resectable gastric or gastro-oesophageal junction adenocarcinoma (FLOT4): a randomised, phase 2/3 trial. *The Lancet*, 393(10184), 1948-1957.
- Alcindor, T., & Beauger, N. (2011). Oxaliplatin: a review in the era of molecularly targeted therapy. *Current oncology (Toronto, Ont.)*, 18(1), 18–25.
- Al-Dasooqi, N., Bowen, J., Bennett, C., Finnie, J., Keefe, D., & Gibson, R. (2017). Cell adhesion molecules are altered during irinotecan-induced mucositis: a qualitative histopathological study. *Supportive Care in Cancer*, 25(2), 391-398.
- Al-Hajeili, M., Marshall, J. L., & Smaglo, B. G. (2016). Neoadjuvant treatment for surgically resectable metastatic colorectal cancer. *Oncology*, 30(1), 10-10.
- Ali, I., A Wani, W., Saleem, K., & Haque, A. (2013). Platinum compounds: a hope for future cancer chemotherapy. *Anti-Cancer Agents in Medicinal Chemistry (Formerly Current Medicinal Chemistry-Anti-Cancer Agents)*, 13(2), 296-306.
- Al-Zwaini, Y. K. H., Al-Mugdadi, S. F. H., & Abbas, W. A. K. (2020). Detection of Novel apyrimidinic Endonuclease 1 (APE1) in a sample of Iraqi cervical cancer patients using Immunohistochemistry Technique. *Research Journal of Pharmacy and Technology*, 13(7), 3193-3198.
- Amado, R. G., Wolf, M., Peeters, M., Van Cutsem, E., Siena, S., Freeman, D. J., ... & Chang, D. D.

- (2008). Wild-type KRAS is required for panitumumab efficacy in patients with metastatic colorectal cancer.
- Ambade, A., & Mandrekar, P. (2012). Oxidative stress and inflammation: essential partners in alcoholic liver disease. *International Journal of hepatology*, 2012.
- Amersi, F., Agustin, M., & Ko, C. Y. (2005). Colorectal cancer: epidemiology, risk factors, and health services. *Clinics in colon and rectal surgery*, 18(03), 133-140.
- André, T., Boni, C., Mounedji-Boudiaf, L., Navarro, M., Tabernero, J., Hickish, T., ... & De Gramont, A. (2004). Oxaliplatin, fluorouracil, and leucovorin as adjuvant treatment for colon cancer. *New England Journal of Medicine*, 350(23), 2343-2351.
- Andreyev, J., Ross, P., Donnellan, C., Lennan, E., Leonard, P., Waters, C., ... & Ferry, D. (2014). Guidance on the management of diarrhoea during cancer chemotherapy. *The Lancet Oncology*, 15(10), e447-e460.
- Angelova, P. R., & Abramov, A. Y. (2016). Functional role of mitochondrial reactive oxygen species in physiology. *Free radical biology and medicine*, 100, 81-85.
- Angelova, P. R., & Abramov, A. Y. (2018). Role of mitochondrial ROS in the brain: from physiology to neurodegeneration. *FEBS letters*, 592(5), 692-702.
- Anthony, L. B., & Chauhan, A. (2018). Diarrhea, constipation, and obstruction in cancer management. In *The MASCC Textbook of Cancer Supportive Care and Survivorship* (pp. 421-436). Springer, Cham.
- Aprile, G., Ongaro, E., Del Re, M., Lutrino, S. E., Bonotto, M., Ferrari, L., ... & Fasola, G. (2015). Angiogenic inhibitors in gastric cancers and gastroesophageal junction carcinomas: A critical insight. *Critical reviews in oncology/hematology*, 95(2), 165-178.
- Aprile, G., Rihawi, K., De Carlo, E., & Sonis, S. T. (2015). Treatment-related gastrointestinal toxicities and advanced colorectal or pancreatic cancer: A critical update. *World journal of gastroenterology*, 21(41), 11793.
- Arbuckle, R. B., Huber, S. L., & Zacker, C. (2000). The consequences of diarrhea occurring during chemotherapy for colorectal cancer: a retrospective study. *The Oncologist*, 5(3), 250-259.
- Ardelean, D. S., Gonska, T., Wires, S., Cutz, E., Griffiths, A., Harvey, E., ... & Benseler, S. M. (2010). Severe ulcerative colitis after rituximab therapy. *Pediatrics*, 126(1), e243-e246.
- Areti, A., Yerra, V. G., Naidu, V. G. M., & Kumar, A. (2014). Oxidative stress and nerve damage: role in chemotherapy-induced peripheral neuropathy. *Redox biology*, 2, 289-295.
- Argyriou, A. A., Bruna, J., Park, S. B., & Cavaletti, G. (2020). Emerging pharmacological strategies for the management of chemotherapy-induced peripheral neurotoxicity (CIPN), based on novel CIPN mechanisms. *Expert review of neurotherapeutics*, 20(10), 1005-1016.
- Argyriou, A. A., Chroni, E., Koutras, A., Iconomou, G., Papapetropoulos, S., Polychronopoulos, P., & Kalofonos, H. P. (2006). Preventing paclitaxel-induced peripheral neuropathy: a phase II trial of vitamin E supplementation. *Journal of Pain and symptom management*, 32(3), 237-244.
- Arifa, R. D., Madeira, M. F., de Paula, T. P., Lima, R. L., Tavares, L. D., Menezes-Garcia, Z., ... & Souza, D. G. (2014). Inflammasome activation is reactive oxygen species-dependent and mediates irinotecan-induced mucositis through IL-1 β and IL-18 in mice. *The American journal of pathology*, 184(7), 2023-2034.
- Athauda, A., Nankivell, M., Langley, R. E., Alderson, D., Allum, W., Grabsch, H. I., ... & Cunningham, D. (2020). Impact of sex and age on chemotherapy efficacy, toxicity and survival in localised oesophagogastric cancer: a pooled analysis of 3265 individual patient data from four large

- randomised trials (OE02, OE05, MAGIC and ST03). *European Journal of Cancer*, 137, 45-56.
- Avallone, A., Piccirillo, M. C., Nasti, G., Rosati, G., Carlomagno, C., Di Gennaro, E., ... & Budillon, A. (2021). Effect of Bevacizumab in Combination With Standard Oxaliplatin-Based Regimens in Patients With Metastatic Colorectal Cancer: A Randomized Clinical Trial. *JAMA network open*, 4(7), e2118475-e2118475.
- Avci, I. A., Altay, B., Cavusoglu, F., Cal, A., Mumcu, N., Eren, D. C., ... & Buberçi, A. (2020). Evaluation of the efficacy of the three-component health care management program HEWCOT in colorectal cancer patients receiving chemotherapy. *Journal of Cancer Education*, 35(2), 274-283.
- Axelrad, J., Kriplani, A., Ozbek, U., Harpaz, N., Colombel, J. F., Itzkowitz, S., ... & Ang, C. (2017). Chemotherapy tolerance and oncologic outcomes in patients with colorectal cancer with and without inflammatory bowel disease. *Clinical colorectal cancer*, 16(3), e205-e210.
- Azizi, E., Carr, A. J., Plitas, G., Cornish, A. E., Konopacki, C., Prabhakaran, S., ... & Pe'er, D. (2018). Single-cell map of diverse immune phenotypes in the breast tumour microenvironment. *Cell*, 174(5), 1293-1308.
- Babu, S. P. S. P., Sishtla, K., Sulaiman, R. S., Park, B., Shetty, T., Shah, F., ... & Corson, T. W. (2018). Ref-1/APE1 inhibition with novel small molecules blocks ocular neovascularization. *bioRxiv*, 296590.
- Bachman, M. A., Miller, V. L., & Weiser, J. N. (2009). Mucosal lipocalin 2 has pro-inflammatory and iron-sequestering effects in response to bacterial enterobactin. *PLoS pathogens*, 5(10), e1000622.
- Badgett, T. C., Laetsch, T., Gore, L., & Macy, M. (2017). A Phase I/Ib Study of Eribulin in Combination with Oral Irinotecan for Adolescent and Young Adult Patients with Relapsed or Refractory Solid Tumors.
- Bae, E. H., Greenwald, M. K., & Schwartz, A. G. (2021). Chemotherapy-Induced Peripheral Neuropathy: Mechanisms and Therapeutic Avenues. *Neurotherapeutics*, 1-13.
- Bai, P., Cantó, C., Oudart, H., Brunyánszki, A., Cen, Y., Thomas, C., ... & Auwerx, J. (2011). PARP-1 inhibition increases mitochondrial metabolism through SIRT1 activation. *Cell metabolism*, 13(4), 461-468.
- Bailly, C. (2019). Irinotecan: 25 years of cancer treatment. *Pharmacological research*, 148, 104398.
- Balko, J. M., & Black, E. P. (2009). A gene expression predictor of response to EGFR-targeted therapy stratifies progression-free survival to cetuximab in KRAS wild-type metastatic colorectal cancer. *BMC Cancer*, 9(1), 1-10.
- Banerjee, A., Pathak, S., Subramaniam, V. D., Dharanivasan, G., Murugesan, R., & Verma, R. S. (2017). Strategies for targeted drug delivery in treatment of colon cancer: current trends and future perspectives. *Drug discovery today*, 22(8), 1224-1232.
- Bano, N. U. S. R. A. T. (2013). Sinusoidal dilatations and splenomegaly as feature specifications of drug-induced thrombocytopenia in oxaliplatin treated Wistar rats. *Asian Journal of Pharmaceutical and Clinical Research*, 6(SUPPL 2), 259-61.
- Bapat, A., Fishel, M. L., & Kelley, M. R. (2009). Going ape as an approach to cancer therapeutics. *Antioxidants & redox signaling*, 11(3), 651-667.
- Bapte, P. S., Pansambal, S. S., & Borgave, S. (2022). Biosynthesized Selenium Nanoparticles: An Excellent Bait for Antioxidant Therapy. *Journal of Nanostructures*, 12(1), 178-193.

- Barchiesi, A., Bazzani, V., Tolotto, V., Elancheliyan, P., Wasilewski, M., Chacinska, A., & Vascotto, C. (2020). Mitochondrial Oxidative Stress Induces Rapid Intermembrane Space/Matrix Translocation of Apurinic/Apyrimidinic Endonuclease 1 Protein through TIM23 Complex. *Journal of Molecular Biology*, 432(24), 166713.
- Barchiesi, A., Wasilewski, M., Chacinska, A., Tell, G., & Vascotto, C. (2015). Mitochondrial translocation of APE1 relies on the MIA pathway. *Nucleic acids research*, 43(11), 5451-5464.
- Bardos, G., Moricz, K., Jaszlits, L., Rabloczky, G., Tory, K., Rácz, I., ... & Literáti-Nagy, P. (2003). BGP-15, a hydroximic acid derivative, protects against cisplatin-or taxol-induced peripheral neuropathy in rats. *Toxicology and applied pharmacology*, 190(1), 9-16.
- Barnieh, F. M., Loadman, P. M., & Falconer, R. A. (2021). Progress towards a clinically-successful ATR inhibitor for cancer therapy. *Current Research in Pharmacology and Drug Discovery*, 2, 100017.
- Barzilai, A., Biton, S., & Shiloh, Y. (2008). The role of the DNA damage response in neuronal development, organization and maintenance. *DNA repair*, 7(7), 1010-1027.
- Bassotti, G., & Villanacci, V. (2006). Slow transit constipation: a functional disorder becomes an enteric neuropathy. *World journal of gastroenterology: WJG*, 12(29), 4609.
- Bassotti, G., & Villanacci, V. (2011). Can "functional" constipation be considered as a form of enteric neuro-ciliopathy?. *Glia*, 59(3), 345-350.
- Bassotti, G., Villanacci, V., Nascimbeni, R., Cadei, M., Fisogni, S., Antonelli, E., ... & Salerni, B. (2009). Enteric neuroglial apoptosis in inflammatory bowel diseases. *Journal of Crohn's and Colitis*, 3(4), 264-270.
- Bassotti, G., Villanacci, V., Nascimbeni, R., Cadei, M., Manenti, S., Sabatino, G., ... & Salerni, B. (2011). Colonic mast cells in controls and slow transit constipation patients. *Alimentary pharmacology & therapeutics*, 34(1), 92-99.
- Bateman, E., Weaver, E., Klein, G., Wignall, A., Wozniak, B., Plews, E., ... & Keefe, D. (2016). Serum-derived bovine immunoglobulin/protein isolate in the alleviation of chemotherapy-induced mucositis. *Supportive Care in Cancer*, 24(1), 377-385.
- Bathe, O. F., Ernst, S., Sutherland, F. R., Dixon, E., Butts, C., Bigam, D., ... & Dowden, S. (2009). A phase II experience with neoadjuvant irinotecan (CPT-11), 5-fluorouracil (5-FU) and leucovorin (LV) for colorectal liver metastases. *BMC Cancer*, 9(1), 1-10.
- Belsky, J. A., Batra, S., Stanek, J. R., & O'Brien, S. H. (2021). Secondary impacts of constipation in acute lymphoblastic leukemia in US children's hospitals. *Pediatric blood & cancer*, 68(11), e29336.
- Belsky, J. A., Wolf, K., & Setty, B. A. (2020). A Case of Resolved Vincristine-Induced Constipation Following Osteopathic Medicine in a Patient With Infantile Fibrosarcoma. *Journal of Osteopathic Medicine*, 120(10), 691-695.
- Benson III, A. B., Ajani, J. A., Catalano, R. B., Engelking, C., Kornblau, S. M., Martenson Jr, J. A., ... & Wadler, S. (2004). Recommended guidelines for the treatment of cancer treatment-induced diarrhea. *Journal of Clinical Oncology*, 22(14), 2918-2926.
- Bernardini, N., Segnani, C., Ippolito, C., De Giorgio, R., Colucci, R., Faussone-Pellegrini, M. S., ... & Dolfi, A. (2012). Immunohistochemical analysis of myenteric ganglia and interstitial cells of Cajal in ulcerative colitis. *Journal of cellular and molecular medicine*, 16(2), 318-327.
- Bertaut, A., Toucheffeu, Y., Blanc, J., Bouché, O., François, E., Conroy, T., ... & Bennouna, J. (2021). Health-Related Quality of Life Analysis in Metastatic Colorectal Cancer Patients Treated by

Second-Line Chemotherapy, Associated With Either Cetuximab or Bevacizumab: The PRODIGE 18 Randomized Phase II Study. *Clinical Colorectal Cancer*.

- Bhakat, K. K., Izumi, T., Yang, S. H., Hazra, T. K., & Mitra, S. (2003). Role of acetylated human AP-endonuclease (APE1/Ref-1) in the regulation of the parathyroid hormone gene. *The EMBO journal*, 22(23), 6299-6309.
- Bhakat, K. K., Mantha, A. K., & Mitra, S. (2009). Transcriptional regulatory functions of mammalian AP-endonuclease (APE1/Ref-1), an essential multifunctional protein. *Antioxidants & redox signaling*, 11(3), 621-637.
- Bhat, M. A., Varshneya, C., Bhardwaj, P., Patil, R. D., & Panda, A. K. (2021). In vitro cytotoxicity, apoptosis, effects on cell cycle kinetics and schedule-dependent effects induced by paclitaxel on c6 and Cho-k1 cell lines. *Indian Journal of Animal Research*, 55(3), 340-346.
- Biswas, A., Khanna, S., Roy, S., Pan, X., Sen, C. K., & Gordillo, G. M. (2015). Endothelial cell tumour growth is Ape/ref-1 dependent. *American Journal of Physiology-Cell Physiology*, 309(5), C296-C307.
- Biswas, S. K. (2016). Does the interdependence between oxidative stress and inflammation explain the antioxidant paradox?. *Oxidative medicine and cellular longevity*, 2016.
- Biswas, S. K., Peixoto, E. B., Souza, D. S., & De Faria, J. B. L. (2008). Hypertension increases pro-oxidant generation and decreases antioxidant defence in the kidney in early diabetes. *American journal of nephrology*, 28(1), 133-142.
- Bleiberg, H. (1998). Oxaliplatin (L-OHP): a new reality in colorectal cancer. *British journal of cancer*, 77(4), 1-3.
- Bleiberg, H., & Cvitkovic, E. (1996). Characterisation and clinical management of CPT-11 (irinotecan)-induced adverse events: the European perspective. *European journal of cancer*, 32, S18-S23.
- Bobola, M. S., Blank, A., Berger, M. S., Stevens, B. A., & Silber, J. R. (2001). Apurinic/aprimidinic endonuclease activity is elevated in human adult gliomas. *Clinical cancer research*, 7(11), 3510-3518.
- Böckelman, C., Engelmann, B. E., Kaprio, T., Hansen, T. F., & Glimelius, B. (2015). Risk of recurrence in patients with colon cancer stage II and III: a systematic review and meta-analysis of recent literature. *Acta oncologica*, 54(1), 5-16.
- Boehm, A. L., Sen, M., Seethala, R., Gooding, W. E., Freilino, M., Wong, S. M. Y., ... & Grandis, J. R. (2008). Combined targeting of epidermal growth factor receptor, signal transducer and activator of transcription-3, and Bcl-XL enhances antitumor effects in squamous cell carcinoma of the head and neck. *Molecular Pharmacology*, 73(6), 1632-1642.
- Boeing, T., Gois, M. B., de Souza, P., Somensi, L. B., & da Silva, L. M. (2021). Irinotecan-induced intestinal mucositis in mice: a histopathological study. *Cancer Chemotherapy and Pharmacology*, 87(3), 327-336.
- Böhm, B., Schwenk, W., Hucke, H. P., & Stock, W. (1993). Does methodic long-term follow-up affect survival after curative resection of colorectal carcinoma?. *Diseases of the colon & rectum*, 36(3), 280-286.
- Bokhari, B., & Sharma, S. (2019). Stress marks on the genome: Use or lose?. *International journal of molecular sciences*, 20(2), 364.
- Bombardi, C., Rambaldi, A. M., Galiazzo, G., Giancola, F., Graic, J. M., Salamanca, G., ... & Chiocchetti, R. (2021). Nitrergic and Substance P Immunoreactive Neurons in the Enteric Nervous System of the Bottlenose Dolphin (*Tursiops truncatus*) Intestine. *Animals*, 11(4), 1057.

- Bornstein, J. C. (2006). Intrinsic sensory neurons of mouse gut—toward a detailed knowledge of enteric neural circuitry across species. Focus on “characterization of myenteric sensory neurons in the mouse small intestine”. *Journal of Neurophysiology*, 96(3), 973-974.
- Bornstein, J. C., & Foong, J. P. (2018). Enteric neural regulation of mucosal secretion. In *Physiology of the gastrointestinal tract* (pp. 429-451). Academic Press.
- Bornstein, J. C., Costa, M., & Grider, J. R. (2004). Enteric motor and interneuronal circuits controlling motility. *Neurogastroenterology & Motility*, 16, 34-38.
- Bornstein, J. C., Furness, J. B., Kunze, W. A. A., & Bertrand, P. P. (2002). Enteric reflexes that influence motility. In *Innervation of the gastrointestinal tract* (pp. 21-76). CRC Press.
- Bossi, P., Delrio, P., Mascheroni, A., & Zanetti, M. (2021). The spectrum of malnutrition/cachexia/sarcopenia in oncology according to different cancer types and settings: A narrative review. *Nutrients*, 13(6), 1980.
- Bouchenaki, H., Danigo, A., Sturtz, F., Hajj, R., Magy, L., & Demiot, C. (2021). An overview of ongoing clinical trials assessing pharmacological therapeutic strategies to manage chemotherapy-induced peripheral neuropathy, based on preclinical studies in rodent models. *Fundamental & Clinical Pharmacology*, 35(3), 506-523.
- Bowen, J. M., Gibson, R. J., Stringer, A. M., Chan, T. W., Prabowo, A. S., Cummins, A. G., & Keefe, D. M. (2007). Role of p53 in irinotecan-induced intestinal cell death and mucosal damage. *Anti-cancer drugs*, 18(2), 197-210.
- Boyer, D. S., Brigell, M., Kolli, A., Rahmani, K., Lazar, A., Sooch, M., ... & Kelley, M. R. (2022). The safety of APX3330, an oral drug candidate for the treatment of diabetic eye disease, in the ongoing masked 24-week ZETA-1 Phase 2 clinical trial. *Investigative Ophthalmology & Visual Science*, 63(7), 675-F0129.
- Boyer, L., Ghoreishi, M., Templeman, V., Vallance, B. A., Buchan, A. M., Jevon, G., & Jacobson, K. (2005). Myenteric plexus injury and apoptosis in experimental colitis. *Autonomic Neuroscience*, 117(1), 41-53.
- Boyle, P., & Langman, M. J. (2000). ABC of colorectal cancer: Epidemiology. *BMJ*, 321(Suppl S6).
- Bradley, C. J., Yabroff, K. R., Warren, J. L., Zeruto, C., Chawla, N., & Lamont, E. B. (2016). Trends in the treatment of metastatic colon and rectal cancer in elderly patients. *Medical care*, 54(5), 490-497.
- Branca, J. J. V., Carrino, D., Gulisano, M., Ghelardini, C., Di Cesare Mannelli, L., & Pacini, A. (2021). Oxaliplatin-Induced Neuropathy: Genetic and Epigenetic Profile to Better Understand How to Ameliorate This Side Effect. *Frontiers in Molecular Biosciences*, 8, 166.
- Breen, D. M., Kim, H., Bennett, D., Calle, R. A., Collins, S., Esquejo, R. M., ... & Birnbaum, M. J. (2020). GDF-15 neutralization alleviates platinum-based chemotherapy-induced emesis, anorexia, and weight loss in mice and nonhuman primates. *Cell Metabolism*, 32(6), 938-950.
- Brewer, J. R., Morrison, G., Dolan, M. E., & Fleming, G. F. (2016). Chemotherapy-induced peripheral neuropathy: Current status and progress. *Gynecologic oncology*, 140(1), 176-183.
- Bristow, R. G., & Hill, R. P. (2008). Hypoxia and metabolism: Hypoxia, DNA repair and genetic instability. *Nature Reviews Cancer*, 8(3).
- Broderson, J. D., Joshi, S. K., Browman, K. E., Mikasa, J., Zhong, C., Gauvin, D., ... & Giranda, V. L. (2012). PARP inhibitors attenuate chemotherapy-induced painful neuropathy. *Journal of the Peripheral Nervous System*, 17(3), 324-330.

- Bromberg, J. F., Wrzeszczynska, M. H., Devgan, G., Zhao, Y., Pestell, R. G., Albanese, C., & Darnell Jr, J. E. (1999). Stat3 as an oncogene. *Cell*, *98*(3), 295-303.
- Brooks, P. J. (2002). DNA repair in neural cells: basic science and clinical implications. *Mutation Research/Fundamental and Molecular Mechanisms of Mutagenesis*, *509*(1-2), 93-108.
- Browning, K. N., & Travagli, R. A. (2014). Central nervous system control of gastrointestinal motility and secretion and modulation of gastrointestinal functions. *Comprehensive Physiology*, *4*(4), 1339.
- Bukowski, K., Kciuk, M., & Kontek, R. (2020). Mechanisms of multidrug resistance in cancer chemotherapy. *International journal of molecular sciences*, *21*(9), 3233.
- Burkholder, B., Huang, R. Y., Burgess, R., Luo, S., Jones, V. S., Zhang, W., ... & Huang, R. P. (2014). Tumour-induced perturbations of cytokines and immune cell networks. *Biochimica et Biophysica Acta (BBA)-Reviews on Cancer*, *1845*(2), 182-201.
- Cachofeiro, V., Goicochea, M., De Vinuesa, S. G., Oubiña, P., Lahera, V., & Luño, J. (2008). Oxidative stress and inflammation, a link between chronic kidney disease and cardiovascular disease: new strategies to prevent cardiovascular risk in chronic kidney disease. *Kidney International*, *74*, S4-S9.
- Camilleri, M. (2004). Chronic diarrhea: a review on pathophysiology and management for the clinical gastroenterologist. *Clinical Gastroenterology and Hepatology*, *2*(3), 198-206.
- Campalans, A., Martin, S., Nakabeppu, Y., O'connor, T. R., Boiteux, S., & Radicella, J. P. (2005). XRCC1 interactions with multiple DNA glycosylases: a model for its recruitment to base excision repair. *DNA repair*, *4*(7), 826-835.
- Campbell, J. M., Stephenson, M. D., Bateman, E., Peters, M. D. J., Keefe, D. M., & Bowen, J. M. (2017). Irinotecan-induced toxicity pharmacogenetics: an umbrella review of systematic reviews and meta-analyses. *The pharmacogenomics journal*, *17*(1), 21-28.
- Cannito, S., Novo, E., Compagnone, A., Valfrè di Bonzo, L., Busletta, C., Zamara, E., ... & Parola, M. (2008). Redox mechanisms switch on hypoxia-dependent epithelial-mesenchymal transition in cancer cells. *Carcinogenesis*, *29*(12), 2267-2278.
- Cappell, M. S. (2005). From colonic polyps to colon cancer: pathophysiology, clinical presentation, and diagnosis. *Clinics in laboratory medicine*, *25*(1), 135-177.
- Cappell, M. S. (2005). The pathophysiology, clinical presentation, and diagnosis of colon cancer and adenomatous polyps. *Medical Clinics*, *89*(1), 1-42.
- Carbine, N. E., Lostumbo, L., Wallace, J., & Ko, H. (2018). Risk-reducing mastectomy for the prevention of primary breast cancer. *Cochrane Database of Systematic Reviews*, (4).
- Carbone, S. E., Jovanovska, V., Brookes, S. J. H., & Nurgali, K. (2016). Electrophysiological and morphological changes in colonic myenteric neurons from chemotherapy-treated patients: a pilot study. *Neurogastroenterology & Motility*, *28*(7), 975-984.
- Carelle, N., Piotto, E., Bellanger, A., Germanaud, J., Thuillier, A., & Khayat, D. (2002). Changing patient perceptions of the side effects of cancer chemotherapy. *Cancer*, *95*(1), 155-163.
- Carla, D. I. (2001). Prognostic significance of Ape1/ref-1 subcellular localization in non-small cell lung carcinomas. *Anticancer Research*, *21*, 4041-4050.
- cARLA, D. I. (2001). Prognostic significance of Ape1/ref-1 subcellular localization in non-small cell lung carcinomas. *Anticancer research*, *21*, 4041-4050.
- Carlsen, L., Schorl, C., Huntington, K., Hernandez-Borrero, L., Jhaveri, A., Zhang, S., ... & El-Deiry, W. S. (2021). Pan-drug and drug-specific mechanisms of 5-FU, irinotecan (CPT-11),

oxaliplatin, and cisplatin identified by comparison of transcriptomic and cytokine responses of colorectal cancer cells. *Oncotarget*, 12(20), 2006.

- Casadaban, L., Rauscher, G., Aklilu, M., Villenes, D., Freels, S., & Maker, A. V. (2016). Adjuvant chemotherapy is associated with improved survival in patients with stage II colon cancer. *Cancer*, 122(21), 3277-3287.
- Cascinu, S., Rosati, G., Nasti, G., Lonardi, S., Zaniboni, A., Marchetti, P., ... & Cozzi, L. (2017). Treatment sequence with either irinotecan/cetuximab followed by FOLFOX-4 or the reverse strategy in metastatic colorectal cancer patients progressing after first-line FOLFIRI/bevacizumab: An Italian Group for the Study of Gastrointestinal Cancer phase III, randomised trial comparing two sequences of therapy in colorectal metastatic patients. *European Journal of Cancer*, 83, 106-115.
- Cassidy, J., & Misset, J. L. (2002, October). Oxaliplatin-related side effects: characteristics and management. In *Seminars in oncology* (Vol. 29, No. 5 Suppl 15, pp. 11-20).
- Cassidy, J., Clarke, S., Díaz-Rubio, E., Scheithauer, W., Figer, A., Wong, R., ... & Saltz, L. (2008). Randomized phase III study of capecitabine plus oxaliplatin compared with fluorouracil/folinic acid plus oxaliplatin as first-line therapy for metastatic colorectal cancer. *Journal of clinical oncology*, 26(12), 2006-2012.
- Cassidy, J., Tabernero, J., Twelves, C., Brunet, R., Butts, C., Conroy, T., ... & Díaz-Rubio, E. (2004). XELOX (capecitabine plus oxaliplatin): active first-line therapy for patients with metastatic colorectal cancer. *Journal of Clinical Oncology*, 22(11), 2084-2091.
- Cassidy, R. J., Liu, Y., Patel, K., Zhong, J., Steuer, C. E., Kooby, D. A., ... & Landry, J. C. (2017). Can we eliminate neoadjuvant chemoradiotherapy in favor of neoadjuvant multiagent chemotherapy for select stage II/III rectal adenocarcinomas: Analysis of the National Cancer Data base. *Cancer*, 123(5), 783-793.
- Caston, R. A., Gampala, S., Armstrong, L., Messmann, R. A., Fishel, M. L., & Kelley, M. R. (2021). The multifunctional APE1 DNA repair–redox signalling protein as a drug target in human disease. *Drug Discovery Today*, 26(1), 218-228.
- Caston, R. A., Gampala, S., Armstrong, L., Messmann, R. A., Fishel, M. L., & Kelley, M. R. (2021). The multifunctional APE1 DNA repair–redox signaling protein as a drug target in human disease. *Drug discovery today*, 26(1), 218-228.
- Caston, R. A., Shah, F., Starcher, C. L., Wireman, R., Babb, O., Grimard, M., ... & Fishel, M. L. (2021). Combined inhibition of Ref-1 and STAT3 leads to synergistic tumour inhibition in multiple cancers using 3D and in vivo tumour co-culture models. *Journal of Cellular and Molecular Medicine*, 25(2), 784-800.
- Cavaletti, G., & Marmiroli, P. (2020). Management of oxaliplatin-induced peripheral sensory neuropathy. *Cancers*, 12(6), 1370.
- Center, M. M., Jemal, A., Smith, R. A., & Ward, E. (2009). Worldwide variations in colorectal cancer. *CA: a cancer journal for clinicians*, 59(6), 366-378.
- Cercek, A., Goodman, K. A., Hajj, C., Weisberger, E., Segal, N. H., Reidy-Lagunes, D. L., ... & Saltz, L. B. (2014). Neoadjuvant chemotherapy first, followed by chemoradiation and then surgery, in the management of locally advanced rectal cancer. *Journal of the National Comprehensive Cancer Network*, 12(4), 513-519.
- Cervi, A. L., Lukewich, M. K., & Lomax, A. E. (2014). Neural regulation of gastrointestinal inflammation: role of the sympathetic nervous system. *Autonomic Neuroscience*, 182, 83-88.
- Chakravarti, A., Delaney, M. A., Noll, E., Black, P. M., Loeffler, J. S., Muzikansky, A., & Dyson, N.

- J. (2001). Prognostic and pathologic significance of quantitative protein expression profiling in human gliomas. *Clinical cancer research*, 7(8), 2387-2395.
- Chami, B., Martin, N. J., Dennis, J. M., & Witting, P. K. (2018). Myeloperoxidase in the inflamed colon: A novel target for treating inflammatory bowel disease. *Archives of biochemistry and biophysics*, 645, 61-71.
- Chandrasekharan, B., Anitha, M., Blatt, R., Shahnavaz, N., Kooby, D., Staley, C., ... & Srinivasan, S. (2011). Colonic motor dysfunction in human diabetes is associated with enteric neuronal loss and increased oxidative stress. *Neurogastroenterology & Motility*, 23(2), 131-e26.
- Chaney, S. G., Campbell, S. L., Temple, B., Bassett, E., Wu, Y., & Faldu, M. (2004). Protein interactions with platinum–DNA adducts: from structure to function. *Journal of inorganic biochemistry*, 98(10), 1551-1559.
- Chassaing, B., Srinivasan, G., Delgado, M. A., Young, A. N., Gewirtz, A. T., & Vijay-Kumar, M. (2012). Fecal lipocalin 2, is a sensitive and broadly dynamic non-invasive biomarker for intestinal inflammation.
- Chattopadhyay, R., Wiederhold, L., Szczesny, B., Boldogh, I., Hazra, T. K., Izumi, T., & Mitra, S. (2006). Identification and characterization of mitochondrial abasic (AP)-endonuclease in mammalian cells. *Nucleic Acids Research*, 34(7), 2067-2076.
- Chen, B., Guan, D., Cui, Z. J., Wang, X., & Shen, X. (2010). Thioredoxin 1 downregulates MCP-1 secretion and expression in human endothelial cells by suppressing nuclear translocation of activator protein 1 and redox factor-1. *American Journal of Physiology-Cell Physiology*, 298(5), C1170-C1179.
- Chen, C., Zhao, S., Karnad, A., & Freeman, J. W. (2018). The biology and role of CD44 in cancer progression: therapeutic implications. *Journal of hematology & oncology*, 11(1), 1-23.
- Chen, D. S., & Olkowski, Z. L. (1994). *Biological responses of human apurinic endonuclease to radiation-induced DNA damage* (No. CONF-9307221-). New York Academy of Sciences, New York, NY (United States).
- Chen, H., Li, Y., Long, Y., Tang, E., Wang, R., Huang, K., ... & Chen, G. (2017). Increased p16 and p53 protein expression predicts poor prognosis in mucosal melanoma. *Oncotarget*, 8(32), 53226.
- Chen, J., Cheuk, I. W., Shin, V. Y., & Kwong, A. (2019). Acetylcholine receptors: Key players in cancer development. *Surgical oncology*, 31, 46-53.
- Chen, L., Deng, H., Cui, H., Fang, J., Zuo, Z., Deng, J., ... & Zhao, L. (2018). Inflammatory responses and inflammation-associated diseases in organs. *Oncotarget*, 9(6), 7204.
- Chen, W., Lian, W., Yuan, Y., & Li, M. (2019). The synergistic effects of oxaliplatin and piperlongumine on colorectal cancer are mediated by oxidative stress. *Cell death & disease*, 10(8), 1-12.
- Cheng, K. W., Tseng, C. H., Tzeng, C. C., Leu, Y. L., Cheng, T. C., Wang, J. Y., ... & Cheng, T. L. (2019). Pharmacological inhibition of bacterial β -glucuronidase prevents irinotecan-induced diarrhea without impairing its antitumor efficacy in vivo. *Pharmacological Research*, 139, 41-49.
- Chiang, S. C., Meagher, M., Kassouf, N., Hafezparast, M., McKinnon, P. J., Haywood, R., & El-Khamisy, S. F. (2017). Mitochondrial protein-linked DNA breaks perturb mitochondrial gene transcription and trigger free radical–induced DNA damage. *Science advances*, 3(4), e1602506.
- Chibaudel, B., Tournigand, C., André, T., & de Gramont, A. (2012). Therapeutic strategy in

- unresectable metastatic colorectal cancer. *Therapeutic advances in medical oncology*, 4(2), 75-89.
- Choi, S., Shin, J. H., Lee, Y. R., Joo, H. K., Song, K. H., Na, Y. G., ... & Jeon, B. H. (2016). Urinary APE1/Ref-1: a potential bladder cancer biomarker. *Disease markers*, 2016.
- Choi, Y. D., Jung, J. Y., Baek, M., Khan, S., Song, P. I., Ryu, S., ... & Kim, M. (2020). APE1 promotes pancreatic cancer proliferation through GFR α 1/Src/ERK axis-cascade signaling in response to GDNF. *International Journal of Molecular Sciences*, 21(10), 3586.
- Chou, K. M., & Cheng, Y. C. (2003). The exonuclease activity of human apurinic/aprimidinic endonuclease (APE1): biochemical properties and inhibition by the natural dinucleotide Gp4G. *Journal of Biological Chemistry*, 278(20), 18289-18296.
- Chou, K. M., Kukhanova, M., & Cheng, Y. C. (2000). A novel action of human apurinic/aprimidinic endonuclease: excision of L-configuration deoxyribonucleoside analogs from the 3' termini of DNA. *Journal of Biological Chemistry*, 275(40), 31009-31015.
- Chung, U. I., Igarashi, T., Nishihara, T., Iwanari, H., Iwamatsu, A., Suwa, A., ... & Okazaki, T. (1996). The Interaction between Ku Antigen and REF1 Protein Mediates Negative Gene Regulation by Extracellular Calcium (*). *Journal of Biological Chemistry*, 271(15), 8593-8598.
- Church, J. M. (2005). Colon cancer screening update and management of the malignant polyp. *Clinics in colon and rectal surgery*, 18(03), 141-149.
- Cinausero, M., Aprile, G., Ermacora, P., Basile, D., Vitale, M. G., Fanotto, V., ... & Sonis, S. T. (2017). New frontiers in the pathobiology and treatment of cancer regimen-related mucosal injury. *Frontiers in pharmacology*, 8, 354.
- Codrich, M., Comelli, M., Malfatti, M. C., Mio, C., Ayyildiz, D., Zhang, C., ... & Tell, G. (2019). Inhibition of APE1-endonuclease activity affects cell metabolism in colon cancer cells via a p53-dependent pathway. *DNA repair*, 82, 102675.
- Codrich, M., Comelli, M., Malfatti, M. C., Mio, C., Ayyildiz, D., Zhang, C., ... & Tell, G. (2019). Inhibition of APE1-endonuclease activity affects cell metabolism in colon cancer cells via a p53-dependent pathway. *DNA repair*, 82, 102675.
- Cole, K. A., Pal, S., Kudgus, R. A., Ijaz, H., Liu, X., Minard, C. G., ... & Weigel, B. J. (2020). Phase I clinical trial of the Wee1 inhibitor adavosertib (AZD1775) with irinotecan in children with relapsed solid tumors: a COG phase I consortium report (ADVL1312). *Clinical Cancer Research*, 26(6), 1213-1219.
- Colucci, G., Gebbia, V., Paoletti, G., Giuliani, F., Caruso, M., Gebbia, N., ... & Maiello, E. (2005). Phase III randomized trial of FOLFIRI versus FOLFOX4 in the treatment of advanced colorectal cancer: a multicenter study of the Gruppo Oncologico Dell'Italia Meridionale. *Journal of Clinical Oncology*, 23(22), 4866-4875.
- Connolly, M., & Larkin, P. (2012). Managing constipation: a focus on care and treatment in the palliative setting. *British journal of community nursing*, 17(2), 60-67.
- Conti, J. A., Kemeny, N. E., Saltz, L. B., Huang, Y., Tong, W. P., Chou, T. C., ... & Gonzalez, C. (1996). Irinotecan is an active agent in untreated patients with metastatic colorectal cancer. *Journal of clinical oncology*, 14(3), 709-715.
- Cooke, H. J. (2000). Neurotransmitters in neuronal reflexes regulating intestinal secretion. *Annals of the New York Academy of Sciences*, 915(1), 77-80.
- Cortejoso, L., García, M. I., García-Alfonso, P., González-Haba, E., Escolar, F., Sanjurjo, M., & López-Fernández, L. A. (2013). Differential toxicity biomarkers for irinotecan-and oxaliplatin-containing chemotherapy in colorectal cancer. *Cancer chemotherapy and pharmacology*, 71(6), 1463-1472.

- Cortesini, C., Cianchi, F., Infantino, A., & Lise, M. (1995). Nitric oxide synthase and VIP distribution in the enteric nervous system in idiopathic chronic constipation. *Digestive diseases and sciences*, 40(11), 2450-2455.
- Costa, L. J., Micallef, I. N., Inwards, D. J., Johnston, P. B., Porrata, L. F., Litzow, M. R., & Ansell, S. M. (2008). Effect of the dose per body weight of conditioning chemotherapy on the severity of mucositis and risk of relapse after autologous haematopoietic stem cell transplantation in relapsed diffuse large B cell lymphoma. *British journal of haematology*, 143(2), 268-273.
- Costa, M., & Brookes, S. H. (2008). The architecture of enteric neural circuits involved in intestinal motility. *Eur Rev Med Pharmacol Sci*, 12(Suppl 1), 3-19.
- Cottone, L., Capobianco, A., Gualteroni, C., Perrotta, C., Bianchi, M. E., Rovere-Querini, P., & Manfredi, A. A. (2015). 5-Fluorouracil causes leukocytes attraction in the peritoneal cavity by activating autophagy and HMGB1 release in colon carcinoma cells. *International journal of cancer*, 136(6), 1381-1389.
- Cremolini, C., Antoniotti, C., Rossini, D., Lonardi, S., Loupakis, F., Pietrantonio, F., ... & Banzi, M. (2020). Upfront FOLFOXIRI plus bevacizumab and reintroduction after progression versus mFOLFOX6 plus bevacizumab followed by FOLFIRI plus bevacizumab in the treatment of patients with metastatic colorectal cancer (TRIBE2): a multicentre, open-label, phase 3, randomised, controlled trial. *The Lancet Oncology*, 21(4), 497-507.
- Cruz-Bermúdez, A., Laza-Briviesca, R., Vicente-Blanco, R. J., García-Grande, A., Coronado, M. J., Laine-Menéndez, S., ... & Provencio, M. (2019). Cisplatin resistance involves a metabolic reprogramming through ROS and PGC-1 α in NSCLC which can be overcome by OXPPOS inhibition. *Free Radical Biology and Medicine*, 135, 167-181.
- Cunningham, D., Pyrhönen, S., James, R. D., Punt, C. J., Hickish, T. F., Heikkilä, R., ... & Herait, P. (1998). A randomised trial of irinotecan plus supportive care versus supportive care alone after fluorouracil failure for patients with metastatic colorectal cancer. *The Lancet*, 352(9138), 1413-1418.
- Curtis, C. D., Thorngren, D. L., Ziegler, Y. S., Sarkeshik, A., Yates, J. R., & Nardulli, A. M. (2009). Apurinic/aprimidinic endonuclease 1 alters estrogen receptor activity and estrogen-responsive gene expression. *Molecular Endocrinology*, 23(9), 1346-1359.
- Dai, J., Chen, Y., Gong, Y., Wei, J., Cui, X., Yu, H., ... & Chen, J. (2019). The efficacy and safety of irinotecan±bevacizumab compared with oxaliplatin±bevacizumab for metastatic colorectal cancer: A meta-analysis. *Medicine*, 98(39).
- Darnell, J. E., Kerr, I. M., & Stark, G. R. (1994). Jak-STAT pathways and transcriptional activation in response to IFNs and other extracellular signalling proteins. *Science*, 264(5164), 1415-1421.
- Dasari, S., & Tchounwou, P. B. (2014). Cisplatin in cancer therapy: molecular mechanisms of action. *European journal of pharmacology*, 740, 364-378.
- Davies, M. J., & Hawkins, C. L. (2020). The role of myeloperoxidase in biomolecule modification, chronic inflammation, and disease. *Antioxidants & Redox Signaling*, 32(13), 957-981.
- de Alencar, N. M. N., da Silveira Bitencourt, F., de Figueiredo, I. S. T., Luz, P. B., Lima-Júnior, R. C. P., Aragão, K. S., ... & Ramos, M. V. (2017). Side-effects of Irinotecan (CPT-11), the clinically used drug for colon cancer therapy, are eliminated in experimental animals treated with latex proteins from *Calotropis procera* (Apocynaceae). *Phytotherapy Research*, 31(2), 312-320.
- De Gramont, A. D., Figer, A., Seymour, M., Homer, M., Hmissi, A., Cassidy, J., ... & Bonetti, A. (2000). Leucovorin and fluorouracil with or without oxaliplatin as first-line treatment in advanced colorectal cancer. *Journal of Clinical Oncology*, 18(16), 2938-2947.

- De Gramont, A., Vignoud, J., Tournigand, C., Louvet, C., Andre, T., Varette, C., ... & Krulik, M. (1997). Oxaliplatin with high-dose leucovorin and 5-fluorouracil 48-hour continuous infusion in pretreated metastatic colorectal cancer. *European Journal of Cancer*, 33(2), 214-219.
- de Pontes Santos, H. B., de Moraes, E. F., Cavalcante, R. B., Nogueira, R. L. M., Nonaka, C. F. W., de Souza, L. B., & de Almeida Freitas, R. (2020). Immunoexpression of DNA base excision repair and nucleotide excision repair proteins in ameloblastomas, syndromic and non-syndromic odontogenic keratocysts and dentigerous cysts. *Archives of Oral Biology*, 110, 104627.
- Dembic, Z. (2020). Antitumor drugs and their targets. *Molecules*, 25(23), 5776.
- Denlinger, C. S., & Barsevick, A. M. (2009). The challenges of colorectal cancer survivorship. *Journal of the National Comprehensive Cancer Network*, 7(8), 883-894.
- Dennison, C., Prasad, M., Lloyd, A., Bhattacharyya, S. K., Dhawan, R., & Coyne, K. (2005). The health-related quality of life and economic burden of constipation. *Pharmacoeconomics*, 23(5), 461-476.
- Denzer, I., Muench, G., & Friedland, K. (2016). Modulation of mitochondrial dysfunction in neurodegenerative diseases via activation of nuclear factor erythroid-2-related factor 2 by food-derived compounds. *Pharmacological research*, 103, 80-94.
- Devanabanda, B., & Kasi, A. (2022). Oxaliplatin. In *StatPearls [Internet]*. StatPearls Publishing.
- Di Fiore, F., & Van Cutsem, E. (2009). Acute and long-term gastrointestinal consequences of chemotherapy. *Best Practice & Research Clinical Gastroenterology*, 23(1), 113-124.
- Di Lisa, F., Menabò, R., Canton, M., Barile, M., & Bernardi, P. (2001). Opening of the mitochondrial permeability transition pore causes depletion of mitochondrial and cytosolic NAD⁺ and is a causative event in the death of myocytes in postischemic reperfusion of the heart. *Journal of Biological Chemistry*, 276(4), 2571-2575.
- Di Maso, V., Avellini, C., Crocè, L. S., Rosso, N., Quadrioglio, F., Cesaratto, L., ... & Tiribelli, C. (2007). Subcellular localization of APE1/Ref-1 in human hepatocellular carcinoma: possible prognostic significance. *Molecular medicine*, 13, 89-96.
- Dianova, I. I., Bohr, V. A., & Dianov, G. L. (2001). Interaction of human AP endonuclease 1 with flap endonuclease 1 and proliferating cell nuclear antigen involved in long-patch base excision repair. *Biochemistry*, 40(42), 12639-12644.
- Dickens, E., & Ahmed, S. (2018). Principles of cancer treatment by chemotherapy. *Surgery (Oxford)*, 36(3), 134-138.
- Dienstmann, R., Mason, M. J., Sinicrope, F. A., Phipps, A. I., Tejpar, S., Nesbakken, A., ... & Guinney, J. (2017). Prediction of overall survival in stage II and III colon cancer beyond TNM system: a retrospective, pooled biomarker study. *Annals of Oncology*, 28(5), 1023-1031.
- Donald, E. L., Stojanovska, L., Apostolopoulos, V., & Nurgali, K. (2017). Resveratrol alleviates oxidative damage in enteric neurons and associated gastrointestinal dysfunction caused by chemotherapeutic agent oxaliplatin. *Maturitas*, 105, 100-106.
- Douglas, J., Androulakis, N., Syrigos, K., Polyzos, A., Zira's, N., Athanasiadis, A., ... & Georgoulas, V. (2006). FOLFOXIRI (folinic acid, 5-fluorouracil, oxaliplatin and irinotecan) vs FOLFIRI (folinic acid, 5-fluorouracil and irinotecan) as first-line treatment in metastatic colorectal cancer (MCC): a multicentre randomised phase III trial from the Hellenic Oncology Research Group (HORG). *British journal of cancer*, 94(6), 798-805.

- Dranitsaris, G., Maroun, J., & Shah, A. (2005). Severe chemotherapy-induced diarrhea in patients with colorectal cancer: a cost of illness analysis. *Supportive Care in Cancer*, 13(5), 318-324.
- Drott, J., Fomichov, V., Starkhammar, H., Börjeson, S., Kjellgren, K., & Berterö, C. (2019). Oxaliplatin-induced neurotoxic side effects and their impact on daily activities: a longitudinal study among patients with colorectal cancer. *Cancer nursing*, 42(6), E40-E48.
- Du Bois, A., Lück, H. J., Meier, W., Adams, H. P., Möbus, V., Costa, S., ... & Pfisterer, J. (2003). A randomized clinical trial of cisplatin/paclitaxel versus carboplatin/paclitaxel as first-line treatment of ovarian cancer. *Journal of the National Cancer Institute*, 95(17), 1320-1329.
- Dudley, J., Das, S., Mukherjee, S., & Das, D. K. (2009). RETRACTED: Resveratrol, a unique phytoalexin present in red wine, delivers either a survival signal or death signal to the ischemic myocardium depending on the dose.
- Dzagnidze, A., Katsarava, Z., Makhlova, J., Liedert, B., Yoon, M. S., Kaube, H., ... & Thomale, J. (2007). Repair capacity for platinum-DNA adducts determines the severity of cisplatin-induced peripheral neuropathy. *Journal of Neuroscience*, 27(35), 9451-9457.
- Eastman, A. (1990). Activation of programmed cell death by anticancer agents: cisplatin as a model system. *Cancer cells (Cold Spring Harbor, NY: 1989)*, 2(8-9), 275-280.
- Egloff, A. M., & Grandis, J. R. (2009). Improving response rates to EGFR-targeted therapies for head and neck squamous cell carcinoma: candidate predictive biomarkers and combination treatment with Src inhibitors. *Journal of oncology*, 2009.
- Elbeddini, A., Hooda, N., Gazarin, M., Webster, P., & McMillan, J. (2020). Irinotecan-Associated Dysarthria in Patients with Pancreatic Cancer: A Single Site Experience. *The American Journal of Case Reports*, 21, e924058-1.
- Ema, M., Hirota, K., Mimura, J., Abe, H., Yodoi, J., Sogawa, K., ... & Fujii-Kuriyama, Y. (1999). Molecular mechanisms of transcription activation by HLF and HIF1 α in response to hypoxia: their stabilization and redox signal-induced interaction with CBP/p300. *The EMBO journal*, 18(7), 1905-1914.
- Emami Nejad, A., Najafgholian, S., Rostami, A., Sistani, A., Shojaeifar, S., Esparvarinha, M., ... & Manian, M. (2021). The role of hypoxia in the tumor microenvironment and development of cancer stem cell: a novel approach to developing treatment. *Cancer Cell International*, 21(1), 1-26.
- Erol Tinaztepe, Ö., Ay, M., & Eser, E. (2017). Nuclear and mitochondrial DNA of age-related cataract patients are susceptible to oxidative damage. *Current eye research*, 42(4), 583-588.
- Escalante, J., McQuade, R. M., Stojanovska, V., & Nurgali, K. (2017). Impact of chemotherapy on gastrointestinal functions and the enteric nervous system. *Maturitas*, 105, 23-29.
- Evans, A. R., Junger, H., Southall, M. D., Nicol, G. D., Sorkin, L. S., Broome, J. T., ... & Vasko, M. R. (2000). Isoprostanol, are novel eicosanoids that produce nociception and sensitize rat sensory neurons. *Journal of Pharmacology and Experimental Therapeutics*, 293(3), 912-920.
- Evans, A. R., Limp-Foster, M., & Kelley, M. R. (2000). Going APE over ref-1. *Mutation Research/DNA Repair*, 461(2), 83-108.
- Falcon, B. L., Chintharlapalli, S., Uhlik, M. T., & Pytowski, B. (2016). Antagonist antibodies to vascular endothelial growth factor receptor 2 (VEGFR-2) as anti-angiogenic agents. *Pharmacology & therapeutics*, 164, 204-225.

- Falcone, A., Masi, G., Allegrini, G., Danesi, R., Pfanner, E., Brunetti, I. M., ... & Conte, P. (2002). Biweekly chemotherapy with oxaliplatin, irinotecan, infusional fluorouracil, and leucovorin: a pilot study in patients with metastatic colorectal cancer. *Journal of clinical oncology*, 20(19), 4006-4014.
- Fan, Y., Mao, R., & Yang, J. (2013). NF- κ B and STAT3 signalling pathways collaboratively link inflammation to cancer. *Protein & cell*, 4(3), 176-185.
- Fan, Z., Beresford, P. J., Zhang, D., Xu, Z., Novina, C. D., Yoshida, A., ... & Lieberman, J. (2003). Cleaving the oxidative repair protein Ape1 enhances cell death mediated by granzyme A. *Nature immunology*, 4(2), 145-153.
- Favoriti, P., Carbone, G., Greco, M., Pirozzi, F., Pirozzi, R. E. M., & Corcione, F. (2016). Worldwide burden of colorectal cancer: a review. *Updates in surgery*, 68(1), 7-11.
- Feeney, B., & Clark, A. C. (2005). Reassembly of active caspase-3 is facilitated by the propeptide. *Journal of Biological Chemistry*, 280(48), 39772-39785.
- Fehrenbacher, J. C., Guo, C., Kelley, M. R., & Vasko, M. R. (2017). DNA damage mediates changes in neuronal sensitivity induced by the inflammatory mediators, MCP-1 and LPS, and can be reversed by enhancing the DNA repair function of APE1. *Neuroscience*, 366, 23-35.
- Felici, R., Lapucci, A., Cavone, L., Pratesi, S., Berlinguer-Palmini, R., & Chiarugi, A. (2015). Pharmacological NAD-boosting strategies improve mitochondrial homeostasis in human complex I-mutant fibroblasts. *Molecular Pharmacology*, 87(6), 965-971.
- Ferrell, B., & Coyle, N. (2006). *Textbook of palliative nursing*. Oxford University Press, USA.
- Feyer, P. C., Maranzano, E., Molassiotis, A., Roila, F., Clark-Snow, R. A., & Jordan, K. (2011). Radiotherapy-induced nausea and vomiting (RINV): MASCC/ESMO guideline for antiemetics in radiotherapy: update 2009. *Supportive Care in Cancer*, 19(1), 5-14.
- Feyer, P., & Jordan, K. (2011). Update and new trends in antiemetic therapy: the continuing need for novel therapies. *Annals of Oncology*, 22(1), 30-38.
- Feyer, P., Jahn, F., & Jordan, K. (2014). Radiation-induced nausea and vomiting. *European journal of pharmacology*, 722, 165-171.
- Feyer, P., Jordan, K., & Schild, S. E. (2011). Radiotherapy-induced nausea and vomiting: prophylaxis and treatment.
- Fischer, R., & Maier, O. (2015). Interrelation of oxidative stress and inflammation in neurodegenerative disease: role of TNF. *Oxidative medicine and cellular longevity*, 2015.
- Fishel, M. L., & Kelley, M. R. (2007). The DNA base excision repair protein Ape1/Ref-1 is a therapeutic and chemopreventive target. *Molecular aspects of medicine*, 28(3-4), 375-395.
- Fishel, M. L., Cheng, H., Shahda, S., & Kelley, M. R. (2015). Abstract B167: APX3330 drug development for clinical trials targeting APE1/Ref-1 in pancreatic cancer.
- Fishel, M. L., He, Y., Smith, M. L., & Kelley, M. R. (2007). Manipulation of base excision repair to sensitize ovarian cancer cells to alkylating agent temozolomide. *Clinical Cancer Research*, 13(1), 260-267.
- Fishel, M. L., Jiang, Y., Rajeshkumar, N. V., Scandura, G., Sinn, A. L., He, Y., ... & Kelley, M. R. (2011). Impact of APE1/Ref-1 Redox Inhibition on Pancreatic Tumor Growth. *Molecular cancer therapeutics*, 10(9), 1698-1708.
- Fishel, M. L., Logsdon, D. P., Grimard, M. L., Supuran, C. T., Zyromski, N., Ivan, M., ... & Shah, F.

- (2016). Targeting Ref-1/APE1 pathway inhibition in pancreatic cancer using APX3330 for clinical trials.
- Fishel, M. L., Vasko, M. R., & Kelley, M. R. (2007). DNA repair in neurons: so if they don't divide what's to repair?. *Mutation Research/Fundamental and Molecular Mechanisms of Mutagenesis*, 614(1-2), 24-36.
- Fletcher, R. H. (2009). The diagnosis of colorectal cancer in patients with symptoms: finding a needle in a haystack. *BMC medicine*, 7(1), 1-3.
- Folkman, J. (2007). Angiogenesis: an organizing principle for drug discovery?. *Nature reviews Drug discovery*, 6(4), 273-286.
- Forootan, M., Bagheri, N., & Darvishi, M. (2018). Chronic constipation: A review of the literature. *Medicine*, 97(20).
- Forsythe, J. A., Jiang, B. H., Iyer, N. V., Agani, F., Leung, S. W., Koos, R. D., & Semenza, G. L. (1996). Activation of vascular endothelial growth factor gene transcription by hypoxia-inducible factor 1. *Molecular and cellular biology*, 16(9), 4604-4613.
- Fortini, P., & Dogliotti, E. (2010). Mechanisms of dealing with DNA damage in terminally differentiated cells. *Mutation Research/Fundamental and Molecular Mechanisms of Mutagenesis*, 685(1-2), 38-44.
- Fox, P., Darley, A., Furlong, E., Miaskowski, C., Patiraki, E., Armes, J., ... & Maguire, R. (2017). The assessment and management of chemotherapy-related toxicities in patients with breast cancer, colorectal cancer, and Hodgkin's and non-Hodgkin's lymphomas: A scoping review. *European Journal of Oncology Nursing*, 26, 63-82.
- Frank, J., Gao, H., Sengupta, J., Gao, N., & Taylor, D. J. (2007). The process of mRNA-tRNA translocation. *Proceedings of the National Academy of Sciences*, 104(50), 19671-19678.
- Frossi, B., Antoniali, G., Yu, K., Akhtar, N., Kaplan, M. H., Kelley, M. R., ... & Pucillo, C. E. (2019). Endonuclease and redox activities of human apurinic/aprimidinic endonuclease 1 have distinctive and essential functions in IgA class switch recombination. *Journal of Biological Chemistry*, 294(13), 5198-5207.
- Fuchs, C., Mitchell, E. P., & Hoff, P. M. (2006). Irinotecan in the treatment of colorectal cancer. *Cancer treatment reviews*, 32(7), 491-503.
- Fuertes, M. A., Castilla, J., Alonso, C., & Prez, J. M. (2003). Cisplatin biochemical mechanism of action: from cytotoxicity to induction of cell death through interconnections between apoptotic and necrotic pathways. *Current medicinal chemistry*, 10(3), 257-266.
- Fujita, K. I., Kubota, Y., Ishida, H., & Sasaki, Y. (2015). Irinotecan is a key chemotherapeutic drug for metastatic colorectal cancer. *World journal of gastroenterology*, 21(43), 12234.
- Fujita, Y., Yagishita, S., Hagiwara, K., Yoshioka, Y., Kosaka, N., Takeshita, F., ... & Ochiya, T. (2015). The clinical relevance of the miR-197/CKS1B/STAT3-mediated PD-L1 network in chemoresistant non-small-cell lung cancer. *Molecular therapy*, 23(4), 717-727.
- Fulda, S., & Debatin, K. M. (2006). Extrinsic versus intrinsic apoptosis pathways in anticancer chemotherapy. *Oncogene*, 25(34), 4798-4811.
- Fumet, J. D., Hervieu, A., Hennequin, A., Zanetta, S., Bertaut, A., & Ghiringhelli, F. (2021). Phase I dose-escalation study of desynchronized irinotecan plus bevacizumab, oxaliplatin, 5-fluorouracil, and folinic acid (bFOLFIRINOX-3) administration in chemorefractory metastatic colorectal cancer patients.
- Fung, C., & Vanden Berghe, P. (2020). Functional circuits and signal processing in the enteric nervous system. *Cellular and Molecular Life Sciences*, 77(22), 4505-4522.

- Furness, J. B. (2012). The enteric nervous system and neurogastroenterology. *Nature Reviews Gastroenterology & Hepatology*, 9(5), 286-294.
- Furness, J. B., Callaghan, B. P., Rivera, L. R., & Cho, H. J. (2014). The enteric nervous system and gastrointestinal innervation: integrated local and central control. *Microbial endocrinology: The microbiota-gut-brain axis in health and disease*, 39-71.
- Furness, J. B., Jones, C., Nurgali, K., & Clerc, N. (2004). Intrinsic primary afferent neurons and nerve circuits within the intestine. *Progress in neurobiology*, 72(2), 143-164.
- Gadina, M., Gazaniga, N., Vian, L., & Furumoto, Y. (2017). Small molecules to the rescue: Inhibition of cytokine signalling in immune-mediated diseases. *Journal of autoimmunity*, 85, 20-31.
- Gampala, S., Caston, R. A., Fishel, M. L., & Kelley, M. R. (2020). Basic, the translational and clinical relevance of the DNA repair and redox signalling protein APE1 in human diseases. In *DNA Damage, DNA Repair and Disease* (pp. 286-318).
- Gampala, S., Shah, F., Lu, X., Moon, H. R., Babb, O., Umesh Ganesh, N., ... & Fishel, M. L. (2021). Ref-1 redox activity alters cancer cell metabolism in pancreatic cancer: Exploiting this novel finding as a potential target. *Journal of Experimental & Clinical Cancer Research*, 40(1), 1-24.
- Gampala, S., Shah, F., Zhang, C., Rhodes, S. D., Babb, O., Grimard, M., ... & Fishel, M. L. (2021). Exploring transcriptional regulators Ref-1 and STAT3 as therapeutic targets in malignant peripheral nerve sheath tumours. *British journal of cancer*, 124(9), 1566-1580.
- Ganguli, S. C., Kamath, M. V., Redmond, K., Chen, Y., Irvine, E. J., Collins, S. M., & Tougas, G. (2007). A comparison of autonomic function in patients with inflammatory bowel disease and in healthy controls. *Neurogastroenterology & Motility*, 19(12), 961-967.
- Gao, D., Herman, J. G., & Guo, M. (2016). The clinical value of aberrant epigenetic changes of DNA damage repair genes in human cancer. *Oncotarget*, 7(24), 37331.
- Gaur, S., Chen, L., Ann, V., Lin, W. C., Wang, Y., Chang, V. H., ... & Yen, Y. (2014). Dovitinib synergizes with oxaliplatin in suppressing cell proliferation and inducing apoptosis in colorectal cancer cells regardless of RAS-RAF mutation status. *Molecular Cancer*, 13(1), 1-16.
- Germain, A. M., Romanik, M. C., Guerra, I., Solari, S., Reyes, M. S., Johnson, R. J., ... & Valdés, G. (2007). Endothelial dysfunction: a link among preeclampsia, recurrent pregnancy loss, and future cardiovascular events?. *Hypertension*, 49(1), 90-95.
- Germain, D., & Frank, D. A. (2007). Targeting the cytoplasmic and nuclear functions of signal transducers and activators of transcription 3 for cancer therapy. *Clinical Cancer Research*, 13(19), 5665-5669.
- Ghobrial, I. M., & Rajkumar, S. V. (2003). Management of thalidomide toxicity. *The journal of supportive oncology*, 1(3), 194.
- Giacchetti, S., Perpoint, B., Zidani, R., Le Bail, N., Faggiuolo, R., Focan, C., ... & Levi, F. (2000). Phase III multicenter randomized trial of oxaliplatin added to chronomodulated fluorouracil-leucovorin as first-line treatment of metastatic colorectal cancer. *Journal of clinical oncology*, 18(1), 136-136.
- Gibson, R. J., & Keefe, D. M. (2006). Cancer chemotherapy-induced diarrhoea and constipation: mechanisms of damage and prevention strategies. *Supportive Care in Cancer*, 14(9), 890-900.
- Gibson, R. J., & Stringer, A. M. (2009). Chemotherapy-induced diarrhoea. *Current opinion in supportive and palliative care*, 3(1), 31-35.

- Gibson, R. J., Bowen, J. M., Inglis, M. R., Cummins, A. G., & Keefe, D. M. (2003). Irinotecan causes severe small intestinal damage, as well as colonic damage, in the rat with implanted breast cancer. *Journal of gastroenterology and hepatology*, 18(9), 1095-1100.
- Gibson, R. J., Cummins, A. G., Bowen, J. M., Logan, R. M., Healey, T., & Keefe, D. M. (2006). Apoptosis occurs early in the basal layer of the oral mucosa following cancer chemotherapy. *Asia-Pacific Journal of Clinical Oncology*, 2(1), 39-49.
- Gibson, R. J., Keefe, D. M., Lalla, R. V., Bateman, E., Blijlevens, N., Fijlstra, M., ... & Bowen, J. M. (2013). A systematic review of agents for the management of gastrointestinal mucositis in cancer patients. *Supportive Care in Cancer*, 21(1), 313-326.
- Glowacki, S., Synowiec, E., & Blasiak, J. (2013). The role of mitochondrial DNA damage and repair in the resistance of BCR/ABL-expressing cells to tyrosine kinase inhibitors. *International journal of molecular sciences*, 14(8), 16348-16364.
- Godlewski, J. (2010). Morphological changes in the enteric nervous system are caused by carcinoma of the human large intestine. *Folia histochemical et cytobiologica*, 48(1), 157-162.
- Goel, S., Duda, D. G., Xu, L., Munn, L. L., Boucher, Y., Fukumura, D., & Jain, R. K. (2011). Normalization of the vasculature for treatment of cancer and other diseases. *Physiological Reviews*, 91(3), 1071-1121.
- Goldberg, R. M. (2005). Advances in the treatment of metastatic colorectal cancer. *The Oncologist*, 10, 40-48.
- Gong, G., Waris, G., Tanveer, R., & Siddiqui, A. (2001). Human hepatitis C virus NS5A protein alters intracellular calcium levels, induces oxidative stress, and activates STAT-3 and NF- κ B. *Proceedings of the National Academy of Sciences*, 98(17), 9599-9604.
- Goodisman, J., Hagrman, D., Tacka, K. A., & Souid, A. K. (2006). Analysis of cytotoxicities of platinum compounds. *Cancer chemotherapy and pharmacology*, 57(2), 257-267.
- Grabenbauer, G. G., & Holger, G. (2016). Management of radiation and chemotherapy related acute toxicity in gastrointestinal cancer. *Best Practice & Research Clinical Gastroenterology*, 30(4), 655-664.
- Graham, M. A., Lockwood, G. F., Greenslade, D., Brienza, S., Bayssas, M., & Gamelin, E. (2000). Clinical pharmacokinetics of oxaliplatin: a critical review. *Clinical Cancer Research*, 6(4), 1205-1218.
- Granados-Romero, J. J., Valderrama-Treviño, A. I., Contreras-Flores, E. H., Barrera-Mera, B., Herrera Enríquez, M., Uriarte-Ruiz, K., ... & Arauz-Peña, G. (2017). Colorectal cancer: a review. *Int J Res Med Sci*, 5(11), 4667-4676.
- Gray, E. J., Darvishzadeh, A., Sharma, A., Ganeshan, D., Faria, S. C., & Lall, C. (2016). Cancer therapy-related complications in the bowel and mesentery: an imaging perspective. *Abdominal Radiology*, 41(10), 2031-2047.
- Grierson, P., Suresh, R., Tan, B. R., Pedersen, K. S., Amin, M. A., Park, H., ... & wang-gillam, A. (2022). A pilot study of liposomal irinotecan plus 5-FU/LV combined with paricalcitol in patients with advanced pancreatic cancer which progressed on gemcitabine-based therapy.
- Grivicich, I., Mans, D. R. A., Peters, G. J., & Schwartzmann, G. (2001). Irinotecan and oxaliplatin: an overview of the novel chemotherapeutic options for the treatment of advanced colorectal cancer. *Brazilian Journal of Medical and Biological Research*, 34(9), 1087-1103.

- Grombacher, T., Eichhorn, U., & Kaina, B. (1998). p53 is involved in the regulation of the DNA repair gene O 6-methylguanine-DNA methyltransferase (MGMT) by DNA damaging agents. *Oncogene*, *17*(7), 845-851.
- Gros, L., Ishchenko, A. A., Ide, H., Elder, R. H., & Saparbaev, M. K. (2004). The major human AP endonuclease (Ape1) is involved in the nucleotide incision repair pathway. *Nucleic acids research*, *32*(1), 73-81.
- Grothey, A., & Goldberg, R. M. (2004). A review of oxaliplatin and its clinical use in colorectal cancer. *Expert Opinion on Pharmacotherapy*, *5*(10), 2159-2170.
- Grothey, A., Sargent, D., Goldberg, R. M., & Schmoll, H. J. (2004). Survival of patients with advanced colorectal cancer improves with the availability of fluorouracil-leucovorin, irinotecan, and oxaliplatin in the course of treatment. *Journal of Clinical Oncology*, *22*(7), 1209-1214.
- Gu, J., Li, Z., Zhou, J., Sun, Z., & Bai, C. (2019). Response prediction to oxaliplatin plus 5-fluorouracil chemotherapy in patients with colorectal cancer using a four-protein immunohistochemical model. *Oncology Letters*, *18*(2), 2091-2101.
- Guanizo, A. C., Fernando, C. D., Garama, D. J., & Gough, D. J. (2018). STAT3: a multifaceted oncoprotein. *Growth Factors*, *36*(1-2), 1-14.
- Guha, P., Gardell, J., Darpolor, J., Cunetta, M., Lima, M., Miller, G., ... & Katz, S. C. (2019). STAT3 inhibition induces Bax-dependent apoptosis in liver tumor myeloid-derived suppressor cells. *Oncogene*, *38*(4), 533-548.
- Guinane, J., & Crone, R. (2018). Management of faecal incontinence in residential aged care. *Australian Journal of General Practice*, *47*(1/2), 40-42.
- Gulati, K., Guhathakurta, S., Joshi, J., Rai, N., & Ray, A. J. M. I. (2016). Cytokines and their role in health and disease: a brief overview. *Moj Immunol*, *4*(2), 1-9.
- Gulbransen, B. D., Bashashati, M., Hirota, S. A., Gui, X., Roberts, J. A., MacDonald, J. A., ... & Sharkey, K. A. (2012). Activation of neuronal P2X7 receptor–pannexin-1 mediates death of enteric neurons during colitis. *Nature medicine*, *18*(4), 600-604.
- Gunasegaran, B., Neilsen, P. M., & Smid, S. D. (2020). P53 activation suppresses irinotecan metabolite SN-38-induced cell damage in non-malignant but not malignant epithelial colonic cells. *Toxicology in Vitro*, *67*, 104908.
- Guo, L. D., Shen, Y. Q., Zhao, X. H., Guo, L. J., Yu, Z. J., Wang, D., ... & Liu, J. Z. (2015). Curcumin combined with oxaliplatin effectively suppress colorectal carcinoma in vivo through inducing apoptosis. *Phytotherapy Research*, *29*(3), 357-365.
- Guo, Y., Chen, J., Zhao, T., & Fan, Z. (2008). Granzyme K degrades the redox/DNA repair enzyme Ape1 to trigger oxidative stress of target cells leading to cytotoxicity. *Molecular immunology*, *45*(8), 2225-2235.
- Gupta, K., Walton, R., & Kataria, S. P. (2021). Chemotherapy-induced nausea and vomiting: pathogenesis, recommendations, and new trends. *Cancer treatment and research communications*, *26*, 100278.
- Gupta, R., & Bhaskar, A. (2016). Chemotherapy-induced peripheral neuropathic pain. *Bja Education*, *16*(4), 115-119.
- Gwynne, R. M., & Bornstein, J. C. (2007). Local inhibitory reflexes excited by the mucosal application of nutrient amino acids in guinea pig jejunum. *American Journal of Physiology-Gastrointestinal and Liver Physiology*, *292*(6), G1660-G1670.

- Gwynne, R. M., & Bornstein, J. C. (2007). Synaptic transmission at functionally identified synapses in the enteric nervous system: roles for both ionotropic and metabotropic receptors. *Current Neuropharmacology*, 5(1), 1-17.
- Hadri, K. E., Mahmood, D. F. D., Couchie, D., Jguirim-Souissi, I., Genze, F., Diderot, V., ... & Rouis, M. (2012). Thioredoxin-1 promotes anti-inflammatory macrophages of the M2 phenotype and antagonizes atherosclerosis. *Arteriosclerosis, thrombosis, and vascular biology*, 32(6), 1445-1452.
- Haggar, F. A., & Boushey, R. P. (2009). Colorectal cancer epidemiology: incidence, mortality, survival, and risk factors. *Clinics in colon and rectal surgery*, 22(04), 191-197.
- Hainaut, P., & Milner, J. (1993). Redox modulation of p53 conformation and sequence-specific DNA binding in vitro. *Cancer Research*, 53(19), 4469-4473.
- Hakem, R. (2008). DNA-damage repair; the good, the bad, and the ugly. *The EMBO journal*, 27(4), 589-605.
- Hald, A., Van Beek, J., & Lotharius, J. (2007). Inflammation in Parkinson's disease. *Inflammation in the Pathogenesis of Chronic Diseases*, 249-279.
- Halestrap, A. P. (2009). What is the mitochondrial permeability transition pore?. *Journal of molecular and cellular cardiology*, 46(6), 821-831.
- Haller, D. G. (2000). Safety of oxaliplatin in the treatment of colorectal cancer. *Oncology (Williston Park, NY)*, 14(12 Suppl 11), 15-20.
- Haller, D. G., Tabernero, J., Maroun, J., De Braud, F., Price, T., Van Cutsem, E., ... & Schmoll, H. J. (2011). Capecitabine plus oxaliplatin compared with fluorouracil and folinic acid as adjuvant therapy for stage III colon cancer. *J Clin Oncol*, 29(11), 1465-1471.
- Hamano, H., Mitsui, M., Zamami, Y., Takechi, K., Nimura, T., Okada, N., ... & Ishizawa, K. (2019). Irinotecan-induced neutropenia is reduced by oral alkalization drugs: analysis using retrospective chart reviews and the spontaneous reporting database. *Supportive Care in Cancer*, 27(3), 849-856.
- Han, C. J., Yang, G. S., & Syrjala, K. (2020). Symptom experiences in colorectal cancer survivors after cancer treatments: A systematic review and meta-analysis. *Cancer nursing*, 43(3), E132.
- Hanahan, D., & Weinberg, R. A. (2011). Hallmarks of cancer: the next generation. *cell*, 144(5), 646-674.
- Hanlon, M. M., Rakovich, T., Cunningham, C. C., Ansboro, S., Veale, D. J., Fearon, U., & McGarry, T. (2019). STAT3 mediates the differential effects of oncostatin M and TNF α on RA synovial fibroblast and endothelial cell function. *Frontiers in immunology*, 10, 2056.
- Hansberry, D. R., Shah, K., Agarwal, P., & Agarwal, N. (2017). Fecal myeloperoxidase as a biomarker for inflammatory bowel disease. *Cureus*, 9(1).
- Hansen, M. B. (2003). The enteric nervous system I: organisation and classification. *Pharmacology & Toxicology*, 92(3), 105-113.
- Hanson, S., Kim, E., & Deppert, W. (2005). Redox factor 1 (Ref-1) enhances specific DNA binding of p53 by promoting p53 tetramerization. *Oncogene*, 24(9), 1641-1647.
- Harrison, J. F., Hollensworth, S. B., Spitz, D. R., Copeland, W. C., Wilson, G. L., & LeDoux, S. P. (2005). Oxidative stress-induced apoptosis in neurons correlates with mitochondrial DNA base excision repair pathway imbalance. *Nucleic acids research*, 33(14), 4660-4671.

- Hartman, G. D., Lambert-Cheatham, N. A., Kelley, M. R., & Corson, T. W. (2021). Inhibition of APE1/Ref-1 for Neovascular Eye Diseases: From Biology to Therapy. *International Journal of Molecular Sciences*, 22(19), 10279.
- He, C. L., Burgart, L., Wang, L., Pemberton, J., Young-Fadok, T., Szurszewski, J., & Farrugia, G. (2000). The decreased interstitial cell of Cajal volume in patients with slow-transit constipation. *Gastroenterology*, 118(1), 14-21.
- Hecht, J. R. (1998). Gastrointestinal toxicity of irinotecan. *Oncology (Williston Park, NY)*, 12(8 Suppl 6), 72-78.
- Heinemann, V., von Weikersthal, L. F., Decker, T., Kiani, A., Kaiser, F., Al-Batran, S. E., ... & Stintzing, S. (2021). FOLFIRI plus cetuximab or bevacizumab for advanced colorectal cancer: final survival and per-protocol analysis of FIRE-3, a randomised clinical trial. *British journal of cancer*, 124(3), 587-594.
- Heinrich, P. C., Behrmann, I., Müller-Newen, G., Schaper, F., & Graeve, L. (1998). Interleukin-6-type cytokine signalling through the gp130/Jak/STAT pathway. *Biochemical Journal*, 334(2), 297-314.
- Heisel, C., Yousif, J., Mijiti, M., Charizanis, K., Brigell, M., Corson, T. W., & Kelley, M. R. (2021). APE1/Ref-1 as a novel target for retinal diseases. *Journal of cellular signaling*, 2(2), 133.
- Hershman, D. L., Lacchetti, C., Dworkin, R. H., Lavoie Smith, E. M., Bleeker, J., Cavaletti, G., ... & Loprinzi, C. L. (2014). Prevention and management of chemotherapy-induced peripheral neuropathy in survivors of adult cancers: American Society of Clinical Oncology clinical practice guideline. *J Clin Oncol*, 32(18), 1941-1967.
- Hetman, M., Vashishta, A., & Rempala, G. (2010). Neurotoxic mechanisms of DNA damage: focus on transcriptional inhibition. *Journal of neurochemistry*, 114(6), 1537-1549.
- Hino, H., Shiomi, A., Kagawa, H., Manabe, S., Yamaoka, Y., Kato, S., & Hanaoka, M. (2022). Neoadjuvant chemoradiotherapy for borderline resectable low rectal cancer: short-and long-term outcomes at a single Japanese center. *Surgery Today*, 1-9.
- Hiramoto, M., Shimizu, N., Sugimoto, K., Tang, J., Kawakami, Y., Ito, M., ... & Handa, H. (1998). Nuclear targeted suppression of NF- κ B activity by the novel quinone derivative E3330. *The Journal of Immunology*, 160(2), 810-819.
- Hirota, K., Murata, M., Sachi, Y., Nakamura, H., Takeuchi, J., Mori, K., & Yodoi, J. (1999). Distinct roles of thioredoxin in the cytoplasm and the nucleus: a two-step mechanism of redox regulation of transcription factor NF- κ B. *Journal of Biological Chemistry*, 274(39), 27891-27897.
- Hong, Y., Kim, J., Choi, Y. J., & Kang, J. G. (2020). Clinical study of colorectal cancer operation: Survival analysis. *Korean Journal of Clinical Oncology*, 16(1), 3-8.
- Hsieh, Y. C., Chang, T. K., Su, W. C., Huang, C. W., Tsai, H. L., Chen, Y. C., ... & Wang, J. Y. (2021). UGT1A1 Polymorphism for Irinotecan Dose Escalation in Patients with BRAF-Mutated Metastatic Colorectal Cancer Treated with First-Line Bevacizumab and FOLFIRI. *Journal of Oncology*, 2021.
- Hu, S., Huang, K. M., Adams, E. J., Loprinzi, C. L., & Lustberg, M. B. (2019). Recent developments of novel pharmacologic therapeutics for the prevention of chemotherapy-induced peripheral neuropathy. *Clinical Cancer Research*, 25(21), 6295-6301.
- Hu, W., Jiang, A., Liang, J., Meng, H., Chang, B., Gao, H., & Qiao, X. (2008). Expression of VLDLR in the retina and evolution of subretinal neovascularization in the knockout mouse model's retinal angiomatous proliferation. *Investigative ophthalmology & visual science*, 49(1), 407-415.

- Hu, Z. P., Yang, X. X., Chan, S. Y., Xu, A. L., Duan, W., Zhu, Y. Z., ... & Zhou, S. F. (2006). St. John's wort attenuates irinotecan-induced diarrhea via down-regulation of intestinal pro-inflammatory cytokines and inhibition of intestinal epithelial apoptosis. *Toxicology and applied pharmacology*, 216(2), 225-237.
- Huang, C. Y., & Ferrell, J. E. (1996). Ultrasensitivity in the mitogen-activated protein kinase cascade. *Proceedings of the National Academy of Sciences*, 93(19), 10078-10083.
- Huang, C., Chen, L., Savage, S. R., Eguez, R. V., Dou, Y., Li, Y., ... & Piehowski, P. D. (2021). Proteogenomic insights into the biology and treatment of HPV-negative head and neck squamous cell carcinoma. *Cancer cell*, 39(3), 361-379.
- Huang, R. P., & Adamson, E. D. (1993). Characterization of the DNA-binding properties of the early growth response-1 (Egr-1) transcription factor: evidence for modulation by a redox mechanism. *DNA and cell biology*, 12(3), 265-273.
- Idrizaj, E., Traini, C., Vannucchi, M. G., & Baccari, M. C. (2021). Nitric Oxide: From Gastric Motility to Gastric Dysmotility. *International Journal of Molecular Sciences*, 22(18), 9990.
- Innominato, P. F., Karaboué, A., Focan, C., Chollet, P., Giacchetti, S., Bouchahda, M., ... & Garufi, C. (2021). Efficacy and safety of chronomodulated irinotecan, oxaliplatin, 5-fluorouracil and leucovorin combination as first-or second-line treatment against metastatic colorectal cancer: Results from the International EORTC 05011 Trial. *International Journal of Cancer*, 148(10), 2512-2521.
- Ishibashi, S., Arai, H., Yokote, K., Araki, E., Suganami, H., Yamashita, S., & K-877 Study Group. (2018). Efficacy and safety of pemafibrate (K-877), a selective peroxisome proliferator-activated receptor α modulator, in patients with dyslipidemia: Results from a 24-week, randomized, double-blind, active-controlled, phase 3 trial. *Journal of clinical lipidology*, 12(1), 173-184.
- Jalaeikhoo, H., Zokaasadi, M., Khajeh-Mehrizi, A., Rajaeinejad, M., Mousavi, S. A., Vaezi, M., ... & Ghavamzadeh, A. (2019). Effectiveness of adjuvant chemotherapy in patients with Stage II colorectal cancer: a multicenter retrospective study. *Journal of Research in Medical Sciences: The Official Journal of Isfahan University of Medical Sciences*, 24.
- Jamieson, E. R., & Lippard, S. J. (1999). Structure, recognition, and processing of cisplatin- DNA adducts. *Chemical Reviews*, 99(9), 2467-2498.
- Javle, M. M., Cao, S., Durrani, F. A., Pendyala, L., Lawrence, D. D., Smith, P. F., ... & Rustum, Y. M. (2007). Celecoxib and mucosal protection: translation from an animal model to a phase I clinical trial of celecoxib, irinotecan, and 5-fluorouracil. *Clinical cancer research*, 13(3), 965-971.
- Jedinak, A., Dudhgaonkar, S., Kelley, M. R., & Sliva, D. (2011). Apurinic/Apyrimidinic endonuclease 1 regulates inflammatory response in macrophages. *Anticancer Research*, 31(2), 379-385.
- Jedinak, A., Dudhgaonkar, S., Kelley, M. R., & Sliva, D. (2011). Apurinic/Apyrimidinic endonuclease 1 regulates inflammatory response in macrophages. *Anticancer research*, 31(2), 379-385.
- Jemal, A., Siegel, R., Ward, E., Hao, Y., Xu, J., Murray, T., & Thun, M. J. (2008). Cancer statistics, 2008. *CA: a cancer journal for clinicians*, 58(2), 71-96.
- Jeon, B. H., Gupta, G., Park, Y. C., Qi, B., Haile, A., Khanday, F. A., ... & Irani, K. (2004). Apurinic/aprimidinic endonuclease 1 regulates endothelial NO production and vascular tone. *Circulation Research*, 95(9), 902-910.
- Jia, J., Zhang, P., Gou, M., Yang, F., Qian, N., & Dai, G. (2019). The role of serum CEA and CA19-9 in efficacy evaluations and progression-free survival predictions for patients treated with cetuximab combined with FOLFOX4 or FOLFIRI as a first-line treatment for advanced colorectal cancer. *Disease Markers*, 2019.

- Jiang, A., Gao, H., Kelley, M. R., & Qiao, X. (2011). Inhibition of APE1/Ref-1 redox activity with APX3330 blocks retinal angiogenesis in vitro and in vivo. *Vision Research*, 51(1), 93-100.
- Jiang, A., Hu, W., Meng, H., Gao, H., & Qiao, X. (2009). Loss of the VLDL receptor activates retinal vascular endothelial cells and promotes angiogenesis. *Investigative ophthalmology & visual science*, 50(2), 844-850.
- Jiang, B. H., Semenza, G. L., Bauer, C., & Marti, H. H. (1996). Hypoxia-inducible factor 1 levels vary exponentially over a physiologically relevant range of O₂ tension. *American Journal of Physiology-Cell Physiology*, 271(4), C1172-C1180.
- Jiang, X., Wang, J., Deng, X., Xiong, F., Zhang, S., Gong, Z., ... & Xiong, W. (2020). The role of microenvironment in tumour angiogenesis. *Journal of Experimental & Clinical Cancer Research*, 39(1), 1-19.
- Jiang, Y., Yuan, H., Li, Z., Ji, X., Shen, Q., Tuo, J., ... & Xiang, Y. (2022). Global pattern and trends of colorectal cancer survival: a systematic review of population-based registration data. *Cancer biology & medicine*, 19(2), 175.
- Jin, H. W., Flatters, S. J., Xiao, W. H., Mulhern, H. L., & Bennett, G. J. (2008). Prevention of paclitaxel-evoked painful peripheral neuropathy by acetyl-L-carnitine: effects on axonal mitochondria, sensory nerve fibre terminal arbores, and cutaneous Langerhans cells. *Experimental neurology*, 210(1), 229-237.
- Jin, Z., May, W. S., Gao, F., Flagg, T., & Deng, X. (2006). Bcl2 suppresses DNA repair by enhancing c-Myc transcriptional activity. *Journal of Biological Chemistry*, 281(20), 14446-14456.
- Jing, L. I. U., & Anning, L. I. N. (2005). Role of JNK activation in apoptosis: a double-edged sword. *Cell research*, 15(1), 36-42.
- Johnson, D. E., O'Keefe, R. A., & Grandis, J. R. (2018). Targeting the IL-6/JAK/STAT3 signalling axis in cancer. *Nature reviews Clinical oncology*, 15(4), 234-248.
- Johnston, F. M., Kneuert, P. J., & Pawlik, T. M. (2012). Resection of non-hepatic colorectal cancer metastasis. *Journal of gastrointestinal oncology*, 3(1), 59.
- Joseph, E. K., & Levine, J. D. (2009). Comparison of oxaliplatin-and cisplatin-induced painful peripheral neuropathy in the rat. *The Journal of Pain*, 10(5), 534-541.
- Jugait, S., Areti, A., Nellaiappan, K., Narwani, P., Saha, P., Velayutham, R., & Kumar, A. (2022). Neuroprotective Effect of Baicalein Against Oxaliplatin-Induced Peripheral Neuropathy: Impact on Oxidative Stress, Neuro-inflammation and WNT/ β -Catenin Signaling. *Molecular Neurobiology*, 1-17.
- Jurkovicova, D., Neophytou, C. M., Gašparović, A. Č., & Gonçalves, A. C. (2022). DNA Damage Response in Cancer Therapy and Resistance: Challenges and Opportunities. *International Journal of Molecular Sciences*, 23(23), 14672.
- Kakolyris, S., Kaklamanis, L., Engels, K., Fox, S. B., Taylor, M., Hickson, I. D., ... & Harris, A. L. (1998). Human AP endonuclease 1 (HAP1) protein expression in breast cancer correlates with lymph node status and angiogenesis. *British journal of cancer*, 77(7), 1169-1173.
- Kang, L., Tian, Y., Xu, S., & Chen, H. (2021). Oxaliplatin-induced peripheral neuropathy: clinical features, mechanisms, prevention and treatment. *Journal of Neurology*, 268(9), 3269-3282.
- Karin, M., Cao, Y., Greten, F. R., & Li, Z. W. (2002). NF- κ B in cancer: from innocent bystander to major culprit. *Nature reviews cancer*, 2(4), 301-310.
- Katsuyuki, M., Kohzo, N., Kotaro, F., Xiangao, S., Shuji, S., & Ken-ichi, Y. (1994). Two different cellular redox systems regulate the DNA-binding activity of the p50 subunit of NF- κ B in vitro. *Gene*, 145(2), 197-203.

- Kawai, S., Takeshima, N., Hayasaka, Y., Notsu, A., Yamazaki, M., Kawabata, T., ... & Yasui, H. (2021). Comparison of irinotecan and oxaliplatin as the first-line therapies for metastatic colorectal cancer: a meta-analysis. *BMC Cancer*, *21*(1), 1-11.
- Kciuk, M., Marciniak, B., & Kontek, R. (2020). Irinotecan—Still an important player in cancer chemotherapy: A comprehensive overview. *International journal of molecular sciences*, *21*(14), 4919.
- Keefe et al (2014) Risk and outcomes of chemotherapy-induced diarrhea (CID) among patients with colorectal cancer receiving multi-cycle chemotherapy. *Cancer Chemother Pharmacology*.74:675.
- Keefe, D. M. (2004). Gastrointestinal mucositis: a new biological model. *Supportive Care in Cancer*, *12*(1), 6-9.
- Keefe, D. M. K., Brealey, J., Goland, G. J., & Cummins, A. (2000). Chemotherapy for cancer causes apoptosis that precedes hypoplasia in crypts of the small intestine in humans. *Gut*, *47*(5), 632-637.
- Keefe, D. M., & Gibson, R. J. (2007). Mucosal injury from targeted anti-cancer therapy. *Supportive Care in Cancer*, *15*(5), 483-490.
- Kehrer, D. F., Sparreboom, A., Verweij, J., de Bruijn, P., Nierop, C. A., van de Schraaf, J., ... & de Jonge, M. J. (2001). Modulation of irinotecan-induced diarrhea by cotreatment with neomycin in cancer patients. *Clinical Cancer Research*, *7*(5), 1136-1141.
- Kelland, L. (2007). The resurgence of platinum-based cancer chemotherapy. *Nature Reviews Cancer*, *7*(8), 573-584.
- Kelley, M. (2020). Basic, Translational and Clinical Relevance of the DNA Repair and Redox Signaling Protein APE1 in Human Diseases. *DNA Damage, DNA Repair and Disease Volume 2*, *15*, 286.
- Kelley, M. R., & Fehrenbacher, J. C. (2017). Challenges and opportunities identifying therapeutic targets for chemotherapy-induced peripheral neuropathy resulting from oxidative DNA damage. *Neural regeneration research*, *12*(1), 72.
- Kelley, M. R., Jiang, Y., Guo, C., Reed, A., Meng, H., & Vasko, M. R. (2014). Role of the DNA base excision repair protein, APE1 in cisplatin, oxaliplatin, or carboplatin induced sensory neuropathy. *PLoS one*, *9*(9), e106485.
- Kelley, M. R., Logsdon, D., & Fishel, M. L. (2014). Targeting DNA repair pathways for cancer treatment: what's new?. *Future Oncology*, *10*(7), 1215-1237.
- Kelley, M. R., Luo, M., Reed, A., Su, D., Delaplane, S., Borch, R. F., ... & Georgiadis, M. M. (2011). Functional analysis of novel analogues of E3330 that block the redox signalling activity of the multifunctional AP endonuclease/redox signalling enzyme APE1/Ref-1. *Antioxidants & redox signaling*, *14*(8), 1387-1401.
- Kelley, M. R., Messmann, R. A., & Fehrenbacher, J. (2018). Novel first-in-class small molecule targeting APE1/Ref-1 to prevent and treat chemotherapy-induced peripheral neuropathy (CIPN).
- Kelley, M. R., Shahda, S., Lakhani, N. J., O'Neil, B., Chu, L., Anderson, A. K., ... & Messmann, R. A. (2019). Abstract PR01: A phase I study targeting the APE1/Ref-1 DNA repair-redox signalling protein with the APX3330 inhibitor.
- Kelley, M. R., Wikel, J. H., Guo, C., Pollok, K. E., Bailey, B. J., Wireman, R., ... & Vasko, M. R. (2016). Identification and characterization of new chemical entities targeting apurinic/apyrimidinic endonuclease 1 for the prevention of chemotherapy-induced peripheral neuropathy. *Journal of Pharmacology and Experimental Therapeutics*, *359*(2),

300-309.

- Kelley, M. R., Wikel, J. H., Guo, C., Pollok, K. E., Bailey, B. J., Wireman, R., ... & Vasko, M. R. (2016). Identification of new chemical entities targeting APE1 for the prevention of chemotherapy-induced peripheral neuropathy (CIPN) (a)
- Kelley, M. R., Wikel, J. H., Guo, C., Pollok, K. E., Bailey, B. J., Wireman, R., ... & Vasko, M. R. (2016). Identification and characterization of new chemical entities targeting apurinic/aprimidinic endonuclease 1 for the prevention of chemotherapy-induced peripheral neuropathy. *Journal of Pharmacology and Experimental Therapeutics*, 359(2), 300-309 (b)
- Kerckhove, N., Collin, A., Condé, S., Chaletex, C., Pezet, D., & Balayssac, D. (2017). Long-term effects, pathophysiological mechanisms, and risk factors of chemotherapy-induced peripheral neuropathies: a comprehensive literature review. *Frontiers in pharmacology*, 8, 86.
- Khattab, A., Park, S. J., Patrui, S., Daboul, N., & Monga, D. K. (2019). Case Series of Irinotecan-Induced-Dysarthria: A Review of Literature and Proposition of a Pre-Medication Regimen. *Mathews Journal of Gastroenterology & Hepatology*, 4(1), 1-5.
- Kim, H. S., Guo, C., Thompson, E. L., Jiang, Y., Kelley, M. R., Vasko, M. R., & Lee, S. H. (2015). APE1, the DNA base excision repair protein, regulates the removal of platinum adducts in sensory neuronal cultures by NER. *Mutation Research/Fundamental and Molecular Mechanisms of Mutagenesis*, 779, 96-104.
- Kim, S. H., & Kim, H. (2018). Inhibitory effect of astaxanthin on oxidative stress-induced mitochondrial dysfunction-a mini-review. *Nutrients*, 10(9), 1137.
- Kleih, M., Böpple, K., Dong, M., Gaißler, A., Heine, S., Olayioye, M. A., ... & Essmann, F. (2019). The direct impact of cisplatin on mitochondria induces ROS production that dictates the cell fate of ovarian cancer cells. *Cell death & disease*, 10(11), 1-12.
- Knauf, C., Abot, A., Wemelle, E., & Cani, P. D. (2020). Targeting the enteric nervous system to treat metabolic disorders? "Enterosynes" as therapeutic gut factors. *Neuroendocrinology*, 110(1-2), 139-146.
- Köhne, C. H., Hofheinz, R., Mineur, L., Letocha, H., Greil, R., Thaler, J., ... & Karthaus, M. (2012). First-line panitumumab plus irinotecan/5-fluorouracil/leucovorin treatment in patients with metastatic colorectal cancer. *Journal of cancer research and clinical oncology*, 138(1), 65-72.
- Kolb, E. A., Houghton, P. J., Kurmasheva, R. T., Mosse, Y. P., Maris, J. M., Erickson, S. W., ... & Gorlick, R. (2020). Preclinical evaluation of the combination of AZD1775 and irinotecan against selected pediatric solid tumors: A Pediatric Preclinical Testing Consortium report. *Pediatric blood & cancer*, 67(5), e28098.
- Koopman, M., Antonini, N. F., Douma, J., Wals, J., Honkoop, A. H., Erdkamp, F. L., ... & Punt, C. J. (2007). Sequential versus combination chemotherapy with capecitabine, irinotecan, and oxaliplatin in advanced colorectal cancer (CAIRO): a phase III randomised controlled trial. *The Lancet*, 370(9582), 135-142.
- Koshiji, M., To, K. K. W., Hammer, S., Kumamoto, K., Harris, A. L., Modrich, P., & Huang, L. E. (2005). HIF-1 α induces genetic instability by transcriptionally downregulating MutSa expression. *Molecular cell*, 17(6), 793-803.
- Koukourakis, M. I., Giatromanolaki, A., Kakolyris, S., Sivridis, E., Georgoulas, V., Funtzilias, G., ... & Harris, A. L. (2001). The nuclear expression of human apurinic/aprimidinic endonuclease (HAP1/Ref-1) in head-and-neck cancer is associated with resistance to chemoradiotherapy and poor outcome. *International Journal of Radiation Oncology* Biology* Physics*, 50(1), 27-36.

- Kowalska, M., Piekut, T., Prendecki, M., Sodel, A., Kozubski, W., & Dorszewska, J. (2020). Mitochondrial and nuclear DNA oxidative damage in physiological and pathological aging. *DNA and cell biology*, 39(8), 1410-1420.
- Kpenu, E., & Kelley, M. (2021). The potential role of STAT3 In the APE1/NF-kB regulatory axis in K-rasLSL. G12D/+; Pdx-1-Cre (KC) pancreatic tumour model. *Proceedings of IMPRS*, 4(1).
- Krishnamurthi, S. S., & Macaron, C. (2019). Management of acute chemotherapy-related diarrhea. *Up-to-date*. Accessed August, 5.
- Kroschinsky, F., Stölzel, F., von Bonin, S., Beutel, G., Kochanek, M., Kiehl, M., & Schellongowski, P. (2017). New drugs, new toxicities: severe side effects of modern targeted and immunotherapy of cancer and their management. *Critical Care*, 21(1), 1-11.
- Kuebler, J. P., Wieand, H. S., O'Connell, M. J., Smith, R. E., Colangelo, L. H., Yothers, G., ... & Wolmark, N. (2007). Oxaliplatin combined with weekly bolus fluorouracil and leucovorin as surgical adjuvant chemotherapy for stage II and III colon cancer: results from NSABP C-07. *Journal of clinical oncology*, 25(16), 2198-2204.
- Kuninger, D. T., Izumi, T., Papaconstantinou, J., & Mitra, S. (2002). Human AP-endonuclease 1 and hnRNP-L interact with a scare-like repressor element in the AP-endonuclease 1 promoter. *Nucleic acids research*, 30(3), 823-829.
- Kunze, W. A., Mao, Y. K., Wang, B., Huizinga, J. D., Ma, X., Forsythe, P., & Bienenstock, J. (2009). Lactobacillus reuteri enhances the excitability of colonic AH neurons by inhibiting calcium-dependent potassium channel opening. *Journal of cellular and molecular medicine*, 13(8b), 2261-2270.
- Kwon, Y. (2016). Mechanism-based management for mucositis: option for treating side effects without compromising the efficacy of cancer therapy. *OncoTargets and therapy*, 9, 2007.
- Laev, S. S., Salakhutdinov, N. F., & Lavrik, O. I. (2017). Inhibitors of nuclease and redox activity of apurinic/aprimidinic endonuclease 1/redox effector factor 1 (APE1/Ref-1). *Bioorganic & medicinal chemistry*, 25(9), 2531-2544.
- Lahtz, C., & Pfeifer, G. P. (2011). Epigenetic changes of DNA repair genes in cancer. *Journal of molecular cell biology*, 3(1), 51-58.
- Lando, D., Pongratz, I., Poellinger, L., & Whitelaw, M. L. (2000). A redox mechanism controls differential DNA binding activities of hypoxia-inducible factor (HIF) 1 α and the HIF-like factor. *Journal of Biological Chemistry*, 275(7), 4618-4627.
- Landre, T., Maillard, E., Taleb, C., Ghebriou, D., Guetz, G. D., Zelek, L., & Aparicio, T. (2018). Impact of the addition of bevacizumab, oxaliplatin, or irinotecan to fluoropyrimidin in the first-line treatment of metastatic colorectal cancer in elderly patients. *International Journal of Colorectal Disease*, 33(8), 1125-1130.
- Langie, S. A., Knaapen, A. M., Houben, J. M., van Kempen, F. C., de Hoon, J. P., Gottschalk, R. W., ... & van Schooten, F. J. (2007). The role of glutathione in the regulation of nucleotide excision repair during oxidative stress. *Toxicology Letters*, 168(3), 302-309.
- Lassmann, H., & van Horssen, J. (2016). Oxidative stress and its impact on neurons and glia in multiple sclerosis lesions. *Biochimica et Biophysica Acta (BBA)-Molecular Basis of Disease*, 1862(3), 506-510.
- Lau, J. P., Weatherdon, K. L., Skalski, V., & Hedley, D. W. (2004). Effects of gemcitabine on APE/ref-1 endonuclease activity in pancreatic cancer cells, and the therapeutic potential of antisense oligonucleotides. *British journal of cancer*, 91(6), 1166-1173.
- Lebwohl, D., & Canetta, R. (1998). Clinical development of platinum complexes in cancer therapy: a historical perspective and an update. *European journal of cancer*, 34(10), 1522-1534.

- Lecarpentier, E., Ouaffi, L., Mir, O., Berveiller, P., Maurel, M., Pujade-Lauraine, E., ... & Veyrie, N. (2011). Bevacizumab-induced small bowel perforation in a patient with breast cancer without intraabdominal metastases. *Investigational new drugs*, 29(6), 1500-1503.
- Lecarpentier, T., Benezit, A., Marostica, A., Brasme, J. F., Vallet, C., Chalumeau, M., ... & Gendrel, D. (2010). Epidemics of gastroenteritis caused by norovirus in Parisian children. *Archives de pediatrie: organe officiel de la Societe francaise de pediatrie*, 17(11), 1522-1526.
- Lecci, A., Santicoli, P., & Maggi, C. A. (2002). Pharmacology of transmission to gastrointestinal muscle. *Current opinion in pharmacology*, 2(6), 630-641.
- Lee, B., Min, J. A., Nashed, A., Lee, S. O., Yoo, J. C., Chi, S. W., & Yi, G. S. (2019). A novel mechanism of irinotecan targeting MDM2 and Bcl-xL. *Biochemical and biophysical research communications*, 514(2), 518-523.
- Lee, E., & Wen, P. Y. (2021). Overview of neurologic complications of platinum-based chemotherapy. *Up to Date, Inc.*
- Lee, H. M., Yuk, J. M., Shin, D. M., Yang, C. S., Kim, K. K., Choi, D. K., ... & Jo, E. K. (2009). Apurinic/aprimidinic endonuclease 1 is a key modulator of keratinocyte inflammatory responses. *The Journal of Immunology*, 183(10), 6839-6848.
- Lee, H., Jeong, A. J., & Ye, S. K. (2019). Highlighted STAT3 as a potential drug target for cancer therapy. *BMB reports*, 52(7), 415.
- Lee, Y. R., Joo, H. K., & Jeon, B. H. (2020). The biological role of apurinic/aprimidinic endonuclease1/redox factor-1 as a therapeutic target for vascular inflammation and as a serologic biomarker. *Biomedicines*, 8(3), 57.
- Leeman, R. J., Lui, V. W. Y., & Grandis, J. R. (2006). STAT3 as a therapeutic target in head and neck cancer. *Expert opinion on biological therapy*, 6(3), 231-241.
- Lehmann, S., Costa, A. C., Celardo, I., Loh, S. H. Y., & Martins, L. M. (2016). Parp mutations protect against mitochondrial dysfunction and neurodegeneration in a PARKIN model of Parkinson's disease. *Cell death & disease*, 7(3), e2166-e2166.
- Lenkiewicz, A. M., Czapski, G. A., Jęsko, H., Wilkaniec, A., Szypuła, W., Pietrosiuk, A., ... & Adamczyk, A. (2016). Potent effects of alkaloid-rich extract from *Huperzia selago* against sodium nitroprusside-evoked PC12 cells damage via attenuation of oxidative stress and apoptosis. *Folia Neuropathologica*, 54(2), 156-166.
- Leonard, P., Seymour, M. T., James, R., Hochhauser, D., & Ledermann, J. A. (2002). Phase II study of irinotecan with bolus and high dose infusional 5-FU and folinic acid (modified de Gramont) for first or second line treatment of advanced or metastatic colorectal cancer. *British journal of cancer*, 87(11), 1216-1220.
- Leslie, T. (2019). Nausea and Vomiting. In *Patient Assessment in Clinical Pharmacy* (pp. 79-89). Springer, Cham.
- Leung, L., Riutta, T., Kotecha, J., & Rosser, W. (2011). Chronic constipation: an evidence-based review. *The Journal of the American Board of Family Medicine*, 24(4), 436-451.
- Levi, F., Pierpoint, B., Garufi, C., Foran, C., Chollet, P., Depres-Brummer, P., ... & Misset, J. L. (1993). Oxaliplatin activity against metastatic colorectal cancer. A phase II study of 5-day continuous venous infusion at circadian rhythm modulated rate. *European Journal of Cancer*, 29(9), 1280-1284.
- Li, J., & Yuan, J. (2008). Caspases in apoptosis and beyond. *Oncogene*, 27(48), 6194-6206.
- Li, M. X., Wang, D., Zhong, Z. Y., Xiang, D. B., Li, Z. P., Xie, J. Y., ... & Qing, Y. (2008). Targeting

truncated APE1 in mitochondria enhances cell survival after oxidative stress. *Free Radical Biology and Medicine*, 45(5), 592-601.

- Li, M., Yang, X., Lu, X., Dai, N., Zhang, S., Cheng, Y., ... & Wilson III, D. M. (2018). APE1 deficiency promotes cellular senescence and premature aging features. *Nucleic acids research*, 46(11), 5664-5677.
- Li, Q., Zhou, Z. W., Duan, W., Qian, C. Y., Wang, S. N., Deng, M. S., ... & Xu, C. X. (2021). Inhibiting the redox function of APE1 suppresses cervical cancer metastasis via disengagement of ZEB1 from E-cadherin in EMT. *Journal of Experimental & Clinical Cancer Research*, 40(1), 1-13.
- Linden, D. R., Couvrette, J. M., Ciolino, A., McQuoid, C., Blaszyk, H., Sharkey, K. A., & Mawe, G. M. (2005). Indiscriminate loss of myenteric neurones in the TNBS-inflamed guinea-pig distal colon. *Neurogastroenterology & Motility*, 17(5), 751-760.
- Liu, P., Kimmoun, E., Legrand, A., Sauvanet, A., Degott, C., Lardeux, B., & Bernuau, D. (2002). Activation of NF-kappaB, AP-1 and STAT transcription factors is a frequent and early event in human hepatocellular carcinomas. *Journal of hepatology*, 37(1), 63-71.
- Liu, Y., Zhang, Z., Zhang, L., & Zhong, Z. (2020). Cytoplasmic APE1 promotes resistance response in osteosarcoma patients with cisplatin treatment. *Cell biochemistry and function*, 38(2), 195-203.
- Logan, R. M., Gibson, R. J., Bowen, J. M., Stringer, A. M., Sonis, S. T., & Keefe, D. M. (2008). Characterisation of mucosal changes in the alimentary tract following administration of irinotecan: implications for the pathobiology of mucositis. *Cancer chemotherapy and pharmacology*, 62(1), 33-41.
- Logan, R. M., Stringer, A. M., Bowen, J. M., Gibson, R. J., Sonis, S. T., & Keefe, D. M. (2009). Is the pathobiology of chemotherapy-induced alimentary tract mucositis influenced by the type of mycotoxin drug administered?. *Cancer chemotherapy and pharmacology*, 63(2), 239-251.
- Lomax, A. E., O'Hara, J. R., Hyland, N. P., Mawe, G. M., & Sharkey, K. A. (2007). Persistent alterations to enteric neural signalling in the guinea pig colon following the resolution of colitis. *American Journal of Physiology-Gastrointestinal and Liver Physiology*, 292(2), G482-G491.
- Long, K., Gu, L., Li, L., Zhang, Z., Li, E., Zhang, Y., ... & Hu, Z. (2021). Small-molecule inhibition of APE1 induces apoptosis, pyroptosis, and necroptosis in non-small cell lung cancer. *Cell death & disease*, 12(6), 1-15.
- López Jiménez, D., Rodríguez Pérez, J. A., & Bañuelos Rodríguez, S. (2021). Molecular Mechanisms Regulating the DNA Repair Protein APE1: A Focus on Its Flexible N-Terminal Tail Domain.
- Louvet, C., Andre, T., Tigaud, J. M., Gamelin, E., Douillard, J. Y., Brunet, R., ... & De Gramont, A. (2002). Phase II study of oxaliplatin, fluorouracil, and folinic acid in locally advanced or metastatic gastric cancer patients. *Journal of Clinical Oncology*, 20(23), 4543-4548.
- Lu, G., Rao, M., Zhu, P., Linendoll, N., Buja, M. L., Bhattacharjee, M. B., ... & Zhu, J. J. (2022). Postmortem Study of Organ-Specific Toxicity in Glioblastoma Patients Treated with a Combination of Temozolomide, Irinotecan and Bevacizumab.
- Lundgren, O., Peregrin, A. T., Persson, K., Kordasti, S., Uhnöo, I., & Svensson, L. (2000). Role of the enteric nervous system in the fluid and electrolyte secretion of rotavirus diarrhea. *Science*, 287(5452), 491-495.
- Luo, M., Delaplane, S., Jiang, A., Reed, A., He, Y., Fishel, M., ... & Kelley, M. R. (2008). Role of the multifunctional DNA repair and redox signalling protein Ape1/Ref-1 in cancer and

- endothelial cells: small-molecule inhibition of the redox function of Ape1. *Antioxidants & redox signaling*, 10(11), 1853-1867.
- Luo, M., He, H., Kelley, M. R., & Georgiadis, M. M. (2010). Redox regulation of DNA repair: implications for human health and cancer therapeutic development. *Antioxidants & redox signaling*, 12(11), 1247-1269.
- Luo, Z. Q., Ma, W. K., So, A. M. C., Ye, Y., & Zhang, S. (2010). Semidefinite relaxation of quadratic optimization problems. *IEEE Signal Processing Magazine*, 27(3), 20-34.b
- Ma, J., Kavelaars, A., Dougherty, P. M., & Heijnen, C. J. (2018). Beyond symptomatic relief for chemotherapy-induced peripheral neuropathy: Targeting the source. *Cancer*, 124(11), 2289-2298.
- Ma, M. K., Zamboni, W. C., Radomski, K. M., Furman, W. L., Santana, V. M., Houghton, P. J., ... & Stewart, C. F. (2000). Pharmacokinetics of irinotecan and its metabolites SN-38 and APC in children with recurrent solid tumors after protracted low-dose irinotecan. *Clinical Cancer Research*, 6(3), 813-819.
- Machover, D., Diaz-Rubio, E., De Gramont, A., Schilf, A., Gastiaburu, J. J., Brienza, S., ... & Ychou, M. (1996). Two consecutive phases II studies of oxaliplatin (L-OHP) for treatment of patients with advanced colorectal carcinoma who were resistant to previous treatment with fluoropyrimidines. *Annals of Oncology*, 7(1), 95-98.
- MacKenzie, S. H., & Clark, A. C. (2012). Death by caspase dimerization. *Protein dimerization and oligomerization in biology*, 55-73.
- Madhusudan, S., Smart, F., Shrimpton, P., Parsons, J. L., Gardiner, L., Houlbrook, S., ... & Hickson, I. D. (2005). Isolation of a small molecule inhibitor of DNA base excision repair. *Nucleic acids research*, 33(15), 4711-4724.
- Makovec, T. (2019). Cisplatin and beyond: molecular mechanisms of action and drug resistance development in cancer chemotherapy. *Radiology and oncology*, 53(2), 148-158.
- Malfatti, M. C., Antoniali, G., Codrich, M., & Tell, G. (2021). Coping with RNA damage with a focus on APE1, a BER enzyme at the crossroad between DNA damage repair and RNA processing/decay. *DNA repair*, 104, 103133.
- Mancini, I., & Bruera, E. (1998). Constipation in advanced cancer patients. *Supportive Care in Cancer*, 6(4), 356-364.
- Mani, S., Manalo, J., & Bregman, D. (2000). Novel combinations with oxaliplatin. *Oncology (Williston Park, NY)*, 14(12 Suppl 11), 52-58.
- Manjelievskaia, J., Brown, D., McGlynn, K. A., Anderson, W., Shriver, C. D., & Zhu, K. (2017). Chemotherapy use and survival among young and middle-aged patients with colon cancer. *JAMA surgery*, 152(5), 452-459.
- Marín-Díez, E., & Del Pozo, J. C. (2021). Diagnostic approach to small-bowel wall thickening: Beyond Crohn's disease and cancer. *Radiología (English Edition)*, 63(6), 519-530.
- Markovina, S., Youssef, F., Roy, A., Aggarwal, S., Khwaja, S., DeWees, T., ... & Olsen, J. R. (2017). Improved metastasis-and disease-free survival with preoperative sequential short-course radiation therapy and FOLFOX chemotherapy for rectal cancer compared with neoadjuvant long-course chemoradiotherapy: results of a matched pair analysis. *International Journal of Radiation Oncology* Biology* Physics*, 99(2), 417-426.
- Maroun, J. A., Anthony, L. B., Blais, N., Burkes, R., Dowden, S. D., Dranitsaris, G., ... & Wong, R. (2007). Prevention and management of chemotherapy-induced diarrhea in patients with colorectal cancer: a consensus statement by the Canadian Working Group on Chemotherapy-Induced Diarrhea. *Current Oncology*, 14(1), 13-20.

- Marschner, N., Arnold, D., Engel, E., Hutzschenreuter, U., Rauh, J., Freier, W., ... & Jänicke, M. (2015). oxaliplatin-based first-line chemotherapy is associated with improved overall survival compared to first-line treatment with irinotecan-based chemotherapy in patients with metastatic colorectal cancer—results from a prospective cohort study. *Clinical epidemiology*, 7, 295.
- Martínez-Ruiz, A., Cadenas, S., & Lamas, S. (2011). Nitric oxide signalling: classical, less classical, and nonclassical mechanisms. *Free Radical Biology and Medicine*, 51(1), 17-29.
- Martini, G., Troiani, T., Cardone, C., Vitiello, P., Sforza, V., Ciardiello, D., ... & Martinelli, E. (2017). Present and future of metastatic colorectal cancer treatment: a review of new candidate targets. *World journal of gastroenterology*, 23(26), 4675.
- Martino, E., Della Volpe, S., Terribile, E., Benetti, E., Sakaj, M., Centamore, A., ... & Collina, S. (2017). The long story of camptothecin: From traditional medicine to drugs. *Bioorganic & medicinal chemistry letters*, 27(4), 701-707.
- Martinvalet, D., Zhu, P., & Lieberman, J. (2005). Granzyme A induces caspase-independent mitochondrial damage, a required first step for apoptosis. *Immunity*, 22(3), 355-370.
- Mastrangelo, S., Attina, G., Triarico, S., Romano, A., Maurizi, P., & Ruggiero, A. (2022). The DNA-topoisomerase Inhibitors in Cancer Therapy. *Biomedical and Pharmacology Journal*, 15(2).
- Maulik, N., & Das, D. K. (2002). Redox signalling in vascular angiogenesis. *Free Radical Biology and Medicine*, 33(8), 1047-1060.
- Mauri, G., Gori, V., Bonazzina, E., Amatu, A., Tosi, F., Bencardino, K., ... & Sartore-Bianchi, A. (2020). Oxaliplatin retreatment in metastatic colorectal cancer: Systematic review and future research opportunities. *Cancer Treatment Reviews*, 91, 102112.
- Mayo, B. J., Stringer, A. M., Bowen, J. M., Bateman, E. H., & Keefe, D. M. (2017). Irinotecan-induced mucositis: the interactions and potential role of GLP-2 analogues. *Cancer chemotherapy and pharmacology*, 79(2), 233-249.
- McCallion, K., Mitchell, R. M. S., Wilson, R. H., Kee, F., Watson, R. G. P., Collins, J. S. A., & Gardiner, K. R. (2001). Flexible sigmoidoscopy and the changing distribution of colorectal cancer: implications for screening. *Gut*, 48(4), 522-525.
- McCulloch, S. M., Aziz, I., Polster, A. V., Pischel, A. B., Stålsmeden, H., Shafazand, M., ... & Simren, M. (2020). The diagnostic value of a change in bowel habit for colorectal cancer within different age groups. *United European Gastroenterology Journal*, 8(2), 211-219.
- McDonald, E. S., & Windebank, A. J. (2002). Cisplatin-induced apoptosis of DRG neurons involves Bax redistribution and cytochrome release but not Fas receptor signalling. *Neurobiology of Disease*, 9(2), 220-233.
- McIlwain, D. R., Berger, T., & Mak, T. W. (2013). Caspase functions in cell death and disease. *Cold Spring Harbor perspectives in biology*, 5(4), a008656.
- McIlwain, D. W., Fishel, M. L., Boos, A., Kelley, M. R., & Jerde, T. J. (2018). APE1/Ref-1 redox-specific inhibition decreases survivin protein levels and induces cell cycle arrest in prostate cancer cells. *Oncotarget*, 9(13), 10962.
- McMahon, G. (2000). VEGF receptor signalling in tumour angiogenesis. *The oncologist*, 5, 3-10.
- McMurray, C. T. (2005). To die or not to die: DNA repair in neurons. *Mutation Research/Fundamental and Molecular Mechanisms of Mutagenesis*, 577(1-2), 260-274.
- McQuade R, Stojanovska V, Abalo R, Bornstein JC, Nurgali K (2016) Chemotherapy-induced constipation and diarrhoea: pathophysiology, current and emerging treatments. Invited review. *Frontiers in Pharmacology* 7:414.

- McQuade R, Stojanovska V, Bornstein JC, Nurgali K (2017) Colorectal cancer chemotherapy: the evolution of treatment and new approaches. *Current Medicinal Chemistry* 24(15):1537-1557.
- McQuade, R. M., Al Thaalibi, M., & Nurgali, K. (2020). Impact of chemotherapy-induced enteric nervous system toxicity on gastrointestinal mucositis. *Current Opinion in Supportive and Palliative Care*, 14(3), 293-300.
- McQuade, R. M., Carbone, S. E., Stojanovska, V., Rahman, A., Gwynne, R. M., Robinson, A. M., ... & Nurgali, K. (2016). Role of oxidative stress in oxaliplatin-induced enteric neuropathy and colonic dysmotility in mice. *British journal of pharmacology*, 173(24), 3502-3521.
- McQuade, R. M., Stojanovska, V., Abalo, R., Bornstein, J. C., & Nurgali, K. (2016). Chemotherapy-induced constipation and diarrhea: pathophysiology, current and emerging treatments. *Frontiers in pharmacology*, 7, 414.
- McQuade, R. M., Stojanovska, V., Donald, E., Abalo, R., Bornstein, J. C., & Nurgali, K. (2016). Gastrointestinal dysfunction and enteric neurotoxicity following treatment with anticancer chemotherapeutic agent 5-fluorouracil. *Neurogastroenterology & Motility*, 28(12), 1861-1875.
- McQuade, R. M., Stojanovska, V., Stavely, R., Timpani, C., Petersen, A. C., Abalo, R., ... & Nurgali, K. (2018). Oxaliplatin-induced enteric neuronal loss and intestinal dysfunction is prevented by co-treatment with BGP-15. *British Journal of Pharmacology*, 175(4), 656-677.
- McQuade, R., Bornstein, J. C., & Nurgali, K. (2014). Anti-colorectal cancer chemotherapy-induced diarrhoea: current treatments and side-effects. *International Journal of Clinical Medicine*, 5(7), 393-406.
- McQuade, R., Stojanovska, V., C Bornstein, J., & Nurgali, K. (2017). Colorectal cancer chemotherapy: the evolution of treatment and new approaches. *Current medicinal chemistry*, 24(15), 1537-1557.
- McQuade, R., Stojanovska, V., Sorensen, J. C., Bornstein, J. C., Petersen, A., Rybalka, E., & Nurgali, K. (2016). BGP-15 co-treatment protects against oxaliplatin-induced neuronal loss and alleviates gastrointestinal dysfunction. *Neurogastroenterology and Motility*, 28(S1), 52-53.
- Mego, M., Chovanec, J., Andrezalova, I., Konkolovsky, P., Mikulova, M., Reckova, M., ... & Drgona, L. (2014). Prevention of irinotecan-induced diarrhea by probiotics: Randomized double-blind, placebo-controlled phase III study.
- Melli, G., Taiana, M., Camozzi, F., Triolo, D., Podini, P., Quattrini, A., ... & Lauria, G. (2008). Alpha-lipoic acid prevents mitochondrial damage and neurotoxicity in experimental chemotherapy neuropathy. *Experimental neurology*, 214(2), 276-284.
- Melzer, C., von der Ohe, J., & Hass, R. (2017). Breast carcinoma: from initial tumor cell detachment to settlement at secondary sites. *BioMed Research International*, 2017.
- Meyerhardt, J. A., & Mayer, R. J. (2005). Systemic therapy for colorectal cancer. *New England journal of medicine*, 352(5), 476-487.
- Mijit, M., Caston, R., Gampala, S., Fishel, M. L., Fehrenbacher, J., & Kelley, M. R. (2021). APE1/Ref-1—One Target with Multiple Indications: Emerging Aspects and New Directions. *Journal of cellular signaling*, 2(3), 151.
- Mijit, M., Liu, S., Sishtla, K., Hartman, G. D., Wan, J., Corson, T. W., & Kelley, M. R. (2023). Identification of Novel Pathways Regulated by APE1/Ref-1 in Human Retinal Endothelial Cells. *International Journal of Molecular Sciences*, 24(2), 1101.

- Mijit, M., Wireman, R., Armstrong, L., Gampala, S., Hassan, Z., Schneeweis, C., ... & Kelley, M. R. (2022). RelA Is an Essential Target for Enhancing Cellular Responses to the DNA Repair/Ref-1 Redox Signaling Protein and Restoring Perturbed Cellular Redox Homeostasis in Mouse PDAC Cells. *Frontiers in oncology*, 12, 826617-826617.
- Miller, K. D., Nogueira, L., Mariotto, A. B., Rowland, J. H., Yabroff, K. R., Alfano, C. M., ... & Siegel, R. L. (2019). Cancer treatment and survivorship statistics, 2019. *CA: a cancer journal for clinicians*, 69(5), 363-385.
- Miller, K. D., Siegel, R. L., Lin, C. C., Mariotto, A. B., Kramer, J. L., Rowland, J. H., ... & Jemal, A. (2016). Cancer treatment and survivorship statistics, 2016. *CA: a cancer journal for clinicians*, 66(4), 271-289.
- Miller, S., Senior, P. V., Prakash, M., Apostolopoulos, V., Sakkal, S., & Nurgali, K. (2016). Leukocyte populations and IL-6 in the tumour microenvironment of an orthotopic colorectal cancer model. *Acta Biochim Biophys Sin*, 48(4), 334-341.
- Mishra, B., & Jha, R. (2019). Oxidative stress in the poultry gut: Potential challenges and interventions. *Frontiers in veterinary science*, 6, 60.
- Mitchel, R. E. (2006). Low doses of radiation are protective in vitro and in vivo: evolutionary origins. *Dose-response*, 4(2), dose-response.
- Mitchell, E. P. (2006, February). Gastrointestinal toxicity of chemotherapeutic agents. In *Seminars in oncology* (Vol. 33, No. 1, pp. 106-120). WB Saunders.
- Mittal, S., Brown, N. J., & Holen, I. (2018). The breast tumor microenvironment: role in cancer development, progression and response to therapy. *Expert review of molecular diagnostics*, 18(3), 227-243.
- Moore, D. H., Michael, H., Tritt, R., Parsons, S. H., & Kelley, M. R. (2000). Alterations in the expression of the DNA repair/redox enzyme APE/ref-1 in epithelial ovarian cancers. *Clinical Cancer Research*, 6(2), 602-609.
- Morris, R., Kershaw, N. J., & Babon, J. J. (2018). The molecular details of cytokine signalling via the JAK/STAT pathway. *Protein Science*, 27(12), 1984-2009.
- Moschen, A. R., Sammy, Y., Marjenberg, Z., Heptinstall, A. B., Pooley, N., & Marczewska, A. M. (2022). The Underestimated and Overlooked Burden of Diarrhea and Constipation in Cancer Patients. *Current Oncology Reports*, 1-14.
- Mourad, F. H., Barada, K. A., Abdel-Malak, N., Rached, N. B., Khoury, C. I., Saade, N. E., & Nassar, C. F. (2003). The interplay between nitric oxide and vasoactive intestinal polypeptide in inducing fluid secretion in rat jejunum. *The Journal of Physiology*, 550(3), 863-871.
- Muggia, F. M., Braly, P. S., Brady, M. F., Sutton, G., Niemann, T. H., Lentz, S. L., ... & Small, J. M. (2000). Phase III randomized study of cisplatin versus paclitaxel versus cisplatin and paclitaxel in patients with suboptimal stage III or IV ovarian cancer: a gynecologic oncology group study. *Journal of Clinical Oncology*, 18(1), 106-106.
- Muniyandi, A., Hartman, G. D., Day, K., Qi, X., Boulton, M., Kelley, M. R., & Corson, T. W. (2022). APE1/Ref-1 is highly expressed in murine laser-induced choroidal neovascularization and human neovascular age-related macular degeneration. *Investigative Ophthalmology & Visual Science*, 63(7), 0005-0005.
- Nagoya, H., Futagami, S., Shimpuku, M., Tatsuguchi, A., Wakabayashi, T., Yamawaki, H., ... & Sakamoto, C. (2014). Apurinic/aprimidinic endonuclease-1 is associated with angiogenesis and VEGF production via upregulation of COX-2 expression in esophageal cancer tissues. *American Journal of Physiology-Gastrointestinal and Liver Physiology*, 306(3), G183-G190.

- Nassour, H., Wang, Z., Saad, A., Papaluca, A., Brosseau, N., Affar, E. B., ... & Ramotar, D. (2016). Peroxiredoxin 1 interacts with and blocks the redox factor APE1 from activating interleukin-8 expression. *Scientific Reports*, 6(1), 29389.
- Nath, S., Roychoudhury, S., Kling, M. J., Song, H., Biswas, P., Shukla, A., ... & Bhakat, K. K. (2017). The extracellular role of DNA damage repair protein APE1 in the regulation of IL-6 expression. *Cellular signalling*, 39, 18-31.
- Nishida, N., Yano, H., Nishida, T., Kamura, T., & Kojiro, M. (2006). Angiogenesis in cancer. *Vascular health and risk management*, 2(3), 213.
- Nishikawa, H., Goto, M., Fukunishi, S., Asai, A., Nishiguchi, S., & Higuchi, K. (2021). Cancer cachexia: its mechanism and clinical significance. *International Journal of Molecular Sciences*, 22(16), 8491.
- Noll, D. M., Mason, T. M., & Miller, P. S. (2006). Formation and repair of interstrand cross-links in DNA. *Chemical Reviews*, 106(2), 277-301.
- Numico, G., Longo, V., Courthod, G., & Silvestris, N. (2015). Cancer survivorship: long-term side-effects of anticancer treatments of gastrointestinal cancer. *Current opinion in oncology*, 27(4), 351-357.
- Nurgali, K. (2009). Plasticity and ambiguity of the electrophysiological phenotypes of enteric neurons. *Neurogastroenterology & Motility*, 21(9), 903-913.
- Nurgali, K., Jagoe, R. T., & Abalo, R. (2018). Adverse effects of cancer chemotherapy: Anything new to improve tolerance and reduce sequelae?. *Frontiers in pharmacology*, 9, 245.
- Nurgali, K., Nguyen, T. V., Matsuyama, H., Thacker, M., Robbins, H. L., & Furness, J. B. (2007). Phenotypic changes of morphologically identified guinea-pig myenteric neurons following intestinal inflammation. *The Journal of Physiology*, 583(2), 593-609.
- Nurgali, K., Nguyen, T. V., Thacker, M., Pontell, L., & Furness, J. B. (2009). Slow synaptic transmission in myenteric AH neurons from the inflamed guinea pig ileum. *American Journal of Physiology-Gastrointestinal and Liver Physiology*, 297(3), G582-G593.
- Nurgali, K., Qu, Z., Hunne, B., Thacker, M., Pontell, L., & Furness, J. B. (2011). Morphological and functional changes in guinea-pig neurons projecting to the ileal mucosa at early stages after inflammatory damage. *The Journal of Physiology*, 589(2), 325-339.
- Nyland, R. L., Luo, M., Kelley, M. R., & Borch, R. F. (2010). Design and synthesis of novel quinone inhibitors targeted to the redox function of apurinic/apyrimidinic endonuclease 1/redox enhancing factor-1 (Ape1/ref-1). *Journal of medicinal chemistry*, 53(3), 1200-1210.
- O'Reilly, M., Mellotte, G., Ryan, B., & O'Connor, A. (2020). Gastrointestinal side effects of cancer treatments. *Therapeutic Advances in Chronic Disease*, 11, 2040622320970354.
- Ochoa-Cortes, F., Turco, F., Linan-Rico, A., Soghomonyan, S., Whitaker, E., Wehner, S., ... & Christofi, F. L. (2016). Enteric glial cells: a new frontier in neurogastroenterology and clinical target for inflammatory bowel diseases. *Inflammatory bowel diseases*, 22(2), 433-449.
- Oechsle, K., Kollmannsberger, C., Honecker, F., Mayer, F., Waller, C. F., Hartmann, J. T., ... & German. Testicular Cancer Study Group. (2011). Long-term survival after treatment with gemcitabine and oxaliplatin with and without paclitaxel plus secondary surgery in patients with cisplatin-refractory and/or multiply relapsed germ cell tumors. *European urology*, 60(4), 850-855.
- Okazaki, T., Chung, U. I., Nishishita, T., Ebisu, S., Usuda, S., Mishiro, S., ... & Ogata, E. (1994). A redox factor protein, ref1, is involved in negative gene regulation by extracellular calcium. *Journal of Biological Chemistry*, 269(45), 27855-27862.

- Okunaka, M., Kano, D., Matsui, R., Kawasaki, T., & Uesawa, Y. (2021). Evaluation of the expression profile of irinotecan-induced diarrhea in patients with colorectal cancer. *Pharmaceuticals*, 14(4), 377.
- Olde Bekkink, M., McCowan, C., Falk, G. A., Teljeur, C., Van de Laar, F. A., & Fahey, T. (2010). Diagnostic accuracy systematic review of rectal bleeding in combination with other symptoms, signs and tests in relation to colorectal cancer. *British journal of cancer*, 102(1), 48-58.
- Oliveira, T. T., Coutinho, L. G., de Oliveira, L. O. A., Timoteo, A. R. D. S., Farias, G. C., & Agnez-Lima, L. F. (2022). APE1/Ref-1 role in inflammation and immune response. *Frontiers in Immunology*, 13, 726.
- Oliveira, T. T., Fontes-Dantas, F. L., de Medeiros Oliveira, R. K., Pinheiro, D. M. L., Coutinho, L. G., Da Silva, V. L., ... & Agnez-Lima, L. F. (2021). Chemical Inhibition of Apurinic-Apyrimidinic Endonuclease 1 Redox and DNA Repair Functions Affects the Inflammatory Response via Different but Overlapping Mechanisms. *Frontiers in cell and developmental biology*, 2583.
- Ono, Y., Furuta, T., Ohmoto, T., Akiyama, K., & Seki, S. (1994). Stable expression in rat glioma cells of sense and antisense nucleic acids to a human multifunctional DNA repair enzyme, APEX nuclease. *Mutation Research/DNA Repair*, 315(1), 55-63.
- Onyango, I. G. (2008). Mitochondrial dysfunction and oxidative stress in Parkinson's disease. *Neurochemical Research*, 33(3), 589-597.
- Oun, R., Moussa, Y. E., & Wheate, N. J. (2018). The side effects of platinum-based chemotherapy drugs: a review for chemists. *Dalton transactions*, 47(19), 6645-6653.
- Ozaki, M., Suzuki, S., & Irani, K. (2002). Redox factor-1/APE suppresses oxidative stress by inhibiting the activity of the rac1 GTPase. *The FASEB Journal*, 16(8), 889-890.
- Ozawa, S., Miura, T., Terashima, J., & Habano, W. (2021). Cellular irinotecan resistance in colorectal cancer and overcoming irinotecan refractoriness through various combination trials including DNA methyltransferase inhibitors: a review. *Cancer Drug Resistance*, 4(4), 946-964.
- Pace, A., Giannarelli, D., Galie, E., Savarese, A., Carpano, S., Della Giulia, M., ... & Cognetti, F. (2010). Vitamin E neuroprotection for cisplatin neuropathy: a randomized, placebo-controlled trial. *Neurology*, 74(9), 762-766.
- Pachman, D. R., Loprinzi, C. L., Grothey, A., & Ta, L. E. (2014). The search for treatments to reduce chemotherapy-induced peripheral neuropathy. *The Journal of clinical investigation*, 124(1), 72-74.
- Pachman, D. R., Watson, J. C., & Loprinzi, C. L. (2014). Therapeutic strategies for cancer treatment-related peripheral neuropathies. *Current treatment options in oncology*, 15(4), 567-580.
- Pachman, D. R., Watson, J. C., Lustberg, M. B., Wagner-Johnston, N. D., Chan, A., Broadfield, L., ... & Loprinzi, C. L. (2014). Management options for established chemotherapy-induced peripheral neuropathy. *Supportive Care in Cancer*, 22(8), 2281-2295.
- Pachmayr, E., Treese, C., & Stein, U. (2017). Underlying mechanisms for distant metastasis-molecular biology. *Visceral Medicine*, 33(1), 11-20.
- Park, H., Sanjeevaiah, A., Hosein, P. J., Mehta, R., Jin, R., Grierson, P., ... & Lockhart, A. C. (2022). Ramucirumab and irinotecan in patients with previously treated gastroesophageal adenocarcinoma: Final analysis of a phase II trial.
- Park, S. J., Ye, W., Xiao, R., Silvin, C., Padget, M., Hodge, J. W., ... & Schmitt, N. C. (2019).

Cisplatin and oxaliplatin induce similar immunogenic changes in preclinical models of head and neck cancer. *Oral oncology*, 95, 127-135.

- Park, S., Lee, H., Lee, B., Lee, S. H., Sun, J. M., Park, W. Y., ... & Park, K. (2019). DNA damage response and repair pathway alteration and its association with tumour mutation burden and platinum-based chemotherapy in SCLC. *Journal of Thoracic Oncology*, 14(9), 1640-1650.
- Parkin, D. M. (2001). Global cancer statistics in the year 2000. *The lancet oncology*, 2(9), 533-543.
- Parrish, A. B., Freel, C. D., & Kornbluth, S. (2013). Cellular mechanisms control caspase activation and function. *Cold Spring Harbor perspectives in biology*, 5(6), a008672.
- Parvez, M. M., Basit, A., Jariwala, P. B., Gáborik, Z., Kis, E., Heyward, S., ... & Prasad, B. (2021). Quantitative Investigation of Irinotecan Metabolism, Transport, and Gut Microbiome Activation. *Drug Metabolism and Disposition*, 49(8), 683-693.
- Pascut, D., Sukowati, C. H. C., Antoniali, G., Mangiapane, G., Burra, S., Mascaretti, L. G., ... & Tell, G. (2019). Serum AP-endonuclease 1 (sAPE1) as novel biomarker for hepatocellular carcinoma. *Oncotarget*, 10(3), 383.
- Pasha, S. P. B. S., Sishtla, K., Sulaiman, R. S., Park, B., Shetty, T., Shah, F., ... & Corson, T. W. (2018). Ref-1/APE1 inhibition with novel small molecules blocks ocular neovascularization. *Journal of Pharmacology and Experimental Therapeutics*, 367(1), 108-118.
- Passardi, A., Nanni, O., Tassinari, D., Turci, D., Cavanna, L., Fontana, A., ... & Amadori, D. (2015). Effectiveness of bevacizumab added to standard chemotherapy in metastatic colorectal cancer: final results for first-line treatment from the ITACa randomized clinical trial. *Annals of Oncology*, 26(6), 1201-1207.
- Pearce, O. M., Delaine-Smith, R. M., Maniatis, E., Nichols, S., Wang, J., Böhm, S., ... & Balkwill, F. R. (2018). Deconstruction of a metastatic tumour microenvironment reveals a common matrix response in human cancers. *Cancer Discovery*, 8(3), 304-319.
- Peddi, S. R., Chattopadhyay, R., Naidu, C. V., & Izumi, T. (2006). The human apurinic/aprimidinic endonuclease-1 suppresses activation of poly (ADP-ribose) polymerase-1 induced by DNA single-strand breaks. *Toxicology*, 224(1-2), 44-55.
- Peter, A. E., Sandeep, B. V., Rao, B. G., & Kalpana, V. L. (2021). Calming the storm: natural Immunosuppressants as adjuvants to target the cytokine storm in COVID-19. *Frontiers in Pharmacology*, 11, 2305.
- Petrioli, R., Pascucci, A., Francini, E., Marsili, S., Sciandivasci, A., Tassi, R., ... & Francini, G. (2008). Neurotoxicity of FOLFOX-4 as adjuvant treatment for patients with colon and gastric cancer: a randomized study of two different schedules of oxaliplatin. *Cancer chemotherapy and pharmacology*, 61(1), 105-111.
- Pezzuto, A., & Carico, E. (2018). Role of HIF-1 in cancer progression: novel insights. A review. *Current molecular medicine*, 18(6), 343-351.
- Philip Kuebler, J., Colangelo, L., O'Connell, M. J., Smith, R. E., Yothers, G., Begovic, M., ... & Wolmark, N. (2007). Severe enteropathy among patients with stage II/III colon cancer treated on a randomized trial of bolus 5-fluorouracil/leucovorin plus or minus oxaliplatin: A prospective analysis. *Cancer*, 110(9), 1945-1950.
- Phuengkham, H., Ren, L., Shin, I. W., & Lim, Y. T. (2019). Nanoengineered immune niches for reprogramming the immunosuppressive tumour microenvironment and enhancing cancer immunotherapy. *Advanced Materials*, 31(34), 1803322.

- Piccolo, J., & Kolesar, J. M. (2014). Prevention and treatment of chemotherapy-induced peripheral neuropathy. *American journal of health-system pharmacy*, 71(1), 19-25.
- Pini, A., Garella, R., Idrizaj, E., Calosi, L., Baccari, M. C., & Vannucchi, M. G. (2016). Glucagon-like peptide 2 counteracts the mucosal damage and the neuropathy induced by chronic treatment with cisplatin in the mouse gastric fundus. *Neurogastroenterology & Motility*, 28(2), 206-216.
- Pirinen, E., Canto, C., Jo, Y. S., Morato, L., Zhang, H., Menzies, K. J., ... & Auwerx, J. (2014). Pharmacological Inhibition of poly (ADP-ribose) polymerases improves fitness and mitochondrial function in skeletal muscle. *Cell metabolism*, 19(6), 1034-1041.
- Podolski, A. J., & Gucalp, R. (2021). GI Toxicities from Cancer Therapy. In *Geriatric Gastroenterology* (pp. 341-379). Cham: Springer International Publishing.
- Podratz, J. L., Knight, A. M., Ta, L. E., Staff, N. P., Gass, J. M., Genelín, K., ... & Windebank, A. J. (2011). Cisplatin-induced mitochondrial DNA damage in dorsal root ganglion neurons. *Neurobiology of Disease*, 41(3), 661-668.
- Pommier, Y., Redon, C., Rao, V. A., Seiler, J. A., Sordet, O., Takemura, H., ... & Kohn, K. W. (2003). Repair of and checkpoint response to topoisomerase I-mediated DNA damage. *Mutation Research/Fundamental and Molecular Mechanisms of Mutagenesis*, 532(1-2), 173-203.
- Porporato, P. E., Filigheddu, N., Bravo-San Pedro, J. M., Kroemer, G., & Galluzzi, L. (2018). Mitochondrial metabolism and cancer. *Cell research*, 28(3), 265-280.
- Preston, T. J., Henderson, J. T., McCallum, G. P., & Wells, P. G. (2009). Base excision repair of reactive oxygen species-initiated 7, 8-dihydro-8-oxo-2'-deoxyguanosine inhibits the cytotoxicity of platinum anticancer drugs. *Molecular cancer therapeutics*, 8(7), 2015-2026.
- Priego, N., Zhu, L., Monteiro, C., Mulders, M., Wasilewski, D., Bindeman, W., ... & Valiente, M. (2018). STAT3 labels a subpopulation of reactive astrocytes required for brain metastasis. *Nature medicine*, 24(7), 1024-1035.
- Puglisi, F., Barbone, F., Tell, G., Aprile, G., Pertoldi, B., Raiti, C., ... & Di Loreto, C. (2002). Prognostic role of Ape/Ref-1 subcellular expression in stage I-III breast carcinomas. *Oncology reports*, 9(1), 11-17.
- Puglisi, F., Barbone, F., Tell, G., Aprile, G., Pertoldi, B., Raiti, C., ... & Di Loreto, C. (2002). Prognostic role of Ape/Ref-1 subcellular expression in stage I-III breast carcinomas. *Oncology reports*, 9(1), 11-17.
- Qi, G., Mi, Y., Wang, Y., Li, R., Huang, S., Li, X., & Liu, X. (2017). Neuroprotective action of tea polyphenols on oxidative stress-induced apoptosis through the activation of the TrkB/CREB/BDNF pathway and Keap1/Nrf2 signaling pathway in SH-SY5Y cells and mice brain. *Food & function*, 8(12), 4421-4432.
- Qu, Z. D., Thacker, M., Castelucci, P., Bagyanszki, M., Epstein, M. L., & Furness, J. B. (2008). Immunohistochemical analysis of neuron types in the mouse small intestine. *Cell and tissue research*, 334(2), 147-161.
- Quesnelle, K. M., Boehm, A. L., & Grandis, J. R. (2007). STAT-mediated EGFR signalling in cancer. *Journal of cellular biochemistry*, 102(2), 311-319.
- R Kelley, M., M Georgiadis, M., & L Fishel, M. (2012). APE1/Ref-1 role in redox signalling: translational applications of targeting the redox function of the DNA repair/redox protein APE1/Ref-1. *Current molecular pharmacology*, 5(1), 36-53.
- Raffoul, J. J., Banerjee, S., Singh-Gupta, V., Knoll, Z. E., Fite, A., Zhang, H., ... & Hillman, G. G. (2007). Down-regulation of apurinic/aprimidinic endonuclease 1/redox factor-1 expression

- by soy isoflavones enhances prostate cancer radiotherapy in vitro and in vivo. *Cancer Research*, 67(5), 2141-2149.
- Rajapakse, A., Suraweera, A., Boucher, D., Naqi, A., O'Byrne, K., Richard, D. J., & Croft, L. V. (2020). Redox regulation in the base excision repair pathway: old and new players as cancer therapeutic targets. *Current Medicinal Chemistry*, 27(12), 1901-1921.
- Ramasubbu, S. K., Mahato, S. K., Agnihotri, A., Pasricha, R. K., & Nath, U. K. (2021). Prevalence, severity, and nature of risk factors associated with drug-drug interactions in geriatric patients receiving cancer chemotherapy: A prospective study in a tertiary care teaching hospital. *Cancer Treatment and Research Communications*, 26, 100277.
- Ranalli, T. A., Tom, S., & Bambara, R. A. (2002). AP endonuclease 1 coordinates flap endonuclease 1 and DNA ligase I activity in long patch base excision repair. *Journal of Biological Chemistry*, 277(44), 41715-41724.
- Ranieri, G., Laforgia, M., Nardulli, P., Ferraiuolo, S., Molinari, P., Marech, I., & Gadaleta, C. D. (2019). Oxaliplatin-based intra-arterial chemotherapy in colo-rectal cancer liver metastases: a review from pharmacology to clinical application. *Cancers*, 11(2), 141.
- Rawlings, J. S., Rosler, K. M., & Harrison, D. A. (2004). The JAK/STAT signalling pathway. *Journal of cell science*, 117(8), 1281-1283.
- Ray, A., & Cleary, M. P. (2017). The potential role of leptin in tumour invasion and metastasis. *Cytokine & growth factor reviews*, 38, 80-97.
- Ray, S., & Ray, M. K. (2009). Bioremediation of heavy metal toxicity-with special reference to chromium. *Al Ameen J Med Sci*, 2(2), 57-63.
- Ray, S., Lee, C., Hou, T., Bhakat, K. K., & Brasier, A. R. (2010). Regulation of signal transducer and activator of transcription 3 enhanceosome formation by apurinic/aprimidinic endonuclease 1 in hepatic acute phase response. *Molecular endocrinology*, 24(2), 391-401.
- Raymond, E., Chaney, S. G., Taamma, A., & Cvitkovic, E. (1998). Oxaliplatin: a review of preclinical and clinical studies. *Annals of Oncology*, 9(10), 1053-1071.
- Raymond, E., Faivre, S., Woynarowski, J. M., & Chaney, S. G. (1998, April). Oxaliplatin: mechanism of action and antineoplastic activity. In *Seminars in oncology* (Vol. 25, No. 2 Suppl 5, pp. 4-12).
- Reagan-Shaw, S., Nihal, M., & Ahmad, N. (2008). Dose translation from animal to human studies revisited. *The FASEB Journal*, 22(3), 659-661.
- Rébé, C., & Ghiringhelli, F. (2019). STAT3, a master regulator of anti-tumor immune response. *Cancers*, 11(9), 1280.
- Reddy, S. M., Vergo, M. T., Paice, J. A., Kwon, N., Helenowski, I. B., Benson, A. B., ... & Harden, R. N. (2016). Quantitative sensory testing at baseline and during cycle 1 oxaliplatin infusion detects subclinical peripheral neuropathy and predicts clinically overt chronic neuropathy in gastrointestinal malignancies. *Clinical colorectal cancer*, 15(1), 37-46.
- Reginelli, A., Sangiovanni, A., Vacca, G., Belfiore, M. P., Pignatiello, M., Viscardi, G., ... & Cappabianca, S. (2021). Chemotherapy-induced bowel ischemia: diagnostic imaging overview. *Abdominal Radiology*, 1-9.
- Regis, G., Pensa, S., Boselli, D., Novelli, F., & Poli, V. (2008, August). Ups and downs: the STAT1: STAT3 seesaw of Interferon and gp130 receptor signalling. In *Seminars in cell & developmental biology* (Vol. 19, No. 4, pp. 351-359). Academic Press.

- Resnikoff, H., Metzger, J. M., Lopez, M., Bondarenko, V., Mejia, A., Simmons, H. A., & Emborg, M. E. (2019). Colonic inflammation affects myenteric alpha-synuclein in nonhuman primates. *Journal of inflammation research*, *12*, 113.
- Ribeiro, E., Uhl, A., Wimmer, G., & Häfner, M. (2016). Exploring deep learning and transfer learning for colonic polyp classification. *Computational and mathematical methods in medicine*, 2016.
- Ribeiro, R. A., Wanderley, C. W., Wong, D. V., Mota, J. M. S., Leite, C. A., Souza, M. H., ... & Lima-Junior, R. C. (2016). Irinotecan-and 5-fluorouracil-induced intestinal mucositis: insights into pathogenesis and therapeutic perspectives. *Cancer chemotherapy and pharmacology*, *78*(5), 881-893.
- Richardson, G., & Dobish, R. (2007). Chemotherapy-induced diarrhea. *Journal of Oncology Pharmacy Practice*, *13*(4), 181-198.
- Riedl, S. J., & Shi, Y. (2004). Molecular mechanisms of caspase regulation during apoptosis. *Nature reviews Molecular cell biology*, *5*(11), 897-907.
- Ries, L. A. G., Melbert, D., Krapcho, M., Stinchcomb, D. G., Howlader, N., Horner, M. J., ... & Edwards, B. (2008). SEER cancer statistics review, 1975–2005. *Bethesda, MD: National Cancer Institute*, 2999.
- Rivera, L. R., Poole, D. P., Thacker, M., & Furness, J. B. (2011). The involvement of nitric oxide synthase neurons in enteric neuropathies. *Neurogastroenterology & Motility*, *23*(11), 980-988.
- Rivera, L. R., Thacker, M., Pontell, L., Cho, H. J., & Furness, J. B. (2011). Deleterious effects of intestinal ischemia/reperfusion injury in the mouse enteric nervous system are associated with protein nitrosylation. *Cell and tissue research*, *344*(1), 111-123.
- Roberts, J. A., Durnin, L., Sharkey, K. A., Mutafova-Yambolieva, V. N., & Mawe, G. M. (2013). Oxidative stress disrupts purinergic neuromuscular transmission in the inflamed colon. *The Journal of Physiology*, *591*(15), 3725-3737.
- Roberts, R. R., Bornstein, J. C., Bergner, A. J., & Young, H. M. (2008). Disturbances of colonic motility in mouse models of Hirschsprung's disease. *American Journal of Physiology-Gastrointestinal and Liver Physiology*, *294*(4), G996-G1008.
- Roberts, R. R., Bornstein, J. C., Bergner, A. J., & Young, H. M. (2008). Disturbances of colonic motility in mouse models of Hirschsprung's disease. *American Journal of Physiology-Gastrointestinal and Liver Physiology*, *294*(4), G996-G1008.
- Roberts, R. R., Murphy, J. F., Young, H. M., & Bornstein, J. C. (2007). Development of colonic motility in the neonatal mouse studies using spatiotemporal maps. *American Journal of Physiology-Gastrointestinal and Liver Physiology*, *292*(3), G930-G938.
- Robertson, K. A., Bullock, H. A., Xu, Y., Tritt, R., Zimmerman, E., Ulbright, T. M., ... & Kelley, M. R. (2001). Altered expression of Ape1/ref-1 in germ cell tumours and overexpression in NT2 cells confers resistance to bleomycin and radiation. *Cancer Research*, *61*(5), 2220-2225.
- Robinson, A. M., Sakkal, S., Park, A., Jovanovska, V., Payne, N., Carbone, S. E., ... & Nurgali, K. (2014). Mesenchymal stem cells and conditioned medium avert enteric neuropathy and colon dysfunction in guinea pig TNBS-induced colitis. *American Journal of Physiology-Gastrointestinal and Liver Physiology*, *307*(11), G1115-G1129.
- Robinson, A. M., Stojanovska, V., Rahman, A. A., McQuade, R. M., Senior, P. V., & Nurgali, K. (2016). Effects of oxaliplatin treatment on the enteric glial cells and neurons in the mouse ileum. *Journal of Histochemistry & Cytochemistry*, *64*(9), 530-545.

- Rojas-Gutierrez, E., Muñoz-Arenas, G., Treviño, S., Espinosa, B., Chavez, R., Rojas, K., ... & Guevara, J. (2017). Alzheimer's disease and metabolic syndrome: A link from oxidative stress and inflammation to neurodegeneration. *Synapse*, 71(10), e21990.
- Rolfe, D. F., & Brown, G. C. (1997). Cellular energy utilization and molecular origin of standard metabolic rate in mammals. *Physiological Reviews*, 77(3), 731-758.
- Rong, X., Liu, H., Yu, H., Zhao, J., Wang, J., & Wang, Y. (2022). Efficacy of apatinib combined with FOLFIRI in the first-line treatment of patients with metastatic colorectal cancer. *Investigational New Drugs*, 1-9.
- Rosenberg, B., Van Camp, L., & Krigas, T. (1965). Inhibition of cell division in *Escherichia coli* by electrolysis products from a platinum electrode. *Nature*, 205(4972), 698-699.
- Rothenberg, M. L. (2001). Irinotecan (CPT-11): Recent Developments and Future Directions—Colorectal Cancer and Beyond. *The oncologist*, 6(1), 66-80.
- Rothenberg, M. L., Kuhn, J. G., Schaaf, L. J., Rodriguez, G. I., Eckhardt, S. G., Villalona-Calero, M. A., ... & Von Hoff, D. D. (2001). Phase I dose-finding and pharmacokinetic trial of irinotecan (CPT-11) administered every two weeks. *Annals of oncology*, 12(11), 1631-1641.
- Rougier, P., Van Cutsem, E., Bajetta, E., Niederle, N., Possinger, K., Labianca, R., ... & Jacques, C. (1998). A randomised trial of irinotecan versus fluorouracil by continuous infusion after fluorouracil failure in patients with metastatic colorectal cancer. *The Lancet*, 352(9138), 1407-1412.
- Roychoudhury, S. (2019). Characterization of the Role of Acetylated APE1 in DNA Damage Repair and Transcriptional Regulation.
- Russo, D., Arturi, F., Bulotta, S., Pellizzari, L., Filetti, S., Manzini, G., ... & Tell, G. (2001). Ape1/Ref-1 expression and cellular localization in human thyroid carcinoma cell lines. *Journal of Endocrinological Investigation*, 24, RC10-RC12.
- Sahakian, L., Filippone, R. T., Stavely, R., Robinson, A. M., Yan, X. S., Abalo, R., ... & Nurgali, K. (2021). Inhibition of APE1/Ref-1 redox signalling alleviates intestinal dysfunction and damage to myenteric neurons in a mouse model of spontaneous chronic colitis. *Inflammatory bowel diseases*, 27(3), 388-406.
- Saifi, M. A., Sangomla, S., Khurana, A., & Godugu, C. (2019). Protective effect of nanoceria on cisplatin-induced nephrotoxicity by amelioration of oxidative stress and pro-inflammatory mechanisms. *Biological trace element research*, 189(1), 145-156.
- Sakanaka, K., Fujii, K., Ishida, Y., Mukumoto, N., Hida, K., Inoo, H., ... & Mizowaki, T. (2022). Preoperative chemoradiotherapy for locally advanced low rectal cancer using intensity-modulated radiotherapy to spare the intestines: a single-institutional pilot trial. *Journal of Radiation Research*, 63(1), 88-97.
- Salat, K. (2020). Chemotherapy-induced peripheral neuropathy—part 2: focus on the prevention of oxaliplatin-induced neurotoxicity. *Pharmacological Reports*, 72(3), 508-527.
- Saliba, F., Hagipantelli, R., Misset, J. L., Bastian, G., Vassal, G., Bonnay, M., ... & Cvitkovic, E. (1998). Pathophysiology and therapy of irinotecan-induced delayed-onset diarrhea in patients with advanced colorectal cancer: a prospective assessment. *Journal of clinical oncology*, 16(8), 2745-2751.
- Saltz, L. B. (2003). Understanding and managing chemotherapy-induced diarrhea. *The journal of supportive oncology*, 1(1), 35-46.
- Saltz, L. B., Cox, J. V., Blanke, C., Rosen, L. S., Fehrenbacher, L., Moore, M. J., ... & Miller, L. L. (2000). Irinotecan plus fluorouracil and leucovorin for metastatic colorectal cancer. *New England Journal of Medicine*, 343(13), 905-914.

- Salvemini, D., Little, J. W., Doyle, T., & Neumann, W. L. (2011). Roles of reactive oxygen and nitrogen species in pain. *Free Radical Biology and Medicine*, 51(5), 951-966.
- Sampath, C., Kalpana, R., Ansah, T., Charlton, C., Hale, A., Channon, K. M., ... & Gangula, P. R. (2019). Impairment of Nrf2-and nitric-oxid-mediated gastrointestinal motility in an MPTP mouse model of Parkinson's disease. *Digestive diseases and sciences*, 64(12), 3502-3517.
- Sarna, S. K. (1993). Colonic motor activity. *Surgical Clinics of North America*, 73(6), 1201-1223.
- Sarna, S. K. (1993). Gastrointestinal longitudinal muscle contractions. *American Journal of Physiology-Gastrointestinal and Liver Physiology*, 265(1), G156-G164.
- Sarna, S. K., Otterson, M. F., Ryan, R. P., & Cowles, V. E. (1993). Nitric oxide regulates migrating motor complex cycling and its postprandial disruption. *American Journal of Physiology-Gastrointestinal and Liver Physiology*, 265(4), G759-G766.
- Savidge, T. (2011). S-nitrosothiol signals in the enteric nervous system: lessons learnt from big brother. *Frontiers in neuroscience*, 5, 31.
- Scheer, A., & Auer, R. A. C. (2009). Surveillance after curative resection of colorectal cancer. *Clinics in colon and rectal surgery*, 22(04), 242-250.
- Schoch, S., Gajewski, S., Rothfuß, J., Hartwig, A., & Köberle, B. (2020). Comparative study of the mode of action of clinically approved platinum-based chemotherapeutics. *International journal of molecular sciences*, 21(18), 6928.
- Schroder, A. L., Chami, B., Liu, Y., Doyle, C. M., El Kazzi, M., Ahlenstiel, G., ... & Witting, P. K. (2021). Neutrophil Extracellular Trap Density Increases With Increasing Histopathological Severity of Crohn's Disease. *Inflammatory bowel diseases*.
- Schulz, C., Heinemann, V., Schalhorn, A., Moosmann, N., Zwingers, T., Boeck, S., ... & Stemmler, H. J. (2009). UGT1A1 gene polymorphism: impact on toxicity and efficacy of irinotecan-based regimens in metastatic colorectal cancer. *World Journal of Gastroenterology: WJG*, 15(40), 5058.
- Secombe, K. R., Crame, E. E., Tam, J. S., Wardill, H. R., Gibson, R. J., Coller, J. K., & Bowen, J. M. (2022). Intestinal toll-like receptor 4 knockout alters the functional capacity of the gut microbiome following irinotecan treatment. *Cancer chemotherapy and pharmacology*, 89(2), 275-281.
- Sengupta, S., Mantha, A. K., Song, H., Roychoudhury, S., Nath, S., Ray, S., & Bhakat, K. K. (2016). Elevated level of acetylation of APE1 in tumor cells modulates DNA damage repair. *Oncotarget*, 7(46), 75197.
- Seo, S. H., Kim, S. E., Kang, Y. K., Ryoo, B. Y., Ryu, M. H., Jeong, J. H., ... & Sung, M. K. (2016). Association of nutritional status-related indices and chemotherapy-induced adverse events in gastric cancer patients. *BMC cancer*, 16(1), 1-9.
- Serrano Falcón, B., Barceló López, M., Mateos Muñoz, B., Álvarez Sánchez, A., & Rey, E. (2016). Fecal impaction: a systematic review of its medical complications. *BMC geriatrics*, 16(1), 1-8.
- Seventy, M., Currie, G. L., Sena, E. S., Ramnarine, S., Grant, R., MacLeod, M. R., ... & Fallon, M. (2014). Incidence, prevalence, and predictors of chemotherapy-induced peripheral neuropathy: a systematic review and meta-analysis. *Pain@*, 155(12), 2461-2470.
- Sgrignani, J., Garofalo, M., Matkovic, M., Merulla, J., Catapano, C. V., & Cavalli, A. (2018). Structural biology of STAT3 and its implications for anticancer therapies development. *International journal of molecular sciences*, 19(6), 1591.

- Shafi, M. A., & Bresalier, R. S. (2010). The gastrointestinal complications of oncologic therapy. *Gastroenterology Clinics*, 39(3), 629-647.
- Shah, F., Logsdon, D., Messmann, R. A., Fehrenbacher, J. C., Fishel, M. L., & Kelley, M. R. (2017). Exploiting the Ref-1-APE1 node in cancer signaling and other diseases: from bench to clinic. *NPJ precision oncology*, 1(1), 1-19.
- Shah, M. A., Bang, Y. J., Lordick, F., Alsina, M., Chen, M., Hack, S. P., ... & Cunningham, D. (2017). Effect of fluorouracil, leucovorin, and oxaliplatin with or without pertuzumab in HER2-negative, MET-positive gastroesophageal adenocarcinoma: the METGastric randomized clinical trial. *JAMA oncology*, 3(5), 620-627.
- Shahda, S., Lakhani, N. J., O'Neil, B., Rasco, D. W., Wan, J., Mosley, A. L., ... & Messmann, R. A. (2019). A phase I study of the APE1 protein inhibitor APX3330 in patients with advanced solid tumours.
- Shahrestani, J., & Das, J. M. (2021). Neuroanatomy, auerbach plexus. *StatPearls [Internet]*.
- Sharif, S., O'Connell, M. J., Yothers, G., Lopa, S., & Wolmark, N. (2008). FOLFOX and FLOX regimens for the adjuvant treatment of resected stage II and III colon cancer. *Cancer Investigation*, 26(9), 956-963.
- Sharma, R., Tobin, P., & Clarke, S. J. (2005). Management of chemotherapy-induced nausea, vomiting, oral mucositis, and diarrhoea. *The lancet oncology*, 6(2), 93-102.
- Sheng, Y., & Zhu, L. (2018). The crosstalk between autonomic nervous system and blood vessels. *International journal of physiology, pathophysiology and pharmacology*, 10(1), 17.
- Shiao, J. C., Fakhoury, K. R., & Olsen, J. (2020). Total Neoadjuvant Therapy for Rectal Cancer: Current Status and Future Directions. *Current Colorectal Cancer Reports*, 16(6), 125-134.
- Shigematsu, N., Kawashiri, T., Kobayashi, D., Shimizu, S., Mine, K., Hiromoto, S., ... & Shimazoe, T. (2020). Neuroprotective effect of alogliptin on oxaliplatin-induced peripheral neuropathy in vivo and in vitro. *Scientific reports*, 10(1), 1-8.
- Shim, H. S., Bae, C., Wang, J., Lee, K. H., Hankerd, K. M., Kim, H. K., ... & La, J. H. (2019). Peripheral and central oxidative stress in chemotherapy-induced neuropathic pain. *Molecular pain*, 15, 1744806919840098.
- Shimizu, N., Sugimoto, K., Tang, J., Nishi, T., Sato, I., Hiramoto, M., ... & Handa, H. (2000). High-performance affinity beads for identifying drug receptors. *Nature Biotechnology*, 18(8), 877-881.
- Shin, J. H., Choi, S., Lee, Y. R., Park, M. S., Na, Y. G., Irani, K., ... & Jeon, B. H. (2015). APE1/Ref-1 as a serological biomarker for the detection of bladder cancer. *Cancer research and treatment: official journal of Korean Cancer Association*, 47(4), 823.
- Shin, S., Asano, T., Yao, Y., Zhang, R., Claret, F. X., Korc, M., ... & Reddy, S. A. (2009). Activator protein-1 has an essential role in pancreatic cancer cells and is regulated by a novel Akt-mediated mechanism. *Molecular Cancer Research*, 7(5), 745-754.
- Shin, W. S., Han, J., Kumar, R., Lee, G. G., Sessler, J. L., Kim, J. H., & Kim, J. S. (2016). Programmed activation of cancer cell apoptosis: A tumor-targeted phototherapeutic topoisomerase I inhibitor. *Scientific reports*, 6(1), 1-11.
- Shinozaki, E., Makiyama, A., Kagawa, Y., Satake, H., Tanizawa, Y., Cai, Z., & Piao, Y. (2021). Treatment sequences of patients with advanced colorectal cancer and use of second-line FOLFIRI with antiangiogenic drugs in Japan: A retrospective observational study using an administrative database. *PloS one*, 16(2), e0246160.

- Siegel, R., DeSantis, C., & Jemal, A. (2014). Colorectal cancer statistics, 2014. *CA: a cancer journal for clinicians*, 64(2), 104-117.
- Silber, J. R., Bobola, M. S., Blank, A., Schoeler, K. D., Haroldson, P. D., Huynh, M. B., & Kolstoe, D. D. (2002). The apurinic/aprimidinic endonuclease activity of Ape1/Ref-1 contributes to human glioma cell resistance to alkylating agents and is elevated by oxidative stress. *Clinical cancer research*, 8(9), 3008-3018.
- Singh-Gupta, V., Zhang, H., Banerjee, S., Kong, D., Raffoul, J. J., Sarkar, F. H., & Hillman, G. G. (2009). Radiation-induced HIF-1 α cell survival pathway is inhibited by soy isoflavones in prostate cancer cells. *International journal of cancer*, 124(7), 1675-1684.
- Siomek, A., Tujakowski, J., Gackowski, D., Rozalski, R., Foksinski, M., Dziaman, T., ... & Olinski, R. (2006). Severe oxidatively damaged DNA after cisplatin treatment of cancer patients. *International journal of cancer*, 119(9), 2228-2230.
- Smith, P., Lavery, A., & Turkington, R. C. (2020). An overview of acute gastrointestinal side effects of systemic anti-cancer therapy and their management. *Best Practice & Research Clinical Gastroenterology*, 48, 101691.
- Sonis, S. T. (2004). The pathobiology of mucositis. *Nature Reviews Cancer*, 4(4), 277-284.
- Sonis, S. T., Elting, L. S., Keefe, D., Peterson, D. E., Schubert, M., Hauer-Jensen, M., ... & Rubenstein, E. B. (2004). Perspectives on cancer therapy-induced mucosal injury: pathogenesis, measurement, epidemiology, and consequences for patients. *Cancer: Interdisciplinary International Journal of the American Cancer Society*, 100(S9), 1995-2025.
- Sougiannis, A. T., VanderVeen, B. N., Davis, J. M., Fan, D., & Murphy, E. A. (2021). Understanding chemotherapy-induced intestinal mucositis and strategies to improve gut resilience. *American Journal of Physiology-Gastrointestinal and Liver Physiology*, 320(5), G712-G719.
- Soveri, L. M. (2019). Adverse events in the treatment of colorectal cancer: Their use as predictive markers and impact on quality of life.
- Spencer, N. J., & Hu, H. (2020). Enteric nervous system: sensory transduction, neural circuits and gastrointestinal motility. *Nature Reviews Gastroenterology & Hepatology*, 17(6), 338-351.
- Spiegel, D. Y., Boyer, M. J., Hong, J. C., Williams, C. D., Kelley, M. J., Salama, J. K., & Palta, M. (2020). Survival advantage with adjuvant chemotherapy for locoregionally advanced rectal cancer: a veterans health administration analysis. *Journal of the National Comprehensive Cancer Network*, 18(1), 52-58.
- Sriramajayam, K., Peng, D., Lu, H., Zhou, S., Bhat, N., McDonald, O. G., ... & El-Rifai, W. (2021). Activation of NRF2 by APE1/REF1 is redox-dependent in Barrett's related esophageal adenocarcinoma cells. *Redox Biology*, 43, 101970.
- Srisajakul, S., Prapaisilp, P., & Bangchokdee, S. (2022). Drug-induced bowel complications and toxicities: imaging findings and pearls. *Abdominal Radiology*, 1-13.
- Staff, N. P., Grisold, A., Grisold, W., & Windebank, A. J. (2017). Chemotherapy-induced peripheral neuropathy: a current review. *Annals of neurology*, 81(6), 772-781.
- Starobova, H., & Vetter, I. (2017). Pathophysiology of chemotherapy-induced peripheral neuropathy. *Frontiers in molecular neuroscience*, 10, 174.
- Stein, A., Voigt, W., & Jordan, K. (2010). Chemotherapy-induced diarrhea: pathophysiology, frequency and guideline-based management. *Therapeutic advances in medical oncology*, 2(1), 51-63.
- Stintzing, S. (2014). Management of colorectal cancer. *F1000prime reports*, 6.

- Stojanovska, V., McQuade, R. M., Stewart, M., Timpani, C. A., Sorensen, J., Orbell, J., & Nurgali, K. (2016, September). Platinum accumulation and changes in mitochondrial function of the longitudinal muscle and myenteric plexus following oxaliplatin administration. In *APS Annual Conference of the Australian Psychology Society: 2015 Hobart*.
- Stojanovska, V., McQuade, R., Rybalka, E., & Nurgali, K. (2017). Neurotoxicity associated with platinum-based anti-cancer agents: what are the implications of copper transporters?. *Current medicinal chemistry*, *24*(15), 1520-1536.
- Stojanovska, V., Sakkal, S., & Nurgali, K. (2015). Platinum-based chemotherapy: gastrointestinal immunomodulation and enteric nervous system toxicity. *American Journal of Physiology-Gastrointestinal and Liver Physiology*.
- Stone, J. B., & DeAngelis, L. M. (2016). Cancer-treatment-induced neurotoxicity—focus on newer treatments. *Nature reviews Clinical oncology*, *13*(2), 92-105.
- Stringer, A. M., Gibson, R. J., Bowen, J. M., Logan, R. M., Ashton, K., Yeoh, A. S., ... & Keefe, D. M. (2009). Irinotecan-induced mucositis manifesting as diarrhoea corresponds with an amended intestinal flora and mucin profile. *International journal of experimental pathology*, *90*(5), 489-499.
- Stringer, A. M., Gibson, R. J., Logan, R. M., Bowen, J. M., Yeoh, A. S., Hamilton, J., & Keefe, D. M. (2009). Gastrointestinal microflora and mucins may play a critical role in the development of 5-fluorouracil-induced gastrointestinal mucositis. *Experimental Biology and Medicine*, *234*(4), 430-441.
- Su, D., Delaplane, S., Luo, M., Rempel, D. L., Vu, B., Kelley, M. R., ... & Georgiadis, M. M. (2011). Interactions of apurinic/aprimidinic endonuclease with a redox inhibitor: evidence for an alternate conformation of the enzyme. *Biochemistry*, *50*(1), 82-92.
- Su, Z., Wang, T., Zhu, H., Zhang, P., Han, R., Liu, Y., ... & Xu, H. (2015). HMGB1 modulates Lewis cell autophagy and promotes cell survival via RAGE-HMGB1-Erk1/2 positive feedback during nutrient depletion. *Immunobiology*, *220*(5), 539-544.
- Subedi, L., Gaire, B. P., Kim, S. Y., & Parveen, A. (2021). Nitric Oxide as a Target for Phytochemicals in Anti-Neuroinflammatory Prevention Therapy. *International journal of molecular sciences*, *22*(9), 4771.
- Sugiyama, K., Shiraishi, K., Sato, M., Nishibori, R., Nozawa, K., & Kitagawa, C. (2021). Salvage chemotherapy by FOLFIRI regimen for poorly differentiated gastrointestinal neuroendocrine carcinoma. *Journal of Gastrointestinal Cancer*, *52*(3), 947-951.
- Sun, R., Zhu, L., Li, L., Song, W., Gong, X., Qi, X., ... & Liu, Z. (2020). Irinotecan-mediated diarrhea is mainly correlated with intestinal exposure to SN-38: critical role of gut Ugt. *Toxicology and Applied Pharmacology*, *398*, 115032.
- Sutton, E. C., & DeRose, V. J. (2021). Early nucleolar responses differentiate mechanisms of cell death induced by oxaliplatin and cisplatin. *Journal of Biological Chemistry*, *296*.
- Ta, L. E., Espeset, L., Podratz, J., & Windebank, A. J. (2006). Neurotoxicity of oxaliplatin and cisplatin for dorsal root ganglion neurons correlates with platinum–DNA binding. *Neurotoxicology*, *27*(6), 992-1002.
- Ta, L. E., Schmelzer, J. D., Bieber, A. J., Loprinzi, C. L., Sieck, G. C., Brederson, J. D., ... & Windebank, A. J. (2013). A novel and selective poly (ADP-ribose) polymerase inhibitor ameliorate chemotherapy-induced painful neuropathy. *PloS one*, *8*(1), e54161.
- Ta, T., & Porter, T. M. (2013). Thermosensitive liposomes for localized delivery and triggered release of chemotherapy. *Journal of controlled release*, *169*(1-2), 112-125.

- Taberero, J., Van Cutsem, E., Díaz-Rubio, E., Cervantes, A., Humblet, Y., André, T., ... & de Gramont, A. (2007). Phase II trial of cetuximab in combination with fluorouracil, leucovorin, and oxaliplatin in the first-line treatment of metastatic colorectal cancer. *Journal of clinical oncology*, 25(33), 5225-5232.
- Tache, Y., Larauche, M., Yuan, P. Q., & Million, M. (2018). Brain and gut CRF signaling: biological actions and role in the gastrointestinal tract. *Current molecular pharmacology*, 11(1), 51-71.
- Tai, D. I., Tsai, S. L., Chang, Y. H., Huang, S. N., Chen, T. C., Chang, K. S., & Liaw, Y. F. (2000). Constitutive activation of nuclear factor κ B in hepatocellular carcinoma. *Cancer: Interdisciplinary International Journal of the American Cancer Society*, 89(11), 2274-22.
- Takahashi, T. (2003). Pathophysiological significance of neuronal nitric oxide synthase in the gastrointestinal tract. *Journal of gastroenterology*, 38(5), 421-430.
- Takasuna, K., Hagiwara, T., Hirohashi, M., Kato, M., Nomura, M., Nagai, E., ... & Kamataki, T. (1998). Inhibition of intestinal microflora β -glucuronidase modifies the distribution of the active metabolite of the antitumor agent, irinotecan hydrochloride (CPT-11) in rats. *Cancer chemotherapy and pharmacology*, 42(4), 280-286.
- Talley, N. J., Dennis, E. H., Schettler-Duncan, V. A., Lacy, B. E., Olden, K. W., & Crowell, M. D. (2003). Overlapping upper and lower gastrointestinal symptoms in irritable bowel syndrome patients with constipation or diarrhea. *The American journal of gastroenterology*, 98(11), 2454-2459.
- Talmadge, J. E., Singh, R. K., Fidler, I. J., & Raz, A. (2007). Murine models to evaluate novel and conventional therapeutic strategies for cancer. *The American journal of pathology*, 170(3), 793-804.
- Tang, X., Metzger, D., Leeman, S., & Amar, S. (2006). LPS-induced TNF- α factor (LITAF)-deficient mice express reduced LPS-induced cytokine: evidence for LITAF-dependent LPS signalling pathways. *Proceedings of the National Academy of Sciences*, 103(37), 13777-13782.
- Tang, Z., Wang, Y., Wan, Y., Xie, Y., Li, S., Tao, D., ... & Sui, J. D. (2021). Apurinic/aprimidinic endonuclease 1/reduction-oxidation effector factor-1 (APE1) regulates the expression of NLR family pyrin domain containing 3 (NLRP3) inflammasome through modulating transcription factor NF- κ B and promoting the secretion of inflammatory mediators in macrophages. *Annals of Translational Medicine*, 9(2).
- Taniguchi, K., & Karin, M. (2018). NF- κ B, inflammation, immunity and cancer: coming of age. *Nature Reviews Immunology*, 18(5), 309-324.
- Tanioka, H., Nagasaka, T., Uno, F., Inoue, M., Okita, H., Katata, Y., ... & Yamaguchi, Y. (2019). The relationship between peripheral neuropathy and efficacy in second-line chemotherapy for unresectable advanced gastric cancer: a prospective observational multicenter study protocol (IVY). *BMC cancer*, 19(1), 1-6.
- Tansky, M. F. (2006). *N-linked glycosylation of the neurokinin 1 receptor: Functional consequences of glycosylation alterations*. Boston University.
- Tell, G., Crivellato, E., Pines, A., Paron, I., Pucillo, C., Manzini, G., ... & Damante, G. (2001). Mitochondrial localization of APE/Ref-1 in thyroid cells. *Mutation Research/DNA Repair*, 485(2), 143-152.
- Tell, G., Damante, G., Caldwell, D., & Kelley, M. R. (2005). The intracellular localization of APE1/Ref-1: more than a passive phenomenon?. *Antioxidants & redox signaling*, 7(3-4), 367-384.
- Tell, G., Pellizzari, L., Pucillo, C., Puglisi, F., Cesselli, D., Kelley, M. R., ... & Damante, G. (2000).

- TSH controls Ref-1 nuclear translocation in thyroid cells. *Journal of Molecular Endocrinology*, 24(3), 383-390.
- Tell, G., Quadrifoglio, F., Tiribelli, C., & Kelley, M. R. (2009). The many functions of APE1/Ref-1: not only a DNA repair enzyme. *Antioxidants & redox signaling*, 11(3), 601-619.
- Tell, G., Zecca, A., Pellizzari, L., Spessotto, P., Colombatti, A., Kelley, M. R., ... & Pucillo, C. (2000). An 'environment to nucleus' signalling system operates in B lymphocytes: redox status modulates BSAP/Pax-5 activation through Ref-1 nuclear translocation. *Nucleic Acids Research*, 28(5), 1099-1105.
- Thomson, B., Tritt, R., Davis, M., & Kelley, M. R. (2001). Histology-specific expression of a DNA repair protein in pediatric rhabdomyosarcomas. *Journal of pediatric hematology/oncology*, 23(4), 234-239.
- Todorov, I. N., & Todorov, G. I. (2009). Multifactorial nature of the high frequency of mitochondrial DNA mutations in somatic mammalian cells. *Biochemistry (Moscow)*, 74(9), 962-970.
- Törnblom, H., Lindberg, G., Nyberg, B., & Veress, B. (2002). Full-thickness biopsy of the jejunum reveals inflammation and enteric neuropathy in irritable bowel syndrome. *Gastroenterology*, 123(6), 1972-1979.
- Tournigand, C., André, T., Achille, E., Lledo, G., Flesh, M., Mery-Mignard, D., ... & de Gramont, A. (2004). FOLFIRI followed by FOLFOX6 or the reverse sequence in advanced colorectal cancer: a randomized GERCOR study. *Journal of Clinical Oncology*, 22(2).
- Trecarichi, A., & Flatters, S. J. (2019). Mitochondrial dysfunction in the pathogenesis of chemotherapy-induced peripheral neuropathy. *International Review of Neurobiology*, 145, 83-126.
- Tzavella, K., Riepl, R. L., Klauser, A. G., Voderholzer, W. A., Schindlbeck, N. E., & Müller-Lissner, S. A. (1996). Decreased substance P levels in rectal biopsies from patients with slow transit constipation. *European journal of gastroenterology & hepatology*, 8(12), 1207-1211.
- Ueno, M., Masutani, H., Arai, R. J., Yamauchi, A., Hirota, K., Sakai, T., ... & Nikaido, T. (1999). Thioredoxin-dependent redox regulation of p53-mediated p21 activation. *Journal of Biological Chemistry*, 274(50), 35809-35815.
- Um, I. S., Armstrong-Gordon, E., Moussa, Y. E., Gnjidic, D., & Wheate, N. J. (2019). Platinum drugs in the Australian cancer chemotherapy healthcare setting: Is it worthwhile for chemists to continue to develop platinum?. *Inorganica Chimica Acta*, 492, 177-181.
- Uttara, B., Singh, A. V., Zamboni, P., & Mahajan, R. (2009). Oxidative stress and neurodegenerative diseases: a review of upstream and downstream antioxidant therapeutic options. *Current Neuropharmacology*, 7(1), 65-74.
- Valko, M., Jomova, K., Rhodes, C. J., Kuča, K., & Musílek, K. (2016). Redox-and non-redox-metal-induced formation of free radicals and their role in human disease. *Archives of toxicology*, 90(1), 1-37.
- Van Cutsem, E., Nordlinger, B., & Cervantes, A. (2010). Advanced colorectal cancer: ESMO Clinical Practice Guidelines for treatment. *Annals of oncology*, 21, v93-v97.
- van der Stok, E. P., Spaander, M. C., Grünhagen, D. J., Verhoef, C., & Kuipers, E. J. (2017). Surveillance after curative treatment for colorectal cancer. *Nature reviews Clinical oncology*, 14(5), 297-315.
- Van Houten, B., Santa-Gonzalez, G. A., & Camargo, M. (2018). DNA repair after oxidative stress: current challenges. *Current opinion in toxicology*, 7, 9-16.

- Vanhoecke, B., Bateman, E., Mayo, B., Vanlancker, E., Stringer, A., Thorpe, D., & Keefe, D. (2015). Dark Agouti rat model of chemotherapy-induced mucositis: establishment and current state of the art. *Experimental Biology and Medicine*, 240(6), 725-741.
- Varadé, J., Magadán, S., & González-Fernández, Á. (2021). Human immunology and immunotherapy: main achievements and challenges. *Cellular & Molecular Immunology*, 18(4), 805-828.
- Vasko, M. R., Guo, C., Thompson, E. L., & Kelley, M. R. (2011). The repair function of the multifunctional DNA repair/redox protein APE1 is neuroprotective after ionizing radiation. *DNA repair*, 10(9), 942-952.
- Vasudev, N. S., & Reynolds, A. R. (2014). Anti-angiogenic therapy for cancer: current progress, unresolved questions and future directions. *Angiogenesis*, 17(3), 471-494.
- Velasco, R., Alemany, M., Villagrán, M., & Argyriou, A. A. (2021). Predictive biomarkers of Oxaliplatin-induced peripheral neurotoxicity. *Journal of Personalized Medicine*, 11(7), 669.
- Vera, G., Castillo, M., Cabezos, P. A., Chiarlone, A., Martín, M. I., Gori, A., & Abalo, R. (2011). Enteric neuropathy evoked by repeated cisplatin in the rat. *Neurogastroenterology & Motility*, 23(4), 370-e163.
- Vera-Ramirez, L., Sanchez-Rovira, P., Ramirez-Tortosa, M. C., Ramirez-Tortosa, C. L., Granados-Principal, S., Lorente, J. A., & Quiles, J. L. (2011). Free radicals in breast carcinogenesis, breast cancer progression and cancer stem cells. Biological bases to develop oxidative-based therapies. *Critical reviews in oncology/hematology*, 80(3), 347-368.
- Verstappen, C. C., Heimans, J. J., Hoekman, K., & Postma, T. J. (2003). Neurotoxic complications of chemotherapy in patients with cancer. *Drugs*, 63(15), 1549-1563.
- Viele, C. S. (2003, November). Overview of chemotherapy-induced diarrhea. In *Seminars in Oncology Nursing* (Vol. 19, pp. 2-5). WB Saunders.
- Vince, J. E., De Nardo, D., Gao, W., Vince, A. J., Hall, C., McArthur, K., & Lawlor, K. E. (2018). The mitochondrial apoptotic effectors BAX/BAK activate caspase-3 and-7 to trigger NLRP3 inflammasome and caspase-8 driven IL-1 β activation. *Cell reports*, 25(9), 2339-2353.
- Vincent, A. M., Russell, J. W., Low, P., & Feldman, E. L. (2004). Oxidative stress in the pathogenesis of diabetic neuropathy. *Endocrine Reviews*, 25(4), 612-628.
- Vinita, M., Dorathi, R. P. J., & Palanivelu, K. (2010). Degradation of 2, 4, 6-trichlorophenol by photo Fenton's like method using nano heterogeneous catalytic ferric ion. *Solar Energy*, 84(9), 1613-1618.
- Vitiello, P. P., Martini, G., Mele, L., Giunta, E. F., De Falco, V., Ciardiello, D., ... & Martinelli, E. (2021). Vulnerability to low-dose combination of irinotecan and niraparib in ATM-mutated colorectal cancer. *Journal of Experimental & Clinical Cancer Research*, 40(1), 1-15.
- Vogelstein, B., Papadopoulos, N., Velculescu, V. E., Zhou, S., Diaz Jr, L. A., & Kinzler, K. W. (2013). Cancer genome landscapes. *science*, 339(6127), 1546-1558.
- Wadler, S., Benson, A. B., Engelking, C., Catalano, R., Field, M., Kornblau, S. M., ... & Vokes, E. (1998). Recommended guidelines for the treatment of chemotherapy-induced diarrhea. *Journal of Clinical Oncology*, 16(9), 3169-3178.
- Wafai, L., Taher, M., Jovanovska, V., Bornstein, J. C., Dass, C. R., & Nurgali, K. (2013). Effects of oxaliplatin on mouse myenteric neurons and colonic motility. *Frontiers in neuroscience*, 7, 30.
- Wainberg, Z. A., Bekaii-Saab, T., Boland, P. M., Dayyani, F., Macarulla, T., Mody, K., ... & Dean, A. (2021). First-line liposomal irinotecan with oxaliplatin, 5-fluorouracil and leucovorin

- (NALIRIFOX) in pancreatic ductal adenocarcinoma: A phase I/II study. *European Journal of Cancer*, 151, 14-24.
- Walke, M. P., & Sakharkar, S. (2021). Review on Constipation in Adults. *Int J Cur Res Revl Vol*, 13(10), 84.
- Wang, B., Mao, Y. K., Diorio, C., Pasyk, M., Wu, R. Y., Bienenstock, J., & Kunze, W. A. (2010). Luminal administration ex vivo of a live *Lactobacillus* species moderates mouse jejunal motility within minutes. *The FASEB Journal*, 24(10), 4078-4088.
- Wang, C. C., & Li, J. (2012). An update on chemotherapy of colorectal liver metastases. *World journal of gastroenterology: WJG*, 18(1), 25.
- Wang, D., Luo, M., & Kelley, M. R. (2004). Human apurinic endonuclease 1 (APE1) expression and prognostic significance in osteosarcoma: enhanced sensitivity of osteosarcoma to DNA damaging agents using silencing RNA APE1 expression inhibition. *Molecular cancer therapeutics*, 3(6), 679-686.
- Wang, K., Ren, Y., Ma, Z., Li, F., Cheng, X., Xiao, J., ... & Jiao, Z. Y. (2019). Docetaxel, oxaliplatin, leucovorin, and 5-fluorouracil (FLOT) as preoperative and postoperative chemotherapy compared with surgery followed by chemotherapy for patients with locally advanced gastric cancer: a propensity score-based analysis. *Cancer Management and Research*, 11, 3009.
- Wang, L. A., Yang, B., Rao, W., Xiao, H., Wang, D., & Jiang, J. (2019). The correlation of BER protein, IRF3 with CD8+ T cell and their prognostic significance in upper tract urothelial carcinoma. *OncoTargets and therapy*, 12, 7725.
- Wang, Y., Branicky, R., Noë, A., & Hekimi, S. (2018). Superoxide dismutases: Dual roles in controlling ROS damage and regulating ROS signalling. *Journal of Cell Biology*, 217(6), 1915-1928.
- Wang, Y., Shen, Y., Wang, S., Shen, Q., & Zhou, X. (2018). The role of STAT3 in leading the crosstalk between human cancers and the immune system. *Cancer letters*, 415, 117-128.
- Wardill, H. R., Gibson, R. J., Van Sebille, Y. Z., Secombe, K. R., Collier, J. K., White, I. A., ... & Bowen, J. M. (2016). Irinotecan-Induced Gastrointestinal Dysfunction and Pain Are Mediated by Common TLR4-Dependent Mechanisms TLR4 and Chemotherapy-Induced Toxicity. *Molecular cancer therapeutics*, 15(6), 1376-1386.
- Waris, G., Huh, K. W., & Siddiqui, A. (2001). Mitochondrially associated hepatitis B virus X protein constitutively activates transcription factors STAT-3 and NF- κ B via oxidative stress. *Molecular and cellular biology*, 21(22), 7721-7730.
- Waseem, M., Kaushik, P., Tabassum, H., & Parvez, S. (2018). Role of mitochondrial mechanism in chemotherapy-induced peripheral neuropathy. *Current Drug Metabolism*, 19(1), 47-54.
- Waseem, M., Sahu, U., Salman, M., Choudhury, A., Kar, S., Tabassum, H., & Parvez, S. (2017). Melatonin pre-treatment mitigates SHSY-5Y cells against oxaliplatin induced mitochondrial stress and apoptotic cell death. *PLoS One*, 12(7), e0180953.
- Wasilewski, A., & Mohile, N. (2021). Meet the expert: How I treat chemotherapy-induced peripheral neuropathy. *Journal of Geriatric Oncology*, 12(1), 1-5.
- Wedel, T., Büsing, V., Heinrichs, G., Nohroudi, K., Bruch, H. P., Roblick, U. J., & Böttner, M. (2010). Diverticular disease is associated with enteric neuropathy as revealed by morphometric analysis. *Neurogastroenterology & Motility*, 22(4), 407-e94.
- Weihe, E., Tao-Cheng, J. H., Schäfer, M. K., Erickson, J. D., & Eiden, L. E. (1996). Visualization of the vesicular acetylcholine transporter in cholinergic nerve terminals and its targeting to a specific population of small synaptic vesicles. *Proceedings of the National Academy of Sciences*, 93(8), 3547-3552.

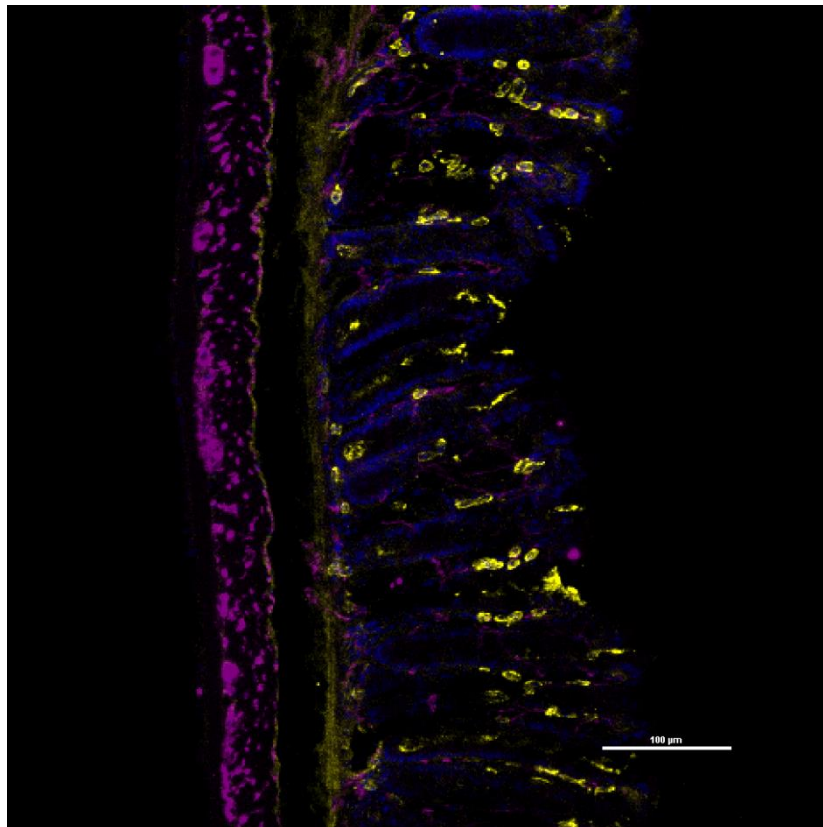
- Wessler, I., & Kirkpatrick, C. J. (2020). Cholinergic signaling controls immune functions and promotes homeostasis. *International Immunopharmacology*, *83*, 106345.
- Wingate, D., Hongo, M., Kellow, J., Lindberg, G., & Smout, A. (2002). Disorders of gastrointestinal motility: Towards a new classification 1. *Journal of gastroenterology and hepatology*, *17*, S1-S14.
- Wong, D. V. T., Holanda, R. B. F., Cajado, A. G., Bandeira, A. M., Pereira, J. F. B., Amorim, J. O., ... & Lima-Júnior, R. C. P. (2021). TLR4 deficiency upregulates TLR9 expression and enhances irinotecan-related intestinal mucositis and late-onset diarrhoea. *British Journal of Pharmacology*, *178*(20), 4193-4209.
- Wong, D. V. T., Ribeiro-Filho, H. V., Wanderley, C. W. S., Leite, C. A. V. G., Lima, J. B., Assef, A. N. B., ... & Lima-Júnior, R. C. P. (2019). SN-38, the active metabolite of irinotecan, inhibits the acute inflammatory response by targeting toll-like receptor 4. *Cancer Chemotherapy and Pharmacology*, *84*(2), 287-298.
- Xanthoudakis, S., & Curran, T. (1992). Identification and characterization of Ref-1, a nuclear protein that facilitates AP-1 DNA-binding activity. *The EMBO journal*, *11*(2), 653-665.
- Xanthoudakis, S., & Curran, T. (1996). Redox regulation of AP-1. *Biological Reactive Intermediates V*, 69-75.
- Xanthoudakis, S., Miao, G., Wang, F., Pan, Y. C., & Curran, T. (1992). Redox activation of Fos-Jun DNA binding activity is mediated by a DNA repair enzyme. *The EMBO journal*, *11*(9), 3323-3335
- Xanthoudakis, S., Smeyne, R. J., Wallace, J. D., & Curran, T. (1996). The redox/DNA repair protein, Ref-1, is essential for early embryonic development in mice. *Proceedings of the National Academy of Sciences*, *93*(17), 8919-8923.
- Xiao, W. H., & Bennett, G. J. (2012). Effects of mitochondrial poisons on the neuropathic pain produced by the chemotherapeutic agents, paclitaxel and oxaliplatin. *Pain*, *153*(3), 704-709.
- Xie, K., Wei, D., & Huang, S. (2006). Transcriptional anti-angiogenesis therapy of human pancreatic cancer. *Cytokine & growth factor reviews*, *17*(3), 147-156.
- Xie, K., Wu, C., & Xiong, L. (2006). Genomic organization, differential expression, and interaction of SQUAMOSA promoter-binding-like transcription factors and microRNA156 in rice. *Plant Physiology*, *142*(1), 280-293.
- Xu, D., & Qu, C. K. (2008). Protein tyrosine phosphatases in the JAK/STAT pathway. *Frontiers in bioscience: a journal and virtual library*, *13*, 4925.
- Xu, Y., & Villalona-Calero, M. A. (2002). Irinotecan: mechanisms of tumour resistance and novel strategies for modulating its activity. *Annals of oncology*, *13*(12), 1841-1851.
- Xue, D. F., Pan, S. T., Huang, G., & Qiu, J. X. (2020). ROS enhances the cytotoxicity of cisplatin by inducing apoptosis and autophagy in tongue squamous cell carcinoma cells. *The international journal of biochemistry & cell biology*, *122*, 105732.
- Yadav, S. K., Ito, N., Mindur, J. E., Kumar, H., Youssef, M., Suresh, S., ... & Ito, K. (2022). Fecal Lcn-2 level is a sensitive biological indicator for gut dysbiosis and intestinal inflammation in multiple sclerosis. *Frontiers in immunology*, *13*.
- Yakes, F. M., & Van Houten, B. (1997). Mitochondrial DNA damage is more extensive and persists longer than nuclear DNA damage in human cells following oxidative stress. *Proceedings of the National Academy of Sciences*, *94*(2), 514-519.

- Yamabe, Y., Shimamoto, A., Goto, M., Yokota, J., Sugawara, M., & Furuichi, Y. (1998). Sp1-mediated transcription of the Werner helicase gene is modulated by Rb and p53. *Molecular and cellular biology*, 18(11), 6191-6200.
- Yamagishi, A., Morita, T., Miyashita, M., & Kimura, F. (2009). Symptom prevalence and longitudinal follow-up in cancer outpatients receiving chemotherapy. *Journal of Pain and symptom management*, 37(5), 823-830.
- Yang, S., & Meyskens, F. L. (2009). Apurinic/aprimidinic endonuclease/redox effector factor-1 (APE/Ref-1): a unique target for the prevention and treatment of human melanoma. *Antioxidants & redox signaling*, 11(3), 639-650.
- Yang, S., Irani, K., Heffron, S. E., Jurnak, F., & Meyskens, F. L. (2005). Alterations in the expression of the apurinic/aprimidinic endonuclease-1/redox factor-1 (APE/Ref-1) in human melanoma and identification of the therapeutic potential of resveratrol as an APE/Ref-1 inhibitor. *Molecular cancer therapeutics*, 4(12), 1923-1935.
- Yang, Y., Karakhanova, S., Hartwig, W., D'Haese, J. G., Philippov, P. P., Werner, J., & Bazhin, A. V. (2016). Mitochondria and mitochondrial ROS in cancer: novel targets for anticancer therapy. *Journal of cellular physiology*, 231(12), 2570-2581.
- Yang, Y., Luo, L., Cai, X., Fang, Y., Wang, J., Chen, G., ... & Cao, P. (2018). Nrf2 inhibits oxaliplatin-induced peripheral neuropathy via protection of mitochondrial function. *Free Radical Biology and Medicine*, 120, 13-24.
- Yang, Z. Z., Chen, X. H., & Wang, D. (2007). Experimental study enhancing the chemosensitivity of multiple myeloma to melphalan by using a tissue-specific APE1-silencing RNA expression vector. *Clinical Lymphoma and Myeloma*, 7(4), 296-304.
- Yu, H., Pardoll, D., & Jove, R. (2009). STATs in cancer inflammation and immunity: a leading role for STAT3. *Nature reviews cancer*, 9(11), 798-809.
- Zabransky, D. J., Jaffee, E. M., & Weeraratna, A. T. (2022). Shared genetic and epigenetic changes link aging and cancer. *Trends in Cell Biology*.
- Zajączkowska, R., Kocot-Kępska, M., Leppert, W., Wrzosek, A., Mika, J., & Wordliczek, J. (2019). Mechanisms of chemotherapy-induced peripheral neuropathy. *International journal of molecular sciences*, 20(6), 1451.
- Zedan, A. H., Hansen, T. F., Svenningsen, Å. F., & Vilholm, O. J. (2014). Oxaliplatin-induced neuropathy in colorectal cancer: many questions with few answers. *Clinical colorectal cancer*, 13(2), 73-80.
- Zhang, C., Ward, J., Dauch, J. R., Tanzi, R. E., & Cheng, H. T. (2018). Cytokine-mediated inflammation mediates painful neuropathy from metabolic syndrome. *PloS one*, 13(2), e0192333.
- Zhang, X., Duan, R., Wang, Y., Liu, X., Zhang, W., Zhu, X., ... & Guo, W. (2022). FOLFIRI (folinic acid, fluorouracil, and irinotecan) increases not efficacy but toxicity compared with single-agent irinotecan as a second-line treatment in metastatic colorectal cancer patients: a randomized clinical trial. *Therapeutic Advances in Medical Oncology*, 14, 17588359211068737.
- Zhang, Y., Zhang, Q., Li, L., Mu, D., Hua, K., Ci, S., ... & Guo, Z. (2020). Arginine methylation of APE1 promotes its mitochondrial translocation to protect cells from oxidative damage. *Free Radical Biology and Medicine*, 158, 60-73.
- Zhao, G., Liu, S., Zhang, Y., Zhao, T., Wang, R., Bian, J., ... & Zhou, J. (2021). Irinotecan eluting beads-transarterial chemoembolization using Callispheres® microspheres is an effective and safe approach in treating unresectable colorectal cancer liver metastases. *Irish Journal of Medical Science (1971-)*, 1-7.

- Zhao, S., Tadesse, S., & Kidane, D. (2021). Significance of base excision repair to human health. *International review of cell and molecular biology*, 364, 163-193.
- Zhao, Z., Nelson, A. R., Betsholtz, C., & Zlokovic, B. V. (2015). Establishment and dysfunction of the blood-brain barrier. *Cell*, 163(5), 1064-1078.
- Zheng, H., Xiao, W. H., & Bennett, G. J. (2012). Cytotoxicity and bortezomib-induced chronic painful peripheral neuropathy. *Experimental neurology*, 238(2), 225-234.
- Zhou, H., & Toan, S. (2020). Pathological roles of mitochondrial oxidative stress and mitochondrial dynamics in cardiac microvascular ischemia/reperfusion injury. *Biomolecules*, 10(1), 85.
- Zhou, L., Liu, R., Huang, D., Li, H., Ning, T., Zhang, L., ... & Ba, Y. (2021). Monosialotetrahexosylganglioside in the treatment of chronic oxaliplatin-induced peripheral neurotoxicity: TJMUCH-GI-001, a randomised controlled trial. *EClinicalMedicine*, 41, 101157.
- Zhou, L., Zhang, Q., Zhang, P., Sun, L., Peng, C., Yuan, Z., & Cheng, J. (2017). c-Abl-mediated Drp1 phosphorylation promotes oxidative stress-induced mitochondrial fragmentation and neuronal cell death. *Cell death & disease*, 8(10), e3117-e3117.
- Zhu, H., Shan, Y., Ge, K., Lu, J., Kong, W., & Jia, C. (2020). Oxaliplatin induces immunogenic cell death in hepatocellular carcinoma cells and synergizes with immune checkpoint blockade therapy. *Cellular Oncology*, 43, 1203-1214.
- Zibara, K., Awada, Z., Dib, L., El-Saghir, J., Al-Ghadban, S., Ibrik, A., ... & El-Sabban, M. (2015). Anti-angiogenesis therapy and gap junction inhibition reduce MDA-MB-231 breast cancer cell invasion and metastasis in vitro and in vivo. *Scientific reports*, 5(1), 1-16.
- Zimmerman, C., Atherton, P. J., Pachman, D., Seisler, D., Wagner-Johnston, N., Dakhil, S., ... & Loprinzi, C. L. (2016). MC11C4: a pilot randomized, placebo-controlled, double-blind study of venlafaxine to prevent oxaliplatin-induced neuropathy. *Supportive Care in Cancer*, 24(3), 1071-1078.
- Zorov, D. B., Bannikova, S. Y., Belousov, V. V., Vyssokikh, M. Y., Zorova, L. D., Isaev, N. K., ... & Plotnikov, E. Y. (2005). Reactive oxygen and nitrogen species: friends or foes?. *Biochemistry (Moscow)*, 70(2), 215-221.
- Zorov, D. B., Filburn, C. R., Klotz, L. O., Zweier, J. L., & Sollott, S. J. (2000). Reactive oxygen species (Ros-Induced) Ros release: a new phenomenon accompanying induction of the mitochondrial permeability transition in cardiac myocytes. *The Journal of experimental medicine*, 192(7), 1001-1014.
- Zorov, D. B., Juhaszova, M., & Sollott, S. J. (2014). Mitochondrial reactive oxygen species (ROS) and ROS-induced ROS release. *Physiological Reviews*, 94(3), 909-950.
- Zorov, D. B., Plotnikov, E. Y., Jankauskas, S. S., Isaev, N. K., Silachev, D. N., Zorova, L. D., ... & Morosanov, M. A. (2012). The phenoptosis problem: what is causing the death of an organism? Lessons from acute kidney injury. *Biochemistry (Moscow)*, 77(7), 742-753.
- Zou, G. M., & Maitra, A. (2008). A small-molecule inhibitor of the AP endonuclease 1/REF-1 E3330 inhibits pancreatic cancer cell growth and migration. *Molecular cancer therapeutics*, 7(7), 2012-2021.
- Zou, G. M., Karikari, C., Kabe, Y., Handa, H., Anders, R. A., & Maitra, A. (2009). The Ape-1/Ref-1 redox antagonist E3330 inhibits the growth of tumour endothelium and endothelial progenitor cells: therapeutic implications in tumour angiogenesis. *Journal of cellular physiology*, 219(1), 209-218.

6

SUPPLEMENTARY DOCUMENTS



Cross-sectional preparation of the distal colon of IRI+VEH-treated mouse with CRC labelled with an anti-MPO antibody (yellow), neuronal marker anti- β Tubulin III antibody (magenta) and DAPI (green) (Scale bar = 100 μ m)

CHAPTER 2

Figure SD 2.14 APE1/Ref-1 protein expression in the distal colon

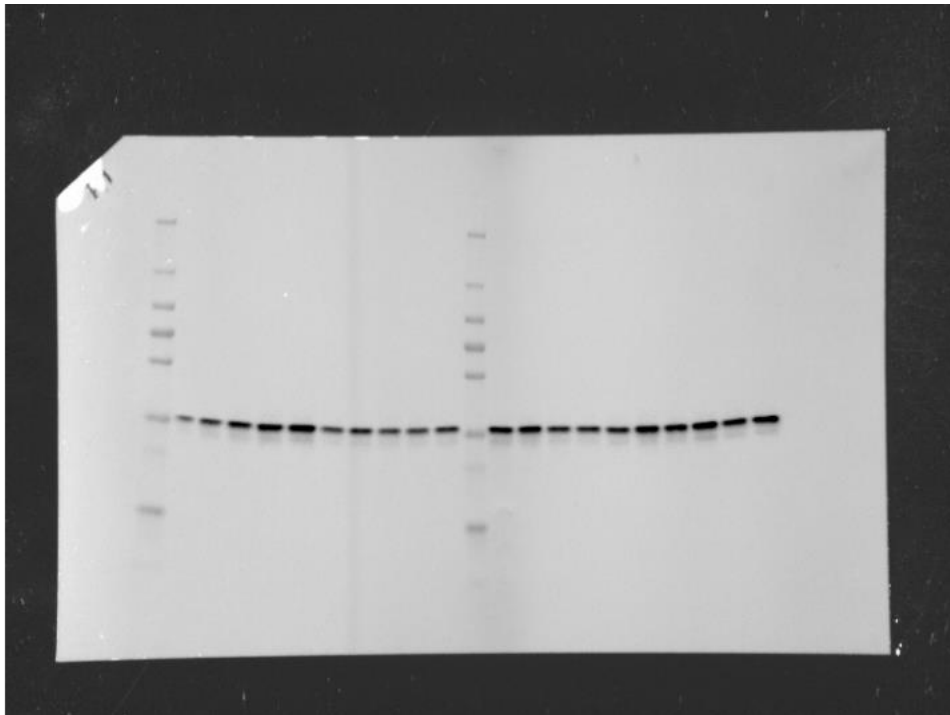


Figure SD 2.17 APE1/Ref-1 protein expression in the distal colon of mice with CRC

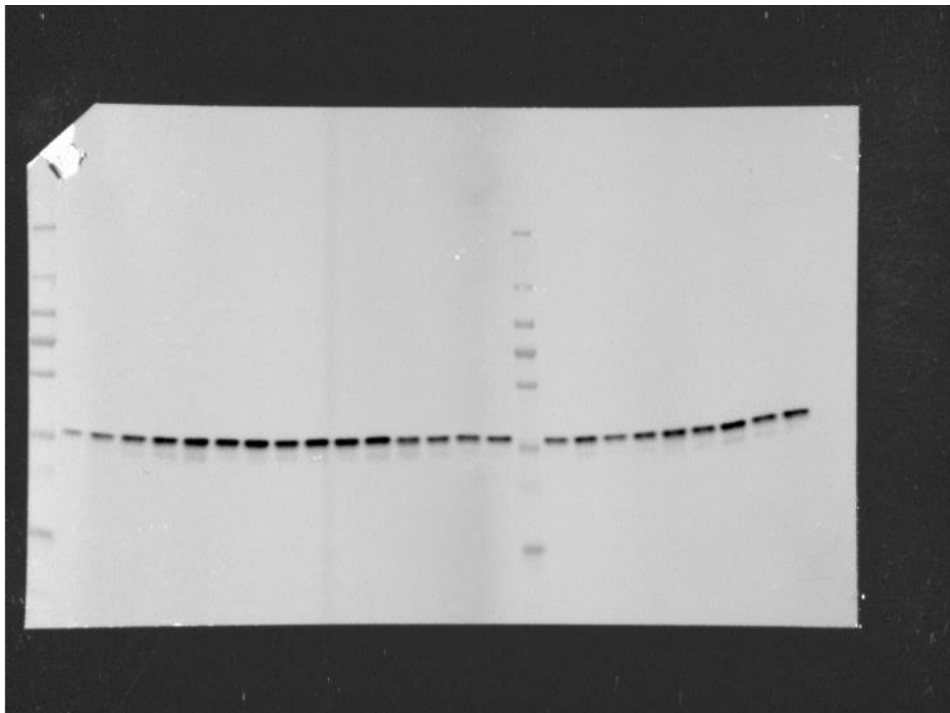


Figure SD 2.22 (A) NF- κ B protein expression in the distal colon

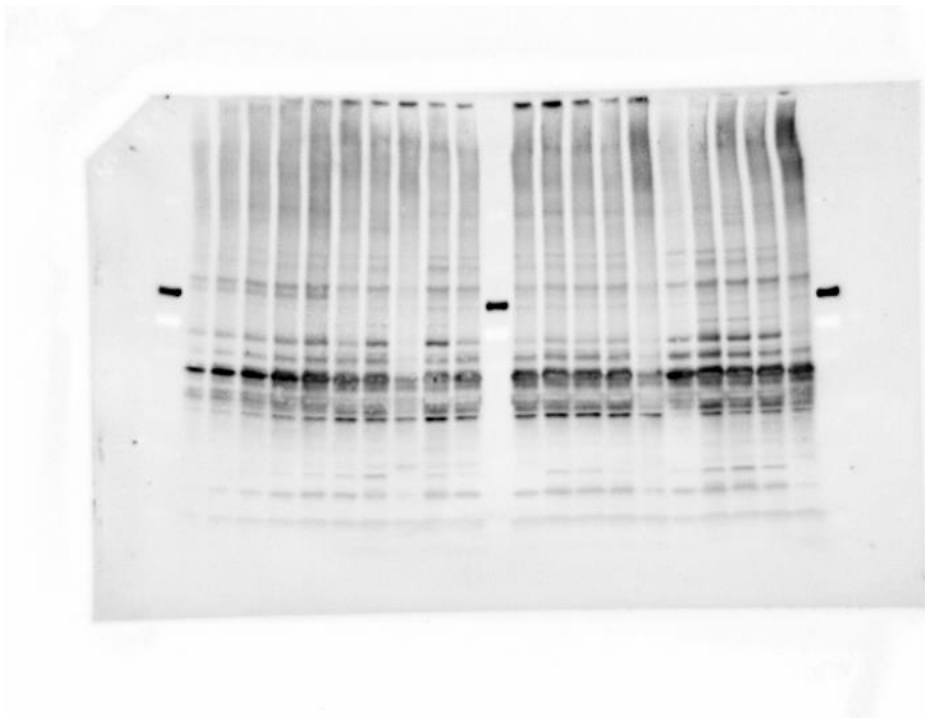


Figure SD 2.22 (B) NF- κ B protein expression in the distal colon

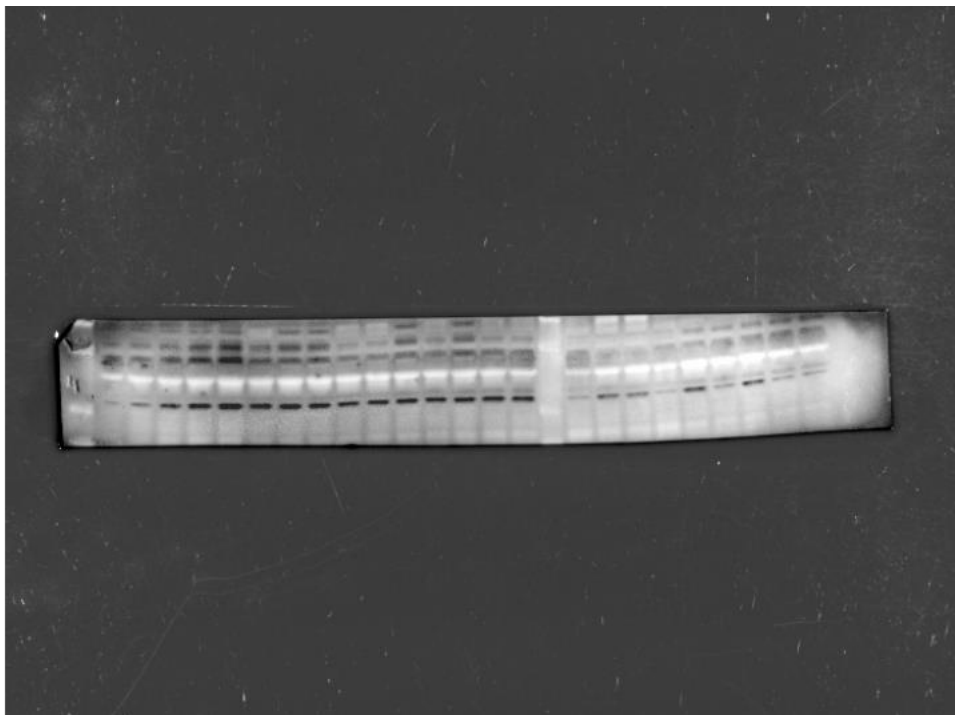


Figure SD 2.23 (A) Signal transducer and activator of transcription 3 in the distal colon in mice without cancer

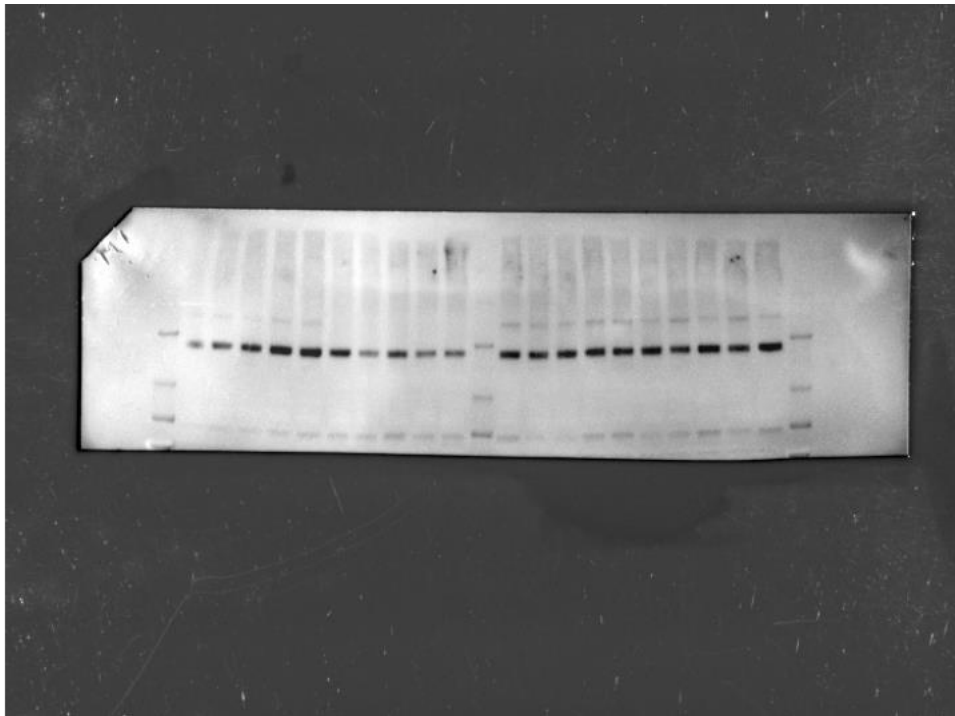


Figure SD 2.23 (B) Phosphor signal transducer and activator of transcription 3 protein expression in the distal colon in mice without cancer

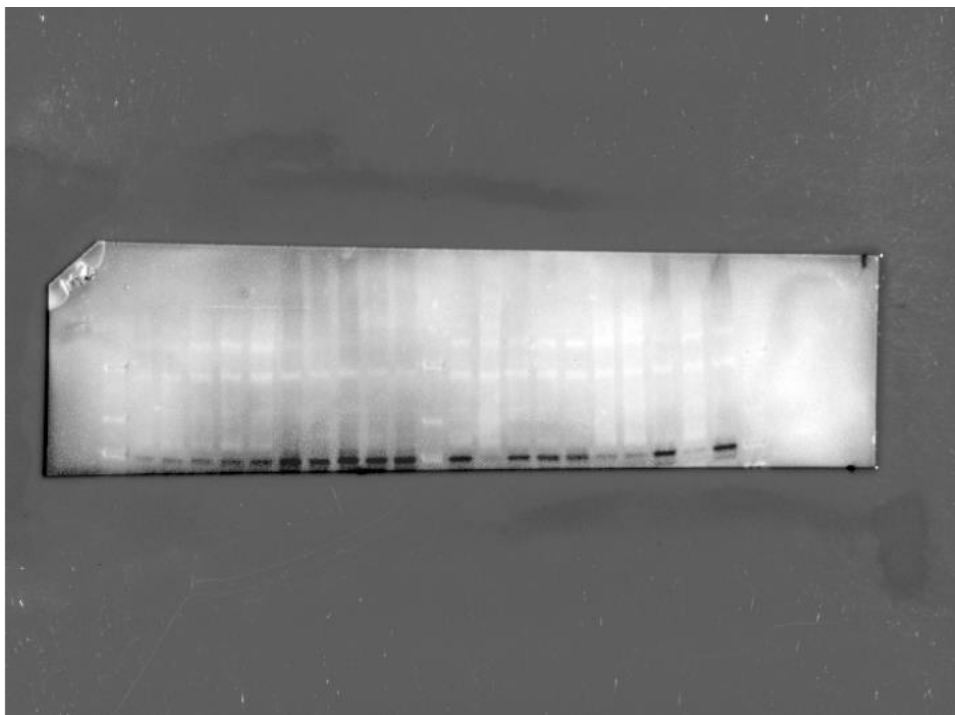


Figure SD 2.24 (A) Signal transducer and activator of transcription 3 protein expression in the distal colon in with CRC

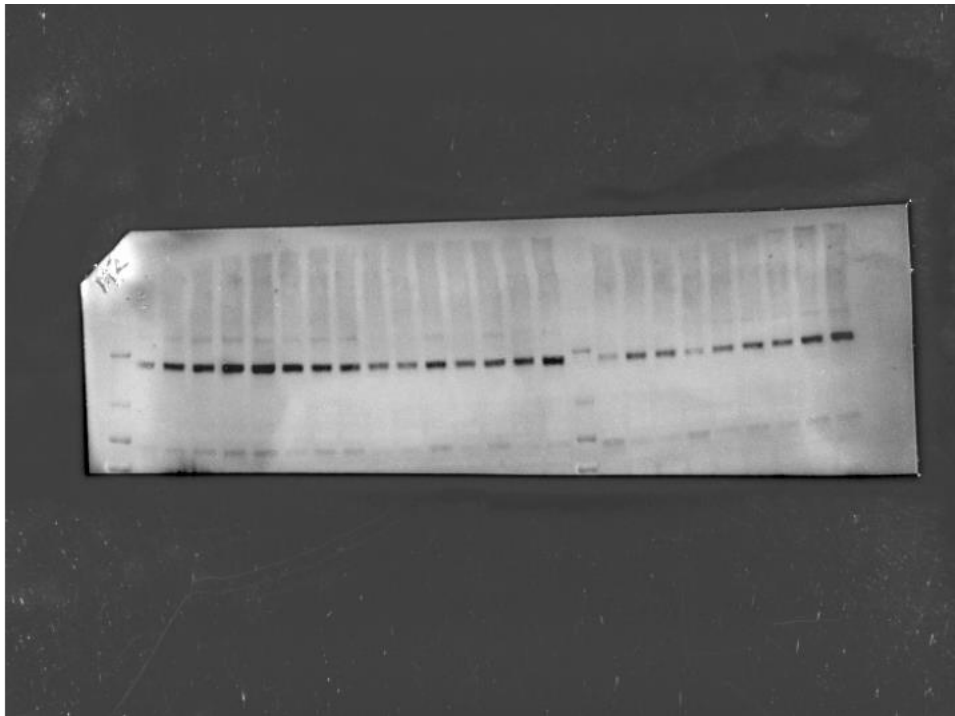


Figure SD 2.24 (B) Phosphor signal transducer and activator of transcription 3 protein expression in the distal colon in with CRC

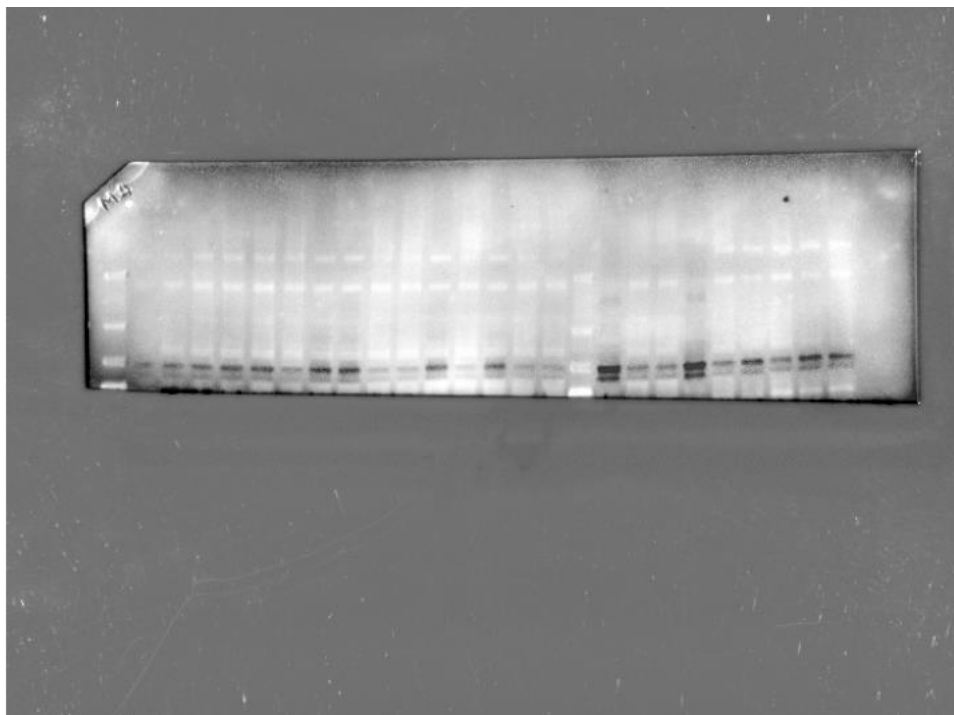
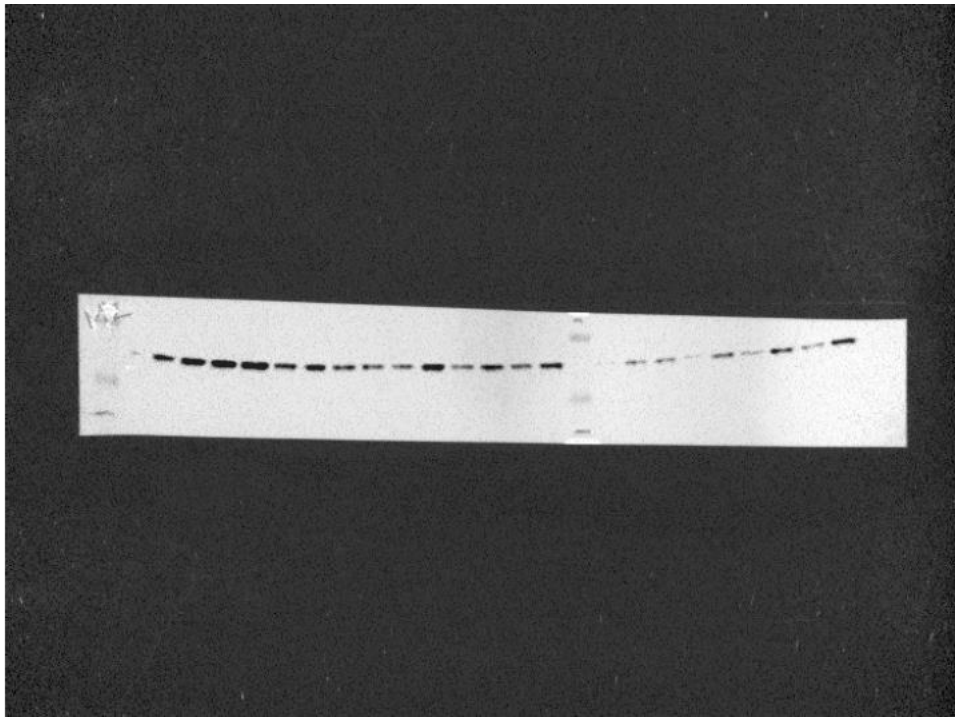


Figure SD 2.27 Vascular endothelial growth factor protein expression following treatments in mice with CRC



CHAPTER 3

Figure SD 3.7 APE1/Ref-1 protein expression in the distal colon of mice without cancer

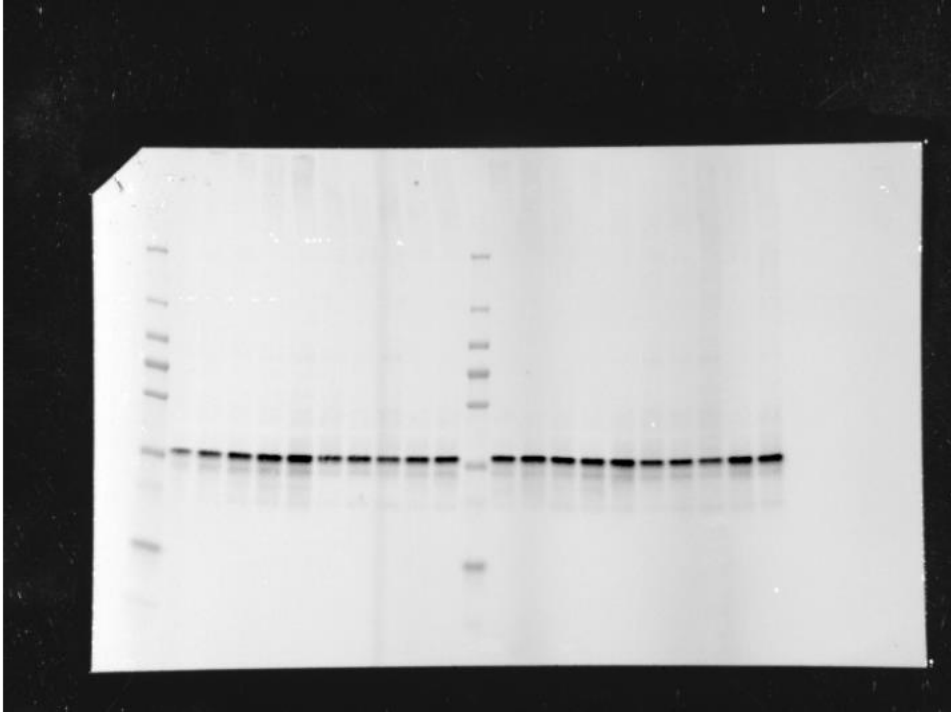


Figure SD 3.10 APE1/Ref-1 protein expression in the distal colon of mice with CRC

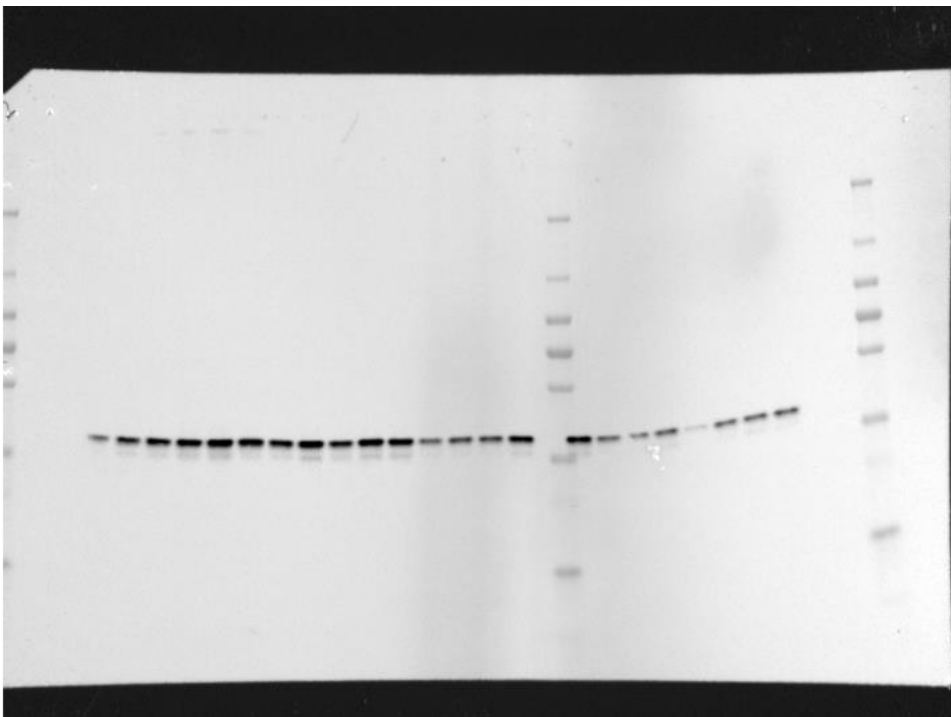


Figure 3.13 (A) Cytochrome c protein expression in the distal colon

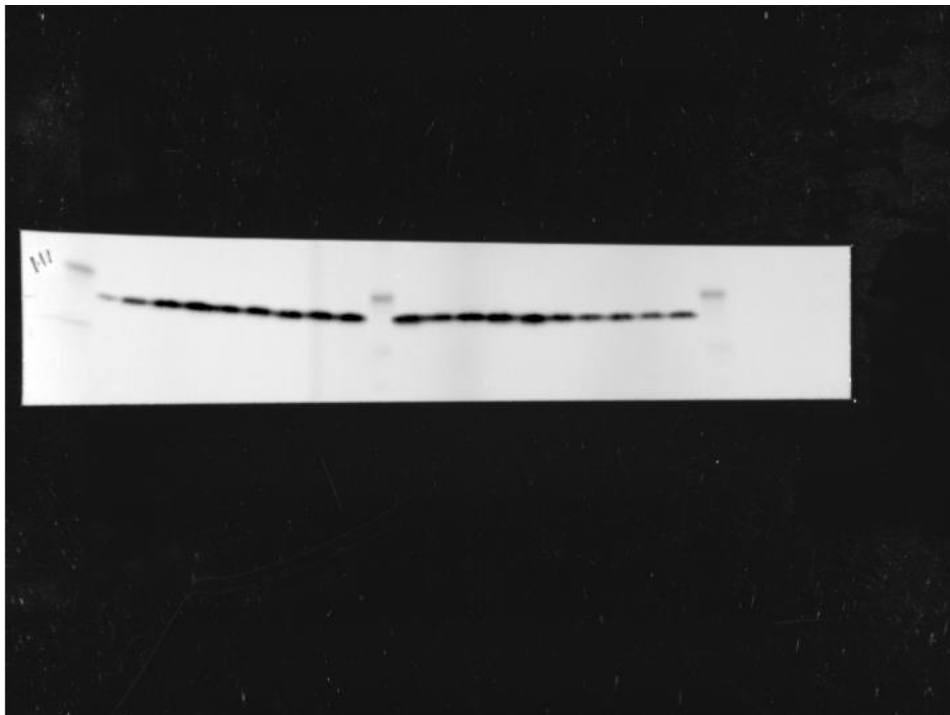


Figure 3.13 (B) Cytochrome c protein expression in the distal colon



Figure 3.14 (A) Signal transducer and activator of transcription 3 protein expression in the distal colon in mice without cancer

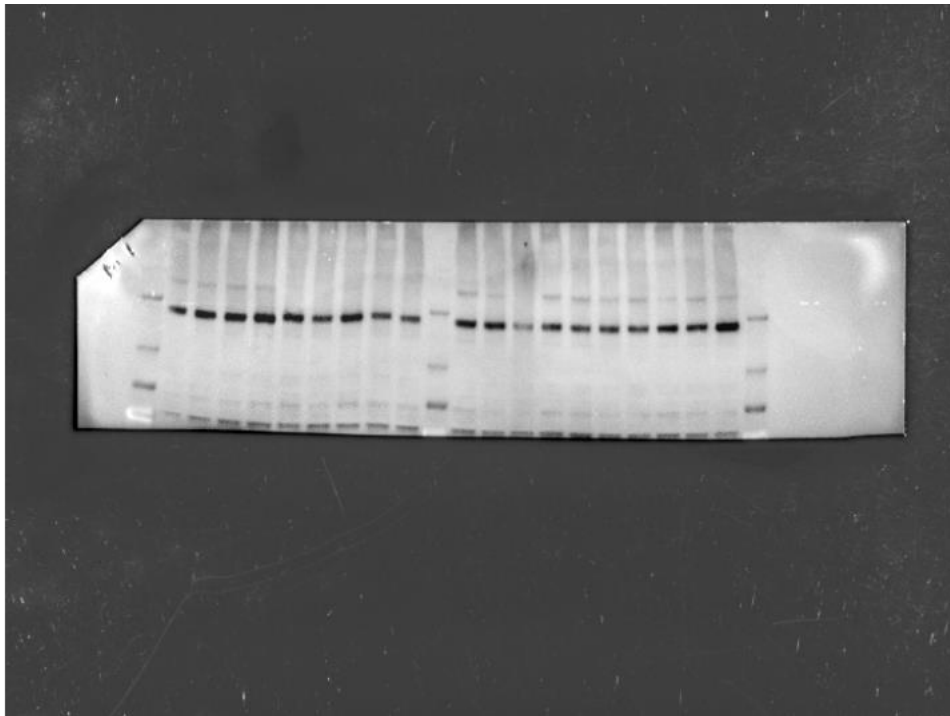


Figure 3.14 (B) Phosphor signal transducer and activator of transcription 3 protein expression in the distal colon in mice without cancer

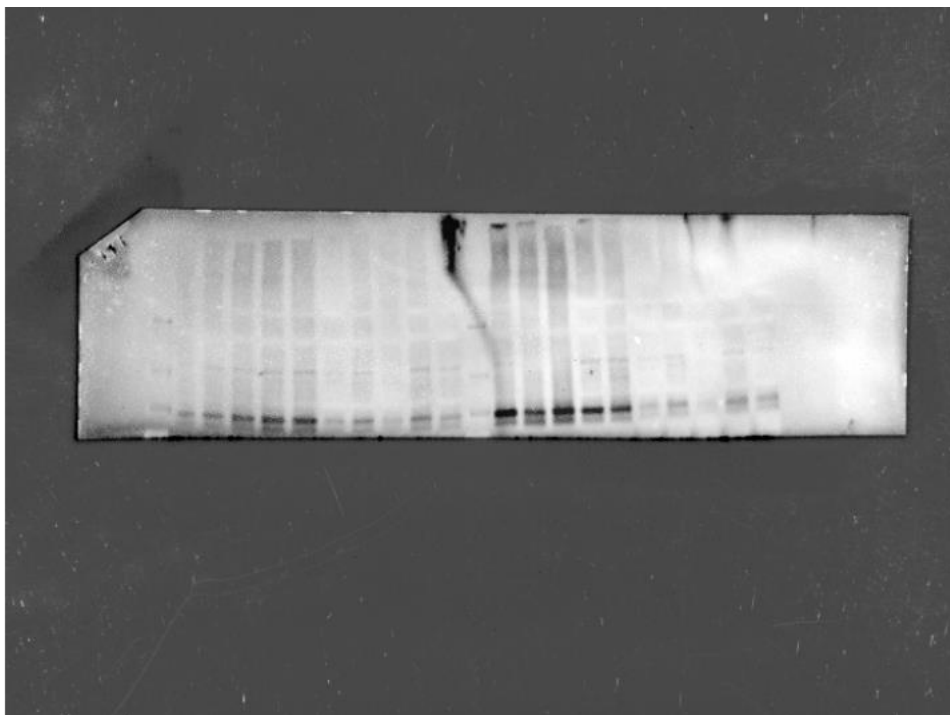


Figure 3.15 (A) Signal transducer and activator of transcription 3 protein expression in the distal colon in CRC-induced mice.

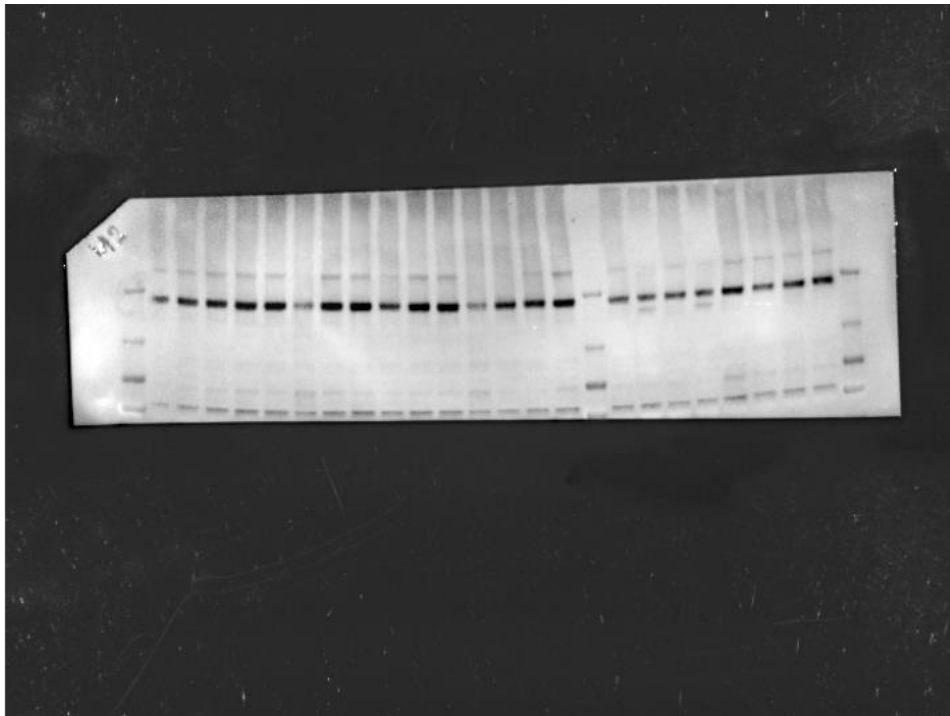


Figure 3.15 (B) Phosphor signal transducer and activator of transcription 3 protein expression in the distal colon in CRC-induced mice

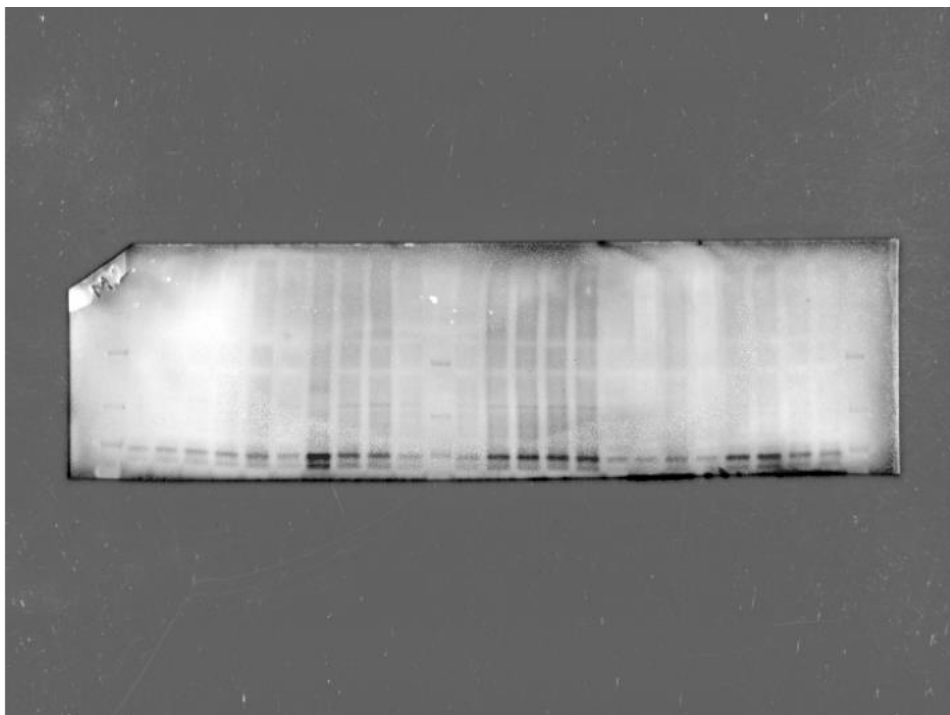


Figure SD 3.18 Vascular endothelial growth factor protein expression following treatments in CRC-induced mice.

